because they were over age 80 and as such, the IHC results were likely due to acquired methylation of the *MLH1* promoter. The remaining 4 patients with absent staining have been referred to Cancer Genetics for possible further work-up. The reimbursement rate and turn-around time for the IHC stains were similar to that for other IHC stains used in clinical practice.

Conclusions: IHC stains for the MMR proteins are fast and relatively easy to institute in routine evaluation of CRC, and we have not had difficulty interpreting the stains leading to additional testing. Furthermore, reimbursement was obtained at a level similar to other IHC stains used in clinical practice. The surgeons and oncologists welcomed the prognostic information. Further study is warranted to confirm these initial findings.

597 High Fidelity Image Cytometry in Neoplastic Lesions in Barrett's Esophagus, Including Basal Crypt Dysplasia-Like Atypia with Surface Maturation

X Zhang, Q Huang, R Goyal, RD Odze. VA Boston Health Care System, Boston, MA; Brigham and Women's Hospital, Boston, MA.

Background: Chromosomal instability and DNA aneuploidy is a key event in the progression of cancer in Barrett's esophagus (BE). Automated image cytometry using high fidelity DNA histograms have been shown to be more sensitive and less susceptible to technical and interpretation issues than flow cytometry for analyzing cellular DNA content. Basal crypt dysplasia-like atypia (BCDA), with surface maturation, has recently been reported to represent an early form of true dysplasia in BE. The aim of this study was to evaluate DNA content in the progression of neoplasia in BE including cases of BCDA, with surface maturation.

Design: Eighty-two formalin fixed mucosal biopsies from 65 BE patients (M/F ratio: 6.3, mean age: 65 yrs.), representing the full range of neoplasia [negative (n = 2), indefinite (n = 2), BCDA (n = 14), low grade dysplasia (LGD, n = 17), high grade dysplasia (HGD, n = 19), and adenocarcinoma (AD, n = 28)] were stained with H and E and Feulgen and evaluated for DNA content using an automated cellular imaging system (ACIS) to generate high fidelity DNA histograms. Histograms consisted of DNA index (DI), representing integrated optical density relative to stromal cells in the same section and were classified into diploid (peak DI = 0.9 – 1.1), mild aneuploidy (peak DI = 1.1 – 1.3), moderate aneuploidy (peak DI = 1.3 – 1.8), and severe aneuploidy (peak DI >1.8).

Results: The prevalence of aneuploidy increased significantly ($p<0.01$) from negative/indefinite (25%) to BCDA (57%), LGD (59%), HGD (100%) and AD (100%). Most aneuploid BCDA (87%) and LGD (100%) were mild in contrast to HGD (32%) and AD (0%), the majority of which showed either moderate (HGD: 26%, AD: 43%) or severe aneuploidy (HGD:42%, AD: 57%, $p<0.01$ vs BCDA or LGD). In addition, both cellular DNA content heterogeneity, and the distribution of cells with DNA content >5N, increased progressively from BCDA and LGD to HGD and AD ($p<0.01$).

Conclusions: High fidelity image cytometry provides objective discriminatory information in BE-associated neoplastic lesions, and may be a useful adjunct to histology and a potential marker of progression of neoplasia in this condition. Ploidy status of BCDA is similar to that of LGD, which supports the concept that this abnormality represents an early neoplastic lesion in BE.

Genitourinary

598 Primary Carcinomas of the Urethra: A Clinicopathologic Analysis of 100 Patients

AJ Adeniran, P Tamboli, PE Spiess, HB Grossman, CPN Dinney, BA Czerniak. M.D. Anderson Cancer Center, Houston, TX.

Background: Primary urethral carcinomas are rare, accounting for <1% of urinary tract malignancies. Since most of these have been reported as small series or cases reports, their clinical and morphologic spectrum remain incompletely defined, and their behavoir is poorly understood.

Design: Retrospective review of all available material from 100 patients diagnosed with primary urethral carcinoma at one center. Primary urethral carcinomas were defined as tumors arising in the urethra; bladder tumors extending to the urethra were excluded.

Results: Patient data: 29-85 year age range; 61 years median age; 3:2 male:female ratio. Median tumor size of 4 cm; 0.5-6.5cm range. Most common tumor location: proximal urethra in females, bulbar urethra in males. Histological types included 27 urothelial carcinoma (UC), 36 squamous cell carcinoma (SC), 17 adenocarcinoma (AC), 6 mixed carcinomas (MC), 11 carcinoma NOS (CN), 2 sarcomatoid carcinoma and 1 lymphoepithelioma-like carcinoma. AC included: 6 clear cell, 3 mucinous, 3 enteric, 2 signet ring and 3 adenocarcinoma NOS. 7 tumors arose from urethral diverticula, 5 were AC; 6 were in women. Most tumors were grade 3 in UC, moderately differentiated in SC and AC. Pathologic stage at diagnosis: 1 pTa (1 MC); 14 pTis (6 UC, 1 AC, 5 SC, 2 CN); 22 pT1 (6 UC, 3 AC, 8 SC, 4 CN, 1 MC); 18 pT2 (5 UC, 4 AC, 8 SC, 1 MC); 17 pT3 (5 UC, 2 AC, 9 SC, 1 MC); 3 pT4 (1 AC, 1 SC, 1 CN). There were lymph node metastasis in 22 cases (7 UC, 5 AC, 7 SC, 2 CN, 1 MC); right inguinal as the commonest site. Distant metastasis in 15 cases (3 UC, 2 AC, 7 SC, 2 MC, 1 CN): 4 liver, 8 lung, 3 bone, 1 adrenal and 2 pelvic soft tissue. Along with surgery, 42 patients had neoadjuvant therapy (22 chemotherapy, 8 radiation, 12 chemoradiation), and 20 had adjuvant therapy (11 chemotherapy, 3 radiation, 6 chemoradiation). Clinical outcome data: 17 alive with no disease (5 UC, 1 AC, 7 SC, 3 MC, 1 Other); 24 alive with disease (5 UC, 4 AC, 11 SC, 1 MC,3 CN); 28 dead of disease (20.9 months average survival; 11 months median survival; 9 women; 19 men; 7 UC, 4 AC, 9 SC, 2 MC, 4 CN, 2 Other;); 2 dead of other causes (1AC, 1 CN); 25 dead of unknown causes (10 UC, 5 AC, 7 SC, 3 CN). Both sarcomatoid carcinoma patients died of disease (2 and 7 months survival).

Conclusions: Primary urethra carcinomas are tumors of older individuals and are more commonly seen in males. The clinicopathologic features of these tumors are different in men compared to women, with men more likely to die of disease. Sarcomatoid carcinoma has the worst outcome.

599 Anterior Predominant Prostate Tumors: A Contemporary Look at Zone of Origin

HA Al-Ahmadie, SK Tickoo, A Gopalan, S Olgac, VE Reuter, SW Fine. Memorial Sloan Kettering Cancer Center, NY, NY.

Background: Aggressive PSA screening and prostate needle biopsy protocols have successfully detected low-volume posterior tumors, with a concurrent increase in anterior-predominant prostate cancer (AT). Zone of origin, patterns of spread, and extraprostatic extension of these tumors have not been well studied.

Design: We greatly expanded and refined our previous studies to include pathologic features of 197 patients with largest tumors anterior to the urethra in whole-mounted radical prostatectomy specimens.

Results: Of 197 AT, 97 (49.2%) were predominantly located in the peripheral zone (PZ-D), 70 (35.5%) in the transition zone (TZ-D), 16 (8.1%) were of indeterminate zone (IND), and 14 (7.1%) in both PZ and TZ (PZ+TZ). **PZ-D tumors:** 34/97 (35%) = Gleason score (GS) 6, 61 (62.9%) = GS 7, and 2 = GS 9; 49 (50.5%) involved anterior fibromuscular stroma (AFMS); 83 (85.6%) were organ confined (OC) and 11 (11.3%) had extraprostatic extension (EPE), with invasion of anterior/anterolateral fat; 4 EPE cases also had a positive anterior margin (M+); 63 (64.9%) invaded the apical-most section, 11 with apical M+; 88 (90.7%) showed additional tumors of posterior PZ origin (GS 6: 66, GS 7: 21, GS 8: 1; posterior EPE: 3; posterior M+: 2). **TZ-D tumors:** 24/70 (34.3%) = GS 6 and 46 (65.7%) = GS 7; 52 (74.3%) involved AFMS; 60 (85.7%) were OC and 7 (10%) showed EPE, with invasion of anterior fat (7/7) and bladder neck [BN] (2/7); 3 EPE cases and 3 OC tumors showed anterior M+; 46 (65.9%) invaded the apical-most section, 4 with apical M+; 64 cases (91.4%) showed additional PZ tumors (GS 6: 45, GS 7: 19; posterior EPE: 3; posterior M+: 2 [1 OC, 1 EPE]). **IND tumors:** 5/16 (31.2%) = GS 6 and 11 (68.8%) = GS 7; 13 involved the AFMS without clear relationship to either TZ or PZ; 12 were OC, 4 had EPE with involvement of anterior fat (4/4) and BN (1/4); 15 cases had additional PZ tumors (GS 6: 12; GS 7: 3). **PZ+TZ:** 2/14 = GS 6 and 12 = GS 7; 12 were OC, 1 with anterior M+; 2 showed EPE, one with anterior/apical M+; 10 involved AFMS; 8 involved the apical-most section, 1 with M+; 13 had other PZ tumors (GS 6: 10; GS 7:3).

Conclusions: PZ-D tumors are more prevalent than TZ-D tumors in the anterior prostate. AT of both zones show similar GS, EPE, and invasion of the apical portion of the prostate. TZ-D tumors more commonly involve AFMS. Tumor extension into anterior fat may represent definitive EPE in this region, where no clear capsule is present. Prostates with AT frequently contain additional PZ tumors which are occasionally stage-determining.

600 Prostate Specific Membrane Antigen (PSMA) Expression in Primary Prostatic Adenocarcinoma: Comparison of Expression with Gleason Grade and Hormonal Therapy

HA Al-Ahmadie, S Prakash, A Gopalan, S Olgac, SK Tickoo, SW Fine, HI Scher, VE Reuter. Memorial Sloan-Kettering Cancer Center, New York, NY.

Background: Prostate specific membrane antigen (PSMA) is a type II transmembrane glycoprotein that is consistently expressed in benign and neoplastic prostatic tissue with its strongest and most diffuse expression being in prostatic adenocarcinoma (PCa). Antibodies directed against PSMA are being utilized in imaging studies for patients with advanced PCa and its efficacy as a therapeutic agent is presently being studied in clinical trials. Previous studies have used proprietary antibodies with limited availability. Taking advantage of a recently developed and commercially available antibody, we studied PSMA expression by immunohistochemistry (IHC) in a large number of hormone naïve primary PCa (PCaN) and after neoadjuvant therapy (PCaT).

Design: Slides from tissue microarrays blocks prepared from formalin-fixed, paraffin-embedded archival material from prostatectomies performed at Memorial Sloan-Kettering Cancer Center were stained by IHC with monoclonal antibody directed against the external domain of PSMA Clone 3E6 (Dako, Carpinteria, CA). The study included 141 PCaN and 106 PCaT. Hormone-naïve non-neoplastic prostatic tissue (NPN) from 316 cases and 66 cases of non-neoplastic prostatic tissue following neoadjuvant therapy (NT) were also included. The extent and intensity of stain were evaluated semi-quantitatively.

Results: Overall, PSMA expression was detected in 140 of 141 PCaN (99.3%). Expression increased in extent and intensity from NPN to PCaN and was most intense and diffuse in tumors with high Gleason score ($p \leq 0.05$) (Table.1). In PCaT, PSMA expression was detected in 92 of 106 cases (86.8%). In non-neoplastic prostatic acinar cells, PSMA expression was present in 86.7% and 92.4% of NPN and NT, respectively.

Conclusions: Utilizing this commercially available antibody, the majority of PCa express PSMA. This expression is stronger and more widespread in PCa with higher Gleason score. Even after neoadjuvant therapy, PSMA expression is retained in both PCa and non-neoplastic prostatic tissue. PSMA is a useful diagnostic tool for PCa independent of grade and hormonal status.

Table.1: PSMA expression in hormone-naïve prostatic tissue

	NPN	GS 3+3	GS 3+4	GS ≥4+3
Negative	42	1	0	0
Focal	75	10	4	2
Diffuse	199	39	34	51
Weak	111	7	3	2
Strong	163	42	35	51

GS: Gleason score

601 The Role of Immunohistochemical Evaluation of Adult Renal Cortical Tumors on Core Biopsy: An Ex-Vivo Study

HA Al-Ahmadie, D Alden, S Olgac, SW Fine, A Gopalan, SK Tickoo, VE Reuter. Memorial Sloan-Kettering Cancer Center, New York, NY.

Background: Renal cortical tumors (RCT) have distinct morphologic and genetic characteristics and clinical outcomes. Due to the dramatic change in management and therapeutic approach to these tumors in recent years, it has become increasingly important to determine tumor type before intervention. Results of studying routine H&E morphology alone of core biopsy (CB) material of RCT are not encouraging. With the advent of new markers that might show differential expression in subtypes of RCT, we studied the utility of a number of such markers on tissue obtained from RCT by CB.

Design: After nephrectomy, two 18-guage needle biopsy cores were obtained and routinely processed. Immunohistochemical (IHC) studies were performed with antibodies against Carbonic anhydrase (CA)-IX, CD117, AMACR, CK7 and CD10. Results were compared to final pathologic diagnosis.

Results: From a cohort of 130 nephrectomies, 110 cases were included in this study and represented the most common subtypes of RCT: 74 clear cell (conventional) carcinoma (CRCC), 17 papillary (PRCC), 14 chromophobe (ChRCC) and 5 oncocytomas (ONCO). Quantitative IHC findings are listed in Table1. CAIX expression in CRCC was widespread and intense but was only focal in both PRCC and ChRCC. AMACR was most intense and diffuse in PRCC but it also showed variable expression in other subtypes. CD117 was expressed in ChRCC in a distinct membranous pattern while it was only cytoplasmic in other subtypes. CK7 was most widespread and intense in ChRCC and PRCC but was only focal in CRCC and ONCO. CD10 was most commonly expressed in CRCC and PRCC. Its expression in PRCC was more pronounced on the apical aspect of the papillary fronds in 7 cases.

Conclusions: Despite quantitative variability and overlapping, the extent and pattern of expression of these markers is a strong adjunct in the classification of the most common renal neoplasms. Diffuse and membranous CAIX expression is only seen in CRCC. Diffuse granular cytoplasmic expression of AMACR is most commonly seen in PRCC. CK7 and CD117 are helpful in differentiating ChRCC and ONCO.

Table.1: Quantitative analysis of IHC markers in RCT

	CRCC	PRCC	ChRCC	ONCO
CAIX	68/68 (100%)	10/14 (71%)	1/11 (9%)	0/5 (0%)
CD117	5/73 (7%)	1/17 (6%)	8/14 (57%)	2/5 (40%)
AMACR	46/68 (68%)	17/17 (100%)	5/13 (38%)	3/5 (60%)
CK7	19/74 (26%)	15/17 (88%)	10/11 (91%)	1/5 (20%)
CD10	67/74 (91%)	13/17 (76%)	3/13 (23%)	3/4 (75%)

602 Prostatic Central Zone: High Grade Prostatic Intraepithelial Neoplasia and Carcinoma

HQ Al-Moghrabi, EC Belanger, KT Mai. The Ottawa Hospital, and University of Ottawa, Ottawa, ON, Canada.

Background: High grade prostatic intraepithelial neoplasia (HGPIN) and prostatic adenocarcinoma (PAC) are encountered in the central zone (CZ), but have not been well studied. Non-CZPAC that spread into the CZ can mimic CZ PAC.

Design: We reviewed 300 consecutive radical prostatectomies performed for PAC to identify cases showing PAC and HGPIN in CZ.

Results: There were nine PAC localized predominantly in the CZ, presenting as a single tumor nodule (8/9) and associated with 4.5±1.1 foci HGPIN in the CZ and with only 1.7±0.5 foci in the PZ. Of the 291 non-CZ PAC, 24 cases showed satellite tumor nodules in the CZ, and 92 cases demonstrated secondary contiguous spread to the CZ. As compared to the non-CZ PAC, CZ PAC tended to have lower tumor volume, but had higher Gleason scores (8.10±0.6 vs. 6.30±0.7, $p<0.05$), as well as a higher incidence of a ductal carcinoma component (6/9), higher rates of capsular penetration, positive resection margins (4/9) and seminal vesicle spread (2/9). The CZ HGPIN associated with CZ PAC demonstrated cells with prominent nucleoli and formed either slender papillary structures or cribriform/solid patterns. The correlating positive biopsy cores were from the mid portion or base of prostate and contained foci of HGPIN in 4/7 cases. CZ PAC are readily palpable, and visible with ultrasound for biopsy.

Conclusions: CZPAC is characteristically accompanied by more foci of HGPIN in CZ than in non-CZ and is associated with high grade and high stage. Preoperative diagnosis of CZPAC can be suspected due to the clinical presentation and histopathological features in the biopsy and is important to improve the free surgical resection rate.

603 Vanishing Prostate Cancer on Radical Prostatectomy (RP): Incidence and Follow-Up Data from a Cohort of 850 Patients between 1998-2006

AL Alvarez, G Venkataraman, K Rycyna, G Barkan, RC Flanigan, EM Wocjik. Loyola University Medical Center, Maywood, IL.

Background: The "vanishing cancer" phenomenon on the radical prostatectomy specimen (RP) is a well-known entity that was first described more than a decade ago. Ever since the first series of 38 cases in 1995, there have been very few studies investigating the incidence and prognostic relevance of this entity in the current decade.

Design: From 1998- 2006, we searched the surgical pathology database at our institution for RPs with minimal or no residual prostatic adenocarcinoma (Pca) in the RP tissues, after biopsy-proven diagnosis of PCa. Among 850 cases, we identified 15 such cases, 4 of which were excluded secondary to post-diagnosis therapy (3 of them received hormonal therapy and one case received immunotherapy). In the remaining 11 cases, we extracted clinical data including age and prebiopsy PSA levels with biopsy data (highest gleason score, highest percentage of carcinoma, number of biopsy sites, number of positive biopsy sites, use of immunohistochemistry and number of previous biopsies), and RPs data (number of examined slides, highest gleason score, percentage of carcinoma, presence of high grade prostatic intraepithelial neoplasia and atrophy).

Results: Our incidence of the vanishing cancer phenomenon was 11/850 RPs (1.3% incidence). Among the 11 RPs studied, 9 had no residual cancer was identified despite careful sampling. Two cases showed microscopic foci of PCa involving less than 0.5% of the tissue. The mean age of the patients was 59.09 (44-75). The total number of biopsy sites range from 2 to 14 with a mean of 7. The mean PSA was 5.8 units (3.6-9.0). The highest score in the biopsy ranges from 4 to 8, with a mean of 6. The mean number of positive biopsy sites was 1.33 (1-4). The number of biopsy sites range from 2 to 14 with a mean of 5.89. The mean number of examined slides is 39.55 (11-63). In the RP, six of these cases show residual high-grade prostatic intraepithelial neoplasia and 2 had atrophy. All patients are currently alive with no cancer recurrence and the serum PSA concentration remaining at < 0.2 ng/mL.

Conclusions: The incidence of 'vanishing cancer' appears to be on the rise, compared to the incidence rates reported in the last decade (0.2%). The prognosis in this cohort of patients is excellent; however, our series does not show apparent clinical significance to microscopic foci of cancer that remains undetected after extensive pathological sampling.

604 Prostatic Capsular Thickness Varies between Gland Regions and Is Impacted by Biologic Factors

M Amin, NS Goldstein. William Beaumont Hospital, Royal Oak, MI.

Background: The prostatic capsule has long been considered a static entity. This study evaluated differences in prostate capsular thickness between gland regions and the impact of age, gland volume, and the grade-amount of carcinoma on capsular thickness.

Design: 638 completely embedded whole-organ mounted prostatectomy specimens were selected based on age, prostate, and Gleason score-amount of adenocarcinoma. Patient age was grouped into 5-year intervals and prostate weight was by 5g increments. Adenocarcinoma Gleason score and amount was grouped as: (Gleason 6 (G6),<15% total area involved); G6,15% – 50% area; G7 (3+4),<15% area; G7 (3+4),15%-50% area; G7 (4+3),15%-50% area; G8,<50% area. Capsular thickness to the nearest um was measured using a Olympus DP70 digital camera in microns. Capsular thickness was measured at the posterior midline, posteriolateral (x3), and lateral locations bilaterally on each slide (mean, 6.9 slides/ case).

Results: The mean case capsular thickness was 534.76 um (range, 67.6 – 1191.38 um). The mean and median capsular thicknesses of the post-midline, postlateral, and lateral regions were 576.59, 519.84, and 550.89 um. The largest difference in capsule thickness between these regions was in the middle third, where the mean posteriolateral capsule thickness was 53 um thinner than the posterior midline capsule, compared to apical and basilar sections, where it was (mean) 37 um amd 22 um thinner. The prostate capsule was significantly more uniform in thickness around the prostate and between apex, mid-gland, and base regions in younger pts (<50 yrs) compared to senior pts (>65 yrs) ($p<0.001$). The mean postlateral capsular thickness in <50, 50 –<65, and $\geq$65 yrs old groups were 658.04, 468.82, 397.19 um, respectively ($p<0.001$). On univariate analysis, increasing pt age ($p = 0.015$), gland wght ($p<0.001$), and Gleason score-area ($p=0.001$) had significant inverse relationships with prostate capsule thickness, however, on multivariate analysis, only prostate weight (Coef = -7.82; $p<0.001$) and Gleason score-area group (Coef = -3.22; $p = 0.012$) retained significant relationships. Larger pste gland volumes, but not higher Gleason score-amounts accentuated the degree of midgland, postlateral capsular thinness in each of the three pt age groups.

Conclusions: The prostate capsule is not a static entity during life. It is most uniform and thickest in young patients and gradually thins with increasing age, primarily due to increasing prostate volume. The greatest amount of capsular thinning occurs in the mid-gland posteriolateral region.

605 Rete Testis-Associated Nodular Steroid Cell Nests: Putative Pluripotential Testicular Hilus Steroid Cells or Testicular Adnexal Leydig Cells. A Report in 3 Orchiectomies with Emphasis on Differential Diagnosis

MB Amin, GP Paner. Cedars-Sinai Medical Center, Los Angeles, CA.

Background: The steroid-producing cells in the human testes that have been proposed include the Leydig cells, adrenocortical rest (ACR) cells and putative hilar pluripotential cells. The prototypic steroid cell is the Leydig cell which is classically situated in the interstitium of the testis. Ectopic Leydig cells-testicular appendiceal Leydig cells (TALC) are relatively common through often inconspicuous. A putative hilus interstitial cell has been proposed as the cell of origin for testicular tumor of androgenital syndrome (TTAGS), but its normal histology is not documented.

Design: In our experience of detailed evaluation of over 300 orchiectomies, we encountered 3 cases of patients with germ cell tumors of the testis in which incidental unique nodular steroid cell rests, distinctive from TALC or ACRs were noted. The histology, immunohistochemical (IHC) profile and differential diagnostic implications are presented.

Results: Closely associated to the rete testis, and situated within the mediastinum of the testis were distinctive circumscribed nodular rests of eosinophilic cells separated from one another by a striking sinusoidal vasculature. The nodules measured 1, 2 and 2.5 mm in size and individual cells were rounded to polygonal with fine evenly distributed eosinophilic cytoplasm. The nuclei were homogenous and round occasionally with prominent nucleoli. Intracytoplasmic crystalloids of Reinke or pigment was not identified. Testicular atrophy or tumor-associated rete-testis hyperplasia was not identified. The differential diagnosis included carcinoid tumorlets, paraganglionic rests, ACRs, and adenomatoid mesothelial proliferation. IHC showed negativity for cytokeratin, WT1, synaptophysin, chromogranin, ACTH and testosterone receptors and positively for melan-A (2/2) and inhibin (2/3), although the immunoreactivity was distinctively different from the intratesticular Leydig cells in all 3 cases. All patients had no signs or symptoms attributable to androgenital syndrome or hormonal imbalance.

Conclusions: We describe hitherto undescribed nodular steroid cell rests that are distinctive in their morphology and IHC profile from Leydig cells, and do not have the morphology of typical extraadrenal cortical rests. The striking predilection for association with the rete testis epithelium in the testicular mediastinum raises the possibility of these cells representing testicular hilus steroid cells, the putative histogenetic cell implicated for TTAGS.

606 EPHB2 Alterations in Prostate Carcinoma. Normal and Neoplastic Prostate Express a Truncated Isoform

A Andea, L Chen, Y Xiao, W Gerald. UAB, Birmingham, AL; Memorial Sloan-Kettering Cancer Center, New York, NY.

Background: Recent work has uncovered that, in prostate carcinoma (PCa), EphB2 gene is the site of frequent mutations and that the gene locus is often deleted, suggesting a possible tumor suppressor role. The EphB2 gene produces by alternative splicing several transcripts resulting in different length proteins. In this study we evaluated the relative mRNA expression level of EphB2 isoforms in tumor and normal tissue. In addition we investigated the incidence of EphB2 gene alterations at DNA levels and analyzed the incidence of loss of heterozygosity involving the EphB2 locus.

Design: Primers specific for RNA isoforms encoding for full length (1055 aa) and truncated (987 aa) proteins were designed. Real-time qPCR was performed using cDNA from 7 samples of PC and 5 normal prostate. For an additional 50 samples of PCa, PCR followed by DNA fragment analysis on agarose gel was performed. Mutational analysis at the DNA level was performed on 15 cases of PCa and 2 cell lines. A total of 40 cases of PCa were analyzed for LOH using BAC CGH arrays and cDNA was sequenced in cases demonstrating loss of genetic material at EphB2 locus.

Results: The results showed that all samples of normal prostate and PCa expressed only the truncated isoform. Two novel mutations were identified at DNA level (P325S and P391S) both involving the Fibronectin type III domain. We also found that a previously reported deletion (3051delA) occurs most likely as the result of a PCR artifact. Three out of 40 cases (7.5%) exhibited losses at the EphB2 locus, one of which upon sequencing revealed E477K mutation.

Conclusions: The findings that PCa and normal prostate express only the truncated EphB2 isoform is relevant in light of recent information regarding EphB2 mutational status in prostate carcinoma. The most frequent mutation reported, K1019X (15%), only affects the full length isoform. In the truncated isoforms expressed by prostate, the above mutation falls within the 3' untranslated region, thus most likely not affecting the protein function. In addition, in our study, the 3051delA appears to be the result of a PCR artifact and not a genetic deletion. We have identified 3 novel mutations however we did not note any of the previously reported mutations of EphB2. Although LOH for the EphB2 locus was identified in 7.5% of the cases, we did not find a clearly inactivating mutation of the retained allele. Our findings question the putative tumor suppressor gene function ascribed to EphB2 gene in prostate carcinoma.

607 Expression of HLA-Related Antigens TAP-2 and HB2 in Prostatic Disease: An Immunohistochemical Study Using Tissue Microarrays (TMA)

RM Angeles, A Liang, M Acquafondata, R Dhir. University of Pittsburgh Medical Center, Pittsburgh, PA.

Background: Immune surveillance is a mechanism by which the body's immune system detects and destroys arising malignant cells. This process is incumbent upon the proper interactions of HLA proteins and related antigens such as transporter associated with antigen processing (TAP) and low molecular weight protein of the proteosome complex (LMP) with effector lymphocytes. The objective of this study is to determine differences in expression of HLA related antigens: TAP-2 and LMP-7 between neoplastic and non-neoplastic prostatic glands by immunohistochemistry using TMA.

Design: The TMA set used in this study includes PCa (137), donor prostatic tissue (24), PIN (33), benign prostatic hypertrophy (35), metastatic PCa (20), and benign prostate adjacent to PCa (36). Immunohistochemical staining using antibodies anti-TAP-2 (1:200) and antiHB2 (1:100) with specificities to TAP-2 and LMP-7 was performed using the ABC method. The differences in staining patterns were graded according to the intensity (grade 0-3) and localization (membranous/cytoplasmic, nuclear, and stromal) of staining. Statistical analysis using t test, ANOVA and Mann Whitney test was performed.

Results: TAP-2 shows a mean intensity of 1.996 in organ donor prostate epithelium. Cytoplasmic expression of TAP-2 is slightly decreased in PIN, decreased in prostate carcinoma, with larger decrease in metastases (mean staining intensity scores of 1.902, 1.553 and 1.466, respectively). Nuclear and stromal expression is not significantly different. HB2 also shows a decrease in cytoplasmic expression in prostatic cancer, high-grade PIN and metastases with mean intensity scores of 0.809, 0.939 and 0.553 respectively. BPH however shows a much higher expression (1.557). In addition, increased HB2 staining correlated with higher stage of carcinoma.

Conclusions: 1. The HLA related antigens TAP-2 and HB2 show significantly decreased expression in high grade PIN, prostatic carcinoma and metastases. This finding suggests a possible mechanism by which malignant cells escape immune detection. 2. Additional studies are needed to delineate the exact mechanisms via which these changes influence immune response. Modulation of TAP-2 and HB2 expression could be utilized both as a treatment option in aggressive disease as well as played a role in designing new prevention strategies.

608 TFEB Immunopositivity in Renal Angiomyolipomas

T Antic, P Meyer, M Pins, MM Picken. Loyola University Medical Center, Maywood, IL; Feinberg School of Medicine, Chicago, IL.

Background: Nuclear labelling for TFE3 and TFEB has been shown to be a sensitive and specific immunohistochemical (IHC) diagnostic marker for Xp11 and t(6;11) renal cell carcinomas (RCCs) respectively. It has been proposed that tumors with these translocations may belong to a larger family of MITF/TFE renal translocation RCCs. Whether this family also encompasses other tumors is an open question. Recently, TFE3 positivity has been reported in a small subset of perivascular epithelioid cell neoplasms (PEComas). TFEB positive RCCs consistently express melanocytic markers on IHC. Conversely, melanomas and angiomyolipomas (AML), express MITF. AML belongs to the family of related mesenchymal neoplasms that include PEComas, lymphangiolyomatosis (LAM), and clear cell 'sugar' tumor of the lung, all of which share a perivascular cell type and co-express muscle and melanocytic markers.

Design: We sought to investigate positivity for TFEB in tumors that were positive for melanoma markers such as AML (classic and fat-poor), epithelioid and LAM. TFEB IHC stains were performed according to a published protocol with cytogenetically confirmed TFEB translocational carcinomas used as positive controls. Only nuclear stains were evaluated. The specimens were graded as follows: diffuse stain: >80% of nuclei, focal: at least 10% of nuclei. Intensity was graded from 0-3+. Conventional sections with 16 tumors and one tissue array with 24 evaluable tumors were studied. The tumors were diagnosed according to current criteria. Fat-poor AMLs were defined as tumors containing <25% of fat.

Results: There were 24 typical AMLs and 16 nonconventional AMLs: 14 fat poor, one epitheliod and one LAM, (total 40 cases). Diffuse stain for TFEB (2-3+) was seen in 7 tumors, focal 2-3+ stain was seen in 7 additional tumors and 3 tumors showed focal stain graded as 1-2+. Adjacent normal tissues were negative. Overall, 17 (42%) of cases showed positivity for TFEB. However, among the nonconventional AMLs 11/16 (69%) were positive for TFEB, while among typical AMLs 6/24 (25%) were positive.

Conclusions: In the current study, positivity for TFEB was detected in >40% of smooth muscle tumors that also expressed other melanocytic markers, with non-conventional AMLs showing 69% positivity. Whether these tumors share pathogenetic pathways with other MITF/TFE3 translocation carcinomas requires further studies. It has been proposed that fat-poor AMLs may be biologically different from "conventional" AMLs and the higher positivity for TFEB is intriguing.

609 Adult Xp11 Translocation Renal Cell Carcinoma (RCC): Expanded Clinical, Pathologic, and Genetic Spectrum

P Argani, S Olgac, S Tickoo, M Goldfischer, H Moch, DY Chan, JN Eble, S Bonsib, M Jimeno, J Lloreta, A Billis, J Hicks, AM De Marzo, VE Reuter, M Ladanyi. Johns Hopkins Medical Institutions, Baltimore, MD; Memorial Sloan-Kettering Cancer Center, New York, NY; Hackensack University Medical Center, Hackensack, NJ; University Hospital, Zurich, Switzerland; Indiana University, Indianapolis, IN; Hospital del Mar, Autonomous University, Barcelona, Spain; Hospital del Mar, Universitat Pompeu Fabra, Barcelona, Spain; Fac De Ciencias Medicas-UNICAMP, Brazil.

Background: The recently recognized Xp11 translocation renal cell carcinomas (RCC), all of which which bear gene fusions involving the *TFE3* transcription factor gene, comprise at least one-third of pediatric RCC. Only rare adult cases have been reported, without detailed pathologic analysis.

Design: Twenty eight Xp11 translocation RCC in patients over the age of 20 years were identified and analyzed. All cases were confirmed by TFE3 immunohistochemistry, a sensitive and specific marker of neoplasms with *TFE3* gene fusions which is applicable to archival material. Three cases were also confirmed genetically.

Results: Patients ranged from ages 22-78, with a strong female predominance (F: M=22:6). These cancers tended to present at advanced stage; 14 of 28 presented at stage 4, while lymph nodes were involved by metastatic carcinoma in 11 of 13 cases in which they were resected. Previously undescribed and distinctive clinical presentations included dense tumor calcifications such that the neoplasm mimicked renal lithiasis, and obstruction of the renal pelvis promoting extensive obscuring xanthogranulomatous pyelonephritis. Previously unreported morphologic variants included tumor giant cells, fascicles of spindle cells mimicking sarcomatoid carcinoma, and a biphasic appearance that simulated the RCC characterized by a t(6;11)(p21;q12) chromosome translocation. One case harbored a novel variant translocation, t(X;3)(p11;q23). Five of six patients with one or more years of follow-up developed hematogenous metastases, with two dying within one year of diagnosis.

Conclusions: Xp11 translocation RCC occur in adults, and are often aggressive cancers that require morphologic distinction from clear cell and papillary RCC. While they are uncommon on a percentage basis, given the vast predominance of RCC in adults compared to children, adult Xp11 translocation RCC may well outnumber their pediatric counterparts.

610 Heterogeous and Differential Immunohistochemical Staining in Chromphobe Renal Cell Carcinoma and Oncocytoma: A Tissue Microarray Study

A Awamleh, S Evren, JM Sweet. University Health Network, Toronto, ON, Canada.

Background: Chromophobe renal cell carcinomas (ChRCCs) and oncocytomas (Onc) arise from the intercalated cell of the distal collecting duct and may show overlapping histologic and immunohistochemical (IHC) features. However, since their prognosis differs significantly, distinctive diagnostic markers are needed. This study evaluates the IHC markers: caveolin 1 (Cav1), a component of the caveolae membrane invagination, kidney specific cadherin (Ksp), a cell adhesion protein, cytokeratin 7 (CK7), an intermediate filament protein, and CD10, a cell surface metalloprotease, in the differential diagnosis of ChRCCs and Onc using a tissue microarry (TMA).

Design: A TMA was constructed from 13 cases of ChRCCs and 20 cases of Onc. Each case was represented by 3 cores. Immunohistochemistry was performed for Cav1 (BD Labs), Ksp (Zymed), CK7 (Dako), and CD10 (Zymed) and the percentage of positive cells was scored. Thirty percent immunoreactivity in an individual case was considered positive, a 20% difference between cores from the same case was considered differential staining, and the co-existence of positive and completely negative cores from an individual case was considered heterogeneous staining.

Results:

Expression profiles of Oncocytomas

	Cav1	Ksp	CK7	CD10
Positive expression	19/20 (95%)	18/20 (90%)	5/20 (25%)	17/20 (85%)
Differential expression	9/17 (52%)	10/15 (66%)	4/16 (25%)	5/15 (33%)
Heterogeneous expression	3/15 (20%)	4/14 (28%)	4/16 (25%)	1/16 (0.06%)

Cases lacking differential or heterogeneous expression in which a core was lost from the TMA were excluded

Expression profiles of Chromophobe Renal Cel Carcinomas

	Cav1	Ksp	CK7	CD10
Positive expression	10/12 (83%)	11/11 (100%)	9/13 (69%)	4/12 (33%)
Differential expression	5/12 (42%)	2/10 (20%)	5/11 (45%)	2/10 (20%)
Heterogeneous expression	3/12 (25%)	1/10 (10%)	2/10 (20%)	2/9 (22%)

Cases lacking differential or heterogeneous expression in which a core was lost from the TMA were excluded

Conclusions: ChRCC and Onc exhibited intrinsic differential and heterogeneous staining, for the IHC panel, signifying extensive cellular pleomorphism. CD10 showed the least heterogeneous and differential staining, rendering it the most consistent and distinctive marker. This study emphasizes the overlapping IHC features of ChRCC and Onc reflecting their intrinsic internal cellular diversity which must be considered in their differential diagnosis especially in limited biopsy samples.

611 Tumor Microenvironment Comprehensive PCa Nomograms

GE Ayala, A Frolov, R Li, H Liu, D Rowley. Baylor College of Medicine, Houston, TX.

Background: A reactive tumor microenvironment co-evolves with human prostate cancer from HGPIN and co-evolves with carcinoma foci into tumors. Our laboratory has demonstrated that stromal grading (RSG) can be used to predict biochemical recurrence in both radical prostatectomies and biopsies, independently. Pre- and post-operative nomograms have been developed to predict recurrent disease probability. Each is based on cancer cell biomarkers. It is our hypothesis that a more precise prediction model can be devised that utilizes existing sets of carcinoma-derived biomarkers together with novel tumor microenvironment-based biomarkers.

Design: Based on the biochemical recurrence-free survival models described above, we developed a preoperative and postoperative nomogram and an electronic calculator for the risk of biochemical recurrence, based on the usual clinical/pathological parameters such as Preoperative PSA, Lymph node status, Margins, ECE, SVI and Gleason Grade, including RSG and PNI diameter.

Results: We have produced 2 nomogram models demonstrating that RSG grading provides significant and different information that carries similar weight to Gleason grading, both in the pre and postoperative scenarios. We have also developed a calculator in the form of an Access program for both scenarios. Input of the required values into a user-friendly program screen displays a probability of staying biochemical recurrence free at 2 and 5-year marks.

Conclusions: This represents a new paradigm in tumor biomarker research. We believe that such a comprehensive prediction model will enable us to predict mortality in addition to biochemical recurrence. The ultimate goal is to create multivariate models that are useful for both radical prostatectomy and biopsy specimens, to predict clinical outcomes including mortality.

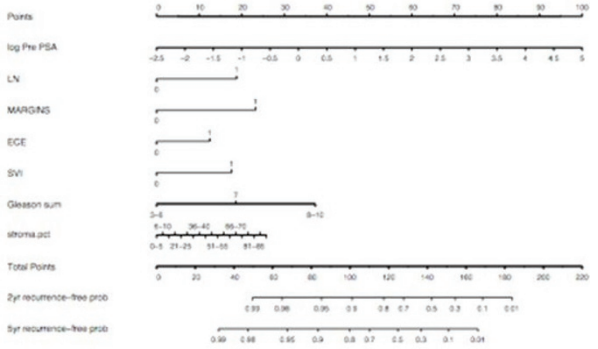

612 Pre-Biopsy Serum PSA and Highest Biopsy Gleason Score (hbGS) Remain Significant Predictors of Extra-Capsular Extension (ECE): A Study of 533 Radical Prostatectomies

AA Bargaje, K Rycyna, G Venkataraman, RC Flanigan, EM Wojcik. Loyola University Medical Center, Maywood, IL; Loyola University Medical Center.

Background: The presence of ECE after prostatectomy for cancer has been reported to be significant source of morbidity measured by recurrence-free survival. Hence, there is a crucial need to develop models using pre-operative clinical, biochemical and biopsy information to accurately identify patients with higher risk of ECE.

Design: From the Loyola University Health System database of prostate cancer, we identified a cohort of 533 patients with a diagnosis of prostatic adenocarcinoma. We selected patients who had diagnostic needle biopsy with concurrent radical prostatectomy (RP) performed. Cases with pre-RP hormonal or radiation therapy were excluded from the analysis. A total of 8 predictors including age, pre-biopsy PSA, highest biopsy Gleason score (hbGS), highest primary Gleason grade (GG), highest secondary GG, presence of perineural invasion (PNI), presence of high-grade prostatic intra-epithelial neoplasia (HGPIN) and, the highest percentage of involvement by carcinoma in the diagnostic biopsy (hPCAbx) were used to model the presence of ECE. PSA was natural log-transformed prior to analysis because of left skew in the distribution. Descriptive statistics and cross-tabulations of the data were examined. A binary logistic regression (LR) model was implemented in SAS v.9 (SAS Institute, Cary, NC) setting an F-value cut-off of 0.05 for entry into the model. Model classification was assessed by the c-statistic, as well as by the overall percentage of correct classifications.

Results: In this data, there were 89 (16.7%) cases with ECE and 444 (83.3%) cases without ECE. There was no significant difference in age between the two groups (p=0.19, Student's t-test). Binary LR selected a parsimonious two-parameter model with only hbGS (Adjusted Odds Ratio [OR_{adj}]:3.1, 95% CI: 1.88-5.12), and serum PSA (OR_{adj}: 2.2, 95% CI: 1.3-3.7) as the most significant parameters that predicted presence of ECE. The resulting model had c-statistic of 0.76 indicating significant predictive ability.

Conclusions: Our study demonstrates that models using hbGS in the diagnostic prostate biopsy and pre-operative serum PSA are able to predict presence of ECE with reasonable accuracy. Our findings concur with the existing data in literature. This information may be useful in identifying potential patients who can be targeted for more aggressive adjuvant therapy in the appropriate clinical setting.

613 Tumors Metastatic to the Kidney: A Clinicopathological Study of 30 Cases

G Barkan, C Magi-Galluzzi, L Sercia, E Wojcik, M Pickens, M Zhou. Cleveland Clinic, Cleveland, OH; Loyola University, Chicago, IL.

Background: The vast majority of the tumors arising in the kidney are primary. Metastatic tumors are exceedingly rare and constitute case reports in the literature. However, these metastatic tumors can histologically mimic and be mistaken for primary renal tumors. This study reports the clinicopathological features of 30 tumors metastatic to the kidney and discusses diagnostic clues as to when to consider a renal tumor as metastatic.

Design: This study included tumors metastatic to kidneys diagnosed on nephrectomy, needle biopsy, aspiration cytology and autopsy. Clinical, radiological and pathological data were reviewed. When available, the slides were also reviewed. Hematopoietic tumors involving the kidney, or the metastatic tumors of unknown primary sites (except melanomas), were excluded.

Results: Between 1981 and 2006, 30/5615 (0.53%) renal masses were metastatic to the kidney. The clinical and radiological features are in Table 1. The primary tumors included lung squamous cell carcinoma (7 cases), lung adenocarcinoma (4), gastrointestinal adenocarcinoma (4), breast adenocarcinoma (2), melanoma (3), seminoma (2), thyroid papillary carcinoma (1), ovarian papillary serous carcinoma (1), uterine leiomyosarcoma (1), brain hemangiopericytoma (1), cervical squamous cell carcinoma (1), small cell carcinoma (1) and adenosqumous carcinoma (1). Of 12 nephrectomies reviewed, multifocal disease, microscopic infiltrative growth pattern, and vascular invasion were present in 6 (50%), 6(50%) and 5 (41.7%) cases. When performed, immunohistochemical stains confirmed the diagnosis.

Gender (Male/Female)	14/16
Age [year, mean (range)]	58.9 (34-86)
Time between primary and metastatic presentation [months, mean (range)]	52.3 (0-360)
Mode of diagnosis (30 cases)	Nephrectomy 17 (56.7%) Biopsy 9 (33.3%)
	FNA 3 (11.1%)
	Autopsy 1 (3.3%)
Radiological Diagnosis (13 cases)	RCC/other primary renal tumor 6 (46.2%)
	RCC vs. metastasis 4 (30.8%)
	Met/probable metastasis 3 (23.1%)

Conclusions: Tumors metastatic to the kidney are rare, and most commonly they are metastatic from squamous cell carcinoma and adenocarcinoma of the lung, gastrointestinal adenocarcinoma, and melanoma, although metastases from other sites are also observed. A possibility of a metastatic tumor should be considered in patients with a prior history of malignancy involving other organs, or when the renal tumor has unusual pathological features, such as multifocal disease and microscopic infiltrative growth patterns.

614 Examination of Osteopontin, Clusterin, Drg-1, BMP7, Survivin, p-Smad, and p-JNK Protein Expression in Adenocarcinoma of the Prostate (CaP)

AM Bell, C Zhong, M Sturm, P Roy-Burman, MB Cohen. U. of Iowa, Iowa City; U. of Southern California, Los Angeles.

Background: Previous work by us and others with mouse models of human prostate cancer have shown that certain relevant proteins are differentially expressed and may be important in the biology of CaP. To confirm in vivo experimental data we analyzed protein expression in human prostate tissue and determined if any of these proteins could serve as prognostic biomarkers. We examined expression of osteopontin, clusterin, Drg-1, BMP7, survivin, p-Smad, and p-JNK proteins in malignant versus benign prostatic epithelium, in adjacent stroma, by Gleason grading, and between primary CaP and disease metastatic to lymph node or bone.

Design: Tissue microarrays were constructed using a manual arrayer from 59 cases of primary CaP, 42 cases of CaP metastatic to lymph node, and 14 cases of CaP metastatic to bone. Immunohistochemistry, with antigen retrieval, was performed using standard techniques. Protein expression was assessed and quantified by intensity (0-3) and proportion (0-3) scores, and a total score (0-6) was calculated.

Results:

Protein	CaP	Benign	Gleason 3	Gleason 4	Gleason 5
Osteopontin	5.34 (53)	5.69 (13)	5.18 (11)	5.42 (26)	5.31 (16)
Clusterin	3.83 (53)	3.54 (13)	3.55 (11)	3.96 (26)	3.81 (16)
BMP7	4.83 (54)	4.37 (19)	4.91 (11)	4.88 (26)	4.71 (17)
Drg-1	5.28 (53)	4.87 (15)	5.45 (11)	5.38 (26)	5.00 (16)
p-Smad	5.16 (43)	4.42 (19)	5.00 (8)	5.10 (20)	5.33 (15)
Survivin	4.33 (42)	2.67 (18)	4.86 (7)	4.65 (20)	3.80 (15)
p-JNK	5.44 (43)	5.05 (20)	5.63 (8)	5.50 (20)	5.27 (15)

[Combined staining score (number of cases)]

Conclusions: Expression of all seven proteins was readily detected in both malignant and benign human prostatic epithelium. Furthermore, survivin expression was significantly higher in malignant epithelium compared to benign. For the remaining six proteins no consistent and significant relationship in protein expression between benign and malignant epithelium was identified, nor was there any remarkable association between protein expression and grade. Of note, comparative scoring of stromal staining revealed preferential epithelial expression of osteopontin, Drg-1, p-Smad, survivin, and p-JNK. There was no significant difference for the remaining proteins. In comparison of primary versus metastatic disease, the only notable trend was of decreased Drg-1 expression in bone metastases. Overall, the data collected to date confirmed that survivin is a potential prognostic biomarker of CaP.

615 The Pathology of Malignant Germ Cell Tumors in the Elderly

DM Berney, M Verma, SC Kudahetti, RTD Oliver. Barts and The London, Queen Mary University of Medicine and Dentistry, London, United Kingdom.

Background: Malignant germ cell tumors (GCT) occur typically in males below 40 and are rare in later life. While spermatocytic seminomas (SS) are a well known entity in elderly males and have a typically indolent natural history, true malignant germ cell tumors may occur in the elderly and require treatment. The pathology and natural history of malignant germ cell tumors in the over 60s has never been systematically investigated. We therefore collected a retrospective series of germ cell tumors, excluding SS, that were diagnosed at the age of 60 or greater to examine their histopathology and compare them with those diagnosed in a younger population.

Design: We searched the files of The British Testicular Tumor Panel (1950-1980) and of St Bartholomew's and The Royal London Hospital for GCTs where the patient was 60 or above at diagnosis. All cases of SS were excluded from the analysis. Slides were reviewed and, where possible, the macroscopic description examined to determine the tumor size and side. Important data retrieved from the slides included tumor type, vascular invasion, stage and presence of intratubular neoplasia (IGCNU).

Results: Thirty tumors were retrieved from the BTTP archive with 10 tumors from the local pathology database. The patients were aged between 60 and 82 . There were 17 right testis tumors, 10 right testis tumors and 13 where side was not stated. Size of tumor was available on 21 tumors and ranged from 2 to 11 cm, with a mean of 6.3cm. There were 31 seminomas, 5 non-seminomas and 4 tumors with mixed seminoma and non-seminoma elements. The non seminomas included a pure embryonal carcioma, with other tumors being a mixture of non-seminomatous elements with yolk sac, teratoma and embyonal elements. Vascular invasion or evidence of metastasis was seen in 15/40 tumors. IGCNU was only seen in 6 cases.

Conclusions: This is, to our knowledge, the largest series of malignant GCTs in the elderly studied. The tumours are significantly larger than those reported in a younger population and appear to be of higher stage. There are a much higher percentage of seminomas, though non-seminomas and mixed tumors were seen. They are associated with IGCNU, though the few cases of IGCNU seen in this series may reflect widespread atrophy as well as limited sampling in older cases. We conclude that germ cell tumors are diagnosed at a later stage than those arising earlier in life and are largely seminomas. However, the variety of non-seminomas seen here, suggests that any GCTs may arise at any age.

616 Topoisomerase I and IIα Expression in Penile Squamous Cell Carcinomas

DM Berney, AMA Adlan, O Biedrzycki, SC Kudahetti, P Hadway, N Watkin, C Corbishley, RTD Oliver. Barts and the London, Queen Mary's University, London, United Kingdom; St George's Hospital, London, United Kingdom.

Background: Squamous cell carcinoma of the penis (SCCP) is a rare disease which is associated with HPV infection. Advanced SCCP has proven mostly unresponsive to chemotherapy regimes, though trials are necessarily small scale with little patient selection. There have been no studies assessing potential chemotherapeutic targets in SCCP. We therefore examined the tissue expression of DNA Topoisomerase I (Topo I) and IIα (Topo IIα) to investigate whether there would be any tissue expression of these proteins and pursue the possibility of tumor selection in SCCP for future chemotherapy regimens. High expression of Topo I may indicate sensitivity to the Camptothecins, whereas high Topo IIα may indicate sensitivity to etoposide.

Design: 73 cases of SCCP, all operated upon at a single institution, were reviewed histologically and then tissue microarrayed into 5 blocks using 1mm diameter cores. These were then stained with immunohistochemistry for topo I, topo IIα and ki-67. Tumor stage, grade and type were all available. Staining was assessed as a percentage of total SCCP cells for each antibody.

Results: Topo IIα showed a strong positive correlation with the proliferation index as measured by Ki-67 ($p<0.0001$) but no correlation with topo I. There were also strong correlations between tumor grade and Ki-67 ($p<0.0001$) and also topo IIα expression ($p<0.0001$). Tumor type was also strongly correlated with topo II and Ki-67 expression, with the highest expression being seen in basaloid carcinomas and the lowest seen in verrucous carcinomas. However, topo I expression was not correlated with any other tumor parameter and appeared to be unrelated to the other markers used. None of the markers were associated with tumor stage.

Conclusions: In keeping with findings in other tumors, topoIIα and Ki-67 were strongly associated with tumour grade and type. However, topo I staining was extremely variable, being present in all grades, stages and types of tumor and showing variable expression within each group. This indicates that its expression is grade and type independent and that chemotherapy using the camptothecins is unlikely to be effective in in a minority of high grade SCCPs. The strong positivity of topo IIα in high grade and basaloid SCCPs suggests that treatment with etoposide or other topoIIα poisons may be efficacious in this subgroup of SCCPs.

617 Secondary Prostatic Adenocarcinoma: A Cytopathological and Immunohistochemical Study of 59 Cases

C Bicamumpaka, C Marginean, KT Mai. University of Ottawa and the Ottawa Hospital, Ottawa, Canada.

Background: Cytopathology of metastatic PCA has not been well documented in large series with a comprehensive study.

Design: Fifty-nine cases of metastatic PCA with cytological specimens consisting of 47 FNAB, 6 pleural fluid and 3 catheterized urine were reviewed with correlating surgical specimens and clinical charts. The cell block sections were submitted for immunostaining for PSA, PAP, cytokeratin AE1+3, CK7, CK20, vimentin, CEA, TTF1 and androgen receptor (AR).

Results: Mean patient age was 77 ± 7 years, serum PSA: 4.1±2.3 and primary PCA Gleason score: 8.1±1.5. Cytologically, the specimens consisted of overlapping cell clusters or cell sheets with uniform hyperchromatic nuclei with or without nucleoli. 12 cases were not reactive for PSA and PAP, 52 cases displayed negative immunoreactivity for both CK7 and CK20, two small cell carcinomas were reactive for TTF1, however, all cases were reactive for AR . Carcinoid-like or small cell carcinomas were seen in 4 cases and were misdiagnosed as of non-prostatic origin. This was due to their negative immunoreactivity for PSA and PAP associated or not with positive reactivity for CEA and to their different histopathological features when compared to the primary PCA.

Conclusions: Awareness of the negative immunoreactivity of PCA for PSA and PAP, and of the negative immunoreactivity for CK7 and CK20, as well as of the NE differentiation and the possible difference in the histopathological patterns between the primary and secondary tumor is helpful in the diagnoses of metastases. AR marker is the most reliable marker in the differential diagnosis.

618 The Impact of the 2005 International Society of Urological Pathology (ISUP) Consensus Conference on Standard Gleason Grading of Prostatic Carcinoma. Part 2

A Billis, LLL Freitas, MS Guimaraes, MM Quintal, LA Magna, U Ferreira. School of Medicine, University of Campinas, Unicamp, Brazil.

Background: In a previous study, we showed that the highest impact of the ISUP consensus recommendations applied on a series of 172 needle prostatic biopsies graded according to the standard Gleason system, was seen on the secondary pattern. It reflected in a change toward a higher Gleason grading group in 46/172 (26.74%) of the cases. In the present study we evaluated how these patients differed according to several clinicopathologic variables.

Design: The study was based on 172 biopsies of patients that were subsequently submitted to radical prostatectomy (RP). Four prognostic grading groups were considered (Gleason scores 2-4, 5-6, 7, and 8-10) and the clinicopathologic variables studied were: preoperative PSA, tumor extent, positive surgical margins, pathologic stage and biochemical (PSA) progression following RP. Tumor extent was evaluated with a point-count semiquantitative method. The data were analyzed using the Mann-Whitney test, Fishers's exact test and the Kaplan-Meier analysis for comparing the time to PSA progression between the groups.

Results: From the total of biopsies, 4/172 (2.33%) patients changed toward a lower Gleason grading group, 122/172 (70.93%) had no change (group A) and 46/172 (26.74%) toward a higher group (group B). The comparison between group A vs group B showed: mean preoperative PSA 9.59 ng/mL and 12.62 ng/mL, respectively ($p=0.019$); mean tumor extent 33.54 positive points and 49.74 positive points, respectively ($p=0.037$); positive surgical margins 33.61% and 65.22%, respectively ($p<0.001$); and, pathologic stage (pT2/pT3a or pT3b) 79.34%/20.66% and 60.87%/39.13%, respectively ($p=0.018$). The mean and median follow-up for the patients was 30.24 and 26 months, respectively (range 2 to 94 months). During the study period, progression occurred in 35.65% and 47.62% of patients in groups A and B, respectively. There was a tendency for patients in Group B to experience shorter progression-free survival (long-rank, $p=0.068$).

Conclusions: The 46/172 (26.74%) patients that changed toward a higher Gleason grading group had significantly a higher preoperative PSA, more extensive tumors, higher positive surgical margins and pathologic stage, and a tendency for shorter time to PSA progression following RP. The recommendations of the ISUP are a valuable refinement for the standard Gleason grading system and should be used by pathologists in their routine practice.

619 Clinicopathologic Features of Small-Volume Prostate Cancer in Patients Submitted to Radical Prostatectomy in Brazil

A Billis, IC Watanabe, MV Costa, GH Telles, LA Magna, U Ferreira. School of Medicine, University of Campinas, Unicamp, Brazil.

Background: There is little information about small-volume (SVOL) prostate carcinoma in radical prostatectomies (RP). The aim of this study was to characterize for the purpose of comparison with other countries the clinicopathologic findings of SVOL tumors in brazilian patients submitted to RP.

Design: The surgical specimens were whole-mount processed. The bladder neck and the apical margins were examined through perpendicular sections. Positive margin was defined as cancer cells touching the inked surface. Extraprostatic extension was diagnosed whenever cancer was seen in adipose tissue and, in case of desmoplastic response, whenever a protuberance corresponding to extension of tumor into the periprostatic tissue was seen. Seminal vesicle invasion was defined as an invasion of the muscular wall. Tumor extent was evaluated with a point-count semiquantitative method previously described. Prostate carcinoma was considered of SVOL whenever corresponded to 10 or less positive points and insignificant SVOL whenever organ-confined, with negative surgical margins and no Gleason pattern 4 or 5. The data were analyzed using the Mann-Whitney test and the Fisher's exact test. Time to biochemical (PSA) progression was compared using the Kaplan-Meier product-limit analysis.

Results: From a total of 268 patients, 47 (17.54%) had SVOL carcinoma. Comparing these 47 cases to 191 non SVOL tumors the findings were as follows: mean age 63.57 yr and 63.43 yr (p=0.868); Whites and African-Brazilians 82.98%/17.02% and 81.91%/18.09% (p>0.999); mean preoperative PSA 8.99ng/mL and 10.11 ng/mL (p=0.604); clinical stage T2 38.64% and 62.30% (p=0.006); non organ-confined tumor 4.26% and 30.89% (p<0.001); positive surgical margins 12.77% and 48.69% (p<0.001); and, Gleason score ≥7 19.59% and 73.82% (p<0.001), respectively. Time of progression-free survival between the groups was not statistically different (log-rank, p=0.288), however, was significantly longer for insignificant SVOL tumors (log-rank, p=0.004).
Conclusions: SVOL prostate cancers corresponded to 17.54% patients submitted to RP. Of these cases, 38.64% were clinical stage T2, 4.26% non organ-confined, 12.77% had positive surgical margins, 19.15% Gleason pattern 4 and, therefore, might be clinically significant. Time of progression-free survival was not statistically different to non SVOL tumors, however, insignificant SVOL tumors experienced significantly longer progression-free survival.

620 Clinicopathologic Trends of Patients with Clinical Stage T1c Submitted to Radical Prostatectomy in Brazil

A Billis, MN Bronner, MF Galvao, L Schultz, LA Magna, U Ferreira. School of Medicine, University of Campinas, Unicamp, Brazil.
Background: The aim of the study is to describe for the purpose of comparison with other countries the clinicopathologic trends of brazilian patients with clinical stage T1c submitted to radical prostatectomy comparing the findings in the periods Jan-1997/2000 vs 2001/May-2006.
Design: The study was based on 264 whole-mount consecutive surgical specimens. The bladder neck and the apical margins were amputated and processed through perpendicular sections. Positive margin was defined as cancer cells touching the inked surface of the prostate. Extraprostatic extension was diagnosed whenever cancer was seen in adipose tissue and, in case of desmoplastic response, whenever a protuberance corresponding to extension of tumor into the periprostatic tissue was seen. Seminal vesicle invasion was defined as an invasion of the muscular wall. Tumor extent was evaluated with a point-count semiquantitative method previously described. The data were analyzed using the Mann-Whitney test and the Fisher's exact test. Time to biochemical (PSA) progression was compared using the Kaplan-Meier product-limit analysis.
Results: Comparing the periods 1997-2000 vs 2001-2006 the findings were as follows: frequency of clinical stage T1c 19.70% and 55.30% (p<0.001); mean age 63.85 yr and 61.85 yr (p=0.176); Whites and African-Brazilians 76.92%/23.08% and 81.69%/18.31% (p=0.577); mean preoperative PSA 9.13ng/mL and 8.88ng/mL (p=0.785); organ-confined tumor 80.77% and 73.97% (p=0.599); positive surgical margins 34.62% and 41.10% (p=0.644); small-volume tumor 36.36% and 23.61% (p=0.274); mean Gleason score on needle biopsy 6.35 and 6.36 (p=0.663); and, mean Gleason score on surgical specimen 6.27 and 6.66 (p=0.094), respectively. Time of progression-free survival was not statistically different between the periods (log-rank, p=0.658).
Conclusions: The striking increase in frequency of clinical stage T1c probably reflects campaigns for early detection of prostate cancer and a higher awareness of brazilian men to engagement. However, in spite of this marked increase there was no statistically significant difference for all clinicopathologic variables studied comparing the periods 1997-2000 vs 2001-2006.

621 CD10 Expression in Prostatic Intraepithelial Neoplasia and Prostatic Carcinoma, and Association with Androgen Receptor

S Bircan, N Kapucuoglu, O Candir. Suleyman Demirel University School of Medicine, Isparta, Turkey.
Background: CD10 has already been implicated in prostate cancer development and progression, and its expression regulated by androgen. The aim of study was to analyze CD10 expression low-grade and high-grade prostatic intraepithelial neoplasia (PIN), and primary prostatic carcinomas (PCs), and investigate the association with androgen receptor (AR) using immunohistochemistry.
Design: The study included 40 primary PCs, 41 cases of PIN including 22 low-grade (LGPIN) and 19 high-grade (HGPIN), and 23 benign prostate (BP) tissues. The cases of PC were new diagnosed and treated surgically hormone naïve primary prostatic carcinoma patients. All slides were re-evaluated histopathologically. Gleason grading and scoring were performed in PC cases. The monoclonal CD10 and AR antibodies were used for immunhistochemistry. The immunoreactivity was evaluated semiquantitatively as negative; 1+, minimal (<10%); 2+, moderate (10-50%); and 3+, diffuse/marked positive (>50%).
Results: The CD10 positivity was confined the luminal apical surface of secretory epithelial cells. All BP and LGPIN cases showed high level (3+) of CD10 positivity in 22 (95.7%) and 21 (95.5%) of cases, respectively. In HGPIN group, 6 (31.6%) and 13 (68.4%) cases showed 1+ and 2+ CD10 staining. In the PCs, it was positive in 17 (42.5%) cases, and remaining 23 (57.5%) cases were negative. This positivity was distributed as 1+ and 2+ in 8 (20%) and 9 (22.5%) of cases, respectively. There were statistically significant differences among the groups in relation to CD10 immunoreactivity (*p=0.000*), except between BP and LGPIN (*p=0.111*). Though not significant, the more cases with higher primary Gleason grade (grades 4 and 5) were positive for CD10 than the lower grades (grades 2 and 3) (*p=0.080*). In addition, the level of CD10 positivity tended to be positively correlated with primary Gleason grade (*p=0.089, r=0.272*). In considering AR expression, all cases showed high level (3+) of nuclear AR immunostaining. There was not a significant difference among the groups in relation to AR expression. In addition, any significant relationship was found between AR and CD10 expression in the groups.
Conclusions: Our results underlined the importance of CD10 expression in development and progression of prostate carcinoma, and suggest that loss of CD10 expression is an early event in human prostate carcinogenesis. CD10 positivity in the primary PCs might suggest the presence of more aggressive clones or the possibility of higher grade tumor.

622 Over-Diagnosis of High-Grade Prostatic Intraepithelial Neoplasia (PIN): Prospective Study of 251 Cases

DG Bostwick, J Ma. Bostwick Laboratories, Glen Allen, VA.
Background: Great differences are reported in the incidence of high-grade prostatic intraepithelial neoplasia (PIN) in contemporary publications probably owing to variance in diagnosis and interpretation of PIN. However, the magnitude and causes of over-diagnosis of PIN have not been previously studied.
Design: Two Urologic pathologists prospectively reviewed 251 consecutive cases received in consultation that were diagnosed and finalized by outside pathologistsas PIN.
Results: The diagnosis of PIN was confirmed in 191 cases (concordance incidence of 76.1% (true positive) and refuted in 60 (discordance incidence of 23.9% (false positive)). The most common histopathologic findings misinterpreted as PIN included basal cell hyperplasia, benign epithelium, low-grade PIN, reactive changes, cribriform hyperplasia, atrophy, and post-atrophic hyperplasia.
Conclusions: There is a high rate of over-diagnosis of PIN, usually owing to misinterpretation of benign mimics. This significant error rate may account for some of the reported differences in incidence of PIN as well as the variable predictive accuracy for cancer.

623 Loss of Chromosome 9p in Clear Cell Renal Cell Carcinoma with Different SSIGN Score

M Brunelli, A Eccher, S Gobbo, MM Mina, P Cossu-Rocca, V Ficarra, F Menestrina, G Martignoni. Università di Verona, Verona, Italy; Università di Sassari, Sassari, Italy.
Background: Loss of chromosome 9p is considered to be a genetic abnormality related to worse prognosis in patients affected by clear cell renal cell carcinoma (RCC). Recently the Mayo Clinic proposed an alghoritm to predict cancer-specific survival according to Stage, Size, Grade and Necrosis (SSIGN). We investigated the correlation between loss of 9p and the SSIGN score and the impact of this genetic abnormality on survival.
Design: We selected 17 patients affected by clear cell RCC with different Mayo Clinic SSIGN score: low (score 0-2); intermediate (score 5-6) and high risk (score ≥ 10) groups. We built two tissue microarrays including at least three cores of neoplastic tissue and two cores for normal renal parenchyma for each case. We performed an fluorescence in situ hybridization analysis using a locus specific probe mapping on chromosome 9p (Abbott) on formalin-fixed-paraffin embedded tissue microarrays. Signal count was scored on 150 neoplastic nuclei per case. Results were correlated with SSIGN score group. Moreover, we evaluated the impact of loss 9p on cancer-specific survival using Kaplan-Meier method and long rank test.
Results: Three cases were not evaluable for technical reasons. Loss of 9p was detected in 3/14 clear cell RCC (21%), in most of neoplastic cells (>70%). Six patients showed a 0-2, six a 5-6 and five a >10 SSIGN score. Nine patients were pT1-2 and eight pT3-4. Three patients showed lymph-nodal (N+) metastases. All patient did not show metastases at diagnosis. Eight were alive-well, five dead of disease. Loss of chromosome 9p was detected in 2/4 (50%) of patients with >10, in 1/5 (20%) with 5-6, and absent (0%) in patients with 0-2 SSIGN score. Loss of 9p resulted significantly related to local extension of the primary tumur (50% pT3-4 Vs 0% pT1-2) and lymph-nodal metastases (67% N+ *Vs* 9% N-, *p=0.03*). Patients with loss of 9p showed a median cancer-specific survival of 9 months whereas those without loss displayed a median cancer-specific survival of 101 months (long rank test, *p=0.01*).
Conclusions: 1) loss of 9p is a genetic abnormality present in 50% of patients with high Mayo Clinic SSIGN score; 2) a correlation with higher SSIGN score does exist; 3) loss of 9p could predict aggressive features of clear cell RCCs such as local invasion and lymph-nodal metastases; 4) and could be added as a cytogenetic marker in the SSIGN score, to predict worse outcome.

624 Chromophobe Renal Cell Carcinoma: Feasibility of Using Tissue Microarrays for the Assessment of Diagnostic Cytogenetic Abnormalities by Fluorescence In Situ Hybridization

M Brunelli, S Gobbo, A Eccher, MM Mina, P Cossu-Rocca, F Menestrina, G Martignoni. Università di Verona, Verona, Italy; Università di Sassari, Sassari, Italy.
Background: Chromophobe renal cell carcinomas (RCCs) have frequent losses of multiple chromosomes from among chromosomes 1, 2, 6, 10, and 17, and this pattern is of diagnostic value. It is uncertain if concordant results can be obtained on tissue microarray (TMA) sections, a high throughput technique that is particularly advantageous in research and validation protocols. Our aim was to compare the results of cytogenetic abnormalities in chromophobe RCC when comparing whole tissue sections with those of TMA.
Design: Standard sections and TMA constructed from archival formalin-fixed and paraffin-embedded chromophobe RCC of 6 patients were subjected to interphase fluorescence in situ hybridization (FISH) using centromeric probes (CEP) for chromosome 1, 2, 6, 10 and 17. The TMA was created using 0.6-mm tissue cores with three sampled cores per tumor from the same tissue block used for whole section FISH. Signals were counted in 100-200 neoplastic nuclei from each tumor.
Results: Chromophobe RCC frequently showed multiple chromosomal losses in 3/6 (50%) cases (>82% neoplastic nuclei), two of them for all chromosomes and one for at least three chromosomes (2, 10 and 17) on whole sections. FISH results in the TMA shared similar score and whole sections were concordant in most of analyzed cases (92%). Two cases (33%) showed two fluorescence signals for chromosome 1 and 6 in

most of neoplastic cells (77%) and a mosaic pattern, a mix of nuclei with signal loss (32%) and gains (27%) for remaining chromosomes, on whole sections. These tumors showed FISH scores consistent among two out of the three cores in TMA, for all chromosomes tested, when comparing them with results obtained by whole sections. One case (17%) prevalently showed two fluorescence signals for all chromosome tested with concordance between TMA and wholes ections. The overall concordance for cytogenetic abnormalities between whole sections and TMA cores was 83%.
Conclusions: 1) TMA could be a reliable approach to study the assessment of diagnostic cytogenetic abnormalities by FISH in a high throughput manner; 2) we suggest to test the cytogenetic abnormalities for all chromosome 1, 2, 6, 10 and 17 on whole tissue sections when a mosaic pattern is found on TMA; 3) FISH performed on renal tumor biopsy could be performed a useful tool for the detection of genetic abnormalities diagnostic of chromophobe RCC.

625 New Immunostains for Extragonadal and Metastatic Germ Cell Tumors

SL Butler, S Kim, GT MacLennan, JH Shanks, D Hossain, A Schall, JK McKenney, I Meiers, C Schlesinger, KA Iczkowski. U. FL, Gainesville, FL; U. Hosps Cleveland, Cleveland, OH; Christie Hosp, Manchester, United Kingdom; U. Mantitoba, Winnipeg, MB, Canada; U. Ark. for Health Sci, Little Rock, AR; Bostwick Labs, Richmond, VA; PCA, Columbia, TN.
Background: Transcription factor OCT3/4, expressed by pluripotent embryonic stem cells, is sensitive and specific for 1º testicular seminoma (S) and embryonal carcinoma (EC). c-kit (CD117), a tyrosine kinase receptor, marks 1º S's. The markers' reactivity in extragonadal germ cell tumors (GCT) merited comparison with established markers.
Design: 52 GCT (20 S, 15 EC, 10 mature teratoma and 7 yolk sac tumor) were obtained from CNS (11), mediastinum (16), retroperitoneal/abdomen (18), and other sites (7). Immunostaining for c-kit, PLAP and OCT3/4 was done on S's; CD30 and EMA were added for non-seminomas. Intensity was graded 0-3+ and % + cells was estimated. Differences in intensity were assessed by Fisher's Exact Test and difference in % by General Linear Mixed Model.
Results: OCT3/4 discriminated S+EC from all other GCT (sensitivity 0.88; specificity 0.94). For EC, OCT3/4 had specificity=0.94, >than CD30 (0.786) owing to CD30 reactivity in 3/10 teratomas. c-kit discriminated S from all other GCT, sensitivity=0.95; but c-kit had low specificity=0.48, due to reactivity with 11/15 EC. However, % of reactive cells in EC was less than in S:

	c-kit (cyto)		PLAP (cyto)		OCT3/4 (nuclear)	
Tumor:	*No. +*	*Int, %cells*	*No. +*	*Int, %cells*	*No. +*	*Int, %cells*
EC	11/15	1.33, 28%†(1-90%)	6/15	0.9, 14%	11/15	1.9*, 53%**
Seminoma	19/20	2.43, 77% (20-100%)	16/20	2.25, 52%‡	20/20	2.6⊕, 73%⊗

* intensity OCT3/4 superior to PLAP, p=.0075 ** % OCT3/4 > PLAP, p=.0011 ⊕ intensity OCT3/4 superior to PLAP, p=.0048 ⊗ % OCT3/4 > PLAP, p=.003 †% cells staining in EC is <than S, p<.0001 ‡% cells in S+ with PLAP is <than with c-kit (p=.006) or OCT3/4 (p=.02). EMA marked teratoma components with sensitivity=1 and specificity=0.76. Low EMA specificity reflected reactivity in EC (3/15) and yolk sac tumor (2/7). Comparing tumor sites, the only significant finding was more intense OCT3/4 reactivity in retroperitoneal/abdominal tumors (3.0+) than at other sites (2.2-2.4+) (p=0.0068).
Conclusions: For extragonadal S, OCT3/4 and c-kit outperformed PLAP. For EC, PLAP was strikingly inferior to OCT3/4. The frequent c-kit reactivity of EC was an unexpected finding, but intensity and % were usually less than in S. CD30 and EMA stained EC and teratoma, respectively, but not with perfect specificity.

626 The Spectrum of Persistence of Testicular Blastema and Ectopic Testicular Parenchyma: A Possible Result of Focal Delay in Gonadal Development

MM Cajaiba, E Garcia-Fernandez, M Reyes-Mugica, M Nistal. Hospital La Paz/ Universidad Autonoma de Madrid, Madrid, Spain; Yale University School of Medicine, New Haven, CT.
Background: Sex-cord formation and organization are important steps in normal testicular development, and depend mainly on adequate interactions between mesenchymal cells, pre-Sertoli cells, and germ cells. These three elements form the testicular blastema, morphologically characterized by poorly organized sex cords and mesenchymal components, precursors of the mature testicular parenchyma. We describe here two groups of testicular lesions that appear to represent a spectrum of developmental derangements.
Design: Two types of uncommon testicular lesions, unrelated to other gonadal anomalies, were studied using both, autopsy and surgical pathology specimens. In the first group, we describe the histological and immunohistochemical features of persistence of testicular blastema (PTB) in 3 fetal autopsy cases, and discuss its possible pathogenesis and clinical importance. In the second group we analyze 11 cases of ectopic testicular parenchyma (ETP) in the tunica albuginea, an uncommon benign condition of uncertain clinical significance, whose main differential diagnosis is testicular dysgenesis.
Results: In all 3 PTB cases, the testicular lesions were incidental findings of fetal autopsies. Light microscopy studies showed well-defined foci of poorly differentiated testicular parenchyma containing ill-organized cords located immediately beneath the testis surface, with a continuous basement membrane between these cords and the celomic epithelium. The rest of the parenchyma was normal for the age. Among all ETP cases, there was no clinical suspicion of anomalies in the tunica albuginea, and the lesions described were incidental findings in both, autopsy and surgical pathology specimens. Histologically, they were characterized by the presence of testicular parenchyma (seminiferous tubules and testicular stroma with Leydig cells) within a normal tunica albuginea. No evidence of gonadal dysgenesis was present in any of the 14 studied cases.
Conclusions: Based on their similar topography within the testis, and on their possibly shared embryological origin, we propose that both lesions may represent the two extremes of a maldevelopmental and clinical spectrum resulting from a focal delay in testicular development.

627 MITF/TFE Renal Carcinomas. Clinico-Pathologic and Genetic Analysis of 31 Cases

P Camparo, V Vassiliu, M Lae, V Molinie, M Sibony, J Couturier, A Vieillefond. Val de Grace, France; Necker, France; Curie, France; Saint Joseph, France; Cochin, Paris, France.
Background: Recently, a subgroup of renal carcinomas (RCCs) associated with translocations resulting in gene fusions involving genes from the MITF/TFE family of transcription factors (TFE3 and TFEB) has been defined. The aim of our study was to regroup a large series of MITF/TFE RCCs in order to precise clinical, immuno-histologic features of these entities.
Design: Between 1997 and 2005, 31 cases of MITF/TFE RCCs were identified by immunohistochemistry or cytogenetics among 3423 RCCs (<1%). TFE3, TFEB, CK7, EMA, AE1-AE3, CD10, vimentin, racemase, Melan A, HMB45 antibodies were tested on a tissue microarray. Histological features, clinical data and follow-up were assessed.
Results: A moderate to strong nuclear expression of TFE3 was observed in 29 cases and of TFEB in 2 cases. Eleven cases had a cytogenetic proven translocation: 5 t(X-1)(p11.2;q21), 4 t(X;17)(p11,2;q23), 1 t(X-1)(p11.2;p34) and 1 t(6.11)(p21;q13). One had a complex caryotype. Two tumors with TFE3 translocation did not expressed TFE3. MITF/TFE carcinomas presented papillary (58%) or nested pattern (45%) and were composed of clear (38 %), eosinophilic cells (45%) or mixed cells (20%). We could not find correlation between histologic features and translocation type. MITF/TFE RCCs were characterized by CD10 (100%), racemase (100%), vimentin (70%), EMA (33%), AE1-AE (27%), CK7 (18 %), Melan-A (84%) and HMB45 (37 %) expression. The two TFEB tumors expressed TFEB, Melan-A, HMB45, Racemase and CD10. The patients were 13 males and 18 females (mean age 24 y.o, range 1 to 64 y.o). Mean tumor size was 7,1 cm. TNM stage was pT1 (n=13), pT2 (n = 3), pT3 (n=3) and N+ /M+ (n = 12). Three patients had incomplete status. Follow-up was available for 28 patients (mean 29 months): 21 patients were alive without disease, 2 patients presented metastasis, 5 patients died of the disease.
Conclusions: We recommend to evaluate the TFE3 and TFEB immunohistochemical expression in RCCs with mixed papillary and clear cell pattern, especially in young patients but also in older patients with unclassified RCCs. Fresh or Frozen material is still needed for cytogenetic and/or molecular biology analysis as we found some discrepancies between IHC and cytogenetic results. The MITF/TFE renal translocation carcinomas immunohistochemical profile (CD10+, Racemase+, CK7-, EMA-) is helpful to separate this entity form other type of RCCs. Clinical presentation at diagnostic and outcome is similar to adult-type RCCs.

628 Significance of Mitotic Activity and Activated Nuclear and Cytoplasmic AKT in Seminoma and Embryonal Carcinoma

JD Cass, C Wong, L Sugar, P Warde, JM Sweet. University of Toronto, Toronto, ON, Canada; University of Toronto and Radiation Medicine Program, Toronto, ON, Canada.
Background: Testicular germ cell tumours (TGCT) are the most common malignancy in men aged 25-40. TGCTs can be divided into seminomas (SE) and non-seminomas. SE accounts for 30-40% and embryonal carcinoma (EC) for about 20% of TGCT. The 5-year survival rate for SE is about 99% and for EC is about 65%. The mitotic index (MI) in seminoma has been linked to prognosis, however identification of mitoses on haematoxylin and eosin (HE) stained sections is unreliable. Histone 3, a DNA-associated protein, is phosphorylated on Ser10 during M-phase of mitosis and is a reliable indicator of MI by immunohistochemistry (IHC). Akt is a component of the phosphoinositide 3-kinase (PI3K) pathway and is activated by phosphorylation at Ser473 after growth factor stimulation, becoming phospho-Akt (pAkt). pAkt translocates to the nucleus and phosphorylates the Ser10 site of histone 3, which becomes phosphohistone-3 (PHH3). This study examines mitotic activity via PHH3 expression and pAkt in EC and SE by IHC.
Design: Two tissue microarrays (TMA) were constructed, one from 36 cases containing SE and the other from 19 cases containing EC from radical orchiectomies. Each case was represented by 3 cores. The expression of pAkt and PHH3 was examined by IHC. In each core, nuclei positive for pAkt were counted in 3 random high power fields (HPF) (50x), and all cores were scored as positive or negative for cytoplasmic reactivity. Mitotic counts were preformed in 3 random HPF per core based on PHH3 positivity and the average mitotic count per case was recorded.
Results: The average mitotic count per case in SE was 2.37 and in EC was 5.76. pAkt showed cytoplasmic expression in 17% of SE and 100% of EC. In SE, an average of 14 nuclei per case expressed reactivity for pAkt. No nuclear localization of pAkt was observed in EC. Although an ANOVA and correlation analysis revealed no statistical significance of cytoplasmic pAkt, nuclear pAkt or mitotic rate within EC and SE, each of these variables were statistically significant when SE and EC were compared.
Conclusions: EC has a higher proliferation rate than SE. pAkt was expressed only in the cytoplasm of EC and in both the cytoplasm and nucleus of SE. Since many targets inhibited by pAkt are nuclear transcription factors, the presence of nuclear pAkt in SE may impact its clinical behaviour. The significance of these markers is currently under investigation.

629 Improved Prognostic Value of a Refined Subclassification of Papillary Renal Cell Carcinoma Evaluated in 74 Cases

HP Cathro, EB Stelow, MR Wick. University of Virginia, Charlottesville, VA.

Background: While the prognosis of most patients with papillary renal cell carcinoma (PRC) is better than that of conventional renal cell carcinoma, a subpopulation of patients has worse survival. Attempts have been made to predict these patients by histologic subclassification into Types 1 and 2; however, this morphologic classification is of controversial utility, perhaps because a proportion of cases is difficult to subclassify. A recent study proposed new Classes 1 and 2 based on gene expression profiling. The current study compares the prognostic value of the 2 schemes.

Design: 74 cases of PRC were reviewed and classified by the 2 schemes. Those tumors with small nuclei, usually Fuhrman Grade 1-2 nucleoli and a small amount of basophilic cytoplasm were designated as Type 1, while Type 2 tumors had larger nuclei with prominent nucleoli and abundant eosinophilic cytoplasm. Class 1 tumors were defined primarily by nucleolar size, (viz only Fuhrman Grade 1-2 nucleoli), with nuclear size and cytoplasmic characteristics disregarded.

Results: Overall, 70% of tumors were classified as Type 1 and 30% as Type 2, with 62% designated Class 1 and 38% Class 2. Fifteen (13.5%) of tumors were reclassified by the new scheme, 80% upgraded from Type 1 to Class 2 and 20% downgraded from Type 2 to Class 1. On examination of a subset of 53 cases with an average follow up of 58 mn, overall survival was 56 mn in Type 1 vs 63 mn in Type 2 cases ($p = 0.29$) , but 62 mn in Class 1 vs 51 mn in Class 2 cases ($p = 0.18$). For Stage 2-4 tumors, class was a more significant predictor of patient survival than type (49 vs 39 mn for Type 1 vs Type 2, and 59 mn vs 34 mn for Class 1 vs Class 2). Overall 11 patients with Type 1 and 4 patients with Type 2 tumors had died of disease, while 8 patients with Class 1 tumors and 7 patients with Class 2 tumors died of disease (overall follow up 48 mn). Metastases or recurrences occured in 2 patients with Type 1/Class 1 tumors and in 6 patients with Type 2/Class 2 tumors.

Conclusions: This refined subclassification of PRC has somewhat better prognostic predictive value than the previously described one. The previous but not uniformly accepted scheme placed emphasis on cell and nucleolar size and cytoplasmic characteristics. The new scheme emphasizes nucleolar size and gross tumor size (average 3.35 cm vs 6.98 cm for Class 1 vs Class 2). This refined PRC subclassification is more straightforward, allowing the pathologist to forgo interpreting tumors as mixed, and provides better prognostic information for patients and clinicians.

630 BFL-1 Expression in Prostate Cancer Cells

XQ Chen, N Chen, H Zeng, R Huang, B Yang, Y Huang, M Xu, Q Zhou. West China Hospital, West China Medical School, Sichuan University, Chengdu, Sichuan, China.

Background: BFL-1 (bcl-2-related gene expressed in fetal liver) is a bcl-2 family member. Expression of BFL-1 appeared to be limited to several tissue types including that of the hematopoietic system, and is under the control of NF-kB pathway, which in turn can be activated by GM-CSF, IL-1, TNF, as well as LPS. BFL-1 can bind to Bid or tBid (truncated BID), thus inhibiting the activation of the mitochondrial pathway of cell death. Expression of BFL-1 and its significance has only rarely been reported in tumors. Here we report the identification of increased BFL-1 expression in prostate carcinoma and the effect of its downregulation by anti-sense approach.

Design: Conventional and quantitative real-time polymerase chain reaction (qPCR) were used to measure expression level of BFL-1 in prostate cancer cells PC3, DU145, and LNcap. Effects on cell growth and expression of molecules involved in cell death and proliferation were assessed in prostate cancer cells treated by BFL-1 antisense oligonucleotide transfected by the Lipofectamine method (Invitrogen).

Results: BFL-1 mRNA level was significantly higher in the androgen-independent cell lines PC3 and DU145 than in the androgen-dependent cell line LNcap and in nodular hyperplasia. The relative copy numbers of BFL-1 mRNA measured by qPCR were increased up to a 1000-fold in PC3 and DU145. BFL-1 antisense oligonucleotide treatment of PC3 and DU145 cells resulted in changes of expression of several genes involved in regulating cell growth and death, including upregulation of AIF (apoptosis-inducing factor).

Conclusions: BFL-1 is upregulated in some prostate cancer cells and may interfere with expression of cell growth or cell death regulators. Expression of BFL-1 in prostate cancer may be associated with poor hormone treatment reponsiveness.

631 Grading of Papillary Urothelial Carcinoma: Significant Interobserver Variations and Survivin as a Useful Marker

YB Chen, JJ Tu, J Kao, XK Zhou, YT Chen. Weill Medical College of Cornell University, New York, NY.

Background: Grading of non-invasive papillary urothelial carcinoma as low-grade (LG) versus high-grade (HG), relying solely on architectural and cytological criteria, can be inconsistent among pathologists due to the heterogeneity of lesions and interobserver variations. Adjunct objective markers would thus be highly desirable.

Design: 51 biopsies of bladder papillary urothelial carcinomas (Ta) were graded blindly by 5 experienced general surgical pathologists. The expression profiles of survivin and Ki-67 were evaluated by immunohistochemistry (IHC) and by quantitative RT-PCR using paraffin-embedded tissues. IHC was quantified using a color deconvolution module of ImageJ (NIH).

Results: The diagnostic agreement of 51 cases among 5 pathologists was fair to poor, with an overall K value of 0.41 (>0.75 as good correlation). Only 66% (34/51) or 44% (22/51) cases were agreed on by 4 or all 5 pathologists respectively. The diagnostic values of survivin and Ki-67 were initially tested in 19 cases with consensus grading (4 or 5 raters agreed; 9 HG and 10 LG). The percentages of urothelial cells with positive survivin nuclear staining (survivin scores) were significantly higher in HG (mean 29.5%, range 14.4-57.4%) than in LG (mean 5.9 %, range 0.9-12.0%) ($p<0.0001$). Ki-67 scores, although also significantly different between the two groups ($p=0.002$), showed substantial overlap in ranges, and survivin was selected for further study. The 51 cases were divided into 3 groups: consensus LG (17), consensus HG (18) and indetermined (IND)(16, <4 raters agreed). The survivin scores were again significantly different between LG and HG (mean 7.7% vs. 22.7%, $p<0.0001$). In comparison, the IND group had survivin scores close to the LG group (mean 10.7%, $p=0.2$), significantly lower than the HG group ($p=0.0002$). Review of the IND cases showed focal high survivin in a few cases, correlating to areas with worse histological features and justifying the diagnosis of HG. However, survivin staining was uniformly low in other cases, implying that they were biologically LG. qRT-PCR showed good correlation between survivin mRNA levels and survivin scores ($\gamma^2=0.79$), confirming the significant difference between LG and HG and the similarity between LG and IND.

Conclusions: Significant interobserver variations exist in the histological grading of papillary urothelial carcinoma. Given our finding of high survivin protein and mRNA levels in HG lesions, IHC for survivin provides an objective criterion in challenging cases and may help prevent over-grading.

632 Evaluation of H2A.X Phosphorylation in Urothelial Carcinoma

WL Cheung, R Sharma, GJ Netto. Johns Hopkins University, Baltimore, MD.

Background: Histone modifications such as acetylation, phosphorylation and methylation have been linked to DNA replication, transcription, mitosis, and DNA damage repair. Specific histone modifications have been shown to alter the nucleosome structure and enhance recruitment of factors required for transcription and DNA damage repair. Phosphorylation of histone H2A.X at serine 139 (H2A.X-phos) is associated with DNA breaks and is involved in the DNA repair pathway by recruiting repair proteins such as BRCA-1 and 53BP1. H2A.X phosphorylation has been suggested to be present in the majority of bladder urothelial carcinoma (URCa) regardless of grade (Bartkova et al. 2005). Studies on the relationship of H2A.X-phos presence with clinical outcome of URCa are lacking. The current study evaluates the rate of H2A.X phosphorylation in high grade (HG-URCa) and low grade (LG-URCa) bladder carcinomas and assesses whether it may help predict LG-URCa recurrence.

Design: A total of 17 archival URCa cases were selected from the surgical pathology file at our institution (2005-2006). Cases included 10 non-invasive LG-URCa from TUR biopsies and 7 invasive HG-URCa from cystectomy specimens. Follow-up cystoscopy data was obtained on all LG-URCa cases. Immunohistochemistry was performed using a polyclonal antibody for H2A.X serine 139 phosphorylation (Upstate Biotech, NY). Tumor was considered to be positive if any nuclear reactivity was encountered.

Results: A higher rate of H2A.X phos positivity was present in non invasive LG-URCa (4/10 ; 40%) compared to invasive HG-URCa (1/7; 14%) cases. On follow-up, cystoscopy and biopsy proven recurrence was demonstrated in 6/10 LG-URCa. In the LG-URCa group, recurrence was much more likely to occur among H2A.X-phos negative cases (5/6; 83 %) compared to H2A.X-phos positive cases (1/4; 25%).

Conclusions: Our study reveal a higher rate of H2A.X-phos positivity in non invasive LG-URCa compared to invasive HG-URCa. In addition, in LG-URCa cases, H2A.X-phos positivity appears to be associated with a lower rate of tumor recurrence. Additional studies are warranted to confirm the current findings and help delineate whether the seemingly protective effect of H2A.X-phos is related to a higher rate of DNA breaks or a preserved DNA repair capacity in such tumors. A tissue microarray based study on a larger cohort of LG-URCa is ongoing.

633 Localized Amyloidosis of Ejaculatory Ducts: A Systematic Study on 447 Prostatectomy Specimens

HY Cho, KH Kee, SS Shen, JH Suh, OJ Lee, AG Ayala, JY Ro. Gachon University Gil Medical Center, Incheon, Republic of Korea; Chosun University Medical College, Kwangju, Republic of Korea; The Methodist Hospital and Weill Medical College of Cornell University, Houston, TX; Ulsan University Hospital, Ulsan, Republic of Korea; Asan Medical Center, Seoul, Republic of Korea.

Background: Although localized amyloidosis of seminal vesicles and vasa deferentia has been reported in the literature, amyloid deposition in ejaculatory ducts has not.

Design: To systematically investigate the incidence and pattern of amyloid deposition in ejaculatory ducts, we reviewed the whole mount sections of 447 radical prostatectomy specimens removed for localized prostatic cancers.

Results: Amyloid deposition in both ejaculatory ducts was found in 21 cases (4.7%), and was invariable accompanied by same deposition in both of the seminal vesicles and vasa deferentia. Deposition was diffuse in 16 cases and focal and patchy in the remaining cases. The deposits were nodular and affected the subepithelial region of ejaculatory ducts, seminal vesicles and vasa deferentia. Blood vessels, muscular walls of the ejaculatory system and prostatic parenchyma were not involved. In none of these cases, prostatic carcinoma involved the ejaculatory system. Patients' age ranged from 51 to 79 years (mean 66.1). Amyloid deposition was found in five patients in the sixth decade (3.4%), in nine patients in the seventh decade (4.7%), and seven patients in the eighth decade (9.3%). No patients under 50 years old, however, showed amyloid deposition.

Conclusions: Conclusion: Our results indicate that amyloid deposition in ejaculatory ducts is an uncommon incidental finding, and is always associated with amyloid deposition in other parts of the ejaculatory system. The incidence increases with advancing age, but is not related to conventional amyloidosis or prostatic carcinoma. Age appears to be the only risk factor for the localized amyloidosis of ejaculatory ducts.

634 Significance of Positive Surgical Margins in Areas of Capsular Incision in Otherwise Organ-Confined Disease at Radical Prostatectomy

AY Chuang, JI Epstein. The Johns Hopkins Hospital, Baltimore, MD.

Background: The significance of capsular incision (CI) into tumor at radical prostatectomy (RP) is not well-understood.

Design: Inclusion criteria were: 1) Positive margin in an area of CI; 2) Elsewhere no extraprostatic extension (EPE), and no seminal vesicle or lymph node spread; 3) Entire prostate submitted for pathological examination; 4) No neoadjuvant therapy. 135 RPs

(1.3% of RPs) from 1993-2004 fit inclusion criteria and were assessed for post-op progression (PSA > 0.2ng/ml). Cases with CI were compared to Gleason score 6 or 7 tumor which was organ-confined margin negative (OC M-, n=7,531), focal EPE margin negative (FEPE M-, n= 1223), extensive EPE margin negative (EEPE M-, n=835), FEPE margin positive (FEPE M+, n=289), & EEPE margin positive (EEPE M+, n=433), using Cox analysis.

Results: The mean length of cancer at the CI site was 2.6 mm. The overall Gleason score in the CI group was 6 (68.9%) & 7 (31.1%), identical to other stages of disease. Location of CI was: posterolateral (61.5%); posterior (18.5%); anterior (8.9%); lateral (8.1%); and apically (3%). The 5-year actuarial freedom from recurrence was 96.7% for OC M-; 89.7% for FEPE M-; 78.6% for FEPE M+; 74% for EEPE M-; 71.3% for CI, and 58.5% for EEPE M+. Men with CI had a worse likelihood of cure than men with OC M- ($p<0.0001$) and FEPE M- ($p=0.02$). The risks of progression for men with CI, FEPE M+ and EEPE M- were not significantly different. Tumors with CI had a greater likelihood of freedom from recurrence than tumors with EEPE M+ ($p<0.0001$). Comparing Gleason score 6 vs. 7 at the CI site was not significant ($p=0.05$), yet there were only 7 men with Gleason score 7 at the CI site. Risk of recurrence correlated with length of tumor at the CI site ($p=0.002$). If there was <3 mm of tumor at the CI site, the 5 year risk of biochemical progression was 20.0% compared to 55% if there was ≥3 mm of tumor cut across.

Conclusions: Isolated CI into tumor is uncommon with experienced urologists and most commonly occurs in the region of the neurovascular bundle, where urologists try to preserve potency and risk incision into the prostate. Most men with CI and otherwise OC disease typically have Gleason score 6 tumor. Men with isolated CI have a significantly higher recurrence rate than patients with OC M- and FEPE M-, yet a significantly lower recurrence rate than patients with EEPE M+. This information along with the extent of CI can be factored in when counseling men with CI in terms of their post-operative chance of cure and consideration of adjuvant therapy.

635 Xanthoma of the Prostate: A Mimicker of High Grade Prostate Adenocarcinoma

AY Chuang, JI Epstein. The Johns Hopkins Hospital, Baltimore, MD.

Background: Prostatic xanthoma may mimic high-grade prostatic adenocarcinoma or prostate cancer treated with hormone therapy.

Design: From 1995-2006, 40 cases of prostatic xanthoma were diagnosed at The Johns Hopkins Hospital. 34 cases were received in consultation from outside institutions. H&E or unstained slides were available in 27 cases (24 consultation cases; 3 in house cases).

Results: Xanthoma was found on needle biopsy in 25 cases, with 2 cases noted on TURP. 26 cases contained only 1 focus of prostatic xanthoma with 1 case having 3 foci on the same core biopsy specimen. In 21 xanthomas, the lesions were small measuring ≤0.5mm. Only 3 xanthomas were >1mm with the largest one measuring 2.5mm. Xanthoma cells had small uniform, benign-appearing nuclei, small inconspicuous nucleoli, and abundant vacuolated foamy cytoplasm. No mitoses were identified. Focal necrosis was identified in one case. Most xanthomas were arranged in circumscribed solid nodular pattern (17 cases). 10 xanthomas consisted of cords and individual cells infiltrating the prostatic stroma, further mimicking high grade prostate carcinoma. 2 xanthomas contained a mixed circumscribed nodular pattern and infiltrating pattern. Of cases with the lesion still present on slides for immunohistochemistry, CD68 was diffusely strongly positive in 18/19 (94.7%) and CAM5.2 was positive in none of the cases 0/14 (0%). One of 15 (6.7%), 2/17 (11.8%) and 1/12 (8.3%) cases were positive for PSA, PSAP, and AMACR, respectively.

Conclusions: Careful attention to morphology with adjunctive use of CD68 and CAM5.2 immunohistochemical stains are helpful in the diagnosis of prostatic xanthoma, especially in difficult cases with an infiltrative pattern.

636 Immunohistochemical Differentiation of High-Grade Prostate Carcinoma (PCa) from Urothelial Carcinoma (UC)

AY Chuang, JI Epstein. The Johns Hopkins Hospital, Baltimore, MD.

Background: The histological distinction of high grade PCa and infiltrating high grade UC may be difficult, and has significant implications because each disease may be treated very differently (ie hormone therapy for PCa and chemotherapy for UC).

Design: Immunohistochemistry of novel and established prostatic and urothelial markers using tissue microarrays (TMAs) were studied. Prostatic markers studied included: PSA; P501s (prostein); PSMA (prostate specific membrane antigen); NKX3.1 (an androgen-related NK-class homeobox gene), proPSA (precursor form of PSA), and AMACR. Urothelial markers included: high molecular weight cytokeratin (HMWCK); p63; thrombomodulin; and S100P (placental S100). TMAs contained 38 poorly differentiated PCa: Gleason score 8 (n=2); Gleason score 9 (n=18); Gleason score 10 (n=18) and 35 high grade invasive UC from radical prostatectomy and cystectomy specimens, respectively. Each case had 3-8 tissue spots (0.6-mm-diameter). If all spots for a case showed negative staining, the case was called negative. Because of PSA's high sensitivity on the TMA, we chose 21 additional poorly differentiated primary PCa which showed variable PSA staining at the time of diagnosis.

Results:

Prostatic Markers

	PSA	P501s	PSMA	NKX3.1	ProPSA	AMACR
Prostate Ca. TMA	37/38 (97.4%)	38/38 (100%)	35/38 (92.1%)	36/38 (94.7%)	36/38(94.7%)	37/38 (97.4%)
Urothelial Ca. TMA	0/35 (0.0%)	2/35 (5.7%)	0/35 (0.0%)	0/35 (0.0%)	0/35 (0.0%)	12/35 (34.3%)
Prostate Ca.-PSA Variable Cases (n=21)						
2-3+ Staining (avg. per case)	19.9%	38.6%	61.6%	66.0%		
Negative Staining (entire case)	1/21 (4.8%)	2/21 (9.5%)	1/21 (4.8%)	0/21 (0.0%)		

Urothelial Markers in TMA

	HMWCK	p63	Thrombomodulin	S100P
Prostate Ca.	3/38(7.9%)	0/38(0%)	2/38(5.3%)	3/38(7.9%)
Urothelial Ca.	32/35(91.4%)	29/35(82.9%)	24/35(68.6%)	25/35(71.4%)

Conclusions: PSA can be used as the 1st screening marker for differentiating high grade PCa from high grade UC. Immunohistochemistry for P501S, PSMA, NKX3.1 and proPSA are useful when high grade PCa is suspected based on the morphology or clinical findings, yet shows negative or focal PSA staining. HMWCK and p63 are superior to the novel markers thrombomodulin and S100P.

637 Increased Expression of STAT-1 in Prostatic Adenocarcinoma

ST Chuang, C Luan, XJ Yang. Feinberg School of Medicine, Northwestern University, Northwestern Memorial Hospital, Chcago, IL.

Background: Signal transducer and activator of transcription (STAT) molecules control the regulatory aspects of the immune system. They are components of the interferon-gamma (IFN-γ) receptor signaling pathway and may play a role in the development of cytokine resistance. STAT-1, one of the seven members of the STAT family, is regarded to have pro-apoptotic activity. An increase of STAT-1 expression has been reported in prostate cancer cell lines; however, its expression in prostatic adenocarcinoma has not been well studied in vivo. The purpose of this study further investigates the STAT-1 expression in prostatic adenocarcinoma with comparison to benign prostatic parenchyma by immunohistochemistry.

Design: Paraffin-embedded tissue sections from 63 cases of prostatic adenocarcinoma (Gleason grade 3, n=31; grade 4 or 5, n=32) and 51 cases of benign prostatic parenchyma that were constructed in tissue microarrays were subjected to immunohistochemistry using a monoclonal antibody specific for STAT-1. The staining intensity was scored on 0 to 3 with 3 being the highest intensity while the distribution of staining was scored as focal (<30%) or diffuse (>30%).

Results: All 63 cases of intermediate and high grade prostatic adenocarcinoma were diffusely positive for STAT-1 with average staining intensities of 2.68 for Gleason 3 and 2.66 for Gleason 4/5 tumors, respectively. All the benign prostatic parenchyma consistently showed absent or weak staining with an average intensity of 1.06.

Conclusions: This study reports the strong STAT-1 immunoreactivity in prostatic adenocarcinoma regardless of the grade with comparison to benign prostatic parenchyma. This finding suggests a possible role of STAT-1 in prostatic carcinogenesis. Additional studies with larger number of cases are necessary to evaluate the diagnostic value of STAT-1.

638 Sporadic Clear Cell Renal Cell Carcinoma (CC-RCC) Commonly Expresses Cytokeratin 7 in Cystic Foci: A Morphologic and Immunohistochemical Study with Emphasis on the Relationship To Clear Cell-Papillary Renal Cell Carcinoma of End-Stage Kidney (CP-RCC-ESK)

WJ Clingan, LA Cerilli, N Gokden, JK McKenney. University of Arkansas for Medical Sciences, Little Rock, AR; University of New Mexico Health Sciences Center, Albuquerque, NM.

Background: Renal neoplasms in end-stage renal disease include CP-RCC-ESK. They are characterized by macrocysts lined by neoplastic cells with clear cytoplasm that form papillae and tufted aggregates, and show immunoreactivity with cytokeratin 7 (CK7). The presence of similar renal neoplasms in a sporadic setting has not been fully described.

Design: H&E-stained slides from consecutive clear cell renal cell carcinomas (CC-RCCs) were retrieved and reviewed to verify diagnoses. Cases with macroscopic cysts of any type (i.e., present grossly) and/or microscopic cysts with intracystic epithelial tufts/papillae were selected as the study group. Immunohistochemistry for CK7 was performed on all available cases from this group, and charts were reviewed for evidence of underlying renal disease.

Results: Of 122 CC-RCC, 25 (20%) contained macrocysts and/or microcysts with intraluminal epithelial tufts/papillae. Of the 25, 15 were CC-RCC with macrocysts (11 with intracystic epithelial tufting), 5 were morphologically identical to CP-RCC-ESK in large foci, 4 were CC-RCC with microscopic cysts and intracystic epithelial tufting, and 1 was multilocular cystic renal cell carcinoma. CK 7 immunoreactivity was present in the cyst lining neoplastic cells in 16/20 cases tested, including cases from all 4 subgroups. The neoplastic cells within septa and the solid foci of CC-RCC surrounding the cysts were typically strongly reactive, while solid foci further from the cystic component were typically negative. None of the 25 patients had clinical history or laboratory evidence of renal failure, but 1 patient had von-Hippel-Lindau disease.

Conclusions: Renal neoplasms morphologically identical to the CP-RCC-ESK occur in a sporadic setting (4/122 consecutive cases: 3%). Otherwise typical CC-RCC with mixed solid and macrocystic growth patterns may have subtle intracystic epithelial tufts/papillae reminiscent of CP-RCC-ESK. The lining epithelial cells of both the microscopic and macroscopic cysts within CC-RCC commonly show strong immunoreactivity to CK7. The morphologic and immunohistochemical overlap between sporadic CC-RCC with cystic change and CP-RCC-ESK suggests a close relationship that warrants further molecular/cytogenetic study.

639 Perineural Invasion (PNI) Predicts Mortality in Penile Squamous Cell Carcinoma. A Long-Term Outcome Study Comparing Clinico-Pathologic Features

AL Cubilla, G Ayala, A Lopes, GC Guimaraes, ML Oliveira, JJ Torres, EF Velazquez, FA Soares. Instituto de Patología e Investigación, Asuncion, Paraguay; Facultad de Ciencias Medicas, Asuncion, Paraguay; Baylor College of Medicine, Houston, TX; Hospital do Cancer AC Camargo, Sao Paulo, Brazil; Harvard Medical School, Boston, MA.

Background: Numerous studies have looked at prediction of lymph node metastasis in penile carcinoma, with the intent of reducing the morbidities associated with inguinal lymph node dissection. However, few studies have looked at factors that predict penile cancer specific mortality.

Design: The cohort includes 375 penectomies for SCC of the penis and 165 groin dissections treated at the Hospital do Cancer AC Camargo in Sao Paulo, Brazil. Data evaluated were: tumor site, size, histological grade (1, 2 and 3), histological subtype, thickness, levels of invasion, prognostic index, vascular and perineural invasion and nodal status. Mann-Whitney test was used for the difference between paired parameters. Spearman test was applied to explore the relationship between parameters and prognostic variables. Possible prognostic significance of parameters was examined by univariate and multivariate analyses using Kaplan Meier and Cox regression, including forward and backward analysis.

Results: Mean age was 55 years (21-88). Follow up ranged from 1 to 459 months (mean 101 months; median 72 months). Cancer specific death was noted in 60 patients (27.5%). Nodal metastasis was identified in 22.4 % of patients with lymphadenectomies. Perineural invasion was identified in 59 patients and vascular invasion in 52. On multivariate analysis and modeling, out of all clinico-pathologic factors, only PNI and nodal metastasis were independently predictive of penile cancer specific mortality.

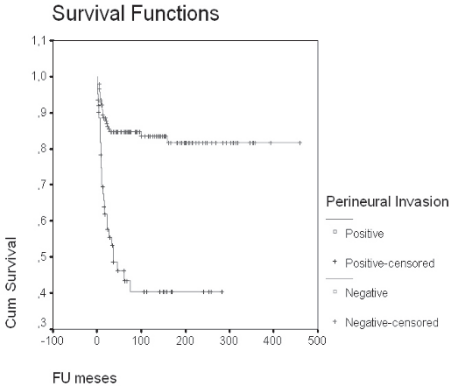

Conclusions: There is limited information on perineural invasion as a prognostic factor in penile SCC, but this study provides exciting data that requires validation. It has been hypothesized that tumor-nerve interaction in prostate cancer produces a microenvironment favorable to tumor spread. It is possible that the predictive value of PNI in penile cancer may also be due to cancer-nerve interactions that favor tumor dissemination.

640 Validation of an Immunohistochemical Panel of Genes for the Prediction of Gleason Pattern 3 vs 4 Prostate Cancer

MW Datta, MB Amin, L True, PS Nelson. Hospital Pathology Associates, University of Minnesota, Minneapolis, MN; Cedars Sinai, University of California Los Angeles, Los Angeles, CA; University of Washington, Seattle, WA; Fred Hutchinson Cancer Research Center, Seattle, WA.

Background: While the Gleason system has been successful in grading prostate cancer, variability in Gleason grading limits its prognostic power. The difference between a Gleason pattern three and four tumor can at times be subtle, and yet is increasingly relied upon for clinical decisions regarding therapy and eligibility for clinical trials.

Design: Our previous work demonstrated the molecular profiling of laser capture microdissected "classic" Gleason pattern three or four tumors (True L, et al. A molecular correlate to the Gleason grading system for prostate adenocarcinoma. Proc Natl Acad Sci U S A. 103:10991, 2006). The study identified a group of genes that can classify the microdissected samples with 100% sensitivity and specificity. These genes were used to develop a panel of antibodies that could be used in an immunohistochemical test on formalin fixed paraffin embedded prostate cancer needle biopsies. Staining tests were developed for seven genes. These were evaluated in a panel of 34 tumors, including 22 tumors with consensus Gleason pattern 3 or 4 diagnoses, and 10 tumors with discrepancies between pathologic Gleason grading (tumors scored as either pattern 3 or pattern 4).

Results: When analyzed, none of the individual seven genes demonstrated a significant correlation with expression and Gleason pattern 3 or 4 tumor. Thus no single gene could accurately differentiate Gleason pattern 3 from pattern 4 tumors. If all seven or six of seven genes were expressed, the gene expression pattern identified Gleason pattern 4 tumor. These profiles were not identified in the Gleason pattern 3 tumors. Thus a separation could be made between Gleason pattern 3 and pattern 4 tumors based on their gene expression profiles. When the gene expression profiles were examined in the cases that demonstrated Gleason grading discrepancies, predicted Gleason pattern classification was made which matched the most common urologic pathologist's diagnosis.

Conclusions: We have been successful in creating a set of seven genes that in preliminary staining of prostate cancer specimens can distinguish Gleason pattern 3 from pattern 4 tumors. These initial results are currently completing validation studies in a panel of 210 additional prostate cancer cases.

641 Positive Urovysion FISH Due to Isolated Loss of 9p21: Comparison with FISH Positive Bladder Tumors Due to Aneuploidy

MN De Peralta-Venturina, R Kanhere, NS Goldstein. William Beaumont Hospital, Royal Oak, MI.

Background: A dual-track pathway in bladder carcinogenesis leading to low-grade papillary non-invasive and high grade non-papillary aggressive bladder tumors is well-recognized. With the increasing usage of Urovysion (Vysis Inc.) fluorescent in-situ hybridization (FISH) testing , this study aims to determine if specific FISH chromosomal abnormalities have characteristic morphologic alterations evident on routine H & E sections, and are therefore predictive of the aggressiveness of the bladder tumor recurrence.

Design: Of the 940 adequate FISH analyses using commercial Urovysion kit performed from May 2003 to August 2006, there were 14 cases which showed homozygous loss of 9p21 and had concurrent or recent bladder biopsies: five with loss of 9p21 in > 2 but <12 urothelial cells (FISH negative) and 9 cases with loss of 9p21 in ≥ 12 cells (FISH positive). These cases were compared with 15 positive FISH cases due to aneuploidy of 3,7, or 17 involving ≥ 2 of these chromosomes in ≥ 4 cells and had concurrent or recent bladder biopsy. Morphologic comparison of the bladder biopsies between these groups was performed.

Results: Four of the five cases (80%) with negative FISH but showed loss of 9p21 in > 2 but < 12 cells were associated with low grade (Grade 1-2) noninvasive papillary tumors. Similarly, eight of the nine cases (89%) with positive FISH due to isolated loss of 9p21 in ≥ 12 cells without aneuploidy showed low grade noninvasive papillary bladder tumors. In these cases the nuclear atypia was mild and uniform throughout the lesion. In contrast, twelve of the fifteen (80%) cases which showed aneuploidy of either 3,7 or 17 on FISH were either high grade bladder tumors which were predominantly muscle-invasive (6 of 10), or flat carcinoma in-situ (2 cases). These cases showed more variation in nuclear atypia ranging from Grade 2 to Grade 3 nuclear features.

Conclusions: The pattern of probe FISH alteration may be indicative of molecular mechanism of bladder carcinogenesis. Isolated loss of 9p21 is more commonly associated with low grade noninvasive papillary neoplasms and uniform mild nuclear atypia in neoplastic cells. In contrast, chromosomal aneuploidy is often seen in high grade muscle invasive bladder cancers and is associated with more severe and variable nuclear changes. Reporting the actual molecular abnormality, i.e. loss of 9p21 versus aneuploidy, on FISH positive cases may be helpful in prognosticating and determining the aggressiveness and extent of follow-up in bladder cancer patients.

642 Adenocarcinomas of the Urinary Bladder and Colorectum Show Distinctive Patterns of Mucin Immunoreactivity

JR deHart, WL Frankel, L Gentchev, RE Jimenez. The Ohio State University, Columbus, OH.

Background: Adenocarcinoma involving the urinary bladder poses a difficult differential diagnosis, as secondary involvement of the bladder by colorectal adenocarcinoma occurs much more frequently and often shares identical morphology. We tried to identify mucin profiles of bladder and colonic adenocarcinoma, to determine whether they could be useful in this differential diagnosis.

Design: Tissue microarrays were created from 26 cases of primary bladder adenocarcinoma (14 enteric, 2 mucinous, 3 signet ring, and 7 NOS) and 18 cases of primary colonic adenocarcinoma, retrieved from archival files. Slides of the microarrays were immunostained with monoclonal antibodies against MUC1, MUC2, MUC4, MUC5AC (MUC5), and MUC6, as well as CK7, CK20, β-Catenin, and CDX-2. Staining was recorded as positive (≥ 5% of cells staining) or negative. For β-Catenin, only nuclear staining was considered positive. Chi-square test was performed to compare frequencies of positive staining. A p-value of <0.05 was considered statistically significant.

Results: MUC2, MUC4 and MUC5 showed variable staining in primary bladder and primary colonic adenocarcinomas, with no significant difference between the two populations. Results of staining for the remaining antibodies are shown below:

	CK7	CK20	β-Catenin	CDX2	MUC1	MUC6
Colon	5/18 (27.8%)	13/18 (72.2%)	17/18 (94.4%)	18/18 (100%)	1/18 (5.56%)	7/17 (41.2%)
Bladder	15/26 (57.7%)	10/26 (38.46%)	6/26 (23.1%)	11/26 (42.3%)	13/23 (56.5%)	0/26 (0%)
p-value	0.050	0.027	<0.001	<0.001	0.001	0.001

Conclusions: While the immunophenotype of primary bladder adenocarcinoma partially overlaps with that of colorectal adenocarcinoma, it shows a distinct mucin expression pattern, with absent MUC6 expression and frequently positive MUC1 expression. An immunohistochemical panel that includes MUC1, MUC6 and β-Catenin may be useful in distinguishing primary adenocarcinomas of the urinary bladder from secondary involvement by colorectal adenocarcinoma.

643 *TMPRSS2: ERG* Gene Fusion Associated with Lethal Prostate Cancer

F Demichelis, K Fall, S Perner, O Andren, FH Schmidt, SR Setlur, Y Hoshida, JM Mosquera, Y Pawitan, C Lee, HO Adami, LA Mucci, PW Kantoff, SO Andersson, AM Chinnaiyan, JE Johansson, MA Rubin. Brigham and Women's Hospital, Boston, MA; Harvard School of Public Health, Boston, MA; Dana Farber Cancer Inst, Boston, MA; Broad Inst. of Harvard and MIT, Cambridge, MA; Univ. Hospital of Ulm, Ulm, Germany; University of Michigan Medical School, Ann Arbor, MI; Univ. Hospital Orebro, Orebro, Sweden; Karolinska Institute, Stockholm, Sweden.

Background: Given the excellent outcome for men with clinically localized prostate cancer (CaP) regardless of treatment, the risks of therapy must be balanced with the risk of disease progression. The recent identification of *TMPRSS2:ERG* gene fusion CaP and its significant association with higher stage disease suggested that gene fusion status might have prognostic implications.

Design: The cohort used to evaluate CaP disease progression was of men followed on a Watchful Waiting trial. Incidental CaP was diagnosed during evaluation for symptomatic benign prostatic hyperplasia at one hospital center (catchment area 190,000 inhabitants).

Follow-up of the cohort with respect to mortality was 100% and no patients were lost to follow-up through October 2005. The endpoint of the present study was lethal CaP, defined as development of distant metastases or CaP specific death (median and max follow-up time 9.1 and 28 yrs). We characterized 111 cases for the *TMPRSS2:ERG* gene fusion using a validated break-apart FISH assay or by Q-PCR when FISH failed.
Results: The frequency of *TMPRSS2:ERG* fusion was 15% (17/111). Q-PCR demonstrated high ERG expression to be associated with *TMPRSS2:ERG* gene fusion ($p<0.005$). *TMPRSS2:ERG* fusion positive tumors were more likely to have a higher Gleason Score (two-sided $P=0.01$). To assess the relationship of fusion status and lethal CaP, we used cumulative incidence regression to account for competing causes of death. We observed a significant association between the presence of the *TMPRSS2:ERG* gene fusion and lethal CaP with a cumulative incidence ratio (CIR) of 2.7 ($P<0.01$, 95%CI=1.3-5.8). When adjusting for Gleason Score, the CIR was 1.8 ($P=0.2$, 95%CI=0.6-5.3).
Conclusions: These data demonstrate for the first time a significant association with *TMPRSS2:ERG* gene fusion lethal CaP and support the critical role of *TMPRSS2:ERG* gene fusion product as a putative oncogene in CaP.

644 Pathological Characteristics of Solitary Small Renal Masses: Implications for Management

T DeRoche, C Magi-Galluzzi, M Zhou. Cleveland Clinic, Cleveland, OH.
Background: With the increasing use of diagnostic imaging, renal neoplasms are frequently detected as solitary small masses in asymptomatic individuals. Partial nephrectomy, ablative techniques, and surveillance have assumed increasing use in the management of such patients. The aim of this study was to examine the pathological characteristics of solitary renal masses measuring ≤ 4 cm and to identify the clinical correlates that may predict the pathological features of small renal lesions.
Design: Patients with a solitary renal mass ≤ 4 cm confirmed by nephrectomy or needle biopsy between 2004 and 2006 were included. In cases with a needle biopsy-proven diagnosis, the tumor size was obtained from preoperative imaging studies. Low-grade renal cell carcinoma (RCC) was defined as an organ-confined tumor (AJCC stage T1a) with a Fuhrman nuclear grade (FNG) ≤ 2 and without vascular invasion. Tumors with any of the following characteristics were categorized as high-grade carcinoma: AJCC stage T3, lymph node involvement, and FNG ≥ 3.
Results: The study population included 301 males and 202 females (ratio 1.5:1) with a mean age of 58.8 years (range 0.25- 84). Non-neoplastic entities, benign neoplasms, low grade RCC and high grade RCC accounted for 1.6%, 18%, 49.8% and 30.6% of cases, respectively. Among the neoplasms, the following distribution was observed: clear cell 56.8%, papillary 15.1%, chromophobe 7.7%, RCC unclassified 1.2%, oncocytoma 11.3% and angiomyolipoma 5%. In patients with masses > 2 cm, 36% had high-grade features compared to 21.1% of masses measuring ≤ 2 cm ($p=0.002$). In females with ≤ 2 cm masses, 37.1% were benign or non-neoplastic, compared to 9.7% ($p<0.001$) in males with ≤ 2 cm masses. In female patients under the age of 50, 30% of all masses were benign or non-neoplastic, compared with 4.5% in males of the same age group ($p<0.01$).

	≤2 cm	>2 cm
Non-neoplastic	1/175 (0.6%)	7/328 (2.1%)
Benign neoplasm	36/175 (20.6%)	53/328 (16.1%)
Low-grade neoplasm	101/175 (57.7%)	150/328 (45.7%)
High-grade neoplasm	37/175 (21.1%)	118/328 (36%)

$p=0.002$
Conclusions: Tumor size, age and gender all contribute to whether a solitary small renal mass may be a benign lesion, low grade or high grade RCC. A tumor > 2 cm is more likely to be a high-grade RCC in both males and females. In female patients under the age of 50, or with a tumor size ≤ 2 cm, 1/3 of masses were non-neoplastic or benign in nature. This information could help clinicians and patients to select the appropriate treatment modalities for solitary small renal masses.

645 Comparison of Urovysion™ Testing, Conventional Cytology and Surgical Biopsy in Evaluation for Recurrent Bladder Cancer

R Dhir, AV Parwani, R Balassanian, R Hrebinko, M Franks, SI Bastacky, C Vrbin, S Raab. University of Pittsburgh, Pittsburgh, PA.
Background: Routine urine cytology (CY) evaluation is the standard method for surveillance of urothelial carcinoma (UC) of the bladder. Fluorescence in-situ hybridization (FISH) using the UroVysion system (UVS) is a molecular cytogenetic based, FDA approved system for screening and surveillance of UC. We present our experience with 218 patient samples to determine the comparative value of these two modalities.
Design: We performed a retrospective analysis of patients under surveillance for UC. The patients included for the study had concurrent CY, UVS and biopsy (BX). BX results were the gold standard for comparison. FISH testing was performed using commercial UVS kit. Standard published and widely accepted criteria for a positive UVS were used. Concordance of CY and UVS results with BX results was assessed and sensitivity and specificity of the two techniques was calculated.
Results: 218 patients had concurrent BX, CY and UVS. 34 patients had low grade UC (LGUC). CY was positive in 3/34 (8.8%) while UVS was positive in 9/34 (26.5%). 99 pts had high grade UC (HGUC). CY was positive in 42/99 (42.4%) while UVS was positive in 48/99 (48.5%). There were 13 pts with a positive CY, with concurrent negative BX. Concurrent UVS was performed on these 13 pts. 6 were positive, 5 were negative and 2 were inconclusive. 22 patients had a positive UVS and negative BX; 6 did have concurrent positive CY while the remainder had no cytologic or surgical confirmation of malignancy. Follow-up of the 16 patients with a positive UVS, without positive CX or BX, has not shown subsequent detection of cancer, although the follow-up is limited, ranging from less than 1 month to 15 months. Statistical evaluation was performed comparing CX and UVS with the BX evaluation. CX had an overall sensitivity of 0.338 and specificity of 0.857. UVS had an overall sensitivity of 0.415 and specificity of 0.750.
Conclusions: 1. Both UroVysion FISH testing and routine cytology have a significant false negative rate. They are both better at detecting HGUC than LGUC. Surveillance urinary cytology should be combined with concurrent biopsy, where clinically feasible. 2. The false negative cases might have chromosomal abnormalities other than those detected by UroVysion FISH. 3. UroVysion FISH has significant false positive results. These may subsequently convert to true positives, although our data does not provide any evidence to that effect.

646 Role of Urovysion™ Fluorescence In-Situ Hybridization (FISH) in the Evaluation of Atypical Urine Cytology from Patients under Surveillance for Recurrent Bladder Cancer

R Dhir, AV Parwani, R Balassanian, SI Bastacky, R Hrebinko, M Franks, K Cieply, C Vrbin, S Raab. University of Pittsburgh, Pittsburgh, PA.
Background: Routine urine cytology (CY) is used for surveillance of urothelial carcinoma (UC) of the bladder. UroVysion FISH testing (UVS) is an adjunct molecular modality, FDA approved for screening and surveillance of UC. UVS is clinically used expecting guidance for managing negative/ atypical CY. This study evaluates UVS in pts. with negative/atypical/ suspicious CY and its concordance with concurrent biopsy (BX).
Design: Retrospective analysis was done of pts. under surveillance for UC. Pts. included for the study had concurrent CY, UVS and BX. BX was the gold standard for comparison. UVS was performed using commercial UroVysion kit. UVS positivity was based on standard published and accepted criteria. The study set consisted of pts. with negative/atypical/suspicious CY results. UVS results on this set were evaluated. Concordance of UVS with BX was assessed.
Results: All 218 pts. had concurrent BX, CY and UVS. 160 CY assessments were negative (52), atypical (69) or suspicious (39). UVS was positive in 8/52 negative CY (15.4%); 3/8 cases were BX positive (1 LGUC & 2 HGUC); concordance rate 37.5%. UVS was positive in 15/69 atypical CY (21.8%); 8/15 cases were BX positive (4 LGUC & 4 HGUC); concordance rate 53.3%. UVS was positive in 21/39 suspicious CY (53.8%); 17/21 cases were BX positive (3 LGUC & 14 HGUC); concordance rate 81%. Overall, 133 cases had UC on BX. CY identified 45/133 cases (sensitivity 0.34, specificity 0.86). UVS identified 57/133 cases (sensitivity 0.42, specificity 0.75). CY identified 13 additional pts. with UC, without a positive BX. UVS had a false positive rate of 28.6% (16/56). Follow-up of these 16 pts. with positive UVS, without positive CY or BX, has not shown subsequent detection of cancer on limited follow-up (less than 1 month to 15 months).
Conclusions: 1. UroVysion FISH testing is fairly specific in identifying cases with UC that might have been missed on urine cytology. The concordance with biopsy increases with increasing cytologic suspicion, being maximal with the cases diagnosed as "suspicious for malignancy". 2. Biopsy seems to be best at detecting cancer and should be performed where clinically feasible and indicated. 3. UroVysion FISH has a high false positive rate. These false positives may subsequently convert to true positives, although our data does not provide any evidence to that effect.

647 Proteomic Changes in the PNI *In Vitro* Model Using Antibody Microarrays

Y Ding, H Dai, GE Ayala. Baylor College of Medicine, Houston, TX.
Background: Perineural invasion (PNI) is the major mechanism of prostate cancer spread outside of the prostate. Our previous studies have shown that prostate cancer cells interact with nerves, stimulating both to grow. In this study we used antibody microarrays to search the molecules involved in this interaction and to understand the mechanisms of this cancer-nerve interaction.
Design: Protein samples were obtained from the *in vitro* PNI model and controls. Du145 alone and Du145 + DRG was cultured in growth factor reduced Matrigel (BD Bioscience) and grown in RPMI 1640 medium contain 10% Nu serum. At day 8, the DRG was removed and cells were recovered by Dispase (BD Bioscience), and protein was extracted by antibody microarray buffer kit (Clontech). Equal amounts of protein from the Du145 or Du145 + DRG cell lysates were labeled by fluorescent Cy3 and Cy5 mono-reactive dye (Amersham biosciences). Unbound dye was removed by protein desalting spin columns (Pierce Biotechnology). Protein was then incubated with antibody microarray slides (Clontech500), washed, and slides scanned using a microarray scanner.
Results: A large number of proteins were over and under expressed in the co-culture models as compared to controls. We found that 5 proteins were under expressed (< 0.5 fold) and 8 proteins were over-expressed (> 2 folds) in the DRG/Du145 co-culture compared to the Du145 alone controls. See table 1.
Conclusions: Four categories of proteins changed in the PNI *in vitro* model(apoptosis, cell cycle, protein kinase and neurobiology). Several caveats can affect these results. Removal of DRG does not guarantee the removal of neurites, and these contain proteins

but no RNA. Therefore, we will cross-reference the antibody array results to the cDNA array results previously performed. Western blots and immunohistochemistry will also be used for confirmation. Further investigation is currently underway.

Table 1

Under expressed		
Gene names	Folds	Categories
Phospholipase(phosphoinositide-specific)	0.25	protein kinase
Caspase 7	0.3	apoptosis
PC4 and SFRS1 interacting protein 1	0.4	protein kinase
diacylglycerol kinase, theta 110 kDa	0.4	protein kinase
nitrooxide synthase 2A	0.5	cell cycle
Over-expressed		
MUPP1	3.3	protein kinase
CDC27	3.3	cell cycle
mitogen-activated protein kinase 5	2.5	protein kinase
protein tyrosine phosphatase, non-receptor type6	2.3	protein kinase
annexin A11	2.3	neurobiology
neuronal Shc	2	neurobiology
cell division cycle 25C	2	cell cycle
neurexin 1	2	neurobiology

648 Androgen Receptor Activity Is Elevated in Prostate Tumors with Decreased PMEPA1 Expression

A Dobi, K Masuda, L Xu, J Cullen, G Petrovics, B Furusato, H Li, S Srivastava. Center for Prostate Disease Research, Rockville, MD; United States Military Cancer Institute, Rockville, MD; Uniformed Services University, Rockville, MD.

Background: Increases in androgen receptor levels are sufficient to convert androgen dependent growth of prostate cancer cells to androgen independent growth. Androgen receptor (AR) levels can be elevated by impaired degradation of the AR protein. Compromised function of AR degradation pathway may contribute to prostate cancer progression. Previously, we reported the loss or decreased expression of PMEPA1 gene in primary prostate tumor specimens. PMEPA1 may function as gate-keeper of the proteasome degradation pathway by its ability to recruit an E3 ubiquitin ligas, and overexpression of PMEPA1 protein can decrease AR levels through the proteasome pathway. Interestingly, PMEPA1 gene can be regulated by AR that lead us to propose a feedback loop model revealing a circuit of AR homeostasis. This model predicts that loss of PMEPA1 expression would result in increases in AR functions.

Design: After laser capture microdissection of tumor and matching benign epithelium cells total RNA was isolated and expression levels were determined by quantitative Real-Time PCR. PMEPA1 and PSA expression relative to GAPDH levels were measured in 105 prostate cancer specimens and were normalized to expression levels in matching benign epithelium. Relative changes between PSA and PMEPA1 were expressed as PSA/PMEPA1 ratios. The ratio of tissue PSA to PMEPA expression was compared to serum PSA doubling time (PSADT) data (<3, 3-8.999, 9-14.999, and >= 15 months) using Analysis of Variance (ANOVA) with Duncan testing to determine statistical significance for each pair-wise comparison of means. Kaplan Meier estimation was used to model time to PSA recurrence by PSA:PMEPA1 strata using the median split to dichotomize this ratio.

Results: Decreases in PMEPA1 expression mirrored increases in AR activity as measured by the expression of PSA gene in laser capture microdissected tumor cells from 105 prostate cancer patients. Furthermore, men with PSADT < 3 months had significantly higher mean PSA:PMEPA expression (Duncan p = 0.0214) as compared to men with PSADT at or beyond 3 months.

Conclusions: Consistent with the proposed model dysregulation of the AR-PMEPA1 feedback loop may allow AR over function promoting the survival of prostate cancer cells. Therefore, PMEPA1 gene activation may be a novel therapeutic strategy in treating prostate cancer.

649 Expression of R- and E-Cadherins in Benign and Neoplastic Prostatic Epithelium

AE Dulau-Florea, J Sunkara, R Hazen, Y Zhong, N Xue, M Li. Montefiore Med Ctr, Bronx, NY; Albert Einstein Coll Med, Bronx, NY.

Background: R-cadherin (R-cad) is a member of cadherin family of calcium-dependent cell adhesion molecules. Animal studies have revealed that R-cad is highly expressed in the nervous system. However, its distribution in human normal tissue and neoplasms are largely unknown although limited data indicates that R-cad is down-regulated in human gastrointestinal cancers due to aberrant methylation. In vitro studies have also suggested that the expression of R-cad is reduced in some human epithelial cancer cell lines.

Design: We studied the expression of R-cad in human prostatic neoplasms and compared it to that of E-cadherin (E-cad). Tissue microarrays, including non-neoplastic epithelium (NE), prostatic intraepithelial neoplasia (PIN), and adenocarcinoma, were constructed from 113 prostatectomy specimens and analyzed immunohistochemically using monoclonal antibody against R-cad and E-cad.

Results: The immunohistochemical staining was semiquantitatively scored by multiplying the % of positive cells and staining intensity (0, 1, 2, 3). For R-cad, the mean scores for carcinoma, PIN and non-neoplastic epithelium were 91, 140, and 179, respectively, with p values of <0.0001 (carcinoma vs. normal), <0.0001 (tumor vs. PIN), and 0.0005 (PIN vs. normal). For E-cad, the mean scores for carcinoma, PIN and non-neoplastic epithelium were 84, 113, and 159, respectively, with p values of <0.0001 (tumor vs. normal), <0.0001 (tumor vs. PIN), and 0.0019 (PIN vs. normal). There was no correlation of immunostaining score with Gleason score, T stage, or margin status for either R-cad or E-cad.

Conclusions: R-cad is normally present in benign prostatic epithelium. Its expression is gradually reduced in PIN and adenocarcinoma, suggesting that the loss of R-cad may play a role in the development of prostate cancer. However, its expression in adenocarcinoma is not correlated with Gleason score, T stage and margin status. These findings are similar to those of E-cad in the current study.

650 Renal Oncocytoma: A Comparative Clinicopathologic Study and Fluorescent In-Situ Hybridization Analysis of 44 Cases with Long-Term Follow-Up

M Dvorakova, R Dhir, FA Monzon, SI Bastacky, KM Cieply, CR Sherer, TL Mercuri, AV Parwani. University of Pittsburgh Medical Center (UPMC), Pittsburgh, PA.

Background: Multiple clinical studies have confirmed that renal oncocytoma (RO) is a benign neoplasm with excellent prognosis. In diagnostically challenging cases of renal oncocytic epithelial neoplasms, fluorescent in-situ hybridization (FISH) is increasingly being used. Since the prognostic significance of FISH abnormalities is unknown, we investigated if FISH results correlate with survival data in a series of patients with RO.

Design: Clinicopathologic data and corresponding glass slides from 44 patients with primary nephrectomy for RO were reviewed. FISH analysis of formalin-fixed, paraffin-embedded sections was performed using centromeric probes for chromosomes 1, 2, 7 and 17 . Signals in at least 60 nuclei were counted for each chromosome in each tumor. Signal loss was considered significant if present in more than 30% of cells, gain if present in more than 20% of cells examined.

Results: The study population included 31 males and 13 females with a mean age of 65 years. The mean tumor size was 4.5 cm (range from 1 to 21 cm). Vascular invasion was present in 3 cases, and invasion into perinephric adipose tissue in 3 cases. None of the patients had evidence of metastatic disease at diagnosis. After a mean follow-up of 98 months (range from 1 to 293 months), 73.1% of patients were alive with no evidence of disease and 26.9% had died of other causes. None of the patients had disease recurrence nor developed metastases. FISH analysis indicated ROs had frequent loss of signal for chromosome 1 (50%), 17 (50%), 2 (34%), and 7 (18.2%). Signal gains were less common (chromosome 7 in 15.9% and 17 in 9.1%). More than 2 losses were observed in 43.2%, and 11.4 % showed loss of one signal in all chromosomes examined. A total of 20.5% cases did not show a significant losses or gains when compared to normal renal tissue.

Conclusions: Based on the current study and contrary to previous reports, chromosomal abnormalities in ROs are common with frequent loss of signal for chromosome 1 and 17, a feature that overlaps with chromophobe renal cell carcinomas and some other "unclassifiable" tumors. No association was found between overall patient survival and the extent and/or degree of chromosomal abnormalities. FISH results, even those showing significant chromosomal abnormalities, should not alter the primarily morphology-based diagnosis of RO.

651 The Use of Fluorescent In-Situ Hybridization and Immunohistochemistry To Differentiate Chromophobe Renal Cell Carcinoma from Renal Oncocytoma

M Dvorakova, R Dhir, FA Monzon, SI Bastacky, KM Cieply, MB Acquafondata, KA Fuhrer, AV Parwani. University of Pittsburgh Medical Center (UPMC), Pittsburgh, PA.

Background: Partial or total loss of chromosome 1 is the most common clonal chromosomal abnormality in renal oncocytomas (RO). Loss of other autosomes is described as infrequent, and fluorescent in-situ hybridization (FISH) is considered a useful tool for distinguishing RO from chromophobe renal cell carcinoma (ChRCC). So far, immunohistochemistry has played a limited role in the distinction of these two tumors. The goal of our study was to compare FISH results as well as caveolin-1 and parvalbumin immunohistochemistry on a series of ChRCCs and ROs.

Design: Formalin-fixed, paraffin-embedded tissue sections of 15 ChRCCs and 44 ROs were analyzed by FISH using centromeric probes for chromosomes 1, 2, 7 and 17. In addition, adjacent tissue sections were subjected to immunohistochemical evaluation using monoclonal antibodies against parvalbumin (1:4000, Sigma) and caveolin-1 (1:200, BD Transduction Laboratories). Cytoplasmic staining of more than 10% of tumor cells was considered positive.

Results: The FISH results are summarized in Table 1. Signal losses for two or more chromosomes were observed in 93.3% of ChRCCs compared to 43.2% of ROs. Signal losses for all chromosomes examined were detected in 54.5% of ChRCCs and 11.4% of ROs. Immunohistochemical analysis revealed that 86.7% of ChRCCs were positive for caveolin-1 as opposed to only 15.9% of ROs. No significant difference was found for parvalbumin (86.7% vs.85%).

Conclusions: FISH analysis revealed significant overlap in the chromosomal abnormality patterns amongst ROs and ChRCCs. Contrary to previous reports, not only ChRCCs but also ROs had a high prevalence of chromosomal abnormalities. Losses involved most frequently chromosomes 1 and 17 in both groups, further supporting the observation that these tumors represent a spectrum of neoplasia rather than two distinct entities. Furthermore, caveolin-1 proved to be a promising immunohistochemical marker that may aid in the differential diagnosis between these two neoplasms even in cases that shared similar chromosomal abnormalities.

FISH result	normal	loss of 1	loss of 2	loss of 7	loss of 17	gain of 7	gain of 17
ChRCC (n=15)	0	80%	80%	60%	93.3%	6.7%	6.7%
RO (n=44)	20.5%	50%	34.2%	18.2%	50%	15.9%	9.1%

652 ProEx™ C (Mcm2 + Topoisomerase II-α) Expression in Urinary Bladder as a Marker of Urothelial Carcinoma

HS Edmunds, V Padmanabhan. Dartmouth Hitchcock Medical Center, Lebanon, NH.

Background: ProEx™C targets Minichromosome maintenance protein 2 (Mcm2) and Topoisomerase II-α (an essential nuclear enzyme); proteins over-expressed in aberrant S-phase induction. MCM proteins (a family of 6 highly conserved and homologous proteins) form a part of the pre-replication complex that licenses DNA replication (increased expression reported in dysplasia and neoplasia). ProEx™ C has been shown to be a useful adjunct in distinguishing CIN1 and CIN2/3 in cervical biopsies. ProEx™ C has hitherto not been studied in the urinary bladder which is the aim of the current study.

Design: Computer-assisted search of archived pathology material between 2005 and 2006 for urinary bladder biopsies/ transurethral bladder resections was performed. Morphology was used as the gold standard in the diagnosis of bladder lesions. Immunohistochemistry was performed using standard techniques with the primary antibody ProEx™C (TriPath Imaging, Inc. Burlington, NC). Slides were scored as percent positive urothelial nuclei/ total number of urothelial cells; initially independently by 2 observers and together with a consensus score. Data was entered in Excel work sheet for analysis.

Results: Of 76 cases (21 Female; 55 Male), ages ranged from 41- 90 years (Mean: 70.06 yrs), 116 areas/ sections were scored with the following diagnosis:

Results

Diagnosis	Number of cases	Mean score % (Range)
Benign Urothelium	12	2.75 (0-5)
Reactive atypia	8	55.6 (0-80)
PUNLMP	7	10.7 (2-40)
Low grade Urothelial carcinoma (LG)	40	25 (2-90)
High grade Urothelail carcinoma, Non invasive (HGNI)	17	46.1 (10-90)
Carcinoma in situ (CIS)	5	83 (75-90)
High grade Urothelial carcinoma, Invasive (HGI)	27	74.07 (35-95)

At or above a score of 35%, sensitivity of ProEx™ C in the diagnosis of high-grade urothelial carcinomas (HGNI, HGI and CIS) was 88% and the specificity was 75%.

Conclusions: Percent positive cells progressively increased from benign (minimal staining) to PUNLMP, LGNI, HGNI/ CIS and HGI (most cells stained) with the exception of reactive atypia, suggesting a step-wise disease progression of carcinogenesis. Nine of 40 cases in the LGNI category showed staining above 35% which may represent transformation at the nuclear/ DNA level; cells in transition to a higher grade lesion, not recognizable at the morphological level. At 35% and above, most HG bladder cancers could be detected. ProEx™ C is a very useful adjunct to morphology in the diagnosis of urinary bladder cancers.

653 Morphologic Heterogeneity of High-Grade Prostatic Adenocarcinoma Corresponds to Molecular Diversity

E Efstathiou, S Wen, CJ Logothetis, KA Do, TJ McDonnell, P Troncoso. UT MD Anderson Cancer Center, Houston, TX.

Background: High-grade prostate cancer (PCa) is a morphologically heterogeneous disease, which displays significant clinical diversity. To determine if the morphologic heterogeneity is linked to biologic differences, we performed a survey of candidate pathways implicated in PCa progression.

Design: We created a tissue microarray from 16 radical prostatectomy specimens (RPS) (Gleason Score ≥7) comprising the following morphologic patterns: cribriform (10 RPS, 56 cores), fused glands (15 RPS, 94 cores), single cells/clusters/cords (10 RPS, 56 cores) and intraductal spread (IDS) (10 RPS, 45 cores). The immunohistochemical expression of three groups of markers related to angiogenesis (bFGF, IL-6, IL-8, PDGF-A, VEGF), broader stromal-epithelial interactions [β-catenin, e-cadherin, MMP-2, MMP-9, TGF-β, TNF-α, hedgehog signaling (sonic hedgehog, smoothened, Gli2)] and the epithelial compartment (active caspase 3, bcl2, bcl-xl, Ki67, p53) was compared.

Results: Hierarchical plotting (vide infra) revealed non-random clustering of marker expression in IDS and cribriform compared to other patterns. This molecularly derived grouping parallels the morphologic similarity in these patterns. Mixed model methodology confirmed that IDS and cribriform exhibit increased proportion of cells expressing markers of angiogenesis and stromal epithelial interaction, including the sonic hedgehog ligand, bFGF, VEGF, MMP-9 and TNF-a. Smoothened (the signaling intermediate of hedgehog signaling) was expressed at higher intensity in cribriform and IDS. Expression of the anti-apoptotic gene, bcl-xl, was increased in IDS. Proliferative fraction (Ki67) was higher in cribriform than in fused glands and similar to single cells and IDS.

Conclusions: These preliminary findings support the hypothesis that morphologic heterogeneity in high grade PCa corresponds to meaningful differences in expression of candidate genes. This may be linked to the heterogeneity of the clinical phenotype. Further study is warranted to explore potential prognostic and predictive implications.

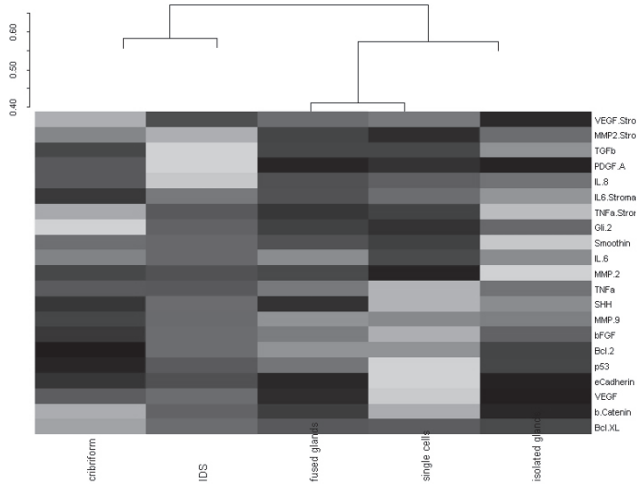

654 Small Foci of Gleason Score 3+3=6 in Modern Needle Biopsy Protocols: Pathologic Outcomes at Radical Prostatectomy

JI Epstein, SW Fine. Johns Hopkins Hospital, Baltimore, MD; Memorial Sloan Kettering Cancer Center, NY, NY.

Background: Modern PSA screening has led to the detection of increasingly smaller foci of prostatic adenocarcinoma on needle biopsy (NB). Few large series have addressed the radical prostatectomy (RP) pathology of patients with these NB findings. The effect of total # of biopsy cores on predicting the pathologic outcomes in this group has not been well studied.

Design: Prostate NB of 1455 patients who underwent RP in 2002-03 were reviewed to determine whether they contained a single small focus of carcinoma (<5%) on one biopsy core only. Findings were correlated with pre-op PSA levels, # of needle biopsy cores taken, and RP Gleason score (RPGS) and pathologic stage (pT2=organ confined; pT3a=extra-prostatic extension and seminal vesicles (SV) negative; pT3b (SV positive).

Results: 116 (8%) of patients constituted the study group, with a mean age of 56.5 years (range: 38 to 70) and mean PSA of 6.2 (range: 0.1 to 32.6). RPGS and stage for these 116 patients are summarized in the table below.

Total (n=116)	pT2	pT3a	pT3b
GS ≤ 6 (n=94)	86	7	1
GS = 7 (n=19)	13	5	1
GS = 8-10 (n=3)	1	1	1

86/116 (74.1%) had organ-confined RPGS 6 tumor. Of patients with RPGS 6, 86/94 (91.5%) had organ-confined disease. For cases with RPGS 7, the incidence of organ confined disease was only 13/19 (68.4%). The mean pre-operative PSA was 6.1-6.2 ng/ml for RPGS 6-7 and 8.0 ng/ml for RPGS 8-10. Serum PSA also increased from pT2 to pT3 disease (5.9 ng/ml to 7.8 ng/ml). For 83 cases, the total # of biopsy cores was available. For patients with < 8 cores, 4/11 (36.4%) had RPGS > 6, as opposed to 12/60 (20%) of those with ≥ 8 cores. Similarly, in the group with < 8 cores, 4/11 (36.4%) had non-organ-confined disease, whereas pT3 disease was found in only 7/56 (12.5%) of those with ≥ 8 cores (p=0.016).

Conclusions: Three quarters of men with a single small focus of Gleason score 3+3=6 on biopsy have RPGS ≤ 6 and organ-confined disease, which is close to 100% curable. With less sampling on biopsy, there is a greater likelihood that a small focus of Gleason score 6 on biopsy is not as representative of the entire tumor with a relatively increased risk of upstaging and upgrading at prostatectomy. Modern biopsy schema with better sampling (i.e. ≥ 8 cores) showing a single small focus of Gleason score 6 more accurately predict organ-confined disease at RP.

655 Lymphovascular Invasion in Prostatic Adenocarcinoma

D Ertoy-Baydar, B Baseskioglu, H Ozen, PO Geyik. Hacettepe University Hospital, Ankara, Turkey.

Background: Whether lymphovascular invasion is an independent prognostic factor for disease progression in prostate cancer is still controversial. We retrospectively investigated lymphovascular involvement as a predictive factor for biochemical failure following radical operation.

Design: The histological sections of radical prostatectomies from 71 prostatic adenocarcinoma patients were reviewed for lymphovascular invasion. Clinical follow-up data were available on 67 cases. Mean follow-up was 65 months (range 4 to 145). Multivariate analysis was performed using the logistic regression model.

Results: Lymphovascular invasion (LVI) was identified in 11 cases (15.5%). Univariate analysis showed a significant association between lymphovascular invasion and advanced pathological stage, higher Gleason score, positive surgical margins, extraprostatic extension, seminal vesicle invasion and lymph node metastasis (each p <0.05). Logistic regression analysis demonstrated that LVI was a strong and independent predictor for disease recurrence (p=0.23), when considered with grade, pT, lymph node involvement, age at diagnosis, preoperative PSA levels and positive margins.

Conclusions: Lymphovascular invasion can be identified in approximately 15.5% of prostate cancer cases. LVI is associated with established markers of biologically aggressive disease and it is an independent risk factor for PSA recurrence.

656 Telomere Shortening Correlates with Short Relapse-Free Survival Time in Prostate Adenocarcinoma

D Ertoy-Baydar, H Ozen, B Gurel, O Saracbasi, PO Geyik, AM De Marzo. Hacettepe University Hospital, Ankara, Turkey; The Johns Hopkins University, Baltimore, MD.

Background: Telomere shortening can be one of the ways that cause chromosomal instability in the pathogenesis of prostatic carcinoma. In the current study, we evaluated the telomere length in prostate tumor and normal tissue, and its association with time to prostate cancer recurrence.

Design: Tissue microarrays were constructed from the paraffin blocks of radical prostatectomy specimens. Sections were hybridized with a Cy3-labeled telomere-specific peptide nucleic acid probe, and counterstained with 4-6-diamidino-2-phenylindole. Telomere length, proportional to probe fluorescence intensity, was visually evaluated, with stromal cells and lymphocytes serving as internal controls. Telomere lengths of the neoplastic cells and normal glands were compared. Gleason scores of the cases ranged from 6-9, and pathological stage ranged from T2N0Mx to T3BN1. The patients' age, serum PSA values and clinical follow-up information were obtained from the hospital records. Relationship between telomere shortening and prognostic factors were analyzed.

Results: 61 primary tumors and non-neoplastic prostate tissue from 61 subjects were studied. The majority (41/61) of prostate cancers displayed abnormally short telomeres. In contrast, in 55/61 cases, telomeres of normal glands were consistently equivalent in length to reference stromal cells. Univariate analysis revealed direct association

between telomere shortening in tumor and lymphovascular invasion (p=0.028) and interestingly inverse correlation with Gleason scores (p=0.029). Short telomeres appeared as independent factor for biochemical recurrence-free survival time in addition to serum PSA, pathological stage and lymphovascular invasion in multivariate Cox regression analysis (p=0.035).

Conclusions: In agreement with previous results, the majority (80.3%) of primary prostate cancers displayed abnormally short telomeres. This pilot study indicated that with decreased telomere length detected by FISH may be predictor of time to disease recurrence in prostatic carcinoma patients.

657 Immunohistochemical Analysis of PTEN Expression in Radical Prostatectomies

D Ertoy-Baydar, H Ozen, O Saracbasi, AM De Marzo. Hacettepe University Hospital, Ankara, Turkey; The Johns Hopkins University, Baltimore, MD.

Background: A tumor suppressor gene, PTEN is located on the q23.3 region of chromosome 10, one of the most frequently deleted regions in prostate. Mutation and down-regulation of the PTEN gene have been detected in various human cancers including that of the prostate. We performed an immunohistochemical study of PTEN protein in malignant and non-neoplastic prostate tissue. Pten status, its relation with prognostic factors and the disease progression were investigated.

Design: Two tissue microarrays constructed by 0.6 mm cores from 71 radical prostatectomy specimens was used. They contained four cores from neoplastic and additional four cores from corresponding non-neoplastic regions. Gleason score ranged from 6-9, and pathological stage ranged from T2N0Mx to T3BN1. A rabbit anti -Pten antibody was used for immunohistochemistry. Staining was scored visually taking percent negative, weak, moderate and strong positivity into consideration. The patients' age and serum PSA values were obtained from the hospital records.

Results: 488 cores were evaluated. Of these, 245 represented the tumor (belonging to 69 cases). Normal epithelium was present in 63 cases. The secretory layer of normal prostatic glands showed high labeling index in the majority. Atrophy and inflammation lead to decrease in the intensity and the extent of staining. 43.5% of adenocarcinomas (n=30) did not express Pten. Univariate analysis revealed that decreased expression and absence of Pten correlated with surgical margin positivity ($p<0.05$). No relation between Pten status and the other well-known clinicopathological prognostic factors were found.

Conclusions: Pten was strongly expressed by secretory cells in normal prostatic glands. Staining was decreased in inflammation, atrophy and most prostate carcinomas. Loss of expression in tumor correlated with positive surgical margins in radical prostatectomy specimens.

658 Effects of Tissue Processing on Biomarker Analysis in Prostate Needle Biopsies: A Multi-Institutional Study

SW Fine, B Trock, VE Reuter, G Ayala, JC Cheville, P Fearn, RB Jenkins, BS Knudsen, M Loda, GJ Netto, J Said, RB Shah, J Simko, P Troncoso, LD True, XJ Yang, MA Rubin, AM DeMarzo. MSKCC, NY; JHU, Baltimore; BCM, Houston; Mayo, Rochester; UWASH/FHCRC, Seattle; Harvard/DFCI, Boston; UCLA, L.A.; UMICH, Ann Arbor; UCSF, S.F.; MDACC, Houston; NWU, Chicago.

Background: Prior studies have suggested that variation in tissue fixation/processing (TFP) may affect prostate cancer (PC) biomarker analysis and be a source of inconsistency across studies of an individual biomarker. Development and validation of prognostic markers for PC increasingly requires multi-institutional collaboration. Inter-institutional variability of TFP and the effect of pre-analytic factors on prostate needle biopsy (PNB) biomarker studies is not known.

Design: Pathologists from 11 centers holding SPORE grants for PC research submitted TFP protocols and 1 H&E / 10 unstained sections of PNB with both cancer (CT) and normal tissue (NT) to central sites. Immunohistochemical (p27, 34βE12, AMACR, Ki-67) and genetic analyses (FISH Chromosome 8) were performed and results analyzed against processing parameters.

Results: Among 11 sites, total processing times ranged 70-570 minutes, with widely varying times/temperatures for post-fixation, dehydration, xylene and paraffin infiltration processing stages. Sections of 4 to 13 cases were submitted per site. Preliminary analyses: 1. p27: no significant difference (SD) in mean % of NT with 3-4+ staining intensity (SI) between sites; 2. 34βE12: SD in mean % of NT with 3+ SI (heavily influenced by low % at one site); 3. AMACR: SD in mean % of CT with 3-4+ SI; 4. Ki-67: SD in ln(%) of tumor cells staining; 5. FISH Chromosome 8: signals required for chromosomal gain/loss evaluation were detectable across sites. Significant associations: A. ↑minimum fixation time and ↓p27 SI (NT), ↓AMACR SI (CT); B. ↑maximum fixation time and ↑34βE12 SI (NT); C. ↑dehydration time and ↑p27 SI (NT), ↑AMACR SI (CT); D. ↑ infiltration temperature and ↓ln(%) cells staining with Ki-67.

Conclusions: There is wide variation in TFP protocols among our centers. Nonetheless, near-equivalent staining may be achieved for markers of NT such as p27 and 34βE12 across sites. For markers such as AMACR, differences seen may reflect pre-analytic factors and/or tumor biology. Additional studies are in progress to determine the true effects of processing using specimens in which pre-/post-processing variables may be controlled/rigorously recorded.

659 Are There Morphologic Correlates of Prostate Cancer Associated with TMPRSS2-ERG Molecular Abnormalities?

SW Fine, A Gopalan, M Leversha, SK Tickoo, HA Al-Ahmadie, S Olgac, W Gerald, VE Reuter. Memorial Sloan Kettering Cancer Center, NY, NY.

Background: Recent studies have shown that TMPRSS2-ERG fusion is common in prostate cancer, varying from 30-70% of cases in published series. The molecular abnormalities include formation of a fusion gene, in a majority of cases due to deletion of a region on chromosome 21. While the histologic features of these tumors have not been elucidated, it has been suggested that these molecular genetic events may be associated with distinct morphologic characteristics, such as cribriform architecture and the presence of blue mucin.

Design: Blinded histologic review was conducted on 67 cases comprising two tissue microarrays (TMA) on which fluorescent in situ hybridization (FISH) had previously been performed to delineate molecular abnormalities.

Results: By FISH, 37/67 cases showed molecular abnormalities, including 21 deletions, 5 translocations, and 11 cases with other abnormalities. The other 30 cases were negative on FISH analysis. The morphologic findings are summarized in the table below.

	Translocation (n=5)	Deletion (n=21)	Other (n=11)	Negative (n=30)
Cribriform/Glomerulation	1	3	4	9
Blue Mucin	3	9	3	11

8/37 (16.7%) cases with and 9/30 (30%) cases without molecular abnormalities showed cribriform glands or glomerulations. Intraluminal blue mucin was present in 15/37 (40.5%) cases with and 11/30 (36.7%) cases without genetic events. Overall, 19/30 (63.3%) cases without FISH abnormalities showed no specific morphologic features. Cribriform glands/glomerulations were present in 8/17 cases with molecular changes and 9/17 FISH negative cases.

Conclusions: In this analysis, we observe that TMPRSS2-ERG-related abnormalities do not correlate with specific tumor histology. Similarly, cribriform architecture is seen equally in cases with and without these genetic events. These findings suggest a lack of association between FISH-detected molecular changes and these morphologic findings. Further studies in larger cohorts of tissue are in progress to confirm these observations.

660 Biochemical Recurrence in Low Grade, Low Stage Prostatic Adenocarcinoma at Radical Prostatectomy: A Multi-Institutional Retrospective Analysis

SW Fine, TM Wheeler, VE Reuter, JI Epstein. Memorial Sloan Kettering Cancer Center, NY, NY; Baylor College of Medicine, Houston, TX; Johns Hopkins Hospital, Baltimore, MD.

Background: Tumor grade, stage, and margin status are important prognostic parameters for prostate cancer (PC) removed by radical prostatectomy (RP). The incidence of biochemical recurrence (BCR) in patients with low grade, low stage disease (LGLS) has not been well studied. LGLS is defined as RP Gleason score (GS) ≤ 6 with organ-confined (OC), negative margins (M-), and negative nodes.

Design: 3 PC centers were searched for men with RP showing LGLS disease and subsequent BCR. All available original slides were obtained and reviewed by genitourinary pathologist(s) at each institution.

Results: A total of 19,545 men underwent RP (1983-1997 Institution #1 1,165 RPs; 1983-2005 Institution #2 5,256 RPs; 1983-2005 Institution #3 13,124 RPs). A total of 7,720 men had LGLS disease. 110 patients developed PSA recurrence following an RP diagnosis of LGLS PC. Upon review, 31 cases had been incompletely submitted precluding definitive assessment of RP GS, stage, and margin status, while an additional 13 entirely-submitted RP had missing slides. The table below summarizes the findings by institution for the remaining 66 men.

	Institution #1	Institution #2	Institution #3	Total
**GS<or=6, OC, M-	4	4	12	20
GS>6, OC, M-	4	5	18	27
GS<or=6, EPE, M-	0	1	3	4
GS<or=6, OC, M+	0	1	2	3
GS>6, EPE, M-	0	7	4	11
GS>6, OC, M+	0	1	0	1

**True LGLS cases with BCR

Only 20/66 (30.3%) cases met criteria for LGLS with BCR. 27/66 (40.9%) cases were excluded from the LGLS category based on GS alone, with 20 GS 3+4= 7 and 7 GS 3+3=6 with tertiary Gleason pattern 4. Exclusion based on extraprostatic extension (EPE) or margin positivity (M+) alone occurred in 4/66 (all focal) and 3/66 men respectively. 12/66 (18.2%) men had both GS > 6 and either EPE (n=11; 7 focal, 4 established) or M+ (n=1). Benign glands at a margin were observed in 2 cases of LGLS with BCR.

Conclusions: True LGLS with BCR is exceedingly rare, representing 0.1% of cases in this series and 0.3% of LGLS disease. The majority of our excluded cases predated 1995. Modern Gleason grading and staging more accurately identifies adverse grade, stage, and margins such that when current RP reports note LGLS, men can be told that they are virtually cured of disease. Finally, although not routinely recorded in RP reports, benign glands at margins in the setting of LGLS disease may occasionally account for BCR.

661 Characteristics and Clinical Implications of Metastases with Extranodal Extension in a Surgically Treated Prostate Cancer Population

A Fleischmann, S Schobinger, R Markwalder, M Schumacher, F Burkhard, GN Thalmann, UE Studer. University of Bern, Bern, Switzerland.

Background: To evaluate histopathological prostate cancer parameters and survival in patients with and without extranodal extension of metastases (ENE).

Design: Analysis includes 102 patients (median age: 65 years) with clinically organ confined disease undergoing extensive standardized bilateral lymphadenectomy at the time of radical prostatectomy and revealing nodal metastases on histological examination. They had no immediate androgen deprivation.

Results: The median number of examined nodes was 21 (range: 9 - 68), median follow up was 92 months. Median recurrence free (RFS), disease specific (DSS) and overall survival (OS) was 23, 128 and 119 months, respectively. ENE was observed in 71 patients (70%) and in a median of 84% of their metastases. Patients with ENE had significantly more, larger and more poorly differentiated nodal metastases, paralleled by significantly larger, advanced stage primaries with higher Gleason scores. ENE defined a subgroup with significantly decreased RFS (p=0.038) and OS (p=0.037) and

a trend toward adverse DSS (p=0.072) having 5 year RFS, DSS and OS probabilities of 26%, 74% and 72%, respectively, compared to 36%, 88% and 85% for patients without ENE. In multivariate analyses only the number of positive nodes (<=2 vs. >2) and the diameter of the largest metastasis (<6 mm vs. >=6 mm) were independent predictors of RFS and DSS/OS, respectively.
Conclusions: While ENE univariately predicts survival, only variables reflecting nodal tumor burden are independent risk factors. However, the common practise of limited lymphadenectomy may not provide an adequate estimation of nodal tumor burden. High-risk cases may additionally be identified by ENE, which should therefore be reported together with the nodal tumor burden.

662 Renal Tubular Epithelial Dysplasia in Sporadic Clear Cell Renal Cell Carcinoma (CCRCC) and CCRCC with Associated Von Hippel Lindau (VHL) Disease

AB Frey, C Nijwaji, M Che, W Sakr, D Grignon. Karmanos Cancer Institute, Detroit Medical Center and Wayne State University, Detroit, MI.
Background: Intratubular epithelial dysplasia has been reported in normal kidney tissue adjacent to human CCRCC in up to 20% of cases and has been proposed as a possible precursor lesion. The term renal intraepithelial neoplasia (RIN) has appeared in the literature. GP250 (carbonic anhydrase [CA]) expression is elevated in CCRCC. This study utilized CA to evaluate the concept of intratubular dysplasia.
Design: From the Department of Pathology files, 64 cases of sporadic CCRCC and 3 cases of CCRCC in patients with VHL disease treated by radical nephrectomy were identified. Slides with benign renal parenchyma adjacent to or distant from the tumor were evaluated for renal tubular dysplasia as was defined (the presence of cells containing enlarged nuclei at least twice as large as surrounding nuclei, with the nuclear enlargement not attributable to inflammatory or reactive processes). In 48 sporadic cases and all VHL cases, 1 – 3 blocks containing tumor and adjacent normal tissue were analyzed for CA expression by immunohistochemistry.
Results: The sporadic cases included 33 male and 31 female patients ranging in age from 34-88 years (mean, 60.1 years). The VHL cases included 2 male patients, ages 36 and 54 years and one female patient, age 55 years. In nine cases of sporadic CCRCC (18.8%; 2/33 males [6.1%], 7/31 females [22.6%] one to five tubules adjacent to the tumor tissue each contained one to six cells with enlarged nuclei, but that did not meet the previously defined criteria for dysplasia. In the VHL cases, occasional tubules were lined by cells with enlarged nuclei and clear cytoplasm similar to CCRCC. In all cases stained for CA CCRCC showed intense positive immunoreactivity. Staining was cytoplasmic and concentrated adjacent to the cell membranes. In the 3 VHL cases clear cells in adjacent tubules showed similar positive immunoreactivity. None of the normal tubules in the 48 sporadic cases stained positive for CA.
Conclusions: These findings show that, in normal renal parenchyma adjacent to CCRCC associated with VHL disease, early neoplastic foci can be identified by high CA expression. Although minute foci of nuclear size variation exists adjacent to sporadic CCRCC, the absence of associated overexpression of CA argues against the concept that this represents a pre-neoplastic "dysplasia." Use of the term renal intraepithelial neoplasia (RIN) is not justified for these changes.

663 The Relationship of Preoperative PSA Levels to Prostatic Weight and Tumor Size

B Furusato, I Rosner, D Osborn, J Cullen, Y Chen, C Davis, I Sesterhenn, D McLeod. Armed Forces Institute of Pathology, Washington, DC; Walter Reed Army Medical Cetner, Washington, DC; Center for Prostate Disease Research, Bethesda, MD.
Background: Estimation of prostate size at the time of biopsy is routine and helpful in diagnostic and treatment procedures. The objective of this study is to determine if there is a relationship between preoperative PSA level, prostate weight and tumor size in radical prostatectomy (RP) specimens.
Design: 717 consecutive hormone naïve RP specimens obtained from the Urology Service at Walter Reed Army Medical Center (WRAMC) were processed as whole-mounts at the Armed Forces Institute of Pathology. They were sectioned at 2.2-2.3 mm intervals and entirely embedded in paraffin. Each tumor was graded separately according to the WHO/Mostofi and Gleason system, staged according to the TNM system, and measured in 3 dimensions (apex to base, right to left and anterior to posterior). The volume of each tumor was calculated using the largest dimension in each direction. The volume did not include the shrinkage factor due to fixation and embedding in prostate with more than one tumor the total tumor volume was the sum of all tumor volumes. Prostatic weight included prostate and seminal vesicles. Clinical information was obtained from Center for Prostate Disease Research (CPDR).
Results: The mean age was 61 years, and mean preoperative PSA was 6.9 ng/ml. Mean prostate weight of the RP specimen was 42.6 gm. Mean index tumor volume was 5.7 cm^3 and mean total tumor volume was 6.7 cm^3. Up to 50 gm, there was a correlation between preoperative PSA level, tumor volume and prostate weight. With increasing PSA levels, there was a parallel increase in prostate weight and tumor volume. However, when the prostate weight exceeded 50 gms, there was positive correlation between preoperative PSA level and prostate weight but an inverse correlation of tumor volume with PSA levels and prostate weight.
Conclusions: In prostates exceeding 50 gms, preoperative PSA levels correlate with the prostatic weight but not with the tumor volume. In prostates less than 50 gm, the preoperative PSA level appears to correlate with both increase in prostate weight and tumor size.

664 Clinico-Pathologic Aspects of Follow-Up on Small Tumor Volume Prostate Cancer after the Radical Prostatectomy at Walter Reed Army Medical Center

B Furusato, D Osborn, I Rosner, J Cullen, C Davis, JW Moul, S Srivastava, D McLeod, I Sesterhenn, A Allen. Armed Forces Institute of Pathology, Washington, DC; Walter Reed Army Medical Center, Washington, DC; Duke University, Durham, NC.
Background: To determine the rate of "serum prostate specific antigen (PSA) recurrence" defined as two consecutive postoperative serum PSA levels of 0.2 ng/ml or greater in patients with tumor volumes of less than 0.5 cc following the radical prostatectomy.
Design: 717 patients underwent radical prostatectomy for localized prostate cancer at the Urology Service of Walter Reed Army Medical Center. Patients hormonally treated prior to surgery were excluded. Fifty of these had total tumor volumes less than 0.5 cc and minimum of 12 months follow up. All specimens were totally embedded. Biochemical recurrence was defined as two consecutive PSA levels equal to or greater than 0.2 ng/ml.
Results: Median followup was 58 month (range 12 to 117 month), mean age at the time of surgery 61 years old (range 41-74 years old) and mean preoperative PSA was 4.9 ng/ml (range 0.4-19.7 ng/ml). Mean total tumor volume was 0.20 cc (range 0.02-0.45 cc). Most tumors were multifocal (mean total number of tumors was 4). All cases were organ confined (pT2) and surgical margin negative. Nineteen cases had benign glands in the surgical margin. Gleason scores were: 4 (1 case), 5 (9 cases), 6 (37 cases), 3+4 (2 cases). In 1 case the tumor was too small for reliable Gleason scoring. In 5 of 50 cases PSA recurrence up to 5.4 ng/ml were observed. These PSA levels had an undulating pattern. All of these cases were well and/or moderately differentiated tumors (Gleason score 6). In 3 of 5 cases benign glands extended into the surgical margin.
Conclusions: Five of 50 cases had "PSA recurrence". In 3 of the 5 patients, capsular incision resulted in benign glands being located in the margins, which may have explained the "PSA recurrence". However, in the other 2 patients, no pathological parameters could explain these measurable PSA levels. The explanation for this is unclear and further studies indicated.

665 Do Prostatic Transition Zone Tumors Have a Distinct Morphology?

JJ Garcia, HA Al-Ahmadie, SK Tickoo, A Gopalan, VE Reuter, SW Fine. Memorial Sloan Kettering Cancer Center, NY, NY.
Background: Previous studies have proposed that the well-differentiated component of tumors arising from the prostatic transition zone (TZ) demonstrates distinct morphologic features. More specifically, it has been suggested that glands of variable size comprised of tall columnar cells with basal nuclei and clear to pale pink cytoplasm (TZ-L) are diagnostic of TZ tumors. However, the specificity of these findings has never been further evaluated.
Design: In a recent review, we identified a large number of peripheral zone (PZ) and TZ tumors with dominant masses located anterior to the prostatic urethra. Three investigators, including an oncologic pathology fellow and two dedicated genitourinary pathologists, examined the histologic features of 146 such tumors in entirely submitted, whole-mounted radical prostatectomies to identify the prevalence of TZ-L in tumors of both zones of origin. Tumors were scored on a scale of 0 to 4, with 0 = no evidence, 1 = 1-25%, 2 = 26-50%, 3 = 51-75%, and 4 = >75% of TZ-L.
Results: 63 tumors of TZ origin and 73 tumors of PZ origin were included in this study. TZ-L scoring is summarized in the table below.

TZ-L Score by Zone of Origin

	0	1	2	3	4
Transition Zone (n=63)	7	13	12	24	7
Peripheral Zone (n=73)	36	20	12	5	0

31/36 (86.1%) cases with TZ-L scores of 3-4 were of TZ origin, accounting for 31/63 (49.2%) of TZ tumors. 36/73 (49.3%) of PZ tumors showed no TZ-L, in contrast with 7/63 (11.1%) of TZ tumors. Of the 37 PZ tumors showing some TZ-L, 17 (23.3%) had scores of 2-3 or >25%. In both TZ and PZ tumors, when TZ-L accounted for the dominant tumor histology (scores 3 to 4), darker glands of more typical acinar adenocarcinoma were often seen at the periphery. In contrast, when TZ-L was present more focally (scores 1-2), these glands tended to be admixed with small glands bearing dark cytoplasm.
Conclusions: Absence of TZ-L is greater than four times as common in anterior PZ tumors as in TZ tumors in this series. Tumors demonstrating >50% TZ-L are very likely of TZ origin, however, dominant (>50%) TZ-L morphology occurs in only 49.2% of TZ tumors. Importantly, nearly one-quarter of anterior PZ show >25% TZ-L morphology. Given the lack of specificity of TZ-L for TZ tumors, caution should be exercised in assigning zone of origin based on TZ-L in limited samples, such as prostate needle biopsy.

666 Histological Correlations between Core Biopsies and Radical Prostatectomies

M Garmendia, C Etxezarraga, J Bilbao, FJ Bilbao, A Gaafar, JI López. Hospital de Basurto, Basque Country University (EHU/UPV), Bilbao, Bizkaia, Spain; Basque Country University (EHU/UPV), Leioa, Bizkaia, Spain.
Background: A wide spectrum of treatment modalities may be undertaken in prostate cancer depending upon clinical staging, PSA levels, and histological features on core biopsies (CB). We evaluate the correlation between histological data found in CBs and in their respective radical prostatectomies (RP) seeking predictive parameters that may help in making therapeutic decisions.

Design: Over a 8-year period (1998-2005), 363 RPs have been performed in our Institution following strict clinical criteria. A number of histological findings detected in their respective CBs [number of tumour foci, total millimetres of cancer, tumour bilaterality, Gleason Index (GI), perineurial invasion, and high grade PIN (HGPIN)] were correlated (Spearman's rho) with several microscopic data found in RPs [pT category, GI, PI, vascular invasion (VI), margin status (MS)].
Results: The average of tumour foci and millimetres of cancer in CBs were 2.5 (range 1-7) and 9.7 mm (range 0.5-58 mm) respectively. Bilateral involvement and HGPIN were detected both in 30% of CBs. pT distribution in RPs was 77 pT2a, 197 pT2b, 46 pT3a, 37 pT3b and 4 pT4. VI and positive MS were detected in 3.8% and 28.7% of RPs respectively. RPs showed a higher GI ($p<0.001$)and more frequent PI ($p>0.001$) than CBs.

	CB	RP
<7	162	93
3+4	108	154
4+3	30	46
>7	45	63
PI	79	229

Spearman's test showed medium intensity correlations between these parameters.

	pT	GI	PI	VI	MS
TM	0.374	0.368	0.283	0.221	
NF	0.369	0.219	0.258		0.160
BI	0.344	0.160	0.209		
HGPIN	0.184				
GI	0.315	0.480	0.166		
PI	0.388	0.281			0.163

GI: Gleason Index, PI: Perineurial Invasion, VI: Vascular Invasion, MS: Margin Status, TM: Tumor Millimeters, NF: Number of Foci, BI: Bilateral involvement
Conclusions: CBs provide histological findings that correlate with parameters of prognostic importance in RPs. Among them, the amount and extent of the neoplasm and the presence of HGPIN and perineurial invasion are the most important.

667 Expression of Platelet Derived Growth Factor Receptor α and β in 175 Renal Cell Neoplasms Using Tissue Microarrays

A Gaspa, A Petit, I Nayach, B Mellado, X García-Albéniz, C Mallofré. Hospital Clinic, Barcelona, Spain.
Background: Platelet derived growth factor receptors (PDGFR) alfa and beta are a transmembrane tyrosin kinase receptors that are involved in cell growth and survival, among other functions. Addicionaly, PDGFR beta has been involved in tumoral angiogenesis. Determining the expression of this protein in different renal cell carcinomas subtypes is interesting due to the potencial therapeuthic use of tyrosin kinase inhibitors, a new kind of drugs which are under clinical trials. The expression of PDGFR in renal cell neoplasms (RCN) has not been extensively studied in vivo although it has great interest since there is no effective treatment for patients with metastatic or recidivant renal cell carcinoma (RCC).
Design: We constructed six tissue arrays consisting of three representative 1 mm cores from formalin-fixed, paraffin-embedded tissue blocks from 64 Clear Cell RCC (CCRCC), 34 Cromophobe RCC (ChRCC), 29 Papillary RCC (PRCC), 24 oncocytomas (O), and 9 miscellaneous. Fiveteen RCC with sarcomatoid differentiation were also evaluated. Immunohistochemical study was performed using policlonal antibody PDGFR α (c-20, Santa Cruz, 1:100) and policlonal antibody PDGFR β (p-20, Santa Cruz, 1:200). Three different pathologist evaluated the inmunohistochemical tumoral cell expression of PDGFR α and β as positive or negative. Also, vasculature PDGFR β expression was evaluated as focally positive, diffuse or negative.
Results:

Percentage of positive cases

	O	ChRCC	PRCC	CCRCC	SRCC
α on tumor cells	20,8%	67,6%	27,6%	39,1%	86,7%
β on tumor cells	29,2%	34,2%	14,8%	11,5%	69,2%
β on vasculature	16,7%	0%	11,1%	42,6%	23,1%

The staining pattern was cytoplasmic and in most of the cases with heterogeneous distribution. In some cases the reactivity evaluation was difficult and doubtfully in epithelial component. Thus only cases in wich the 3 pathologists agree were considered.
Conclusions: Interestingly, sarcomatoid differentiation of RCC shows a higher staining porcentage than the other neoplasms. If this data could be related with a different clinical behavior or treatment is something that we thing deserve more studies. The expression of PDGFRβ on vasculature is focal and scanty for all RCC subtypes, except CCRCC, in which was diffuse and intense.This result could be related with the special pathogenesis of CCRCC (higer levels of hipoxia inducible factor that induce greater expression of VEGF, PDGF, EGF and TGFα and β genes, among others).

668 Cox2 in Renomedullary Interstitial Cell Tumors

Z Gatalica, O Hes, M Michal, B Wang, T Vanacek, M Koul, SL Lilleberg. Creighton University Medical Center, Omaha, NE; Medical Faculty Hospital, Plzen, Czech Republic; Transgenomic, Inc, Omaha, NE.
Background: Normal renomedullary interstitial cell function and survival depends on tightly regulated cyclooxygenase-2 (*Cox-2*) expression and prostaglandin synthesis. Upregulation of *Cox-2* occurs in various cancers; it is estimated that more than 85% of human colon cancers and 50% of colorectal adenomas have elevated levels of *Cox-2*.Polymorphisms affecting coding and non-coding regions have been reported (including the promoter, intronic regions, and the 3'untranslated region (UTR), that can affect the expression or stability of *Cox-2* mRNA. We investigate polymorphisms in the *Cox-2* gene and their contribution to development of renomedullary interstitial cell tumors (RMICT).
Design: Fourteen patients with fifteen RMICT were studied. Eleven polymorphisms in *Cox-2* gene were investigated using DHPLC and sequence analysis including: promoter polymorphisms (1) C/T at position -645; (2) GT insertion/deletion at position -663; (3) G/C at -765; (4) A/G at position -798; (5) T/G at position – 1186; (6) G/A at -1195; and (7) A/G at -1290; coding SNP (8) Met1Ile G/T polymorphism in exon 2; intronic SNPs (9) T/G polymorphism at IVS5-275; (10) C/T at IVS7+111C> and (11) T/C polymorphism at position 8473 in the 3'UTR. Expression of *Cox-2* enzyme, microsomal prostaglandin E-synthase-1 (mPES-1) and receptor for prostaglandin E2 (EP2) were investigated using immunohistochemistry. X-chromosome inactivation (HUMARA) was performed in selected cases.
Results: Patients with RMICT showed no insertion or deletion in -663 promoter but exhibited unusually rare homozygous or heterozygous genotypes at 7 other polymorphic sites. This was associated with strong (3+) and diffuse (>50% of cells) expression of *Cox-2* protein in the majority (86%) of tumors. Concomitant expression of mPES-1 and the EP2, indicating the presence of an autocrine growth loop was seen in 91% of tumors. X-chromosome inactivation (HUMARA) showed that two of three tumors were clonal.
Conclusions: We showed for the first time that renomedullary interstitial cell tumors are true neoplasms of interstitial cells with autocrine growth stimulation involving prostaglandin E2 signaling pathway. Patients with unusual *Cox-2* genotypes favoring overexpression of *Cox-2* may be exceptionally susceptible to development of these neoplasms. This is also the first study implicating *Cox-2* in the risk of kidney neoplasms.

669 p16 Expression, Human Papilloma Virus and Inverted Papillomas of the Urinary Bladder

P Gattuso, A Alonso, S Vinokurova, M Schmitt, VB Reddy, P Bitterman, VE Gould. Rush University Medical Center, Chicago, IL; Deutsches Krebsforschungszentrum, Heidelberg, Germany.
Background: Recent studies have shown that cervical lesions associated with high-risk human papilloma virus (HPV) also have a high overexpression of the p16 protein. However, similar studies in the genitourinary tract are sparse and inconclusive. Inverted papillomas of the urinary bladder are regarded as lesions with malignant potential. The present study investigated the relationship between p16 protein overexpression and HPV detection by multiplex techniques in inverted papilloma.
Design: Between 1981 and 2005 a total of 23 inverted papillomas of the urinary bladder were recorded at Rush University Medical Center. There were 15 male and 8 female patients ranging in age from 17 to 75 years with a mean age of 59. In addition, 12 cases (4 transitional cell carcinomas (TCC), 3 high grade and 1 low grade, 4 cystitis and 4 normal urothelial tissue) were used as controls. p16 protein expression was studied by immunohistochemistry technique using formalin-fixed, paraffin-embedded material. Multiplex technique was used to detect HPV DNA sequences.
Results: 16 out of 23 cases of inverted papilloma overexpressed p16 protein. HPV DNA was isolated in three out of 14 cases analyzed (2-HPV-16 and 1-HPV 11/16), which also expressed p16. p16 overexpression was seen in 10 out of 12 control cases (4 TCC, 4 cystitis and 2 normal urothelial tissue). HPV DNA in the control group was detected in 2 cases of high grade TCC (both cases were HPV 16 subtype), and 3 cases using general primers for HPV sequences. In addition, 4 benign cases from the control group overexpressed p16 in the stromal cells.
Conclusions: 1) p16 protein overexpression in inverted papillomas is not predictive of the presence of high-risk HPV infection. 2) p16 protein overexpression seen in 16 out of 23 (70%) cases of inverted papillomas suggest that HPV may play a role in the urothelial carcinogenesis. These observations indicate that different mechanisms are involved in the pathogenesis of urothelial carcinogenesis. It appears that p16 overexpression serves as an indication of Rb dysfunctioning in neoplasia which could result from high-risk HPV infection. 3) No significant difference in association with HPV was found between inverted papillomas and the control group.

670 Can Lymphatic Drainage from the Kidney Be Predicted? – Retrospective Study Based on 389 Nephrectomies from a Single Institution

R Ghai, M Quek, RC Flanigan, MM Picken. Loyola University Medical Center, Maywood, IL.
Background: New therapies for renal cell carcinoma (RCC) raise hope for the application of adjuvant treatment. Lymphadenectomy with curative intent is also being tried for several cancers, including RCC. While the need for adequate staging is clear, there is a paucity of data regarding lymphatic drainage from the kidney. We sought to address this issue using archival material.
Design: We reviewed 389 recent (5 y) adult nephrectomies from a single Institution. We recorded the total # of cases with harvested lymph nodes (LNs), the location, and the # and distribution of LNs with metastases (mets). The LNs were either submitted separately by the surgeon or by the pathologist if identifiable grossly (gross); a sample of hilar fat, routinely examined microscopically, yielded additional microscopic (micro) LNs.
Results: There were 364 RCC, 24 pelvic urothelial carcinomas and one adrenocortical carcinoma, all primary tumors; total 389 kidneys. In 119 cases 592 LNs were recovered (avg 6.8 LNs/kidney). In 69 kidneys 190 hilar LNs (120 micro + 70 gross) were examined. All micro LNs were negative while 46/70 (67%) gross LNs (from 18 patients) had mets. Among cases with positive hilar LNs, 1 tumor was confined to the kidney and all others had stage T3 or higher. Among regional LNs 28/402 (from 16/78 examined kidneys) had mets. The distribution of involved LNs/# kidneys with LNs examined was as follows: peri and paraaortic: 8/39, para and pericaval 6/17, interaortic caval 1/14 and retroperitoneal NOS 1/3; five preaortic and/or retrocaval, were all negative. Among kidneys with regional LN mets 3 tumors were confined to the kidney and rest were T3 or higher. A total of 32 kidneys had mets in 74/146 LNs examined. In 2 cases (both

pT3a) both hilar and regional LNs were involved. However, in 14 cases regional LNs were positive while the hilar LNs were not recovered (in 13 cases) or were negative (1 case). In this group only 2 cases had tumor limited to the kidney. 15 pts had distal mets at the time of nephrectomy, of whom 8 had no hilar and/or regional LNs.
Conclusions: The largest yield of positive LNs was from the hilum. With micro LNs being consistently negative, the gross hilar LNs were positive in 67%. However, 44% of patients with LN mets, had regional LN mets with negative or not detectable hilar LNs. Eight patients had distal mets without hilar and/or regional LN involvement. This indicates an alternative to the hilar lymphatic drainage route.

671 Allelic Loss of Cyclin D1, an Oncogene, in Clear Cell Renal Cell Carcinoma and Renal Oncocytoma

N Gokden, L Li, S Schichman, BR Smoller, CY Fan. University of Arkansas for Medical Sciences, Little Rock, AR.
Background: Clear cell renal cell carcinoma (CC-RCC) differs significantly from renal oncocytoma in terms of biologic behavior and histology. Genetically, CC-RCC is characterized by frequent allelic loss in the short arm of chromosome 3 (3p). By contrast, renal oncocytoma has been shown to contain translocation of cyclin D1, an oncogene located at chromosomal region 11q13 with overexpression of the Cyclin D1 gene reported in up to 50% of the tumors. These results indicate that cyclin D1 amplification and overexpression may play an important role in the pathogenesis of renal oncocytoma. Allelic loss of cyclin D1 locus has not been thoroughly examined in CC-RCC and renal oncocytoma. In order to determine roles of cyclin D1 gene in the development of renal neoplasms, we performed LOH analysis of cyclin D1 gene in CC-RCC and renal oncocytoma.
Design: 20 cases of CC-RCC and 20 cases of renal oncocytoma were included in this study. DNA samples from all cases were obtained from tissue sections collected using manual microdissection. All DNA samples were subjected to PCR amplification using 2 fluorescent-labeled microsatellite markers adjacent to the cyclin D1 locus (11S534 and 11S490), followed by fragment analysis using ABI PRISM 3100 Genetic Analyzer.
Results: 14 of 20 (70%) cases of CC-RCC and 11 of 20 (55%) cases of renal oncocytoma are informative for at least one of the 2 markers used. Among these cases, 8 (57%) and 3 (27%) showed evidence of cyclin D1 LOH for CC-RCC and oncocytoma, respectively.
Conclusions: Allelic loss at cyclin D1 locus occurs in CC-RCC (57%) much more frequently than in renal oncocytoma (27%). Cyclin D1 allelic loss is possibly due to amplification of one allele of the gene. These results indicate that while cyclin D1 allelic loss represents an important underlying mechanism for the pathogenesis of both CC-RCC and renal oncocytoma, cyclin D1 abnormality appears to play a more dominant role in the development of CC-RCC.

672 Small Cell Carcinoma of the Renal Pelvis: A Clinicopathologic and Immunhistochemical Studies of 4 Cases

D Goldfarb, JY Ro, SJ Jung, J Kang, YM Cho, RA Goldfarb, SS Shen. The Methodist Hospital and Weill Medical College of Cornell University, Houston, TX; Inje University College of Medicine, Paik Hospital, Busan, Korea; Ulsan University, Asan Medical Center, Seoul, Korea; Urologic Clinic of Houston, Houston, TX.
Background: Small cell carcinomas (SCC) of genitourinary tract are mostly common seen in urinary bladder and prostate, but have rarely been reported in kidney. Authors described four cases of SCC of the renal pelvis. The clincopathologic features as well as selective immunohistochemical stain results are summarized.
Design: We reviewed 155 cases of renal pelvic urothelial carcinoma from 2 large hospitals. H&E slides from each case were reviewed and 4 cases of SCC was identified by large solid sheets or nests of undifferentiated small cells with prominent necrosis and typical nuclear features. Selective immunohistochemical stains for neuroendocrine markers were performed on all cases.
Results: Four cases kidney SCC were identified from 155 pelvic urothelial carcinomas. The average age of patients was 68 years (62-77). None of patients had history of SCC of the lung or other extrapulmonary sites. Three patients were men and 1 was a woman. The epicenters of all four tumors were in the renal pelvis. Average tumor size was 4.1 cm. All 4 cases had peripelvic fat invasion, and 2 cases also had renal parenchymal invasion. Urothelial carcinoma in-situ was identified in 2 of 4 cases. Two patients had history of bladder cancers. Three of the 4 tumors were originally diagnosed as high grade urothelial carcinoma of renal pelvis. By immunohistochemistry, tumor cells were positive for CD56 (2/4), synaptophysin (3/4), chromogranin (2/4). Three of four patients had regional lymph node metastasis and one had distant metastasis. All patients were treated by radical nephroureterectomy and three received carboplatinum-based chemotherapy. All 4 patients are alive with a 6 month average follow-up (4-9 months).
Conclusions: We reported here 4 cases of SCC of kidney arising from the renal pelvis. All patients presented with relatively bulky and advanced disease and three had nodal or distant metastasis. With the identification of urothelial CIS, pelvic location, as well as association of history of bladder tumor, we propose that renal SCC may have a similar carcinogenic pathway as that of SCC of urinary bladder.

673 The Prostatic Capsule Is an Integral Biologic Factor in the Presence or Absence of Extracapsular Extension by Adenocarcinoma

NS Goldstein. William Beaumont Hospital, Royal Oak, MI.
Background: Extracapsular extension (ECE) has long been attributed to inherent biologic properties of prostatic adenocarcinoma. This study evaluated whether the prostate capsule, specifically capsular thickness, is a factor in ECE.
Design: 168 completely embedded whole-organ mounted prostatectomy specimens with unilateral, unifocal ECE and negative peripheral-capsular margins were selected based on Gleason score-amount group (Gleason 6 (G6) <15% total area involved), G6 15% – 50% area, G7 (3+4) <15% area, G7 (3+4) 15%-50% area, G7 (4+3) 15%-50% area, G8 <50% area and patient age group (<50 years, 50-<65, ≥65). 470 non-ECE cases, matched for Gleason score-area and patient age group (2.5:1 control:case ratio) were used as controls. Capsular thickness to the nearest um was measured using a Olympus DP70 digital camera in microns. Capsular thickness was measured in 3 locations in the posteriolateral region bilaterally on each macrosection slide (mean, 6.9 slides/ case).
Results: ECE occurred most commonly in the mid-prostate, most often (137/ 168 cases 81.5%) in the 2 cm cephalid to the verumontanum base. The mean posteriolateral capsular thickness in ECE-positive cases was 317.25 um compared to 573.61 um in non-ECE control cases (p< 0.001). The capsule was significantly thinner (mean = 62 um) in the posteriolateral region with ECE compared to the non-ECE contralateral posteriolateral region (p=0.002). When controlled for patient age and Gleason score-amount group, ECE+ prostates were significantly heavier (51g vs 39g, p<001) than non-ECE prostates. On univariate analysis, ECE+ was significantly associated with older age, higher Gleason score-amount group, greater prostate weight, and thinner mean prostate capsule thickness. On multivariate analysis, prostate weight (Coef. = -3.82; p<0.001) and capsular thickness (Coef. = -2.17; p=0.013) were independently associated with ECE. Of the 36 <50-year old patients with Gleason 7 or 8 15% - 50% area, none of the 8 patients with prostates weights <32g and overall posteriolateral capsular mean thickness of >650 um had ECE (0/8), whereas 7/17 (41%) with weights >32g and capsular thickness <650 um had ECE.
Conclusions: The prostate capsule is an integral biologic factor related to ECE. Prostate capsules which are thin due to larger gland volumes, are less effective in this regard. A thick posteriolateral region capsule (and small prostate gland) appears to be a barrier to ECE, which includes young patients with high-grade, high-volume adenocarcinoma.

674 The TMPRSS2-ERG Fusion in Prostate Cancer Is Associated with ERG Expression, but Not with Outcome

A Gopalan, M Leversha, J Satagopan, HA Al-Ahmadie, SW Fine, S Olgac, SK Tickoo, VE Reuter, WL Gerald. Memorial Sloan Kettering Cancer Center, NY, NY.
Background: Recent studies have reported functional fusion of the TMPRSS2 and ERG genes with consequent ERG overexpression in a large proportion of prostate cancer (PC). Some data suggest that ERG expression is higher in less aggressive PC while others show an association between specific TMPRSS2-ERG fusion types and aggressive PC. We determined the translocation (T) status in a well characterized cohort of patients with early stage (ES) PC to evaluate clinicopathologic and molecular associations.
Design: Interphase fluorescent in situ hybridization (FISH) was performed on tissue microarrays constructed from 67 patients with clinically localized PC treated solely by radical prostatectomy. Case control sampling was enriched for outcome events such that 28 patients had biochemical recurrences (BCR), 7 developed metastases (M) and 2 died of PC. Cases without BCR have at least 5 years follow-up (F/U). Tumor samples had been studied using Affymetrix HU133A gene expression arrays. FISH breakapart probes used two BAC DNA clones each at the 3' and 5' ends of both TMPRSS2 and ERG. FISH scoring was based on agreement of patterns for T and deletion (D) with both probe sets. Correlations with outcome used two-sample T-test and Fisher's exact test. F/U ranged from 25.16 to 154.25 months.
Results: 46% of PC had T or D of TMPRSS2 and ERG. About half of this group had polyploidy (PP). 10% had PP without T/D. HGPIN associated with T/D tumors also had T/D. There was no association between PC with T/D versus those without for clinicopathologic features examined but there was strong correlation with ERG transcript levels (Table 1).

Table 1: Correlation of T/D with various parameters

	T/D	NO T/D	p-VALUE
Gleason<7 (13)	7	6	0.84
Gleason≥7 (54)	24	30	0.84
ECE/SVI (+) (40)	20	20	0.62
ECE/SVI (-) (27)*	11	16	0.62
BCR (28)	12	16	0.80
Mets (7)	1	6	0.11
Mean ERG (log)**	7.5	5.62	<0.0001

* Higher odds of organ confined (OC) PC in cases with PP alone versus those having PP+T/D or T/D alone ** Mean ERG not significantly correlated with BCR, M or overall survival; M had lower ERG in general

Conclusions: TMPRSS2-ERG T or D occur in about half of ES PC. T/D and D alone were strongly correlated with ERG overexpression but not with outcome. PP alone had higher odds of having OC PC versus PP coexisting with T/D or T/D without PP. Cases with M tended to have lower ERG expression than those without.

675 Urothelial Neoplasms in Young Adults (≤40 Years of Age): A Clinicopathological Study

K Guggisberg, N Lange, K Trpkov, A Yilmaz. Calgary Laboratory Services and University of Calgary, Calgary, AB, Canada.
Background: Urothelial neoplasms are mostly encountered after the sixth decade and are rare in adults under 40 years of age. Men are more commonly affected than women. Previous studies suggested an increased risk in patients with positive family history of bladder cancer, cigarette smoking, and occupational exposure to carcinogens. We studied the clinical and the pathological features of urothelial neoplasms in patients ≤40 years.
Design: We identified a total of 37 urothelial neoplasms from 28 patients, diagnosed in our institution from1999 to 2006. We limited our study to patients ≤40 years at the time of initial diagnosis. All cases were reviewed and the diagnoses were reclassified using the 2004 WHO/ISUP classification. The clinical data included patient age, gender, family history of bladder cancer, history of cigarette smoking, radiation, and exposure to occupational carcinogens. Complete clinical data was collected for 21/28 (75%) patients.
Results: Mean age at diagnosis was 35 years (range 19-40). There were 19 males and 9 females (M:F ratio 2.1:1). Initial biopsies revealed non-invasive urothelial neoplasms in 25/28 (89%) patients: 14 low-grade papillary urothelial carcinomas

(LGUC), 8 papillary urothelial neoplasms of low malignant potential (PUNLMP), 2 urothelial papillomas, and 1 in situ carcinoma. Recurrences were documented in 2/25 (8%) patients with non-invasive neoplasms. One patient had 8 biopsies (7 with LGUC and one with PUNLMP) and one patient had initial PUNLMP which recurred once with the same diagnosis. Invasive high grade urothelial carcinomas were identified in 3/28 (11%) patients. Two patients had muscle invasive tumors and underwent radical cystectomy that showed no residual tumor in both. One of those patients subsequently died of disease with distant metastasis. History of cigarette smoking was identified in 13/21 (62%) patients and two additional patients reported significant second hand smoking. Only one patient had a history of radiation exposure due to treatment for rectal carcinoma 6 years prior to developing urothelial neoplasm. One patient had occupational exposure (possible arylamine) for 16 years. Family history of bladder cancer was not documented in any patients.

Conclusions: Great majority of urothelial neoplasms in patients ≤40 years are non-invasive and they have favorable clinical outcome with low recurrence rates. Half of our patients had LGUC. History of cigarette smoking was present in majority of our patients, but none had family history of bladder cancer.

676 WHO Histological Classification, Regional Metastasis and Outcome in 372 Surgically Treated Patients with Penile Squamous Cell Carcinomas

GC Guimaraes, I Werneck da Cunha, FA Soares, A Lopes, JJ Torres, A Chaux, EF Velazquez, AL Cubilla. Hospital do Cancer AC Camargo, Sao Paulo, Brazil; Instituto de Patologia e Investigacion, Asuncion, Paraguay; Harvard Medical School, Boston, MA; Facultad de Ciencias Medicas, Asuncion, Paraguay.

Background: The WHO histological classification of penile squamous cell carcinoma (SCC) was recently published but there is no comprehensive evaluation of differential outcome of the various subtypes.

Design: The aim of the study was to evaluate regional spread and mortality in subtypes of SCCs in a large cohort of patients with homogeneous primary surgical treatment in a single institution. Clinical charts and pathologic materials from 372 surgically treated patients, 162 of which also had a bilateral groin dissections were evaluated. Follow up information was obtained in 339 patients (91%) and ranged from 0.8 to 460 months (average 101 months).

Results:

SCC type (WHO)	# cases (%)	% positive nodes	% mortality
Usual	239 (64)	26	19
Basaloid	14 (4)	50	21
Warty	25 (7)	16	8
Verrucous	25 (7)	0	0
Papillary NOS	18 (5)	11	11
Sarcomatoid	4 (1)	75	75
Adenosquamous	4 (1)	50	0
Mixed	43 (12)	10	7

Conclusions: The majority of penile cancers are SCCs of the usual type but there is a variegated spectrum of histological subtypes. A more aggressive biologic behavior was demonstrated for basaloid, adenosquamous and sarcomatoid carcinomas. Verrucous, papillary, warty and mixed carcinomas carried the best prognosis. An intermediate behavior was documented for usual SCC.

677 Prognostic Significance of Positive Surgical Margins in Radical Prostatectomies: An Analysis Based on Their Anatomic Locations

CC Guo, E Tamas, B Trock, JI Epstein. Johns Hopkins University School of Medicine, Baltimore, MD.

Background: There is limited and controversial information regarding the impact of anatomic location of positive surgical margins on prostate cancer recurrence.

Design: We retrospectively reviewed clinical and pathological information on 3742 patients who had undergone radical retropubic prostatectomy between 1994 and 2003 for clinically localized prostate cancer. The average follow-up period was 4.6 years (range: 2-11 years). Margin positivity was broken down into: posterior vs anterior; and distal (apical) vs proximal (bladder neck) vs. other. Progression (recurrence) was defined as biochemical progression (which accounted for the vast majority of cases with progression), local recurrence, or distant metastases.

Results: Positive surgical margins were present in 389 patients (10.4%) with the most common anatomic location at the distal (apex). In 33 cases, surgical margins were positive at more than one anatomic location. The actuarial probability of progression-free survival at five years was 0.69 for patients with a positive surgical margin at a single anatomic location, 0.52 for patients with positive margins at more than one location, and 0.92 in patients with negative surgical margins. A significant risk for cancer recurrence was observed for positive surgical margins at all the anatomic locations except for the anterior region probably due to the limited number of cases in this area in our study. The rate of cancer recurrence was the highest for positive margins at the bladder neck margin. Margin positivity at the apex and other posterior areas of the gland had the same twofold risk of recurrence. When the model was adjusted for other prognostic factors (PSA, Gleason score, or pathologic stage), the location of positive margins did not add to the ability to predict a patient's risk of progression.

Conclusions: Positive surgical margins in radical prostatectomy carry a significant risk for prostate cancer progression. The risk for cancer progression is highest when the positive surgical margin is located at the bladder neck. However, the site of positive margins does not increase the accuracy of predicting progression beyond that achievable with routine clinical and pathological variables.

678 Large Cell Undifferentiated Carcinoma (LCUC) in the Urinary Bladder: A Clinicopathological Study of 33 Cases

CC Guo, ME Nielson, JI Epstein. Johns Hopkins University School of Medicine, Baltimore, MD.

Background: LCUC is a rare urinary bladder tumor. Its morphological features and clinical significance remains unknown.

Design: We identified 33 cases of LCUC from our institution (1994-2005). The original slides were obtained for analysis in 31 cases, and IHC was performed in 11 cases. We compared LCUC with usual urothelial carcinoma of similar stages (III or IV) in our institution (n=76).

Results: The average age of the LCUC patients was 65.6 years old (range: 40-84) with a male predominance (76%). LCUC was characterized by sheets or isolated large polygonal or round cells with moderate to abundant cytoplasm. Nuclei were vesicular with prominent nucleoli, with the exception of cases with isolated tumor cells where nucleoli were not as visible. Other morphological features included marked pleomorphism (n=21), prominent cytoplasmic vacuoles (n=24), focal coagulative necrosis (n=15), and a desmoplastic stromal response (n=20). Tumor cells had an average of 16 mitotic figures/10 HPF (range: 2-72). Focal areas of urothelial, squamous or glandular differentiation were seen in 9 cases (5%-30% of the tumor). In the 12 cystectomy specimens, lymphovascular invasion was observed in 6 cases, and perivesicular fat invasion in 7 cases. Stains were positive for CK7 (n=8/11), CK20 (n=2/11), p53 (n=8/11) and Ki-67 (labeling index 50-100%), yet negative for synaptophysin, chromogranin A, and PSA. Of the12 patients undergoing cystectomy, 5 patients died at an average of 26 months (range 8-67) following surgery, 5 were alive at 37 months (range 10-82) post-operatively, and 2 were lost to follow-up. For the 21 patients who did not receive cystectomy, 10 patients died at an average of 13 months (range 4-55) after diagnosis; 9 patients were alive with a follow-up period of <9 months (2 with distant metastasis and 1 with local recurrence); 1 patient with no tumor in a subsequent partial cystectomy was still alive at 40 months of follow-up; and 1 patient was lost to follow-up. The 12 and 48 month actuarial cancer specific survivals were 61% and 41%, respectively, for LCUC compared to 81% and 59%, respectively, for usual conventional high grade urothelial carcinoma.

Conclusions: LCUC does not morphologically resemble urothelial or adenocarcinoma and if present in a metastatic site would not suggest a urothelial primary. LCUC either pure or with minor urothelial, squamous, or glandular components is associated with a worse prognosis than conventional high grade urothelial carcinoma and merits recognition as a separate clinicopathological entity.

679 Cellular Interactions of the Phosphorilated Form of Akt in Prostate Cancer

K Hammerich, A Manzoni, TM Wheeler, GE Ayala. Baylor College of Medicine, Houston, TX.

Background: Previous studies showed that the kinase P-Akt1 plays a central role in regulating several pathways. P-Akt1 promotes proliferation and increased survival in vitro and plays an important role in prostate cancer progression. We have previously demonstrated that higher levels of P-Akt1 in PCa is independently predictive of a higher probability of recurrence.

Design: Tissue microarrays from index tumors of 640 patients were immunostained with antibody to P-Akt1 (Ser473) and p27, FKHR, P-FKHR, GSK, P-GSK, and NFkB. Ki67 was used to measure proliferation index and Tunnel for apoptotic index. Slides were digitized and semiquantified. The expression index (Intensity*Percentage) was used for statistical analysis. For P-Akt-1 we used the overall index (P-Akt1 max) and then the nuclear and cytoplasmic expression separately (P-Akt1-n & P-Akt1-c).

Results: P-Akt-1 staining was found in both primary tumor and metastatic tissues, but was increased in metastasis (1.56 vs. 2.1; p=0.00). Increased expression of P-Akt1 was associated with an increased proliferation (r^2=0.34, p=0.00), but inversely correlated with apoptotic index (r^2=0.19, p=0.00). The expression of AKT correlates with all forms of p27. Higher levels of P-Akt are associated with both higher levels of cytoplasmic p27 (r^2=0.20, p=0.00) and higher levels of nuclear p27 (r^2=0.40, p=0.00), suggesting an involvement in both cytoplasmic entrapment and phosphorylation of p27. We were not able to identify any correlation between P-Akt-1 and PTEN staining in tumors. P-Akt1 expression significantly correlated with nuclear and cytoplasmic staining of FHKR and GSK. The strongest correlations were found with the -P forms of both. The curves show order 0 in non-P correlations and order 1 with -P forms, suggesting enzyme kinetics in the latter. Our data suggests that phosphorylation is the principal method of FHKR and GSK inactivation and cytoplasmic entrapment secondary. P-Akt1 correlated with NFkB, but P-Akt1-c (r^2=.27) was stronger than P-Akt1-n (r^2=.18) suggesting a role in the inhibition through phosphorilation of IkB.

Conclusions: The results are unique for the scope of the markers and the size of the population. This study confirms, in human PCa tissues, in vitro and in vivo derived P-Akt1 and its downstream effectors data. However, some of our results were surprising, as we found no correlation with PTEN. This and the relatively low correlation coefficients suggest that PCa uses multiple mechanisms to regulate this pathway and substantiates the concept of redundancy in cancer pathway regulation.

680 Renal Carcinoid Tumor: A Clinicopathologic Study of 21 Cases

DE Hansel, JC Cheville, E Berbescu, S Fine, RH Young, JI Epstein. The Johns Hopkins Hospital, Baltimore, MD; Mayo Clinic, Rochester, MN; Memorial Sloan-Kettering, New York, NY; Massachusetts General Hospital, Boston, MA.

Background: Renal carcinoid tumors are rare tumors that have been primarily documented as case reports in the literature. In this study, we report a series of 21 renal carcinoid tumors, with emphasis on histopathologic features and clinical outcomes.

Design: Twenty-one patients with renal carcinoid tumors from 5 separate institutions were identified. Clinicohistopathologic findings and clinical outcomes were examined.

Results: Patients were equally distributed between male (n=10/20) and female (n=10/20) patients. Patient age ranged from 27 to 78 years (average 52 years). Nine of 19 tumors were present in the left kidney and 10/19 were present in the right. Tumors ranged in size from 2.6 to 17 cm. Four patients had a documented history of a horseshoe kidney. Presenting signs and symptoms included back or flank pain (n = 6/9), enlarging abdominal mass (n = 2/9), hematuria (n = 2/9), and anemia (n = 1/9). Fifteen patients had concurrent metastases and the time of surgery, including lymph nodes (n = 9/15), liver alone (n = 4/15), liver and bone (n = 1/15), and lung (n = 1/15). Tumor morphology included tightly packed cords and trabeculae with minimal stroma (n = 17/21) or trabecular growth with prominent stroma (n = 4/21), as well as focal solid nests (n = 4/21), and focal gland-like lumina (n = 4/21). The border between tumor and normal kidney was sharply defined in most cases (n = 16/21). Extracapsular extension was present in 11/21 cases. Calcifications were present in 5/21 cases. Mitotic activity ranged from 0 to 2 mitoses/10 HPF in most cases. Immunostains were often positive for synaptophysin (n = 18/20), chromogranin (n = 13/20), Cam5.2 (n = 14/16), and vimentin (n = 12/15). CK 7 was focally positive in a small subset of cases (n = 3/18). TTF-1 and WT-1 were negative in all cases examined. Clinical followup was available on 15 patients. One patient died of disease at 8 months following surgery. Of the remaining patients, 1 patient was dead without disease, 7 patients were alive without disease and 6 patients were alive with disease.

Conclusions: In conclusion, this study presents the largest collection of primary renal carcinoid tumors to date. Morphologically, renal carcinoid tumor is consistent with carcinoid tumors present at other anatomic sites. Patients frequently present with early metastases, but usually have a subsequent prolonged clinical course.

681 Myxoid Nephrogenic Adenoma

DE Hansel, T Nadasdy, JI Epstein. The Johns Hopkins Hospital, Baltimore, MD; Ohio State University Medical Center, Columbus, OH.

Background: Nephrogenic adenomas demonstrate a variety of morphologic patterns that may occasionally be confused with malignant processes, including urothelial and prostatic carcinoma. In this series, we describe 6 cases of nephrogenic adenoma that contain an admixture of the classic tubular form of nephrogenic adenoma and an unusual spindled and myxoid form of nephrogenic adenoma that closely mimics infiltrating mucinous adenocarcinoma.

Design: Four cases were received in consultation from outside institutions and 2 cases were reviewed from in-house material. Patient demographics and prior genitourinary tract history were examined. Immunostains for AE1/3 (predilute, Ventana, Tucson, AZ), A-methylacyl-CoA racemase (AMACR; racemase Zeta; 1:100, DAKO, Carpinteria, CA) type IV collagen (1:100, DAKO), PAX2 (1:100, Zymed, Carlsbad, CA), prostate-specific antigen (PSA; predilute, Ventana), and Tamm-Horsfall protein (THP; 1:10,000, Biomedical Technologies, Stoughton, MA) were performed. Special stains were performed and included alcian blue/PAS, reticulin, Congo red, and mucicarmine.

Results: In all cases, the classic tubular form of nephrogenic adenoma composed only a small proportion of the lesion, whereas the remainder consisted of compressed spindled cells within a background of mucin, with only rare tubular and cord-like structures. On close examination, minimal nuclear atypia was identified in 2 cases, which included small, pinpoint nucleoli and nuclear pseudoinclusions, respectively. All 6 patients were elderly men that had a prior history of prostate cancer (n = 3), combined prostate and urothelial carcinoma (n = 1), bladder carcinoma (n = 1), or no prior reported prostatic or urothelial abnormalities (n = 1). Four patients received prior treatment with radiotherapy and 1 patient received intravesical mitomycin-C. The epithelial component of the lesions was positive in all cases for AE1/3 and racemase and demonstrated a variable cuff of type IV collagen surrounding the tubules. PAX-2 was focally to rarely positive. Immunostains for PSA were negative. Special stains identified the background matrix as mucin, with intense staining for PAS and focal staining for mucicarmine. Special stains for reticulin and amyloid (Congo red stain) and immunohistochemistry for Tamm-Horsfall protein were negative.

Conclusions: This case series is the first report of a myxoid subtype of nephrogenic adenoma. Awareness of this entity and the use of ancillary techniques can aid in the diagnosis of this unusual form of nephrogenic adenoma.

682 Utility of Early Prostate Cancer Antigen (EPCA) Expression in Predicting Presence of Prostate Cancer in Men with Histologically Negative Biopsies

DE Hansel, AM DeMarzo, EA Platz, J Hicks, JI Epstein, A Partin, GJ Netto. Johns Hopkins Univ, Baltimore.

Background: EPCA, a nuclear matrix protein, was recently shown to be expressed in prostate carcinoma (PCa) and adjacent benign tissue. Previous studies have demonstrated EPCA expression in benign prostate tissue up to 5 years prior to a diagnosis of PCa; EPCA is currently clinically marketed as a predictive marker for PCa.

Design: We evaluated EPCA expression by immunohistochemistry using a polyclonal antibody (Onconome,WA) on benign biopsies (Bxs) from 98 patients (pts). Cases included 39 pts undergoing first time negative Bx (1stNeg group), 24 pts with persistently negative Bxs (PrstNeg group), 8 pts with initially negative Bx who were subsequently diagnosed with PCa (NegF/UPCa group) and negative Bx obtained from 27 pts where other concurrent Bx contained PCa (Neg$_{\&}$PCa group). EPCA staining was blindly assessed by two of the authors. Staining intensity (0-3) and extent (1-3) scores were assigned. The presence of any intensity 3 staining in any of the blocks of a given Bx specimen was considered as positive for EPCA for the primary outcome in the statistical analysis. Additionally, as secondary outcomes, we evaluated the data factoring exent of EPCA staining.

Results: Proportion of EPCA positivity was highest in NegF/UPCa group (6/8; 75%) and lowest in PrstNeg group (7/24; 29%; P=0.04). A relatively higher than expected proportion of EPCA positivity was present in the 1stNeg group (23/39; 59%). EPCA was negative in 41% of the Neg$_{\&}$PCa group known to harbor PCa. A lower proportion of EPCA positivity was encountered in older archival blocks (p<0.0001). Corrected for block age, the NegF/UPCa was the only group to remain statistically significantly different in EPCA positivity compared to the reference PrstNeg. Similar findings were obtained when adjustments for pts age were made and when analysis was based on secondary outcome measurements.

Conclusions: Our study showed a higher proportion of EPCA expression in initial negative prostate Bx of pts who were subsequently diagnosed with PCa. We found a relatively high proportion of EPCA positivity (59%) in 1stNeg group and a 41% rate of "false negative" results in benign Bxs from cases with documented PCa on concurrent cores. The lower EPCA positivity in cases with older blocks raises the question of a confounding effect. Additional studies on the antigenic properties of EPCA in archival material are required to further delineate the clinical utility of EPCA in prostate Bx.

683 Morphologic Assessment of Bladder Carcinomas in Cystectomy Specimens Post Neoadjuvant Chemotherapy

LR Harik, S Olgac, SK Tickoo, H Al-Ahmadie, SW Fine, A Gopalan, VE Reuter. Memorial Sloan Kettering Cancer Center, New York City, NY.

Background: Neoadjuvant chemotherapy (NC) is being offered to an increasing number of patients with bladder cancer before undergoing radical cystectomy (RC). In fact it has been suggested that the use of NC should be standard of care in these patients. There are no detailed histologic studies on the effect on morphology of treated bladder cancer or the normal urothelium in RC post-NC. We present the first study available on the subject.

Design: Morphologic assessment of RC post-NC between 1993-2004 was performed. When available pre-NC TURBT were compared to the corresponding post-NC carcinoma (Ca).

Results: Initial data is available on 23 patients. At the time of RC, 11(48%) patients were downstaged and 12(52%) upstaged or remained the same. Seven patients had pT0 (30%). Ca in situ (CIS) was present in 10 cases, 4 of which (40%) had denuded/clinging morphology. Urothelial atypia, defined as nuclear enlargement and irregularity not reaching the levels of CIS was present (15/23;65%). Invasive Ca was present in 15 RC. Pre-NC TURBT were available in 13 cases, only 9 of which had residual Ca on RC. Differences noticed comparing pre-NC and post-NC specimens included 1-Squamous differentiation (8/9;89%). 2-Spindle cell/sarcomatoid morphology (2/9;22%) 3-Plasmacytoid (1/9;11%) or basaloid (2/9;22%) change. 4-Increase in peri-tumoral fibrosis (5/9;56%) and tumoral necrosis (4/9;44%). The majority of the Ca (12/15;80%) showed divergent differentiation: squamous alone (11) and glandular, plasmacytoid and lympho-epithelioma like Ca with or without squamous (1 each). The predominant growth pattern was in small nests (6/15;40%) and/or single cells (4/15;27%). Intra-cytoplasmic hyaline globules were identified in 10 (67%) and tumor giant cells in 9 (60%) cases. Desmoplastic reaction/sclerosing fibrosis surrounding tumor was classified as mild (3/15;20%), moderate (7/15;47%) and extensive (3/15;20%). In addition, hyalinized fibrosis was present in the lamina propria (18/23;78%) and muscularis propria (23/23;100%). Multinucleated fibroblast were present (20/23;87%).

Conclusions: Post-NC bladder Ca was downstaged in almost half of the patients with complete remission in 30% (pT0). - Ca in post-NC RC show a higher incidence of divergent differentiation (80%) than non-treated bladder Ca. This finding might be important in directing post RC therapy. - Denuded/clinging CIS as well as urothelial atypia are common in post-NC and may cause diagnostic difficulty on small bladder biopsies.

684 PP2A Expression Correlates with Gleason Score and Clinical Stage of Prostate Cancer

HY He, PG Chu, WG Fang. Peking University, Health Science Center, Beijing, China; City of Hope, National Medical Center, Duarte, CA.

Background: PP2A accounts for most intracellular serine-threonine phosphatase activity and has been implicated in the regulation of diverse cellular functions as cell cycle progression, differentiation, oncogenic transformation and apoptosis. PP2A can act as tumor suppressor gene in some human cancers. A recent report showed that the PP2A expression was significantly decreased or absence in breast carcinomas. However, PP2A expression in human prostate cancer (PCa) has not been studied.

Design: Paraffin immunohistochemistry of PP2A-A (the regulatory subunit of PP2A) was performed in 268 cases of human PCa from radical prostatectomy specimens. The immunohistochemical-staining was scored 0-3 based on intensity (weak, moderate, and strong) of positive cells in PCa, prostatic intraepithelial neoplasia (PIN) and normal prostate tissue adjacent to tumor (NAT). Score 0-1 was evaluated as low expression group and score 2-3 was evaluated as high expression group. The data was then correlated with Gleason score and pathological stage.

Results: PP2A-A positivity was observed in cytoplasm of benign and neoplastic prostate glandular cells. Compared to NAT (9/268, 3%), the incidence of high PP2A-A expression was significantly increased in PCa (110/268, 41%; p<0.0001) and in PIN (62/246, 25%; p<0.0001). Compared to PIN, the incidence of high PP2A-A expression was significantly increased in PCa (p=0.0001) (Table). The high expression of PP2A-A was statistically significant between tumors with Gleason score ≥ 7 and tumors with Gleason score < 7 (p=0.0051), and between pT2 tumors and pT3 tumors (p=0.0001). The level of PP2A-A expression had no statistic significance in tumors with high or low volume of prostate involvement and status of surgical margins and pelvic lymph nodes.

Conclusions: PP2A-A is overexpressed in PCa and PIN compared to normal tissue, which is correlated to high Gleason score and high clinical stage. These findings suggest that PP2A may play a role in carcinogenesis and progression of PCa.

Expression of PP2A-A in PCa, PIN and NAT

PP2A-A score		PCa (n=268)			PIN (n=246)	NAT (n=268)
	Gleason score	Cases	Tumor stage	Cases		
	6	71	T2	134		
0-1	7	59				
	8-10	28	T3	24		
	Total	158		158	184	259
	6	27	T2	52		
2-3	7	51				
	8-10	32	T3	58		
	Total	110		110	62	9

685 Differential VHL Immunohistochemical Staining in Clear Cell Renal Cell Carcinoma: Evidence for Differing Mechanisms of VHL Inactivation as a Function of Fuhrman Grade and Clinical Behavior

PC Henry, A Saravanan, N Burry, M Ohh, AJ Evans. University Health Network, Toronto, ON, Canada; University of Toronto, Toronto, ON, Canada.

Background: A well-described early event in the molecular pathogenesis of hereditary and sporadic clear cell renal cell carcinoma (CC-RCC) is the functional loss of the von Hippel-Lindau (VHL) tumor suppressor gene. This loss of function is thought to occur by gene deletion, mutation and/or promoter methylation. The most important prognostic factors in CC-RCC are Fuhrman grade and tumor stage. Preserved VHL immunohistochemical staining in CC-RCC has been described, although the association between immunohistochemical detection of VHL and Fuhrman grade, stage and tumor behavior has not been well characterized.

Design: Tissue microarrays (TMA) were created from a series of 50 CC-RCC. For purposes of this study, the tumors were categorized as either low-grade (Fuhrman 1 and 2) or high-grade (Fuhrman 3 and 4). The TMA's were stained for VHL using monoclonal anti-VHL antibody IG32, and the each tumor was scored as being either positive or negative. In order to assess the relationship between VHL immunoreactivity and tumor behavior, representative sections from 19 CC-RCC were stained for VHL expression. These cases were divided into good prognosis (no recurrence with 5 years follow-up) and poor prognosis groups (metastases at presentation or within 1 year of nephrectomy). VHL staining for these sections was scored semi-quantitatively as being negative, weak/focal, moderate or strong/diffuse.

Results: 26/35 (70%) low-grade tumors on the TMA's had positive VHL immunoreactivity in contrast to 7/15 (47%) of the high-grade tumors. Of the 10 tumors from the good prognosis group, 6/10 (60%) showed strong/diffuse VHL immunoreactivity as compared to 2/9 (22%) of tumors from the poor prognosis group. Moreover, none of the good prognosis tumors showed negative VHL expression (4/10 had moderate or weak/focal staining), while 7/10 of the poor prognosis tumors showed only moderate or weak/focal expression, including one case that was negative for VHL expression.

Conclusions: In CC-RCC, reduced VHL immunoreactivity is observed in higher grade, more aggressive tumors, while preserved VHL immunoreactivity appears to be associated with low-grade tumors with favorable clinical behavior. This differential VHL immunoreactivity suggests that loss of VHL function may occur through different mechanisms in aggressive versus indolent tumors.

686 Expression of PAX-2 and Alpha-Methylacyl-CoA Racemase in Clear Cell Adenocarcinoma of the Bladder and Urethra

M Herawi, JI Epstein. Henry Ford Hospital, Detroit, MI; Johns Hopkins Hospital, Baltimore, MD.

Background: PAX2, a probable transcription factor involved in kidney cell differentiation, has recently been reported to be consistently expressed in nephrogenic adenoma (NA) and proposed as a reliable marker for NA. Alpha-Methylacyl-CoA Racemase (AMACR), a prostate cancer marker, has been extensively studied in NA and shown to be positive in a subset of NA. These markers have not been analyzed in detail in clear cell adenocarcinoma (CCA) of the lower urinary tract. We studied the immunohistochemical expression and diagnostic utility of PAX2 and AMACR in CCA versus NA.

Design: The study included 19 CCA of the bladder (n=9) and the urethra (n=10) from 4 men and 15 women with a mean age of 62 years (range: 36 to 91 years). 10 NA were also included. 4 μm thick sections were prepared from representative formalin fixed paraffin embedded archival tissue blocks and immunostained with PAX2 and AMACR antibodies. The expression of 34βE12 and p63 in conjunction with AMACR was also analyzed.

Results: Of 19 CCA, 9 (47%) were positive for PAX2 and 16 (82%) were positive for AMACR. In comparison, 9 of 10 NAs (90%) were positive for PAX2 and all 8 of 8 NAs (100%) were positive for AMACR. All 19 cases of CCA and 8 cases of NA were negative for 34βE12. P63 was positive in only one case of CCA and in none of NAs examined. Although the staining intensity for PAX2 was strong, the extent of staining ranged from focal to diffuse. The staining for AMACR ranged from weak to strong in intensity and focal to diffuse in extent.

Conclusions: 1) The vast majority of NA showed positive nuclear immunostaining for PAX2, while more than half of the CCA were negative for this marker. Because PAX2 is positive in almost 50% of CCA, it cannot reliably be used as a marker for NA versus CCA in limited biopsy material. 2) Although 100% of NA expressed AMACR, a small fraction of CCA was negative for the marker. AMACR is expressed in the great majority of NA and CCA and therefore is not helpful in distinction of the two entities. 3) PAX2 and AMACR staining extent ranged from focal to diffuse and was seen in tubulopapillary and solid areas of CCA.

687 Renal Oncocytoma with Renal Vein Extension

O Hes, M Michal, R Sima, N Kuroda, G Martignoni, M Brunelli, I Alvarado Cabrero, M Hora, X Yang. Charles University Hospital, Plzen, Czech Republic; Red Cross Hospital, Kochi, Japan; University Verona, Verona, Italy; Centro Medico, Mexico City, Mexico; Northwestern University, Chicago, IL.

Background: Renal vein invasion is one of the most important prognostic factors in renal cell carcinomas (RCC). Although such a phenomenon has been also observed in renal oncocytomas (RO), very few studies have addressed its clinical relevance. We attempted to investigate the clinicopathological correlation of RO with renal vein extension.

Design: From 210 RO in our registry, we identified 7 RO with extension into the branches of renal vein and studied their clinical behaviors, morphological, ultrastructural and cytogenetic features.

Results: The age of 7 patients (5 males and 2 females) ranged from 61 to 82 years (mean = 72.9). Five cases were identified incidentally, 2 patients had gross hematuria. After surgery, all 7 patients were alive and free of tumors with fellow-up of 1 to 5 years (mean = 3.6). Oncocytomas measured from 2.2 cm to 7.5 cm (mean = 4.97). Renal vein extension was grossly suspected in 5/7 cases and confirmed in all 7 cases. Tumors cells were positive for cytokeratins (CAM5.2, AE1/AE3), MIA, EMA and parvalbumin, 5/7 focaly positive for CD 117. Hale colloidal iron stain was negative in all cases. Ultrastructurally, the cytoplasm was packed by mitochondria without membrane-bound vesicles typical of chromophobe RCC. Cytogenetically, only one case showed monosomy of chromosome 17. Molecular genetic analysis did not detected abnormal numbers of chromosomes 7 and XY, LOH on 3p and mutation of VHL gene in all cases.

Conclusions: Although renal vein extension can be occasionally seen in oncocytomas, this event does not affect its benign behavior. In a renal tumor with granular cytoplasm showing renal vein extension, it is necessary to carefully exclude renal cell carcinomas such as chromophobe RCC, oncocytic variant of papillary RCC and granular variant of clear cell RCC.

688 The Fusion of TMPRSS2: ERG and an Intronic Deletion Is Associated with Hereditary Prostate Cancer

MD Hofer, R Kuefer, S Perner, C Maier, K Herkommer, T Paiss, F Demichelis, W Vogel, J Hoegel, AM Chinnaiyan, MA Rubin. Brigham and Women's Hospital, Boston, MA; Urologic University Hospital Ulm, Ulm, Germany; University Hospital Ulm, Ulm, Germany; University of Michigan School of Medicine, Ann Arbor, MI.

Background: Gene fusions have been well described in hematological disorders and sarcomas but are not as widely observed in epithelial tumors. The recent discovery that up to 50% of prostate cancers harbor *TMPRSS2:ETS* gene fusions with *TMPRSS2: ERG* being the most common dramatically changes our understanding of epithelial tumors. Emerging data also suggests that *TMPRSS2:ERG* prostate cancer is associated with more aggressive disease. The objective of the current study was to analyze the frequency of the *TMPRSS2:ERG* fusion in a large cohort of patients with hereditary prostate cancer.

Design: Hereditary prostate cancer was defined as 3 or more first-degree relatives having prostate cancer. Three tissue microarrays were constructed consisting of samples from 284 hereditary prostate cancer patients and benign controls. They were analyzed using a previously validated break-apart fluorescent in-situ hybridization (FISH) assay.

Results: Sufficient data of 212 patients from 45 families could be obtained. The fusion of *TMPRSS2* and *ERG* was identified in 117 cases (55%). In 65 of these cases (56%), the fusion was accompanied by an intronic deletion. This deletion was significantly associated with higher Gleason scores (GS 8-10, p=0.04, Kruskal-Wallis analysis of variance). Of the 45 families with a history of prostate cancer, the translocation was consistently present in all family members in 19 families (42%). Inconsistent translocation defined as one or more members without translocation was present in 15 cases (33%). Of the 19 fusion positive families, 7 families (37%) showed a consistent intronic deletion.

Conclusions: The fusion of *TMPRSS2* and *ERG* as well as the concurrent intronic deletion can be found in the majority of patients with hereditary prostate cancer. The observed frequencies appear to be higher than in sporadic cases of prostate cancer. We are currently working on a linkage analysis to expand these findings.

689 Prostatic Stromal Hyperplasia with Atypia: A Benign, Histologically Worrisome Lesion of the Prostate

D Hossain, I Meiers, J Qian, GT MacLennan, DG Bostwick. University of Maniboba, Winnipeg, Winnipeg, MB, Canada; Bostwick Laboratories, Glen Allen, VA; University Hospital of Cleveland, Cleveland, OH.

Background: Prostatic stromal hyperplasia with atypia is a rare lesion that may be mistaken for sarcoma because of the presence of bizarre nuclei.

Design: We studied the clinical and histologic features of 26 cases of stromal hyperplasia with atypia. Immunohistochemical studies were undertaken in 15 cases. Patient follow-up was obtained in all cases. Patients ranged in age from 46-82 yr (mean 65 yr), and presented with urinary obstructive symptoms in 18 cases, abnormal digital rectal examination (DRE) in 5 cases and incidental finding in 3 cases.

Results: Two histologic patterns of stromal hyperplasia with atypia were identified, both of which contained variable numbers of large bizarre giant cells with vacuolated nuclei, smudged chromatin, and frequent multinucleation. The most common pattern, the infiltrative pattern (19 cases), consisted of an ill-defined hyperplastic stromal nodule with an admixture of atypi-cal bizarre giant cells infiltrating the hyperplasic epithelium. The stroma consisted of a hypocellular loose myxoid matrix accompa-nied by ectatic hyalinized vessels arid mild to moderate chronic inflammation. The less common pattern, the leiomyoma-like pattern (7 cases), consisted of a solid circumscribed expansile stromal nodule with abundant smooth muscle. The cells in the infiltrative pattern displayed intense immunoreactivity for vimentin, but weak or no reactivity for desmin and actin. Conversely the leiomyoma-like pattern displayed intense immunoreactivity for desmin and actin, and weak to moder-ate reactivity for vimentin. Both patterns

displayed intense immunoreactivity for androgen receptors, variable reactivity for progesterone receptors, but no reactivity for estrogen receptors. Four recurrences were seen with mean follow-up of 6.3 years (range 3months-16 yr) but no evidence of sarcomatous transformation occurred.
Conclusions: Prostate stromal hyperplasia with atypia is benign lesion and should not be interpreted as sarcoma or stromal lesion with uncertain malignant potential.

690 Oncocytoma Has High Endogenous Avidin-Binding Activity (EABA): Can EABA Be Used as a Marker in Differentiating Oncocytoma from Other Renal Cell Carcinoma (RCC) Mimics?

J Hu, K Kanehira, T Pier, L Sebree, W Huang. University of Wisconsin, Madison, WI.
Background: Avidin-Biotin complex (ABC) detection system is commonly used in immunohistochemical laboratories (IHC) to increase target antigen detecting sensitivity. It has been documented that some paraffin-embedded tissues have higher level of EABA such as ductal epithelial cells of salivary gland, liver cells and cardiac and skeletal muscles and kidney. Limited data is available on EABA in renal cell neoplasm.
Design: A renal cell neoplasm tissue microarray (TMA) was constructed including oncocytoma (n=32), chromophobe RCC (RCCchr, n=17), clear cell RCC (RCCcl, n=61), papillary RCC (RCCp, n=50) and benign renal tissues (n=31). Duplicate cores were obtained from each tumor/tissue. Three negative control TMA slides were studied for EABA in renal neoplasm (no primary antibody was applied). Slide #1 was stained on Ventana automated system. Slide #2 and #3 were stained manually with Biocare avidin-biotin detection kit. Endogenous peroxidase (EP) blocker was used for all three slides. Biotin (EB) blocker was applied only to slide #1. No biotinylated 2nd antibody was applied to slide #2. No avidin-HRP was applied to slide #3. A semiautomated quantitative image analysis system, ACIS[reg (Clarient, Inc, Alisa Viego, CA), was used to evaluate the TMA slides. The core staining intensities (INT) vary from 0 to 210; core staining percentages (S %), 0 to 100%. A composite score (CS = INT x S %) for each core is obtained and analyzed. A positive threshold is defined as CS = 25% of maximal INT x 10% (staining percentage).
Results: Without EB blocker (slide #2), the oncocytoma demonstrated a high positive rate of EABA: 19/32 (60%, oncocytoma), 18/61 (30%, Benign), 11/50 (22%, RCCp), 4/61 (6%, RCCcl) and 1/17 (3%, RCCchr). With EB blocker (slide #1), the EABA was reduced mostly in benign renal tissue, but only slightly in renal neoplasm: 1/61 (2%, Benign), 14/32 (44%, oncocytoma), 10/50 (20%, RCCp), 2/61 (3%, RCCcl) and 1/17 (6%, RCCchr). No staining signal was observed on slide #3, as expected.
Conclusions: The staining results must be interpreted with caution when avidin-biotin detection system is used in diagnosing renal neoplasm, especially oncocytoma and RCCp. Oncocytoma has high EABA compared to RCCs suggesting EABA could be used as a marker in differentiating oncocytoma from RCC, especially RCCchr.

691 Testicular Lymphoma: A Clinico-Pathological Study of 25 Cases

HF Huwait, A Yilmaz, K Sircar, K Trpkov, F Brimo, M Alrefae, T Cheng, L Begin, TA Bismar. McGill University, Montreal, QC, Canada; University of Calgary, Calgary, AB, Canada.
Background: Testicular lymphoma is an uncommon disease reported in 1 to 7% of all testicular neoplasms. It is the most common testicular tumor in men older than 50 years. We describe the clinical and the pathological features of testicular lymphomas seen in our institutions.
Design: We undertook a retrospective review of testicular lymphomas in our institutions between 07/89 and 07/06. Pathological parameters included lymphoma type and involvement of the following structures: seminipherous tubules, spermatic cord (SC), epididymis (EP), tunica albuginea, and tunica vaginalis. Clinical data included existence of extra-testicular disease, clinical stage, treatment, and outcome.
Results: Of a total of 25 lymphomas, 23 (92%) were primary testicular lymphomas. Two were secondary lymphomas of testis. Mean patient age was 66.8 (31-87) years. All documented cases were diffuse large B-cell lymphomas. Invasion of seminipherous tubules was identified in 90% of cases. SC and EP invasion was present in 11/23 (47.8%) and 30% (7/23) of all primary testicular lymphomas, respectively. Tunica albuginea was involved in 16/23 (69.6%) of cases, but tunica vaginalis was involved in only 2/23 (8.7%) of cases. Localized disease (stage I or II) was present in 84% of patients 17/23 (69.6%) of primary lymphomas were treated with adjuvant therapy. Complete follow-up was available for 17 patients. Intrathecal (IT) prophylactic chemotherapy was given to 10/17 (59%) of patients. During a mean follow-up of 49.9 (8-138) months, 8/17 (47%) of patients had disease progression, and 4 of those developed CNS relapse. CNS relapse rate was 20% (2/10) for patients who had IT chemotherapy vs. 14% (1/7) for those who did not. The overall relapse rate for stage I disease was higher than stage II and IV (46% vs. 33%). Two patients died of disease progression at 2 and 10 months after the initial presentation. No significant relationship was found between any of the pathological parameters and the relapse rate.
Conclusions: Primary testicular lymphoma is significantly more common than secondary lymphoma of the testis. The main histological type is large B-cell lymphoma, as previously reported. In primary lymphomas, no significant association was found between the pathological features and the rate of relapse.

692 *MDM2* Amplification Is an Uncommon Oncogenic Mechanism in Sarcomatoid Renal Cell Carcinoma: Biologic and Diagnostic Implications

CM Ida, JC Cheville, WR Sukov, MR Erickson-Johnson, X Wang, AM Oliveira. Universidade de Sao Paulo, Sao Paulo, SP, Brazil; Mayo Clinic, Rochester, MN.
Background: Sarcomatoid renal cell carcinoma (SRCC) represents 5% of renal cell carcinomas and can be difficult to distinguish from primary retroperitoneal sarcomas due to the frequent absence of cytokeratin expression in the sarcomatoid component and an inconspicuous epithelial component. Among retroperitoneal spindle cell/pleomorphic sarcomas, dedifferentiated liposarcoma (DDL) is among the most common differential diagnoses. Similar to SRCC, the well-differentiated component of DDL may be of difficult recognition - especially in small biopsies - and overlap histologically with the sarcomatoid component of SRCC. Since amplification of the *MDM2* oncogene is a common genetic event observed in a variety of sarcomas, and is virtually present in all cases of DDL, we aimed to investigate whether the identification of *MDM2* amplification is useful in discriminating SRCC from DDL.
Design: Representative 4 µm sections of paraffin-embedded, formalin-fixed tissue specimen from 15 SRCC and 30 DDL were evaluated for *MDM2* amplification by fluorescence in situ hybridization (FISH). All experiments were performed by co-hybridizing a custom designed spectrum-orange probe for *MDM2* with a commercially available spectrum-green centromere 12 specific probe [CEP12(D12Z3), Vysis®]. Signal pattern evaluation was performed in 200 cells/tumor. *MDM2* amplification was defined as *MDM2*/CEP12 signal ratio of >=3.
Results: While all 30 DDL showed evidence of *MDM2* amplification with often >25-50 *MDM2* copies/cell (*MDM2*/CEP12 ratio > 25), only a single (of 15) SRCC showed *MDM2* amplification (20 copies/cell) ($p<0.0001$). In contrast, these tumors showed a FISH signal pattern consistent with an aneuploidy/polyploidy involving chromosome 12 (*MDM2*/CEP12 ratio = 1; median, 4-5 CEP12/*MDM2* signal pairs/cell).
Conclusions: In contrast to DDL and other sarcomas, *MDM2* amplification is a rare oncogenic event in sarcomatoid RCC. This finding supports the hypothesis that the biologic mechanisms operating in the sarcomatoid component of RCC are distinct from those found in primary sarcomas despite their overlapping morphologic features. This difference may also be of diagnostic relevance, especially when dealing with small biopsies of spindle cell/pleomorphic retroperitoneal malignancies.

693 Overexpression of p4EBP1 in High Grade PIN Predicts and Associates with Prostatic Cancer

C Iglesias, I de Torres, F Rojo, J Castellvi, MT Salcedo, A Amoros, J Morote, J Raventos, S Ramon y Cajal. Vall d'Hebron University Hospital, Barcelona, Spain; Vall'hebron University Hospital, Barcelona, Spain.
Background: HGPIN as an isolated finding occurs in 2,7% to 14,2% of needle biopsies. The predictive value for cancer on repeat biopsy is considered nowadays less than 21% due to wide prostate sampling in most biopsies. Nevertheless, there are a subgroup of HGPIN which progress or is associated with cancer and there are not pathological criteria to identify them. In most prostate cancers there is activation of the signalling pathways with several oncogenic alterations activated. Most of the signals converge and activates the mTOR pathway and specially in the downstream factor 4EBP1 which is the key factor in the control of protein synthesis and apoptosis. Because, previously, we have described high levels of p4EBP1 in HGPIN associated to carcinomas, we hypothesized that p4EBP1 could be a marker of progression in HGPIN.
Design: We have analyzed the immunohistochemical expression of phosphorilated form of 4EBP1 (p4EBP1) in 76 prostatic needle biopsies with HGPIN. All the 76 patients had several later biopsies (55/76 with persistent HGPIN or normal histology; 21/76 with progression to prostatic cancer –PC-), with a mean follow-up of 19 month (range from 3 to 49). Positivity was semiquantitatively scored, including intensity (from 0 to 3) and percentage of positive cells, obtaining the HScore for statistical analysis.
Results: P4EBP1 expression pattern in epithelium was citoplasmatic and/or nuclear. Interestingly, p4EBP1 expression was significantly higher in HGPIN focus corresponding to cases with progression to PC than in the cases without it (p=0,000). Considering an Hscore>50 as "positive", the Sensibility and Specificity of the marker to predict a malignant progression were 63% and 100%, with a Positive Predictive Value and Negative Predictive Value of 100% and 21%.
Conclusions: We have found significant differences in p4EBP1 expression in HGPIN focus from needle biopsies related to the presence or not of future progression to histologically demonstrated PC. These results suggest the capability of p4EBP1 to detect a "high-risk" group of the patients. Therefore, we propose p4EBP1 overexpression as a good histological prognostic marker of progression risk in HGPIN. That could help to identify the subgroup of really high risk of HGPIN.

694 The RNA-Binding Protein IMP3: A Novel Molecular Marker Predicts Metastasis and Progression of Renal Cell Carcinomas

Z Jiang, PG Chu, BA Woda, Q Liu, C Li, KL Rock, C-L Wu. University of Massachusetts Medical Center, Worcester, MA; City of Hope National Medical Center, Los Angeles, CA; Massachusetts General Hospital, Boston, MA.
Background: Distant metastatic potential of localized renal cell carcinoma (RCC) is often unpredictable. In this study, we used quantitative analysis of the immunohistochemistry (IHC) to investigate whether the RNA binding protein (IMP3), an oncofetal protein, can serve as a new biomarker to predict metastasis and prognosis of RCC.
Design: The 371 patients with localized RCCs (stage I: N=216; II: N=64; III: N=91) from three institutions were investigated by use of survival analysis. The expression of IMP3 was evaluated by IHC with a computerized image analyzer (ACIS). IMP3 expression in RCCs was considered to be negative [average ACIS value/case(ACISV): <1] and positive (ACISV: ≥1; low levels of expression: ACISV = 1 to 10, and high levels of expression: ACISV = >10).
Results: The expression of IMP3 was only observed in the cytoplasm of tumor cells but not in benign tissue adjacent to cancer. Kaplan-Meier plots in all patients and in patients separated in each stage showed that patients with IMP3-negative RCCs (ACISV = 0.08±0.09) had a significantly longer metastasis-free and overall survival than did those with IMP3-positive RCCs (ACISV =16.9±24.8, $P<0.0001$). In patients whose localized RCCs were negative for IMP3, the 5-year metastasis-free and overall survival rates were 98% and 89% (stage I), 94% and 88% (stage II), and 62% and 58% (stage III) respectively, whereas in patients with IMP3 positive RCCs, the metastatic free and overall survival rates were 44% and 32% (stage I), 41% and 41% (stage II), and 16% and 14% (stage III) respectively. Patients with low levels of IMP3 in their

tumors (ACISV = 3.9±2.5) were also had better metastasis-free and overall survival rates than did those with high levels of IMP3(ACISV = 40.6±29.4, P<0.001). Multivariable analysis showed that IMP3 status in primary RCCs was a strong independent predictor of clinical outcome. The hazard ratios were 6.08 (metastasis-free survival, P<0.0001) and 4.06 (overall survival, P<0.0001), which were much higher than hazard ratios associated with other independent risk factors.
Conclusions: IMP3 is an excellent independent prognostic marker that can be used at the time of initial diagnosis of RCC to identify patients who have a high potential to develop metastasis and who might benefit from early systemic therapy.

695 Intracellular Signaling Via Tyrosine 1062 in Ret Mediates Proliferation of Spermatogonia

M Jijiwa, K Kawai, N Asai, M Takahashi. Nagoya University Graduate School of Medicine, Nagoya, Aichi, Japan.
Background: The *RET* receptor tyrosine kinase is essential for the organogenesis, such as enteric nervous system, kidney, some ganglions, and germ cells. Intracellular signaling via Ret is mediated by the autophosphorylation of specific tyrosine residues in Ret. Tyrosine 1062 is one of the important residues leading to activation of PI3-K/AKT and RAS/ERK pathways, which are critical for cell survival, proliferation and differentiation. As for spermatogenesis, Ret and its co-receptor GFRα1 are expressed in the undifferentiated spermatogonia, considered as germline stem cell, and their ligand GDNF is expressed in Sertoli cell. Some reports showed the fact that the testes lucking Ret demonstrate the reduction of germ cell and no sperm. But the detailed function of signaling via Ret in spermatogenesis is not known yet.
Design: To identify the role of intracellular signaling via Ret Tyrosine 1062 in spermatogenesis, we investigated the testes of the RET Y1062F knock-in mice in which tyrosine 1062 in Ret was replaced with phenylalanine. Testes of knock-in mice were resected and weight were measured. The number of germcells, and RET, PLZF (stem cell marker) positive cells were counted by histological method using hematoxylin and eosin staining and immunohistochemistry, respectively. To know whether apoptosis was responsible for the reduction of spermatogonia or not, TUNEL staining was done and the location of TUNEL positive cells was evaluated. Each result was compared between wild type and homozygous mice, at postnatal day (P) 0, 7, 14, 28.
Results: The testis weight-to-body weight and the number of germcells did not show significant difference between wild type mice and homozygote at P0, 7, 14. At P28, the homozygous testis weight-to-body weight was obviously less than that of wild type and the number of germcells in testes of homozygotes were reduced apparently. The RET and PLZF positive cells were decreased gradually in both wild type and homozygotes. But while wild type mice kept a little number of RET and PLZF positive cells at P28, homozygous mice completely lost those positive cells and no sperm was detected. TUNEL staining showed that the apoptosis occurred equally in both genotype and the TUNEL positive cells were located mainly inside of the seminiferous tubules.
Conclusions: Intracellular signaling via Tyrosine 1062 in Ret plays an important role in the proliferation of undifferentiated spermatogonia, in other words, in the self-renewal of germline stem cell.

696 Urothelial Carcinoma with an Inverted Growth Pattern May Be Distinguished from Inverted Papilloma by UroVision Fluorescence In Situ Hybridization and Immunohistochemistry

TD Jones, S Zhang, A Lopez-Beltran, JN Eble, MT Sung, GT MacLennan, R Montironi, PH Tan, LA Baldridge, L Cheng. Indiana University School of Medicine, Indianapolis, IN; Cordoba University, Cordoba, Spain; Chang Gung Memorial Hospital-Kaohsiung Medical Center, and Chang Gung University College of Medicine, Kaohsiung, Taiwan; Case Western Reserve University, Cleveland, OH; School of Medicine, Polytechnic University of the Marche Region (Ancona), United Hospitals, Ancona, Italy; Singapore General Hospital, Singapore, Singapore.
Background: Inverted papilloma of the urinary bladder and urothelial carcinoma with an inverted growth pattern may be difficult to distinguish histologically, especially in small biopsies. The distinction is important as these lesions have very different biological behaviors and are treated differently. We undertook immunohistochemical staining and UroVysion fluorescence in situ hybridization (FISH) to determine if these methods could aid in making this distinction.
Design: We examined histologic sections from 15 inverted papillomas and 25 urothelial carcinomas with an inverted growth pattern. Each tumor was stained with antibodies to Ki-67, p53, and cytokeratin 20 (CK20). In addition, each tumor was examined with UroVysion FISH for gains of chromosomes 3, 7, and 17 and for the loss of chromosome 9p21 signals.
Results: None of the inverted papillomas stained positively for Ki-67 or for CK20. Only 1 of 15 inverted papillomas stained positively for p53. By contrast, 64%, 56%, and 60% of urothelial carcinomas with an inverted growth pattern stained positively for Ki-67, p53, and CK20, respectively. Only one of the urothelial carcinomas stained negatively for all three immunohistochemical markers. UroVysion FISH produced normal results for all cases of inverted papilloma. By contrast, 14 of 25 (56%) cases of urothelial carcinoma with an inverted growth pattern demonstrated chromosomal abnormalities typical of urothelial cancer.
Conclusions: A panel of immunohistochemical stains (including stains for Ki-67, p53, and CK20) and/or UroVysion FISH can help to distinguish inverted papilloma from urothelial carcinoma with an inverted growth pattern.

697 Telomere Length Analysis of High-Grade Prostatic Intraepithelial Neoplasia (HPIN) and Adjacent Stroma Predicts Outcome in Prostate Cancer and Provides Evidence of Field Carcinogenesis

AM Joshua, B Vukovic, I Braude, S Hussein, M Zielenska, JR Srigley, AJ Evans, JA Squire. University Health Network/Ontario Cancer Institute, Toronto, ON, Canada; Hospital for Sick Children, Toronto, ON, Canada; The Credit Valley Hospital, Mississauga, ON, Canada.
Background: The causes of the genomic events underlying the development of prostate cancer (CaP) remain unclear. Chromosomal instability is evident in many karyotypes of CaP, with frequent and consistent changes characterizing this malignancy. Telomere dysfunction is one potential mechanism associated with the generation of chromosomal instability. We have previously demonstrated a decrease in telomere length in HPIN with increasing proximity to CaP in a series of radical prostatectomy specimens.
Design: In this study, we examined normalized telomere lengths in prostate biopsies. The biopsies, performed between 1998 and 2000, were obtained from 69 men and contained only HPIN. Quantitative fluorescence in situ hybridization (QFISH) was performed on unstained sections from HPIN biopsies using pan-telomeric and pan-centromeric probes. Quantitative assessment of telomere/centromere signal intensity was performed on 10 consecutive images that were z-stacked into a composite image and exported to ImageJ software. An average of 50 non-overlapping HPIN and 50 stromal nuclei were scored on each slide to determine relative changes in telomere lengths and DNA ploidy.
Results: In men with isolated HPIN on biopsy, we observed an association between shorter telomeres in both the HPIN and the adjacent stroma and an eventual diagnosis of CaP. Multivariate Cox regression modelling demonstrated a significant predictive value for time to the diagnosis of CaP using telomere length for both HPIN and the surrounding stroma. This relationship was maintained both alone and in combination with baseline PSA. Finally, Kaplan-Meier analysis of telomere length demonstrated a significantly increased probability of having a follow-up biopsy that was positive for CaP with short telomeres in the surrounding stroma (p=0.035, HR=2.12). A similar trend was noted for HPIN itself (p=0.126, HR=1.72).
Conclusions: Our findings of telomere shortening in both HPIN and the adjacent stroma provide evidence for the existence of field cancerization in CaP and generate important insights into its molecular pathogenesis. Our observations also lend support to the hypothesis that telomere erosion may be fundamental to the generation of the chromosomal instability associated with CaP.

698 Clusterin Expression and Hormone Therapy Effect in Prostatic Adenocarcinoma: A Tissue Microarray Study

N Juanpere, JA Lorente, A Doll, M Abal, T Baro, P Garcia, C Allepuz, L Plaza, A Munne, LA Rioja, J Reventos, S Serrano, A Gelabert, J Lloreta. Hospital del Mar, Barcelona, Spain; UPF, Barcelona, Spain; UAB, Barcelona, Spain; University Hospital Vall Hebron, Barcelona, Spain; University Hospital Miguel Servet, Zaragoza, Spain.
Background: Clusterin is a secretory glycoprotein that is present in many tissues. It has been identified as one of the main prostasomal proteins. It has dual functional properties related to both apoptotic and antiapoptotic signals. Clusterin expression is upregulated in prostatic tumor tissue after neoadjuvant hormone therapy (NHT). On the other hand, increased expression of clusterin has been associated with shorter biochemical recurrence-free survival. We conducted the present tissue microarray (TMA) study to further elucidate the relationship of clusterin expression with the effect of NHT in tumor cells, as well as with standard clinico-pathological variables.
Design: Two TMA blocks with 233 prostatic adenocarcinoma samples, selected from radical prostatectomy specimens, were constructed. They included 175 cases with and 58 without previous NHT. Sections were stained with a Clusterinβ antibody (M-18, dilution 1:600. Santa Cruz Biotechnology, Santa Cruz, CA). Intensity of clusterin staining was recorded (0-3), as well as the severity of the NHT-induced changes in tumor cells (also scored 0 to 3). ANOVA tests were performed to study relationship of clusterin expression with treatment and with treatment-induced changes, pathologic stage, and biochemical recurrence-free survival.
Results: The intensity of clusterin expression was significantly related to previous NHT (Chi^2 34.042, p=0.0001). It was also significantly higher in cases with greater tumor response to NHT (Chi^2 46.882, p=0.0001). There was no statistically significant relationship between clusterin expression and pathologic stage or biochemical recurrence-free survival, regardless of previous NHT.
Conclusions: The strong association between intensity of clusterin expression and the presence and effect of NHT in tumor cells suggests that clusterin may be involved in the mechanisms that are responsible for this effect. Alternatively, clusterin expression could be the consequence of such changes. The biological role of clusterin in prostatic adenocarcinoma needs to be further elucidated, and it could have potential therapeutic implications related to the availability of clusterin antisense oligonucleotides.

699 Reappraisal of TNM T3a Renal Cell Carcinoma: Significance of Extent of Fat Invasion and Direct Extension

SJ Jung, DS Paick, JY Ro, LD Truong, AG Ayala, SS Shen. College of Medicine of Inje University, Busan, Korea; The Methodist Hospital and Weill Medical College of Cornell University, Houston, TX.
Background: Renal cell carcinomas (RCC) with direct extension to adrenal gland, or perinephric or renal sinus fat invasion are all staged as T3a tumors in current TNM staging system. The aim of this study was to evaluate whether the extent of fat invasion as well as adrenal gland direct extension have a similar prognosis.
Design: Of the 660 patients who underwent radical nephrectomy for RCC at one single hospital, 241 patients had T3 tumors. Forty-two patients (17.4%) had either nodal or distant metastasis and were excluded from the analysis. Pathology reports and glass slides from the remaining 199 cases were evaluated. Fat invasion was subclassified as

focal (≤5 mm into the fat) or extensive (>5 mm). Direct adrenal invasion was defined as contiguous involvement of adrenal parenchyma by renal tumor. Survival analysis was performed by the Kaplan-Meier method and differences were evaluated by the log rank test.

Results: Among the 199 evaluated cases of T3 RCCs, focal and extensive fat invasions were identified in 59 and 62 cases, respectively; renal vein invasion and direct adrenal invasion were seen in 73 and 5 cases, respectively. The average age of the patents was 62.9 years and 146 patients were male and 53 were females. With an average follow-up of 38.9 months (range 0.2-154.2), the 2-year and 5-year survival rates were 86% and 56% for focal fat invasion, 76% and 70% for extensive fat invasion, and 54% and 31% for renal vein invasion, respectively. All the patients with direct adrenal extension by tumor died within 2 years. No significant survival difference was seen in patients with RCCs with focal and extensive fat invasion (p=0.884). The survival in patients with renal vein invasion by tumor was significantly worse than that of patients with perinephric fat invasion (p<0.001). Finally, the patients with direct adrenal extension had the worst survival, worse than that of either fat invasion or renal vein invasion (p<0.01).

Conclusions: Our studies show that T3 RCCs with focal or extensive perinephric fat invasion has a similar prognosis, and is significantly more favorable than that of renal vein invasion. In contrast, tumors with direct adrenal gland extension carry a dismal prognosis, which is worse than that of perinephric fat or renal vein invasion. Therefore, RCC with contiguous adrenal involvement may be staged as T4, rather than T3a disease.

700 CK7 and CD10 May Be Useful Markers in Differentiating Oncocytoma from Chromophobe Renal Cell Carcinoma

K Kanehira, T Pier, L Sebree, W Huang. University of Wisconsin, Madison, WI.

Background: Renal cell carcinoma (RCC), especially chromophobe renal cell carcinoma (RCCchr) and renal oncocytoma may resemble each other morphologically, especially on needle core biopsy specimen. Several markers have been suggested as useful in differentiating oncocytoma from its mimics. None has been established for this purpose.

Design: A renal cell neoplasm tissue microarray (TMA) is constructed including oncocytoma (n=32), RCCchr (n=17), clear cell RCC (RCCcl, n=61), papillary RCC (RCCp, n=50) and benign renal tissues (n=31). Duplicate cores were obtained from each tumor/tissue. CK7, CD10. EMA, RCCma and vimentin immunostains were performed on Ventana automated system. A semiautomated quantitative image analysis system, ACIS® (Clarient, Inc, Alisa Viego, CA), was used to evaluate the TMA slides. Core staining intensities (INT) vary from 0 to 210; and core staining percentages (S %), 0 to 100%. A composite score of each core (CS = INT x S %) is obtained and analyzed. A positive threshold is defined as CS = 25% of maximal INT x 10% (staining percentage) for epithelial markers (CK7, EMA and RCC). A positive threshold is defined as CS = 25% of maximal INT x 20% (staining percentage) for stromal markers (CD10 and vimentin).

Results: RCCchr has a low CD10 positive rate: 3/17 (**18%,** RCCchr), 20/32 (**62%,** oncocytoma), 57/61 (93%, RCCcl), 34/50 (67%, RCCp). RCCcl and oncocytoma have a low CK7 positive rate: 11/32 (**33%,** oncocytoma), 4/61 (**7%**, RCCcl), 13/17 (**76%)** (RCCchr), 36/50 (**78%**, RCCp). A high RCCma positive rate is observed in RCCcl and RCCp: 46/61 (76%, RCCcl), 27/50 (54%) (RCCp), 2/17 (12%, RCCchr), 7/32 (21%, oncocytoma). High EMA positive rates are observed in all tumors: 16/17 (97%, RCCchr), 31/32 (98%, oncocytoma), 54/61 (88%, RCCcl), 49/50 (97%, RCCp). High vimentin positive rates are seen in RCCcl and RCCp: 43/61 (70%, RCCcl), 37/50 (73%, RCCp), 18/32 (56%, oncocytoma), 5/17 (32%, RCCchr).

Conclusions: CK7 and CD10 may be useful markers in differentiating oncocytoma from RCCchr. RCCma is confirmed as a marker for RCCcl and RCCp. EMA and vimentin in combination may be useful in diagnosing RCCcl and RCCp.

701 Correlation of Pelvic Biopsies and Nephrouretectomy Specimens for Renal Pelvic Transitional Cell Carcinoma

J Kang, SS Shen, SJ Jung, YM Cho, SP Lerner, JY Ro. Ulsan University, Asan Medical Center, Seoul, Korea; The Methodist Hospital and Weill Medical College of Cornell University, Houston, TX; Inje University College of Medicine, Paik Hospital, Busan, Korea; Baylor College of Medicine, Houston, TX.

Background: Upper urinary tract transitional cell carcinoma (TCC) accounts for approximately 5% of all urologic malignancies and its incidence has been reported to be increasing. Cytologic studies have variable benefit in the evaluation, particularly for low grade lesions. With increasing use of ureteropyeloscopy, biopsy is frequently attempted for pelvic tumor. The aim of this study was to determine the detection rate, concordance of grading and diagnosis by biopsy and final diagnosis from nephroureterectomy specimens.

Design: Pathology reports and all available slides from 32 nephrouretectomies with matched previous biopsies of renal pelvis from two large tertiary hospitals in US and Korea were evaluated. The histologic type, grade, tumor size, number of tumor, as well as extent of invasion were evaluated and compared. Grading was based on 1973 World Health Organization 3 tiered system and staging was based on the current TNM staging system.

Results: In 32 cases of nephrouretectomy for pelvic TCC , 24 patients were males and 8 were females with an average age of 65.6 years (range 45 to 88), number of tumor ranged from 1-4 (mean=1.9), and average tumor size was 3.8 cm (0.3 to 10.0). Examination of nephrouretectomy specimens revealed that the T stages were: Ta (8), Tis (3), T1 (4), T2 (4), and T3 (5). The tumor grades were G2(13 cases) and G3(19) with no G1 tumors. In 2 cases of invasive carcinomas, the biopsies one each were hyperplasia and grade 1 non-invasive papillary carcinoma. Pelvic biopsy results were: non-diagnostic (7 cases, 22%), suspicious (2, 6.2%), hyperplasia or dysplasia (2, 6.2%), Ta (10, 31.3%), Tis (6, 18.9%) and invasive carcinoma (5, 15.6%). In patients with a sufficient biopsy (exclude non-diagnostic category), the accuracy of diagnosis was 92% with grading concordance rate of 84%. In 7 cases of non-diagnostic pelvic biopsies, the diagnoses of nephroureterectomy were TaG1 or 2 (3), Tis (1) and invasive carcinoma (3).

Conclusions: Diagnosis of renal pelvic biopsy with high accuracy (92%) and accurate grading (84%) can be achieved when an adequate specimen is obtained. Failure to obtain a representative sample (22%) accounts for significant proportion of non-diagnostic findings.

702 Potential Role of 15-Lipoxygenase-1, in Inflammation and Bladder Cancer Initiation: A Hypothesis

UP Kelavkar, M Sen, AV Parwani. University of Pittsburgh Medical Center, Pittsburgh, PA; University of Pittsburgh Cancer Institute, Pittsburgh, PA.

Background: Fifteen (15)-Lipoxygenase type 1 (15-LO-1, ALOX15), a highly regulated, tissue- and cell-type-specific lipid-peroxidating enzyme has several functions ranging from physiological membrane remodeling, pathogenesis of atherosclerosis, inflammation, and carcinogenesis. Our previous study in prostate cancer tissues has shown that hypermethylation leads to the upregulation of 15-LO-1 expression and vice versa. Our study has also shown that expression of 15-LO-1 was high in normal and low in bladder cancer tissues. Therefore, this study examined for hypermethylation status for a specific CpG within the 15-LO-1 promoter in bladder tissues.

Design: We hypothesized that the expression of 15-LO-1 can be co-induced with artificially inducing inflammation and that aberrant 15-LO-1 overexpression in primary urothelial cells is key for bladder cancer "initiation." To test our hypothesis we first examined microdissected "normal appearing" surrounding bladder tumors (n=7) and low and high grade invasive and non-invsive bladder tumors (WHO 2004) [n=12] by combined bisulfite restriction analysis (COBRA) analyses for methylation status of a specific CpG within the 15-LO-1 promoter.

Results: Our results demonstrate that 15-LO-1 promoter methylation is frequently present in "normal appearing" surrounding bladder tumors and reduced in bladder tumors. These results provide preliminary evidence on the possible role of "aberrant" 15-LO-1 expression as a marker during bladder cancer initiation, but not in progression.

Conclusions: In an anti-inflammatory role, 15-LO-1 is generally induced or "aberrantly expressed" in response to inflammation. This process if remains uncontrolled can cause carcinogenesis. One of the most common treatments of bladder cancer patients is by inducing inflammation in bladder. However, inducing bladder inflammation as a treatment may not always be beneficial for every patient since 15-LO-1 can be induced and could have unfavorable consequences. Thus screening of bladder cancer patients, for e.g., treated with BCG, for 15-LO-1 may provide means of alternative treatment strategies to 15-LO-1 positive patients who may either be unresponsive to BCG treatment or may recur.

703 Oxidative Stress; an Etiologic Factor of Prostate Cancer? A Tissue Microarray (TMA) and Marker Study of Age, Race and Neoplastic Progression

S Khayyata, G Yildirim Kupesiz, A Andea, S Sheng, D Grignon, W Sakr. Wayne State University, Karmanos Cancer, Detroit Medical Center, Detroit, MI; University of Alabama, Burminghom, AL.

Background: Oxidative stress (OS) is implicated in prostate carcinogenesis with recent studies suggesting linking higher expression of OS markers and the development of PCa. With the age and ethnic attributes of PCa, the objectives of this study were to investigate the potential increase in the immunohistochemical (IHC) expression of OS markers with advancing age and with the progression of malignant transformation of benign prostatic epithelium (BPE) to prostatic intraepithelial neoplasia (PIN) and to carcinoma, in a racially balanced group of Pca patients of a wide age spectrum.

Design: Radical prostatectomy specimens with Gleason score 7 from 120 consecutive African American and Caucasian patients (60 each), with 40 patients form each of the age brackets of <= 50, 51-64, and >=65 years, were identified. Three -120-cores TMAs of BPE, high grade PIN and PCa respectively were constructed with a consistent age and race representation. The TMAs were stained with GST p, HDAC-1, HSP 90, Maspin, NOS 1, NOS 2 and COX 2. The distribution and intensity of expression were correlated with the three histological categories, age and race using Kendal's tau correlation test.

Results: There was a statistically significant increase in the intensity of expression of HSP-90, NOS-1, NOS-2, COX-2 and HDAC-1 from BPE to PIN and to Pca. A trend linking advancing age to higher expression of NOS-1 and COX 2 was observed with moderate/strong expression in patients averaging 68 years of age and with weak or no expression for patients averaging 57.9 years. (p=0.07). There were no race-related differences in HIC expression.

Conclusions: Our data demonstrate a progressive increase in the expression of OS markers across the spectrum of neoplastic transformation of the prostate. The expression of HDAC 1, an androgen receptor (AR) regulator exhibited a similar trend suggesting that both OS pathway and AR dependability of neoplastic transformation may have an interrelated role in prostatic carcinogenesis.

Table 1. Proportion of cases with strong staining.

Histology	HSP-90	NOS 1	NOS 2	COX 2	HDAC-1
Benign	36.5%	1%	28.8%	6%	35.3%
High Grade PIN	38.1%	3.8%	39.8%	7.3%	30%
PCa	58.5%	38%	59.6%	16.7%	86.5%
p-value	<0.0001	<0.0001	<0.0001	<0.0001	<0.0001

704 Lymphatic Vessel Density in Prostate Adenocarcinoma; Correlation with Clinicopathological Factors

KH Kim, S Lee, YW Kim, SG Chang, YK Park. Kyung Hee University, College of Medicine, Seoul, Korea; Kyung Hee University, Collge of Medicine, Seoul, Korea.

Background: Lymph node metastasis is one of the major causes of treatment failure of prostate cancer. Recently, several reports had suggested that the dissemination of neoplastic cells and cancer progression was associated with lymphatic vessel density (LVD). To determine the clinical significance of LVD in prostate adenocarcinoma, we analyzed the LVD in prostate adenocarcinoma and correlated the results with the clinicopathological factors including patients' age, serum PSA level, Gleason score, pTNM stage.

Design: A total 40 patients who had received radical prostatectomy for prostate adenocarcinoma were included. Formalin fixed and paraffin-embedded prostate carcinoma tissues were subjected for immunohistochemistry using lymphatic endothelial marker, D2-40 (Signet laboratories). Three hot spots were selected in each case with agreements of two pathologists and LVD was counted within 5 fields from each hot spot at 200 magnifications in intra-tumoral, peri-tumoral, and normal areas, and mean value was determined. Clinicopathological parameters of 40 patients with prostate carcinoma were reviewed. SPSS software (version 12.0, IL, Chicago) was used for statistical analysis.

Results: The age of the patients ranged from 49 to 78 years old (average, 63.8±5.7). The Gleason sore was 4 (n=5), 5 (n=3), 6 (n=15), 7 (n=13), 8 (n=2), and 9 (n=2). pT stage was pT2 in 32, pT3 in 7, and pT4 in 1 case out of 40 tumors. Two of 40 (5%) cases had regional lymph node metastasis. Average LVDs in intra-tumoral, peri-tumoral and normal areas were 3.2±1.9, 4.8±1.6, 2.2±1.3, respectively. LVD from intra-tumoral, peri-tumoral, normal areas showed significant statistical difference ($p<0.001$) with the highest value in peri-tumoral areas. Peri-tumoral LVD was significantly associated with higher pT stage ($p=0.059$). Any significant correlation was not found between the peri-tumoral LVD and patients' age, Gleason score, serum PSA level, or pN stage.

Conclusions: LVD showed the highest value in peri-tumoral areas compared to intratumoral or normal areas. Peri-tumoral LVD was associated with higher pT stage in prostate carcinoma and it suggested that LVD may be the candidate prognostic factor. However, our study included the limited number of cases and short follow-up periods. To confirm the prognostic implication of LVD, larger scale of the study should be followed.

705 Diagnostic and Prognostic Utility of Cyclin D1, Cyclin D3, Cyclin E, P27, MUC1, CD44, CK7 and CK20 in Renal Cell Carcinoma

S Kiremitci, O Tulunay, S Baltaci, O Gogus. Medical School of Ankara University, Ankara, Sihhiye, Turkey.

Background: Renal epithelial tumors comprise several kinds of tumors, differing in their prognosis and therapeutic response. Renal Cell Carcinoma (RCC) comprises several subtypes with different prognosis and therapeutic response. The prognosis is directly related to biological tumor characteristics. The current prognostic factors include tumor grade, and clinical stage. Immunohistochemistry (IHC) have been used increasingly to support a correct histological diagnostic decision, and only a limited number of markers are available to aid differential diagnosis of these neoplasms, as well as to predict individual tumor behavior.

Design: IHC was performed on tissue microarray (TMA) sections of 83 cases of RCC (62 clear cell RCC-CRCC, 6 chromophobe RCC-ChRCC, 13 papillary RCC-PRCC, 2 unclassified RCC) and 6 cases of renal oncocytoma (RO), using antibodies against cyclin D1, cyclin D3, cyclin E, P27, MUC1, CD44, CK7 and CK20.

Results: CK7 expression was diffuse in ChRCCs and PRCCs, focal (negative) in ROs. CK7 expression was higher in type 1 than in type 2 PRCCs. CK7 expression pattern was significantly different between "clear" and "nonclear" variants of RCC. Prognostic factors identified in this study were high nuclear grade, regional lymph node involvement, distant metastasis, advanced stage, histological tumor necrosis, renal capsule invasion, severe inflammation, lenfovascular invasion and multifocality. Tumor stage and lenfovascular invasion were independent prognostic factors in RCCs. Multifocality of the tumor and high MUC1 expression were correlated and both were associated with distant metastasis. A significant correlation was found between high nuclear cyclin D3 protein expression and distant metastasis which leads to poor survival. P27 expression was significantly correlated with tumor size and regional lymph node involvement.

Conclusions: The majority of ChRCCs and PRCCs express CK7. Negativity of CK7 in CRCC and RO help to differentiate "clear cell" and "nonclear cell" RCCs. Tumor stage and lenfovascular invasion are strongly related to increased metastatic potential and biological aggresiveness, and reduced survival. The association of MUC1 overexpression with distant metastasis indicates a potential therapeutic target in RCC. For the first time it is shown that cyclin D3 protein is an independent prognostic factor in RCC; patients with high nuclear cyclin D3 expression have worse clinical outcome and short survival.

706 APRIN/AS3 Immunohistochemical Expression and Promoter Methylation in Prostatic Adenocarcinoma, Prostatic Intraepithelial Neoplasia and Benign Prostatic Tissue

S Klepper, V Denes, G Carpinito, A Makarowskiy, P Geck, M Pilichowska. Tufts-New England Medical Center, Boston, MA; Tufts University School of Medicine, Boston, MA.

Background: Aprin/AS3 is an androgen-regulated protein mediating proliferative arrest in prostatic cancer cells in culture and highly expressed in prostates of castrated rats. Data derived from animal studies indicate that loss of APRIN/AS3 is important in the development of prostatic carcinoma as well as in breast and ovarian cancers. There is no data on APRIN/AS3 expression and expression regulation in human prostatic adenocarcinoma, prostatic intraepithelial neoplasia (HPIN) and benign prostatic tissue.

Design: Immunohistochemical expression of APRIN/AS3 was examined in 38 archival specimens from 33 patients including: 9 prostatectomies and 29 biopsies (21 adenocarcinomas, 6 HPIN, 2 BNH). Rabbit polyclonal antibody to a synthetic oligopeptide corresponding to C-terminus of APRIN/AS3 molecule was used (P. Geck). The staining was performed according to routine methods and scored semiquantitatively. Methylation studies using quantitative **real-t**ime PCR were performed on carcinoma and normal tissue derived from 3 prostatectomy cases, and compared to the patients' matched blood samples. DNA was extracted from fresh-frozen tissue mapped to corresponding areas in routine histology as well as microdissected from formalin-fixed and paraffin-embedded tissue mapped to the same areas.

Results: All cases (38/38) showed nuclear APRIN/AS3 immunoreactivity in normal and benign tissue, HPIN, and carcinoma present in stromal and epithelial cells and blood vessels. Normal and benign tissue, and HPIN showed similar staining. The basal cells and atrophic glands showed stronger staining comparable to this seen in stroma. The epithelial cells showed less intense and heterogenous staining. In carcinomas the nuclear immunoreactivity was heterogeneous, decreased or lost (5/21 biopsies and 9/9 prostatectomies). There was no correlation with Gleason grade. In comparison with matched normal prostatic tissue and blood, the carcinomas showed two, seven and nine fold increase of APRIN/AS3 promotor methylation in all the three cases examined.

Conclusions: APRIN/AS3 plays a role in growth regulation of human prostatic tissue including adenocarcinoma. In carcinoma decreased or lost APRIN/AS3 expression seen in association with promotor hypermethylation may indicate a putative tumor suppressor function.

707 Histogenesis of Sarcomatoid Urothelial Carcinoma of the Urinary Bladder: Evidence for a Common Clonal Origin with Divergent Differentiation

M Kuhar, MT Sung, M Wang, GT MacLennan, JN Eble, PH Tan, A Lopez-Beltran, R Montironi, L Cheng. Indiana University School of Medicine, Indianapolis, IN; Chang Gung Memorial Hospital-Kaohsiung Medical Center, and Chang Gung University College of Medicine, Kaohsiung, Taiwan; Case Western Reserve University, Cleveland, OH; Singapore General Hospital, Singapore; Cordoba University, Cordoba, Spain; School of Medicine, Polytechnic University of the Marche Region (Ancona), United Hospitals, Ancona, Italy.

Background: Sarcomatoid urothelial carcinoma of the urinary bladder is an uncommon neoplasm which exhibits morphologic and/or immunohistochemical evidence of bidirectional epithelial and mesenchymal differentiation. The histogenesis of sarcomatoid urothelial carcinoma is uncertain.

Design: Separate carcinomatous and sarcomatous components from 30 sarcomatoid urothelial carcinomas, including 20 from men and 10 from women, were analyzed for loss of heterozygosity. We examined six polymorphic microsatellite markers where genetic alterations occur frequently in urothelial carcinomas. Additionally, the status of inactivation of X-chromosome was examined in ten female patients.

Results: Among the tumors demonstrating loss of heterozygosity, an identical pattern of allelic loss between carcinomatous and sarcomatous components was found in 2 of 5 cases (40%) at D3S3050, in 6 of 7 cases (86%) at D8S261, in 4 of 7 cases (57%) at IFNA, in 3 of 4 cases (75%) at D9S177, in 7 of 9 cases (78%) at D11S569 and in 4 of 10 cases (40%) at TP53. Clonality studies revealed the same pattern of nonrandom X-chromosome inactivation in both carcinomatous and sarcomatous components in 5 of 8 informative female patients.

Conclusions: The identical X-chromosome inactivation and significant overlap of loss of heterozygosity support the contention that both carcinomatous and sarcomatous tumor components arise from a monoclonal cell origin and that clonal divergence may occur during tumor progression and differentiation. Genetic divergence following the initial neoplastic transformation is reflected in the discordant allelic loss of microsatellite markers that occurs as these bladder tumors undergo advanced carcinogenesis.

708 Expression of Microsomal Epoxide Hydrolase in Clear Cell Renal Cell Carcinoma

JK Kuhnmuench, SS Shen, HY Zhi, K Nithipatikom, C Wynveen, P Langenstroer, HY Yang, SK Zhu, R Li. Medical College of Wisconsin, Milwaukee, WI; The Methodist Hospital, Houston, TX.

Background: The kidney is a major site of the xenobiotic metabolism and the development of renal cell carcinoma (RCC) may be associated with exposure of renal epithelium to carcinogens and mutagens. Microsomal epoxide hydrolase (mEH), a detoxifying enzyme, is frequently expressed in the normal epithelium of kidney, but is down-regulated in clear cell RCC (CRCC) in studies with small sample sizes. These findings suggest that mEH may have a role in tumor suppression in CRCC. We evaluated the mEH expression in a larger series of CRCC by immunohistochemistry and Western blot analysis.

Design: Twenty-one frozen CRCCs and matched benign kidney tissues were collected for Western blotting study using a monoclonal anti-mEH antibody. Tissue microarray (TMA) sections containing 139 CRCCs and 12 normal kidneys were immunostained using the same antibody and a biotin-free envision system (DAKO). An intensity weaker than benign tissue was considered to represent mEH down-regulation in Western blot. A staining intensity weaker than normal epithelium was considered to represent mEH down-regulation in the immunohistochemical study.

Results: In the Western blotting study, a group (15/21, 71%) of CRCCs showed decreased mEH expression. 6/21 (29%) CRCCs showed either up-regulated or unchanged expression. Immunostaining of TMA section revealed strong staining in benign proximal tubules. 113/139 (81.3%) CRCCs showed decreased staining, and 26/139 (18.7%) showed either equal or increased staining. These cases were considered to belong to the down-regulated and up-regulated groups respectively. Of the 113 down-regulated CRCCs, 75 (66.4%) had a low nuclear grade and 38 (33.6%) had a high nuclear grade. In contrast, in the 26 up-regulated CRCCs, 10 (38.5%) had

a low nuclear grade and 16 (61.5%) had a high nuclear grade. The difference between the two groups was significant (P=0.008). The mean survival time of down-regulated CRCCs was 66.6 months which is significantly longer than a mean of 46.4 months in up-regulated CRCCs (P=0.02).
Conclusions: mEH expression was down-regulated in the majority of CRCC and was associated with lower nuclear grade and favorable prognosis. On the other hand, a small group of CRCC showed increased expression of mEH and was strongly correlated with high nuclear grade and shorter survival. These results suggest that mEH may have a role as a tumor suppressor and may be a potential prognostic marker for CRCC.

709 Clonality of Tumor-Infiltrating Lymphocytes in Testicular Seminoma

KC Kurek, E Yakirevich, P Meitner, R Tavares, MB Resnick. Rhode Island Hospital and Brown Medical School, Providence, RI.
Background: Testicular seminoma is characterized by prominent lymphoid infiltrates containing both T- and B-lymphocytes. However, it is unclear whether these infiltrates represent a tumor antigen-specific clonal immune response or merely a non-specific component of the inflammatory response. The goal of this study was to evaluate whether a tumor-specific response is detectable in seminoma by analysis of T- and B-cell clonality.
Design: Clonality was assessed in 12 seminoma cases, including two tumors with corresponding lymph node metastases. Laser capture microdissection (LCM) was performed on CD20 and CD3 IHC stained paraffinized tumor sections to isolate cells of interest. Lymphocytes were captured separately from tumor cell nests and from surrounding peritumoral stromal aggregates. At least 2,000 lymphocytes were targeted in each of 56 captures. T-cell receptor and immunoglobulin heavy chain (IgH) gene rearrangement PCR analysis was used for T- and B-cell clonality, respectively. PCR products were evaluated using high-resolution microcapillary electrophoresis with the DNA 500 LabChip and Agilent Bioanalyzer.
Results: Analysis of whole tissue sections did not demonstrate clonal lymphocytic populations. However, LCM revealed oligoclonal (2-4 clones) B-cell IgH rearrangements in the majority (11 of 12; 92%) of tumors and lymph nodes, both within tumor nests and in peritumoral areas. The majority (9 of 12; 75%) of cases contained intratumoral clones that were distinct from those in peritumoral areas, indicative of clonal heterogeneity. In three cases, single B-cell clones were detected in tumor cell nests. In four cases, germinal centers (GC) were captured and revealed an oligoclonal pattern. Identical clones were demonstrated between different GCs and intratumoral lymphocytes. Moreover, one lymph node contained clones identical to those in the primary tumor. Similar to B-cells, the majority of cases exhibited an oligoclonal T-cell response. In each of these cases, at least one T-cell clone was identical between intratumoral and peritumoral lymphocytes.
Conclusions: LCM coupled with microcapillary electrophoresis is a useful tool for lymphocyte clonality analysis in tumors. Our study is the first to simultaneously demonstrate an oligoclonal expansion of both B- and T-lymphocytes in testicular seminoma. Heterogeneity of the lymphocytic clones may reflect a variety of tumor-associated antigens. Characterization and expansion of these clones may lead to the development of novel immunotherapies in the treatment of seminoma patients.

710 Prostate and Seminal Vesicle Anatomy in Motheaten Viable (me^v) Mice

JI López, A Ferruelo, J González-Ubreva, B Colás, P López-Ruiz, M Luján, A Berenguer, JC Angulo. Hospital de Basurto, Basque Country University (EHU/UPV), Bilbao, Bizkaia, Spain; Hospital de Getafe, Getafe, Madrid, Spain; University of Alcalá, Alcalá de Henares, Madrid, Spain.
Background: Viable motheaten (me^v) mice carry mutations in the SHP-1 gene leading to 80-90% reduction in the activity of this protein tyrosine phosphatase. Homozygous me^v mice exhibit multiple anomalies that include immunodeficiencies, increased proliferation of macrophage, neutrophil, and erythrocyte progenitors, decreased bone density, and sterility. Reduced testosterone levels in these mice is associated with impaired spermatogenesis, partially rescued with testosterone treatment. Aberrant development appears in the proximal segments of epididymis, but changes in prostate and seminal vesicle anatomy have not been studied so far.
Design: We analyze the seminal vesicle and prostate macro and microscopic anatomy and establish differences between 5 me^v/me^v and 8 wt/wt adult 7 week old mice. Morphometric analysis has been performed to measure the relative changes appearing in the different lobes of mouse prostate.
Results: All me^v/me^v mice were devoid of seminal vesicles and ampulla, but penis, testis, epididymis, vas deferens and bladder develop normally. All prostatic lobes were atrophied, especially ventral and anterior gland. Prostate size reduction was not proportional to reduced body weight of me^v/me^v mice. Anterior prostate was 0.2, ventral prostate 0.15, dorsal 0.3, and lateral 0.35 times larger than those of wild type mice. Prostatic ducts were scarce and of bigger size, and acini were severely atrophied with empty lumina and loosing epithelial tufting and infoldings. The stroma showed fibromuscular hyperplastic changes. Epididymal atrophy, diminished spermatogenesis and decreased number of Leydig cell were also evident.
Conclusions: The prostate of me^v mice exhibits signs of aberrant differentiation and the resulting phenotype may be related to the loss of function of SHP-1. Prostatic anomalies in these mice account, together with defects in sperm maduration, for sterility. These data suggest SHP-1 plays an important role in prostate epithelial morphogenesis. Supported by the grant ISCIII PI020964.

711 MIB-1 Expression Is a Strong Prognostic Predictor in Prostate Cancer

JI López, A Ferruelo, JM Rodriguez-Barbero, A Santana, FJ Bilbao, JC Angulo. Hospital de Basurto, Basque Country University (EHU/UPV), Bilbao, Bizkaia, Spain; Hospital de Getafe, Getafe, Madrid, Spain; Hospital de Alcalá, Alcalá de Henares, Madrid, Spain.
Background: The identification of reliable predictors of prognosis in prostate cancer is a crucial issue to optimize the rational use of treatment modalities. The purpose of this study is to investigate the usefulness of Ki-67 expression in predicting the clinical evolution of a selected series of prostate cancer patients that includes all types of disease.
Design: A total of 114 cases with long term follow-up treated with radical surgery (75%) or with transurethral resection (25%) were included in the series. Additionally, 60 patients (53%) received hormone blockage at the beginning of the disease or after biochemical progression. The proliferation index was measured by conventional immunohistochemistry with MIB-1 antibody and distributed by quartils (<5%, 6-12%, 13-25%, >25%). SPSS (13.0) was used for statistical analysis.
Results: The average of Ki-67 expression was 8.29% (CI 5.83-10.75). The distribution by quartils were: 75 cases (68%) <5%, 17 cases (15%) 6-12%, 8 cases (7%) 13-25%, and 10 cases (9%) >25%. Ki-67 index was associated with Gleason sum (ANOVA, p=0.001), tumor-associated inflammation (ANOVA, p=0.02), clinical progression (t Student, p=0.000), and tumor-related death (t Student, p=0.000). Conversely, it was neither associated with PSA levels (Pearson, p=0.186), T (ANOVA, p=0.076), N (t Student p=0.185), nor M (t Student, p=0.084) categories. One, five, and ten year tumor-specific survival was 98.2% (SD 0.013), 76.1 % (SD 0.043), and 62% (SD 0.084), respectively. Univariant analysis showed T, N, and M categories, Gleason sum, presence of tumor-associated inflammation, and Ki-67 index were predictive factors of survival. However, Cox multivariant model only identified M+, Gleason sum >7, and Ki-67 >25% as independent factors.
Conclusions: The immunohistochemical expression of Ki-67 is a first-line predictor of prognosis in prostate cancer and could be included in the routine strategy when evaluating core biopsies to preoperatively predict cancer behavior. Supported by the grant ISCIII-PI020964.

712 Squamous Cell Carcinoma of the Bladder: A Study of 55 Radical Cystectomy Cases

N Lagwinski, DE Hansel. Cleveland Clinic, Cleveland, OH.
Background: Squamous cell carcinoma of the bladder (SCC) is a rare tumor and its long-term prognosis has remained controversial. We examined a large series of patients who underwent radical cystectomy for SCC in order to identify histopathologic features and clinical outcomes associated with these tumors.
Design: Radical cystectomy specimens of pure SCC of the bladder were identified from The Cleveland Clinic archives between 1981 and 2006.
Results: Demographics: Of 2783 radical cystectomies, 55 cases of SCC were identified (2%). Patient age ranged from 38 to 83 yrs (mean 66 yrs) with a M:F ratio of 3:2. Fifty-three patients were Caucasian. No history of schistosomiasis infection was reported; only 1 patient had a history of HPV. Thirteen patients presented with hematuria and 2 patients with dysuria. Prior specimens: Prior bladder biopsies or TURs were performed 2 days to 6 mo prior in 41 patients (75%). Thirty-one specimens were diagnosed as pure SCC, 6 cases as invasive urothelial carcinoma with squamous differentiation, and 4 cases as pure invasive urothelial carcinoma. Histopathologic findings: Tumor size ranged from 0.8 to 7 cm (average 3.6 cm). Most tumors were moderately (28/53) or poorly (22/53) differentiated, and only 3 tumors were well-differentiated (3/53). Most cases demonstrated SCC in situ (14/53), squamous metaplasia with dysplasia (9/53), or keratinizing (7/53) or nonkeratinizing (10/53) squamous metaplasia. However, 15 cases also demonstrated separate foci of flat urothelial CIS. Keratinization was present in all cases (5-100%). Necrosis (0-60%) inversely correlated with tumor differentiation. Some cases showed a giant-cell reaction to keratin (10/25), and a desmoplastic reaction (18/25). Invasion was identified into the lamina propria (3/49), muscularis propria (15/49), perivesical fat (24/49), and adjacent structures (7/49). Metastases at surgery were identified in 16/55 patients (29%) to pelvic lymph nodes (13/55), mesentery (2/55) or pelvic sidewall (1/55). Followup: Clinical follow-up was available on 24 patients (1 to 184 mo, mean 44.9 mo). Five patients developed subsequent metastatic disease. Fifteen patients were alive without disease from 2 to 184 months postoperatively (mean 65 months), whereas only 2 patients died of disease within 2 years of diagnosis.
Conclusions: SCC of the bladder frequently presents at high stage and often with metastatic disease within months of first diagnosis. In this large series of radical cystectomy specimens, however, current surgical treatment appears to provide a substantial benefit in long-term survival.

713 Cystitis with Pseudocarcinomatous Epithelial Hyperplasia Not Associated with Prior Irradiation/Chemotherapy

Z Lane, JI Epstein. Johns Hopkins Hospital, Baltimore, MD.
Background: Pseudocarcinomatous epithelial hyperplasia is a little known phenomenon, recognized to be associated with prior irradiation and/or chemotherapy. Whether this process can occur outside of this setting has not been studied.
Design: We identified 9 of these cases from our consultation files (07/04-07/06) with no prior history of radiation or chemotherapy.
Results: The mean age at diagnosis was 65 years (range, 42-81 years). 70% were males. 8 patients had a potential etiology for these changes. 4 patients had underlying vascular conditions that could have resulted in localized ischemia. These included: 1st case) atrial fibrillation (afib), hypertension, CHF, GI bleed, and CAVD; 2nd case) coronary angioplasty, afib, hyperlipidemia, and amputation of arm for ischemia; 3rd case) hypertension, uncontrolled diabetes, hyperlipidemia, and afib. A 4th case had an underlying arteriovenous malformation of the bladder. 3 patients had a history of indwelling Foley catheter. 1 patient had a h/o radical prostatectomy for prostate cancer

but no radiation. 1 patient had no potential contributing factors. 8 patients presented with gross hematuria. At cystoscopy, 8 patients had polypoid lesions with 1 appearing non polypoid. Histologically, all cases showed epithelial proliferation mimicking invasive cancer within the lamina propria, with marked proliferation in 3 cases (33%). Moderate nuclear pleomorphism was seen in 6 cases (67%). Only one case revealed mitoses. Ulceration was seen in 1 case. All cases had some degree of hemorrhage with hemosiderin deposition identified in 3 cases (33%). Fibrin deposition was present in 2 cases within stroma, 3 cases in vessels, and 4 cases in both. 5 cases showed stromal fibrosis. Edema and vascular congestion were common features, 90% and 100% respectively, with 6/9 cases accompanied by moderate-marked acute and chronic inflammation. Epithelium tended to contain prominent eosinophilic cytoplasm. Original diagnoses included nested variant urothelial carcinoma (1 case), atypical suspicious for invasive carcinoma (6 cases), and hemangioma (1 case), and eosinophilic cystitis (1 case). 9 patients were followed for a mean of 7 months (range 1-25 months), and none developed bladder cancer.

Conclusions: As a rare response to ischemia and chronic irritation, pseudocarcinomatous epithelial proliferations in the bladder may be confused with invasive urothelial carcinoma. Pathologists must be aware of the histological changes mimicking cancer, and recognize that it can occur outside of the setting of prior irradiation or chemotherapy.

714 Prosatic Adenocarcinoma in Colorectal Biopsy: Clinical and Pathologic Features of 21 Cases

ZL Lane, S Ayub, JI Epstein, GJ Netto. Johns Hopkins Univ, Baltimore.

Background: Locally advanced prostate carcinoma (PCa) can involve adjacent rectal tissue. In such cases, accurate assignment of primary source may prove difficult on a small biopsy. Given the difference in therapy and prognosis between PCa and colorectal carcinoma (CRCa), an accurate diagnosis is crucial.

Design: 29 cases with a Dx of PCa on colorectal biopsy (CRBx) were identified from surgical pathology and consultation files at our institution between 1987-2006. Histologic and clinical data were available in 21 cases.

Results: At the time of CRBx, mean age was 74 years (range 63-85). Main clinical presentation was rectal bleeding in 6 men and obstruction due to a rectal mass in 15. The Dx of PCa was made for the first time at the time of the colorectal presentation in 4 men. 3 of the latter underwent colectomy: one following a CRBx that was misinterpreted as CRCa, the second to relieve obstruction due to PCa diagnosed on CRBx and the third based on clinical/radiologic impression of an obstructive colonic mass. Among the remaining 17 men with prior documented diagnosis of PCa, the overall clinical/endoscopic impression favored a second primary CRCa in 10 cases. The latter was due in part to the chronologically distant prior PCa diagnosis (mean 7 years; range 2-12). Serum PSA levels at time of CRBx was available in 14 men with a median of 22.4 ng/ml (range 0-643). Serum PSA was <4 ng/ml in 4 men, and between 4-10 in one. 9/12 prior PCa were of Gleason score (GSc) >6 with 8/12 prostatectomies showing extraprostatic extension. None of the CRBx demonstrated CIS or dysplastic colonic mucosa. Lymphovascular involvement was absent in all cases. The PCa in CRBx was of GSc 9-10 in 18 cases and of GSc 8 in 3 (only one with pattern 3). Microacinar architecture typical of PCa was seen in 10 cases. 11 cases had absent to only rare mitotic figures. Focal necrosis was present in 9 cases. Immunostains were positive for PSA, P501S (prostein) and PSAP in 14/19, 6/8 and 11/18 cases respectively. CDX2 and B-Catenin were negative in all tested cases (0/9 and 0/8 respectively). CK20 was positive in 2/12 cases.

Conclusions: Although relatively rare, initial presentation of PCa as a rectal lesion may lead to an erroneous clinical and or histologic impression of CRCa. As prior history of PCa is often remote, clinical findings may be misleading, and histology is poorly differentiated, pathologists should rule out a prostatic origin based on morphological and immunohistochemical studies in a poorly differentiated carcinoma on colorectal biopsy in the absence of an in-situ component.

715 Expression of Claudins 1, 4 and 7 in Human Renal Tumors

M Lechpammer, W Greaves, E Sabo, E Yakirevich, R Tavares, L Noble, MB Resnick, LJ Wang. Rhode Island Hospital, Brown University, Providence, RI.

Background: Claudins form the family of more then 20 proteins that are involved in the formation of tight junctions in epithelial and endothelial cells. Although alterations in the expression of individual claudins have been related to progression and invasion of several human tumors, their role in carcinogenesis remains controversial. We evaluated the expression patterns of claudins 1, 4 and 7 in human renal tumors.

Design: Tissue microarrays were created from paraffin-embedded tissue samples from 97 patients diagnosed with renal cell carcinoma (RCC) or oncocytoma. The array included 62 clear cell (cRCC), 12 papillary (pRCC), 12 chromophobe (chRCC), and 11 oncocytomas (OC). Representative areas of non-neoplastic renal tissue were included for all cases. The microarrays were stained for claudins 1, 4 and 7 with epitope specific rabbit antibodies. The immunoreactivity was assessed based on a combined score of the extent and intensity of staining.

Results: The staining pattern for claudins 4 and 7 was membranous and cytoplasmic while claudin 1 staining was predominantly membranous in both non-neoplastic renal tissue and tumors. All tested claudins were detected in the distal convoluted tubules and collecting ducts, with more intense staining of claudins 4 and 7 than claudin 1. Claudin 1 was also detected in Bowman's capsule and the loop of Henle, while weak claudin 4 was present in proximal convoluted tubules. Moderate to strong claudin 1 staining differentiated pRCC (58%) and cRCC (22%) from the chRCC and OC groups, which demonstrated only negative/weak staining ($p<0.005$). Moderate to strong claudin 4 and 7 was present in all of the chRCC tumors and in 55% and 54% of the OCs, whereas fewer of the cRCC stained significantly with claudin 4 and 7 (39% and 38% respectively, $p<0.001$). Eighty three percent of the pRCC stained moderate/strongly for claudin 7 and 67% for claudin 4.

Conclusions: Distinct expression patterns of claudins 1, 4 and 7 were detected in normal renal parenchyma and in the renal cell carcinoma subgroups. All of the chRCCs and majority of the OCs stained moderately/strongly for claudins 4 and 7 and were negative for claudin 1, which reflects the histogenic origin of chRCC and OC from the distal nephron, which has a similar claudin phenotype. Claudins 1, 4 and 7 could thus serve as useful molecular markers for the classification of renal tumors.

716 Further Evidence Supporting the Concept of Alternative Target Genes Contiguous to RB1 Involved in Clonal Expansion of *In Situ* Urothelial Neoplasia

S Lee, T Majewski, J Jeong, A Bhattacharya, TC Kuang, K Baggerly, B Czerniak. The University of Texas M. D. Anderson Cancer Center, Houston, TX.

Background: Identification of chromosomal regions containing genes involved in the development of occult *in situ* neoplastic lesions may provide valuable clues to the incipient events of carcinogenesis.

Design: For High-resolution mapping with SNPs, the sequence-based maps spanning approximately 27 Mb corresponding to microsatellite-defined deleted regions in 13q14 were assembled. SNPs were genotyped by pyrosequencing. Mapping was performed on whole-organ histologic maps of eight cystectomies with invasive urothelial carcinoma. We performed functional studies of alternative target candidate genes contiguous to RB1 involved in clonal expansion of in situ urothelial neoplasia using gene constructs, siRNA, DNA fragmentation and cell proliferation assays on bladder cancer cells grown *in vitro*.

Results: We identified clusters of discontinuous allelic loss mapping to 13q14 containing the model tumor suppressor gene RB1. The clusters represented discontinuous segments of allelic losses ranging in size from 0.1 to 4.6 Mb separated by non-deleted regions. By comparing the patterns of allelic losses from eight cystectomy specimens, we identified minimal deleted regions associated with clonal expansion of in situ neoplasia. The minimal deleted regions near RB1 included its flanking segments and contained several positional candidate genes such as ITM2B and CHC1L. Since the loss of just one RB1 allele was also an early event associated with clonal expansion, the P2RY5 gene located within intron 17 of RB1 was considered a third alternative candidate gene. We found that ITM2B, CHC1L, and P2RY5 were frequently down-regulated in bladder cancer cell lines with inactivated RB1 as well as in those cell lines with wild-type RB1. These genes were often down-regulated in both superficial and invasive TCCs and in corresponding samples of adjacent surface urothelium, indicating their involvement in early *in situ* phases of bladder neoplasia. Ectopically driven expression of ITM2B and P2RY5 reduced proliferation and induced apoptosis in bladder cancer cells.

Conclusions: In vitro functional studies provide evidence that alternative target genes contiguous to RB1 contribute to growth advantage of *in situ* neoplasia by modulation of cell survival *via* apoptosis.

717 Expression of Thrombin in the Prostate: Implications for Carcinogenesis and Tumor-Associated Hypercoagulation

TR Lester, M Kohli, A Quinn, JE Reeder, JL Yao, PA di Sant'Agnese, PA Bourne, J Huang. University of Rochester Medical Center, Rochester, NY.

Background: Malignancies, including prostate cancer (PC), are associated with increased thrombotic state, suggesting activation of coagulation cascade, in which thrombin is a key player. Thrombin is expressed by pulmonary small cell carcinoma, clear cell renal cell carcinoma and multiple myeloma. Expression of thrombin in PC has not been studied.

Design: RT-PCR was performed with primers for prothrombin in 16 fresh PCs (9 localized, 7 hormonally treated). Tissue microarrays containing benign prostate, PIN and PC were stained with a polyclonal anti-thrombin antibody (American Diagnostics, Cat#4702, 1:400 dilution). Epithelium and stroma were separately scored by multiplying staining intensity (0 to 3+) and percentage of stained cells (0-100) to arrive at a score (0-300). A score of 100 or higher was considered positive. In-situ hybridization was performed with a riboprobe for prothrombin. Statistical analysis was performed by Fisher Exact Test.

Results: RT-PCR yielded bands with the size expected of prothrombin/thrombin in all 16 PC samples and were confirmed by sequencing. Immunohistochemical study showed thrombin expression in epithelium and stroma (Tables 1 and 2) and there were no statistically significant differences among benign prostate, PIN and PC. In-situ hybridization showed positive signal in epithelium and stroma of benign prostate and PC with the anti-sense probe, not the sense probe.

Conclusions: Thrombin is produced in the prostate rather than being transported to and deposited in this organ. Neovascularization associated with PC may increase access of prostatic thrombin to circulation, leading to hyper-coagulative state. It has been shown that thrombin receptor PAR-1 is overexpressed in PC which stimulates proliferation, invasion and metastasis. Thus locally produced thrombin, through activation of overexpressed PAR-1, may contribute to carcinogenesis and progression of PC in addition to coagulation activation.

Expression of thrombin in prostatic epithelium

	Positive	Negative
Benign	65% (76/117)	35 (41/117)
PIN	50% (13/26)	50% (13/26)
Low Grade PC (Gleason 2&3)	45% (31/69)	55% (38/69)
High Grade PC (Gleason 4&5)	37% (16/43)	63% (27/43)

Expression of thrombin in prostatic stroma

	Positive	Negative
Benign	72% (84/116)	28% (32/116)
PIN	96% (26/27)	4% (1/27)
Low Grade PC	77% (53/69)	23% (16/69)
High Grade PC	84% (36/43)	16% (7/43)

718 Myosin VI, a Mediator of the P53-Dependent Cell Survival Pathway, Is Overexpressed in Adenocarcinoma of the Prostate

L Li, PA Bourne, JL Yao, PA di Sant'Agnese, Z Zhuang, C Yin, C Wu, J Huang. University of Rochester Medical Center, Rochester, NY; NINDS, National Institute of Health, Bethesda, MD.

Background: Androgen ablation is effective in treating advanced prostate cancer (PC). Androgen withdrawal in some PC cell lines such as LNCaP causes growth inhibition. We hypothesize that by comparing the protein expression profiles of LNCaP cells cultured with or without androgen, we may identify proteins involved in PC proliferation.

Design: Proteins from LNCaP cells cultured with or without androgen were separated by 2-D gel electrophoresis. Differentially expressed proteins were identified with Liquid Chromatography Mass Spectrometry and validated by immunohistochemical staining using tissue microarrays containing benign prostate, PIN and PC.

Results: Ten differerentially expressed proteins were sequenced. Among them, Myosin VI was expressed at high levels in LNCaP cells in the presence of androgen and underexpressed after androgen withdrawal. Immunohistochemical study was performed on tissue microarrays using a monoclonal anti-myosin VI antibody (Sigma, M0691, 1:100 dilution). The staining intensity (0 to 3+) and the percentage of positively-stained cells (0-100) were multiplied to obtain a score of 0-300. A score of 100 or more was considered positive. Positive staining was seen in a minority of benign cores and the majority of PIN, low grade (Gleason pattern 2 or 3) and high grade (Gleason pattern 4 or 5) PC. The differences of myosin VI expression between benign prostate and PIN, and between benign prostate and PC were statistically significant ($p<0.001$).

Conclusions: Myosin VI is a motor protein required for many cellular functions. It is induced by p53. Besides being a tumor suppressor, p53 upregulates pro-survival genes and myosin VI mediates the pro-survival function of p53. We have shown that expression of myosin VI is associated with increased proliferation of PC cells in-vitro and malignant cells of PIN and PC in human tissue, suggesting that it may play an important role in PC, possibly through participating in p53-dependent pro-survival pathway. Overexpression of Myosin VI in PIN suggests that its aberrant expression may be an early event of carcinogenesis.

Expression of Myosin VI in Benign and Malignant Prostate

	Positive	Negative
Benign	30% (33/109)	70% (76/109)
PIN	85% (22/26)	15% (4/26)
Low Grade PC	92% (60/65)	8% (5/65)
High Grade PC	76% (31/41)	24% (10/41)
Total PC	86% (91/106)	14% (15/106)

719 KOC Is a Useful Marker for the Classification of Urothelial Neoplasms of the Bladder

L Li, R Simon, BO Spauldin, PA Bourne, JL Yao, PA di Sant'Agnese, H Xu, J Huang. University of Rochester Medical Center, Rochester, NY; Dako North America, Carpinteria, CA.

Background: KOC (K Homology Domain Containing Protein Overexpressed in Cancer) is an oncofetal protein identified through screening differentially expressed genes in pancreatic cancer. Immunohistochemical study has confirmed that KOC is overexpressed in pancreatic carcinoma in comparison to benign pancreas. The possible value of this marker in the classification of urothelial neoplasms of the bladder has not been studied.

Design: Immunohistochemical staining was performed on 80 slides containing benign urothelium and various urothelial lesions using a monoclonal anti-KOC antibody (Dako, L523S, 1:100 dilution). The intensity of cytoplasmic staining (0 to 3+) and percentage of cells stained (0-100%) were recorded. Positive staining was defined as 2+ or 3+ intensity in 10% or more cells. Statistic analysis was performed using Fisher Exact Test.

Results: Positive staining was observed in the majority of lesions in the high grade group, including invasive urothelial carcinoma (UC), urothelial carcinoma in-situ (CIS), and high grade papillary UC (HG-PUC). No expression of KOC was detected in low grade PUC (LG-PUC), and the group of benign to borderline lesions, including normal urothelium (n=14), papillary urothelial neoplasm of low malignant potential (PUNLMP) (n=3) and urothelial atypia of unknown significance (UAUS) (n=1) (Table 1). Expression of KOC between LG-PUC and each lesion in the high grade group was statistically significant($P<0.001$), as was that between benign to borderline group and each lesion of the high grade group.

Conclusions: High grade papillary UC and CIS as defined by the new WHO classification belong to the genetically unstable category which also includes invasive UC. Our study shows that these entities overexpress KOC in comparison to benign urothelium. borderline and low grade lesions that are genetically stable, supporting the usefulness of the grading system. KOC, whose function includes regulation of IGF-II transcripts and posttranslational regulation of embryogenesis, may also be important in carcinogenesis. Immunohistochemical staining for KOC may help in grading difficult cases of urothelial tumors.

KOC expression in benign and malignant urothelialium

	Positive	Negative
Normal Urothelium, PUNLMP&UAUS	0% (0/18)	100% (18/18)
LG-PUC	0% (0/39)	100% (39/39)
HG-PUC	72% (13/18)	28% (5/18)
CIS	100% (6/6)	0% (0/6)
Invasive UC	92% (12/13)	8% (1/13)

720 Elevated Expression of MAGMAS in Prostatic Neoplasia

M Li, T Hebert, A Dulou, J Sunkara, Y Zhong, N Xue, P Jubinsky. Albert Einstein College of Medicine/Montefiore Medical Center, Bronx, NY; Albert Einstein College of Medicine, Bronx, NY.

Background: Magmas is a 13-kDa mitochondrial protein encoded by a chromosomal gene located at 16p13.3 and plays a key role in transporting mitochondrial proteins in yeast. The expression of Magmas is regulated by granulocyte-macrophage-colony stimulating growth factor (GM-CSF), an important regulator of prostatic carcinoma cells. Our previous study with a small number of cases showed that Magmas protein was increased in prostatic cancer cells.

Design: To explore the potential role of Magmas in prostatic cancer, we investigated the expression of Magmas in prostatic neoplasms. Tissue microarrays, including non-neoplastic epithelium (NE), prostatic intraepithelial neoplasia (PIN), and adenocarcinoma, were constructed from 113 prostatectomy specimens and analyzed immunohistochemically using a rabbit polyclonal antibody against Magmas. The immunohistochemical staining was semiquantitatively scored by multiplying the % of positive cells and the staining intensity (0, 1, 2).

Results: Among the 113 cases, NE, PIN and carcinoma were successfully analyzed in 92, 65 and 88 cases, respectively. Focal weak staining was observed in 15% cases of NE. Positive staining was increased to 66% cases of PIN and 76% cases of carcinoma. The mean scores for NE, PIN and carcinoma were 1.3, 13.5 and 24.0, respectively. The difference was statistically significant with p values <0.0001 (carcinoma vs. NE, PIN vs. NE, and carcinoma vs. PIN). Among the carcinomas, there was no correlation of Magmas staining score with Gleason score, T stage, and margin status.

Conclusions: Compared to NE, the expression of Magmas is gradually increased in prostatic neoplasia, particularly in adenocarcinoma, suggesting that Magmas may play a role in the development of prostatic cancer. However, There is no correlation between the expression of Magmas and Gleason score, T stage and margin status.

721 Prognostic Value of Akt-1 in Prostate Cancer: A Computerized Quantitative Approach with Quantum Dot Technology

R Li, H Dai, TM Wheeler, GE Ayala. Baylor College of Medicine, Houston, TX.

Background: Akt/PKB has been implicated in tumorigenesis and progression. We previously demonstrated that phosphorylated Akt-1 (P-Akt-1) is independently predictive of biochemical recurrence. However, P-Akt-1 is quickly degraded. Therefore, determining the pathological significance of non-phosphorylated Akt-1(or Akt-1 in short) in human prostate cancer (PCa) could provide more reliable information. Here we utilized image deconvolution, nanotechnology (quantum dots (Qdots)), and image analysis to eliminate autofluorescence and improve quantification of Akt-1.

Design: This study included 840 radical prostatectomy cases. Formalin-fixed paraffin-embedded blocks were used to build a 2mm tissue microarray. Slides were incubated with an antibody against non-phosphorylated Akt-1, followed by biotinylated-secondary antibody, then by Qdot655® Streptavidin conjugate. Slides were imaged under fluorescence microscope and spectral deconvolution (CRI-Nuance Imaging System) and quantified by plug-in software. The output of the measurement includes average intensity of Akt-1 signal (AI) and maximum intensity (MI). Cox regression was applied to assess the prognostic value of Akt-1 against clinical stage, preoperative PSA (PrePSA), extracapsular extension (ECE), seminal vesicle invasion (SVI), margins, and Gleason grade. PCa recurrence is defined as a PSA level> 0.4 ng/ml after radical prostatectomy or clinical progression. Akt-1 expression was also correlated with other biomarkers in our database.

Results: Multivariate analysis revealed that Akt-1 AI and MI were independently predictive of biochemical recurrence. Higher levels of Akt-1 were associated with reduced biochemical recurrence-free survival. In the model, Gleason, PrePSA, SVI, and ECE were also independently significant. Clinical stage, lymph node status, and margins status were all dropped out of the model when assessed against Akt-1. Akt-1 MI was inversely correlated with P10 (rho= -0.182, p=0.034). Both Akt-1 AI and MI were inversely correlated with apoptotic index by TUNEL (rho=-0.203, p=0.004; rho=-0.189, p=0.007). No significant correlations were identified with proliferative index or P-Akt-1.

Conclusions: Upregulation of Akt-1 pathway may enhance survival and accelerate PCa progression via an anti-apoptotic mechanism. Akt-1 may become a novel prognostic biomarker in human PCa treated with radical prostatectomy. Computerized quantification of protein levels detected by quantum dot technology might provide advantages over traditional semi-quantitative scoring system.

722 Glycogen Synthase Kinase-3 (GSK-3) Expression in Prostate Cancer with Perineural Invasion

R Li, H Dai, TM Wheeler, GE Ayala. Baylor College of Medicine, Houston, TX.

Background: Activation of Glycogen synthase Kinase-3 (GSK-3) is involved in the regulation of cell growth, differentiation, mobility, proliferation and survival. It is not clear if GSK-3 is associated with development and progression of perineural invasion (PNI) of human prostate cancer (PCa).

Design: Over 1000 patients who underwent radical prostatectomy at Baylor College of Medicine affiliated hospitals were enrolled for this study. All specimens were fixed in formalin and embedded in paraffin to produce whole mount blocks. Whole mount H&E slides were examined and areas of cancer with PNI were selected (226 cases in a 2mm array). The PNI array slides were immunostained with GSK-3β and scored semi-quantitatively using an expression index (EI) (intensity x percentage). Clinical and pathological correlations and prognostic significance were evaluated with Spearman correlation test, Kaplan-Meier survival analysis and Cox regression.

Results: GSK-3β was expressed both in cytoplasm and nuclei of PCa cells in PNI. It was higher in the latter (EI 5.26±2.54 in nuclei *vs.* 3.02±1.39 in cytoplasm; $p<0.005$). Lower nuclear GSK-3β (rho=-0.199, p=0.0314) and higher cytoplasmic GSK-3β were associated with a higher rate of seminal vesicle invasion (rho=0.235,p=0.0107). The

latter was also positively correlated with PNI diameter (rho=0.280,p=0.0108). On survival analysis, lower nuclear GSK-3β was associated with decreased recurrence-free biochemical survival using a cutoff of EI ≤6 and >6 (82 vs. 117 months). Cytoplasmic expression of GSK-3β was not associated with survival.
Conclusions: The close association of GSK-3β with perineural invasion and disease progression suggests that GSK-3β is an important molecule in PCa with PNI. GSK-3β may involve PNI development by facilitating invasion and survival possibly via intracellular redistribution mechanism.

723 MHC Class II Immune Response and Prostate Adenocarcinoma

AF Liang, MB Acquafondata, RM Angeles, R Dhir. University of Pittsburgh School of Medicine, Pittsburgh, PA.
Background: Immunotherapy for prostate adenocarcinoma (PCa) is a new and exciting field. To create a cogent therapy, the immune response and its effect on the developing neoplasm must be well understood. MHC Class II, found on antigen presenting cells such as macrophages, Langerhans cells, B cells and activated T cells, incites both a humoral and a cell-mediated immune response. LG11, a component of the MHC Class II complex, is evaluated through immunohistochemistry (IHC) in a variety of prostate tissues, including benign donor prostate tissue, prostate adenocarcinoma, benign prostatic hypertrophy (BPH), prostatic intraepithelial neoplasia (PIN), stroma adjacent to PCa and metastatic PCa.
Design: A six-slide tissue microarray (TMA) set was used to stain 572 tissue specimens. The TMA set includes PCa (137), benign donor prostate tissue (24), PIN (33), BPH (35), metastatic PCa (20), and benign prostate adjacent to PCa (36). IHC was performed on these tissue sets using the monoclonal antibody LG11 (1:800). Nuclear, cytoplasmic and stromal staining patterns were evaluated using a scale of 0 to 3. A minimum of 10% of the cells had to stain to be considered positive.
Results: Nuclear and cytoplasmic expression of LG11 is minimal; LG11 expression is most prominent in the stroma. The mean values of LG11 expresion are 1.996 in PCa, 1.440 in adjacent normal tissue, 1.180 in foci of PIN and 0.887 in normal donor prostate tissue. LG11 is significantly upregulated in PCa as compared to adjacent normal tissue, PIN and benign donor prostate tissue ($p < 0.001$, $p < 0.001$, $p = 0.008$).
Conclusions: 1. MHC Class II, using the component protein LG11 as a surrogate marker, shows a significant increase in the stroma of PCa as compared to benign donor prostate tissue, PIN and benign prostate adjacent to PCa. 2. This suggests that MHC Class II cells are activated in prostatic stroma in malignant conditions; pre-malignant conditions also show upregulation of expression compared with benign prostate tissue. 3. Modulation of MHC Class II expression could be utilized as a treatment option. In addition, this could also lead to new prevention strategies. 4. Additional studies are needed to understand the role of MHC-II expression in the stroma of PCa.

724 Utility of S-100 and MSH-2 in Differentiating Chromophobe Renal Cell Carcinoma from Renal Oncocytoma

F Lin, J Shi, XJ Yang, HL Wang, SS Shen, D Rukstails, C Schuerch. Geisinger Medical Center, Danville, PA; Northwestern Memorial Hospital, Chicago, IL; Washington University, St. Louis, MO; The Methodist Hospital, Houston, TX.
Background: Our recent studies demonstrated that antibodies to S-100 protein (Human Pathology 2006;37:462) and MSH-2 may have a diagnostic value in distinguishing chromophobe renal cell carcinoma (ChRCC) from oncocytoma based on a small number of cases on tissue microarray sections. In this study, we further test and confirm the utility of S-100 and MSH-2 in differentiating ChRCC from oncocytoma in a large number of cases.
Design: We evaluated the diagnostic value of S-100 and MSH-2 on conventional tissue sections from 37 cases of ChRCC and 26 cases of oncocytoma by immunohistochemistry. The staining intensity (weak or strong) and the distribution(negative, 1+, 2+, 3+, or 4+) were recorded. Western blot using the same anti-MSH-2 antibody was performed on 5 cases of renal tumors, including 1 ChRCC, 2 oncocytomas, and 2 clear cell RCCs. Reverse transcription-polymerase chain reaction (RT-PCR) was also performed on the same cases.
Results: The results demonstrated a nuclear and cytoplasmic staining of S-100 in 26 of 26 oncocytomas with 3+ or 4+ staining in 18 cases, and 0 cases of ChRCC. For MSH-2, all oncocytomas showed various degrees of nuclear staining with 2 key staining patterns. One was strong apical cytoplasmic and weak nuclear staining in 13 cases (50%); the other pattern was strong nuclear and weak cytoplasmic staining in 13 cases (50%). In contrast, 34 of 37 cases (92%) of ChRCC showed strong cytoplasmic/membranous staining. Weak nuclear staining was only seen in 3 cases of ChRCC. Western blotting demonstrated MSH-2 expression in both renal cell neoplasm and normal renal tissue, with a stronger expression (>10 fold) in both ChRCC and oncocytoma than in clear cell RCC. RT-PCR revealed 3.7-fold and 3.8-fold increases in mRNA levels for ChRCC and oncocytoma, respectively, when compared to clear cell RCC.
Conclusions: The results demonstrate that 1) overexpression of MSH-2 in both ChRCC and oncocytoma is consistently confirmed at protein (immunostaining and Western blot) and mRNA (RT-PCR) levels; 2) strong nuclear staining or apical cytoplasmic staining for oncocytoma and strong cytoplasmic staining and lack of nuclear staining for ChRCC are the typical findings; 3) a characteristic staining profile is useful in differentiating oncocytoma from ChRCC: for oncocytoma, S100+/MSH-2 nuclear and/or apical cytoplasmic staining; for ChRCC, S100-/MSH-2 cytoplasmic staining.

725 Expression of Human Kidney Injury Molecule-1 (hKIM-1) in Papillary Renal Adenoma

F Lin, XJ Yang, PL Zhang, J Shi, WK Han, JV Bonventre. Geisinger Medical Center, Danville, PA; Northwestern Memorial Hospital, Chicago, IL; Brigham and Women's Hospital, Boston, MA.
Background: Papillary renal adenoma (PRA) is characterized by a varying portion of papillary or tubular architecture with low nuclear grade and is defined by the World Health Organization (WHO) as smaller than 5 mm. It has been proposed that PRA may represent a putative precursor of papillary renal cell carcinoma (PRCC) (Hum Pathol, in press). It is well known that there are immunohistochemical and genetic similarities between PRA and PRCC. However, reliable tumor-associated markers to differentiate these two entities are not available. Recently, we have reported the expression of human kidney injury molecule-1 (hKIM-1) in over 70% of clear cell renal cell carcinoma (CRCC) and 93% of PRCC (Am J Surg Pathol, in press). The expression of hKIM-1 in PRA and the relationship with PRCC has not been investigated.
Design: Sixteen cases of PRA were included in this study. Sections were incubated with AKG7 anti-hKIM-1 monoclonal antibody using an EnVision-HRP detection kit. The scoring system was classified as negative - no staining; 1+, 25% of tumor staining; 2+, 26-49% of tumor staining; 3+, 50-75% of tumor staining; or 4+, >75% of tumor staining. The intensity of the staining was recorded as weak, intermediate or strong.
Results: Among these 16 cases, an association with PRCC, CRCC, benign renal cysts, and end-stage kidney disease was as follows: 4, 3, 2, and 7 cases, respectively. Tumor size ranged from less than 1 mm to 4 mm. Multifocal adenomas were identified in 7 cases (44%). The results demonstrated that membranous and cytoplasmic staining was observed in 3 of 16 cases (19%), with 2+ staining in 2 cases and 1+ staining in 1 case. Importantly, all 3 positive cases were associated with PRCC (3 of the 4 PRCC cases).
Conclusions: Preliminary data suggest that hKIM-1 may play a potential role in the pathogenesis/transformation of papillary renal adenoma to papillary renal cell carcinoma, which further supports the notion of papillary renal adenoma being a precursor of papillary renal cell carcinoma. Therefore, hKIM-1 can be employed as a useful marker in identifying a subset of papillary renal adenoma with more aggressive biological behavior, instead of depending on tumor size alone (5 mm cutoff by WHO criterion). Additional study in a large series is underway to confirm this finding.

726 Characterization of Prostatic Adenocarcinoma Associated with Granulomatous Prostatitis

YQ Liu, H Lou, JY Lei. Zhengzhou University School of Medicine, Zhengzhou, Henan, China; Cblpath, Rye Brook, NY.
Background: Granulomatous prostatitis (GP) is a well-known mimicker of prostatic adenocarcinoma (PA), not only clinically but also pathologically. Its association with PA, however, has not been very well characterized.
Design: Cases of GP with PA were selected from 9707 consecutive needle biopsies of prostate. The lesions of PA were characterized based on H&E stained slides, and immunohistochemically stained with CK34BE12, p63, and racemase (P504S). GP was subdivided, based on histological and clinical criteria as well as special stain results, into non-specific (NSGP), infectious (IGP), and post-biopsy (PBGP). Mann-Whitney test was used for statistical analysis.
Results: A total of 126 cases of GP was identified and 23 (18.3%) of them exhibited concomitant PA (N=21) or atypical prostatic glands suspicious for cancer (N=2). PA was associated with all types of GPs (17 NSGP, 3 IGP, and 1 PGP). Out of 21 cases of PA with GP, 13 (61.9%) cases showed PA either admixed with GP in the same focus (N=10) or co-existed in the same biopsy core (N=3). Most of these 21 cases showed Gleason grade 6 (N=13, 61.9%) or 7 (N=4, 19.1%), and a few of them (N=4, 19.1%) showed Gleason grade 8-10. Tumor presented in only one biopsy core in nearly half cases of PA with GP (N=10, 47.6%) and occupied ≤ 5% of core tissue in a single small focus in 1/3 of those cases (33.33%). The average age and PSA levels of the patients with PA and GP were higher than those of the patients with GP only (age: 68.24 vs. 64.13, and PSA: 6.4 vs. 6.12), but the differences were not significant (P >0.5). There was no correlation between extent of PA with digital rectal examination and extent of GP. In 2 cases of GP with atypical prostatic glands, lesion was admixed with GP in one case and separate from GP in another.
Conclusions: 1) Nearly 1/5 of GP harbor concomitant PA or atypical prostate glands suspicious for cancer; 2) When associated with GP, PA can be easily missed since tumor presents as a single focus in 47.6% of cases and often involves ≤ 5% of tissue; 3) PA showed bland morphology with Gleason grade 6 in over 60% of cases of PA and GP. Thus, any atypical glands, when co-existed with GP, should be carefully examined and investigated; 4) The atypical cells admixed with GP should raise the concern of high grade PA.

727 Lymphocytic Vasculitis of the Prostate Transition Zone: Incidence in Surgical Specimens and Clinical Significance

A Lopez-Beltran, A Vidal, L Cheng, R Montironi. Cordoba University Medical School, Cordoba, Spain; Indiana University, Indianapolis, IN; Marche Region University, Ancona, Marche Region, Italy.
Background: Lymphocytic vasculitis of the prostate transition zone (LVPTZ) is an exceedingly rare form of localized vasculitis of the prostate that presents without systemic involvement, and is illustrated with anecdotal case reports. True incidence and clinical significance of LVPTZ are virtually unknown.
Design: A sequential cohort series of 400 surgical specimens removed because of benign prostatic hyperplasia (BPH) related symptoms, including simple prostatectomy (N=258) and transurethral resection of the prostate (TURP) (N=142) was the study group. All patients had histological diagnosis of BPH and received surgical therapy only. LVPTZ was seen in variable number of small-to-medium size parenchyma arteries with streaking transmural lymphocytic inflammation. None of the cases having vasculitis had previous surgery or granulomatous prostatitis. The patient's mean age at diagnosis was 71 years.

Results: LVPTZ was present in 43 (10.7 %) out of 400 specimens, irrespective of being simple prostatectomy or TURP (P=0.070). Trans-mural T-cells infiltrate was predominant (>95%) with less than 5% B-cells. One case additionally had some eosinophils (<5%), and another case had focal fibrinoid necrosis. LVPTZ was present in 12 (100.0 %) out of 12 specimens having associated prostatic infarction (P<0.0001) with an increased risk of 9.63 (odds ratio) as compared with BPH cases unassociated to LVPTZ. Mean±SD age at diagnosis was similar in patients with LVPTZ or prostatic infarction. During follow-up, none of the patients with LVPTZ developed systemic disease.
Conclusions: LVPTZ is associated to prostatic infarction thus suggesting a pathogenetic link. Finding of LVPTZ without fibrinoid necrosis should be considered a localized vasculitis in the prostate that does not necessitate additional work up for systemic disease; but the significance of LVPTZ with fibrinoid necrosis remains uncertain. The potential clinical relevance of LVPTZ in patients with BPH warrants further investigation.

728 Upregulation of MKK4, MKK6 and MKK7 during Prostate Cancer Progression

TL Lotan, MB Lyon, D Huo, JB Taxy, CB Brendler, CW Rinker-Schaeffer, WM Stadler. University of Chicago, Chicago, IL.
Background: The Mitogen-Activated Protein Kinase (MAPK) signaling cascade culminates in the phosphorylation of the JNK and p38 MAPKs, two proteins that play a complex role in cancer progression. Recently, upstream activators of these proteins, the MAP kinase kinases (MKKs), have been implicated as metastasis suppressor proteins in animal models of prostate cancer. We looked at the expression of MKK4, 6 and 7 during human prostate cancer (PCa) progression.
Design: Six tissue microarrays (TMA) were constructed from a matched group of 107 men undergoing radical prostatectomy between 1996 and 2001. Immunostaining intensity for MKK4, 6 and 7 was scored in neoplastic and surrounding normal glands in triplicate samples for each patient. Wilcoxon signed-rank test was used to compare intensities between neoplastic and normal glands. Immunostaining intensities were also correlated with pathologic stage, grade and time to biochemical recurrence data using Spearman correlations and Cox proportional hazard ratios.
Results: MKK4, 6 and 7 were each significantly upregulated in PCa when compared to surrounding normal glands (p<0.0001 for all markers). There was, however, no or weak correlation between expression levels of the three kinases within each tumor. Increased expression of MKK4 or 7 was correlated with higher pathologic stage at prostatectomy (p=0.006 and p=0.015) while increased MKK6 expression was correlated with decreased preoperative PSA (p=0.035). Overall, the biochemical recurrence rate was 49% at 5 years, and higher preoperative PSA, Gleason score, and pathologic stage were significantly correlated with decreased time to biochemical recurrence. In multivariate analysis, there was no consistent association between expression of MKK4, 6 or 7 and time to biochemical recurrence.
Conclusions: While the MKKs are metastasis suppressors in murine models of PCa, their generalized upregulation in human PCa is a novel finding. The increased expression of these proteins is likely part of a MAPK-regulated stress response program during tumor progression. Surprisingly, higher levels of MKK4 and 7 were associated with *higher* stage tumors, although there was no correlation with time to biochemical recurrence. Additional studies examining other components of the MAPK signaling cascade may help to clarify the complex role of these proteins in PCa progression.

729 Chemokine CXCL12 Is Upregulated in a Subset of Human Prostate Cancers and Is Inversely Correlated with CXCR4 Expression

TL Lotan, MB Lyon, D Huo, M Tretiakova, WM Stadler, T Krausz. University of Chicago, Chicago, IL.
Background: The chemokine receptor CXCR4 has been implicated as an important modulator of prostate cancer (PCa) dissemination. CXCL12, the ligand for CXCR4, is highly expressed by stromal tissues at metastatic sites and CXCR4 is upregulated in metastatic prostate tumors. However, recent *in vitro* studies have shown that CXCL12 is also expressed by PCa cell lines and have suggested the presence of an autocrine signaling loop augmenting cellular proliferation in these tumors. We looked at the relationship between CXCL12 and CXCR4 expression during human PCa progression.
Design: Six tissue microarrays were constructed from a group of 107 matched men undergoing radical prostatectomy between 1996 and 2001. Immunostaining frequency or intensity for CXCL12 and CXCR4 was scored on a scale of 0 to 3 in triplicate samples for each patient. This data was correlated with pathologic stage, grade and time to biochemical recurrence data using Spearman correlations and Cox proportional hazard ratios.
Results: CXCL12 was predominantly negative in normal prostate epithelial cells and was highly expressed by basal cells and glands with transitional metaplasia. CXCL12 was moderately or highly expressed by 46% of PCa cases studied, and its expression was negatively correlated with both CXCR4 expression (p=0.01) and preoperative PSA (p=0.02). Neither marker showed significant correlation with Gleason grade, pathologic stage or margin involvement. However, consistent with previous studies, a borderline significant correlation between higher CXCR4 expression and shorter time to biochemical recurrence was observed (p=0.09).
Conclusions: CXCL12 is upregulated in a significant subset of prostate tumors, a novel finding that suggests the presence of an autocrine signaling loop in PCa. Such a pathway may initially drive tumor cell proliferation via the JNK/ERK/AKT pathways, as recent *in vitro* work has demonstrated. Significantly, however, there is an inverse correlation between CXCL12 and CXCR4 expression in PCa, consistent with recent work in colorectal carcinoma. While upregulation of CXCR4 is a crucial event in the development of a metastatic tumor phenotype, it may be equally important to downregulate tumor expression of CXCL12, enabling more efficient sensitization towards external endothelial and stromal-derived ligand signals.

730 Evolution of Granulomatous Prostatitis

X Lou, HX Li, JY Lei. Zhengzhou University Schoold of Medicine, Zhengzhou, Henan, China; Cblpath, Rye Brook, NY.
Background: Granulomatous prostatitis (GP) is one of many mimickers of prostatic adenocarcinoma (PA). It is difficult not only for urologists but also for pathologists to distinguish these two extremely distinct lesions. To better understand GP, this study was performed.
Design: A file of 9707 consecutive needle biopsies of prostate was searched for cases with a diagnosis of GP. Clinical correlations were analyzed for all the cases. Selected GP cases were characterized based on H&E stained slides, and subdivided, based on histological and clinical criteria as well as special stain results, into non-specific (NSGP), infectious (IGP), and post-biopsy (PBGP). Any GP cases suspicious for an infectious etiology were stained for mycobacterium tuberculosis with AFB and for fungi with GMS and PAS-Diastase. Mann-Whitney test was used for statistical analysis.
Results: One hundred and twenty six (1.3%) cases of GP were identified and composed of 87 (69.05%) cases of NSGP, 31 (24.60%) IGP, and 8 (6.35%) PBGP. All the IGP cases had either history of immunotherapy with BCG or positive staining results. The majority of them exhibited a segmental or extensive lesion with caseating necrosis (23/31, 74.2%), and involved more than 2 cores (20/31, 64.5%). Special staining for microorganisms were performed in 97 cases and revealed small yeast fungi consistent with histoplasma in 6 cases. Mycobacterium tuberculosis was not identified in any cases. All the PBGP had a history of previous prostate biopsy from at least 4 months prior and presented with focal GP, often in only one core. NSGP showed small focal lesion with early transformation of inflammation to GP in 39% (34/87) cases. Sixty percent of NSGP involved only 1-2 cores. The extent or number of core involvement of GP showed no correlation with digital rectal exam and PSA levels in all the groups. In addition, out of 126 cases of GP, 21 cases contained concomitant PA, 2 cases had atypical glands suspicious for PA, and 7 cases showed high grade prostatic intraepithelial neoplasm (PIN).
Conclusions: 1) A remarkable increase (3.6 fold) in incidence of GP was observed in our prostate needle biopsy, from 0.36% reported in 1997 to current 1.3%; 2) the percentage of IGP has also increased, from 18.1% reported in 1997 to current 24.6%; 3) NSGP and PBGP tend to exhibit focal and early transformation of GP, while IGP often involves more biopsy cores with more extensive lesion; 4) GP not only can mimic PA clinically and pathologically, but also can contain concomitant PA, atypical glands suspicious for PA, and high grade PIN.

731 Expression of Claudin 4 in Renal Cell Carcinoma

Y Lu, HG Strawn, ST Chuang, BT Teh, XY Yang. Feinberg School of Medicine, Northwestern University, Northwestern Memorial Hospital, Chicago, IL; Van Andel Research Institute, Grand Rapids, MI.
Background: Claudin family members are components of tight junctions that are important in the formation of intercellular barriers. It has been suggested that the loss of function in tight junctions may relate to the spread of tumors. Although the role of claudin in the development of other cancers has been speculated, little is known about its expression and localization in renal cell carcinomas (RCC). Previously, we observed an elevated claudin 4 mRNA level in papillary RCC. In this study, we examined the expression of claudin 4 at mRNA and protein levels using expression microarrays and immunohistochemistry in papillary RCC with comparison to other types of RCC in order to understand its possible role in renal tumor development and its value as a RCC marker.
Design: Claudin 4 mRNA levels were evaluated in expression microarrays chips from 143 RCC as well as 12 normal kidneys. In addition, immunohistochemistry using a monoclonal antibody specific for claudin 4 (clone3E2C1, Zymed, San Francisco, CA; 1/50) was carried out on tissue microarray sections containing 109 RCC, including papillary RCC (n=75), clear cell RCC (n=23), and chromophobe RCC (n=11). Claudin 4 immunoreactivity was interpreted using a scoring system of 0 (no staining), 1 (weak staining), 2 (moderate staining), and 3 (strong staining).
Results: Based on expression microarrays, the mean of claudin 4 mRNA levels were measured with results listed as follows: 361 for normal kidneys (n=12), 638 for papillary RCC (n=23), 394 for chromophobe RCC (n=15), and 237 for clear cell RCC (n=105). By immunohistochemistry, claudin 4 reactivity was found in 68.0% of papillary RCC (51/75) and 90.9% of chromophobe RCC (10/11). In contrast, only 8.7% of clear cell RCC (2/23) showed immunoreactivity. Among papillary RCC, 81.7% of low grade tumors (49/60) were positive while only 13.3% of high grade tumors (2/15) were positive.
Conclusions: Claudin 4 was present in both papillary and chromophobe RCC although they displayed different staining patterns with papillary RCC showing cytoplasmic staining and chromophobe RCC showing membranous staining. Claudin 4 was absent in the majority of clear cell RCC and high grade papillary RCC, which are responsible for most metastatic RCC. Our findings suggest that the loss of claudin 4 expression may be related to the metastatic potential of renal cell carcinoma.

732 Proliferative Activity of Prostatic Ductal Adenocarcinoma

A Luong, ST Chuang, XJ Yang. Feinberg School of Medicine, Northwestern University, Northwestern Memorial Hospital, Chicago, IL.
Background: Prostatic ductal adenocarcinoma has been suggested to be an aggressive variant of prostate cancer. There is controversy regarding its biological behavior and the applicability of Gleason grading of this tumor. Although it has been studied previously in conventional acinar adenocarcinoma, Ki67 index has not been well studied in ductal adenocarcinoma. This study investigated the proliferative activity and possibility of grading ductal adenocarcinoma of the prostate.
Design: Through the use of immunohistochemistry, we compared the Ki67 proliferative index of ductal adenocarcinoma (n=21) to that of the conventional acinar type (n=28). We further stratified the Ki67 indices of each group into 3 subsets based on the Gleason

grading system. Benign prostate tissues and high grade intraepithelial neoplasia (HGPIN) were also analyzed for comparison. Ten additional random samples were subjected to automatic counting using the ChromaVision Automatic Cellular Imaging System II to confirm the accuracy of the manual counting.

Results: The average Ki67 indices for both the ductal and acinar adenocarcinoma are listed in the table. Stratification of the ductal group based on features of the Gleason grading system yielded three patterns that parallel those of Gleason patterns 3, 4, and 5 (See Table). In addition, HGPIN was found to have an average Ki67 of 10.1 while normal prostate tissue had a value of 3.8. Of the 10 random samples processed via ChromaVision, 70% showed a trend consistent with the manual counting.

Conclusions: Prostatic ductal adenocarcinoma typically showed high proliferative activity similar to that of acinar adenocarcinoma of Gleason pattern 4 or higher. The possibility of grading ductal carcinoma was not concluded from this study suggesting that ductal adenocarcinoma is an aggressive cancer in general regardless of its patterns. Furthermore, Ki67 index may be useful in differentiating HGPIN from ductal adenocarcinoma.

Ki67 Indices for Prostatic Adenocarcinoma

	Ductal (n=21)			Acinar (n=28)		
Before Stratification (Mean)	44.5			46.0		
After Stratification (Gleason patterns 3,4,5)	G3	G4	G5	G3	G4	G5
	40.2	45.3	57.2	27.3	46.1	67.9

733 Neuregulin-1 Expression in Papillary Renal Cell Carcinoma

A Luong, ST Chuang, BT Teh, XJ Yang. Feinberg School of Medicine, Northwestern University, Northwestern Memorial Hospital, Chicago, IL; Van Andel Research Institute, Grand Rapids, MI.

Background: Neuregulin-1 (NRG-1) belongs to a family of epidermal growth factor-like (EGF) ligands that activate EGF tyrosine kinase receptors (HER3 and HER4). Previous studies have suggested a role of NRG-1 in tumor initiation and progression, but few have explored its function in the development and progression of renal cell neoplasms. Based on gene expression profiling, there has been recent observation of overexpression of NRG-1 in papillary renal cell carcinoma (RCC). This study aimed to evaluate the level of NRG-1 expression in papillary RCC compared to other histological RCC subtypes and to investigate its diagnostic utility.

Design: Gene expression microarrays from 105 clear cell RCC (55 low grade and 50 high grade), 23 papillary RCC (14 low grade and 9 high grade), 15 chromophobe RCC, 15 oncocytoma, and 12 normal kidneys were analyzed to determine their NRG-1 mRNA levels. In addition, immunostaining of NRG-1 was carried out in a total of 35 cases of papillary RCC (grade 1=5, grade 2=11, grade 3=17, and grade 4=2). Immunoreactivity based on stain intensity was scored from 0 to 3+.

Results: Based on expression microarrays, the mean NRG-1 mRNA levels were measured as 323 in papillary RCC, 123 in normal kidney tissues, 104 in clear cell RCC, 14 in chromophobe RCC, and 8 in oncocytoma. In particular, the high grade papillary RCC showed greater levels of NRG-1 mRNA (mean=496, n=9) than low grade papillary RCC (mean=151, n=14). Immunostaining of the papillary RCC generated average NRG-1 staining intensities of 0.8, 1.4, 2.2, and 2.5, in ascending order of Fuhrman grades. The average SI for low grade (grades 1 and 2) and high grade papillary RCC (grades 3 and 4) were 1.2 and 2.2, respectively while normal kidney tissues showed minimal to low NRG-1 staining.

Conclusions: We conclude that NRG-1 expression is elevated in papillary RCC, particularly high grade tumors. In addition, NRG-1 may have a diagnostic value in differentiating high grade papillary RCC from its low grade counterpart as well as other renal tumors based on its elevated mRNA level and stronger immunoreactivity. Furthermore, elevated NRG-1 expression in high grade papillary RCC may suggest that it has a role in tumor progression through the activation of EGF tyrosine kinase receptors. Finally, the potential therapeutic correlation between increased NRG-1 expression in RCC with their responses to tyrosine kinase inhibitors, such as Gleevec, needs further investigation.

734 Multifocal High-Grade Prostatic Intraepithelial Neoplasia on First-Time Saturation Prostate Biopsy Is Associated with High Cancer Detection Rate on Repeat Biopsy

C Magi-Galluzzi, L Schoenfield, AM Reuther, E Klein, JS Jones, M Zhou. Cleveland Clinic, Cleveland, OH.

Background: Although the optimal extent of prostate biopsy (PBx) is controversial, there is a trend to increase the number of cores taken. The identification of high-grade prostatic intraepithelial neoplasia (HGPIN) and atypical glands suspicious for cancer (ATYP) is associated with increased risk of finding PCa in subsequent biopsies and warrants close follow-up. We investigated the HGPIN and ATYP detection rate by 1st time 24-core saturation PBx (sPBx) and the cancer risk in subsequent biopsies.

Design: One hundred sPBx were included in the study group. Indications for sPBx were abnormal DRE and/or serum PSA >2.5 ng/ml. Each specimen was retrospectively reviewed by two pathologists to confirm the diagnosis. The number and percentage of cores positive for HGPIN, and multifocality (HGPIN involving ≥ 2 cores) were recorded in each case. The presence of ATYP and PCa was also recorded. Extended repeat biopsy was available in 23 patients.

Results: The mean age and serum PSA of the patients was 62.8 years and 6.1 ng/ml, respectively. Thirty-four patients had normal findings (BPT), 39 PCa, 22 HGPIN, and 5 ATYP. The mean time between sPBx and repeat biopsy was 11.7 months (range 4 to 36). PCa was detected on repeat biopsy in 33% and 25% of patients with HGPIN and ATYP, respectively. None of the patients with BPT was found to have PCa on re-biopsy (table). PCa detection was significantly greater in patients with multifocal HGPIN than in those with monofocal HGPIN (80% vs. 0%, p=0.0101). The mean number of biopsy cores and % of tissue involved by HGPIN were 3.5 (range 2 to 5) and 0.9% (range 0.5 to 1.2), respectively, in patients with PCa detected on repeat biopsy, compared to 1.2 (range 1 to 3) and 0.3% (range 0.2 to 0.6) in patients without PCa on repeat biopsies (p=0.023 and 0.015, respectively).

Conclusions: Identification of multifocal HGPIN on 1st time sPBx is associated with an overall cancer detection rate of 80% on extended repeat biopsy. Although the number of cases studied is limited, the detection of multifocal HGPIN warrants additional searches for concurrent invasive carcinoma by repeated biopsy.

Repeat biopsy findings

Initial biopsy findings	# repeat biopsy cases	BPT	ATYP	HGPIN	PCa
HGPIN*	9/22	5 (55%)	0	1 (11%)	3 (33%)*
ATYP	4/5	2 (50%)	1 (25%)	0	1 (25%)
BPT*	10/34	7 (70%)	0	3 (30%)	0*
Total	23/61	14 (61%)	1 (4%)	4 (17%)	4 (17%)

* p<0.05 by chi-square test

735 Neoadjuvant Androgen Deprivation Therapy Down-Regulates Prostein (P501S) Expression in Prostate Cancer

C Magi-Galluzzi, L Sercia, E Kodjoe, J Myles, R Dreicer, E Klein, M Zhou. Cleveland Clinic, Cleveland, OH.

Background: Prostein (P501S) is a novel prostate-specific gene, identified by a combination of cDNA subtraction and high-throughput microarray screening. Prostein expression is androgen responsive as the treatment of LNCaP cells with androgen up-regulates P501S mRNA and protein levels. Moreover, prostein antibody stained LNCaP cells, but failed to react with androgen unresponsive DU-145 cells. We examined the expression of prostein by immunohistochemisty in hormonally treated and untreated adenocarcinomas of the prostate (PCA).

Design: We studied 49 radical prostatectomies, transurethral resections and needle biopsies of the prostate, including 28 untreated acinar PCA of various Gleason grades (uPCA), 12 PCA treated (tPCA) with androgen deprivation therapy (ADT) prior to RP, 3 mucinous (colloid) adenocarcinomas (muPCA), and 6 PCA with focal mucinous features (PCAfmu). Tissue sections were selected to include lesions of interest and adjacent non-neoplastic prostate glands. P501S immunoreactivity (perinuclear punctuate plasma membrane) was graded for staining intensity (weak and strong) and extent (focal or diffuse). The P501S expression in cancer glands was compared to that of the adjacent non-neoplastic prostate tissue, when present, and recorded as increased, decreased or comparable.

Results: All uPCA, muPCA, and PCAfmu showed diffuse P501S expression, and 92% of these cases exhibited strong staining comparable to the surrounding non-neoplastic prostate glands. In contrast, half of the tPCA (6/12) demonstrated weak and focal staining, and the remaining cases showed no detectable immunoreactivity. In tPCA, the lack of P501S expression seemed to be associated with the degree of androgen deprivation effect. The atrophic non-neoplastic parenchyma surrounding tPCA showed decreased staining when compared to non-atrophic non-neoplastic prostate glands.

Conclusions: Neoadjuvant androgen deprivation therapy down-regulates P501S expression in prostate cancer and 50% of such cases have no P501S expression by immunohistochemistry. The potential utility of prostein as a prostate specific marker and as a potential target for PCA antibody therapy is limited in PCA treated with hormonal ablation.

Prostein expression in PCA

	Intensity of staining		Extent of staining	
	weak	strong	focal	diffuse
uPCA	3/28	25/28	0/28	28/28
muPCA	0/3	3/3	0/3	3/3
PCAfmu	0/6	3/3	0/6	6/6
tPCA	6/12	0/12	6/12	0/12

736 Detection of Bladder Cancer by Proteomics of Urine

T Majewski, PE Spiess, J Bondaruk, C Clarke, WF Benedict, CPN Dinney, HB Grossman, KS Tang, KA Baggerly, B Czerniak. The University of Texas M. D. Anderson Cancer Center, Houston, TX; Ciphergen Biosystems, Inc, Fremont, CA.

Background: Application of new technologies for detection of cancer could have an important effect on patient survival and overall quality of life. This is particularly urgent in reference to common carcinomas such as those that arise in the bladder and affect a substantial proportion of the population having a major impact on public health.

Design: We used protein matrix-assisted laser desorption and ionization time-of-flight (MALDI-TOF) and surface-enhanced laser desorption and ionization time-of-flight (SELDI-TOF) to study protein profiles in progression of bladder neoplasia from *in situ* conditions to invasive disease and to detect bladder cancer in urine. We initially analyzed proteomic profiles of bladder cancer development from in situ neoplasia in 18 samples to tumor and adjacent urothelium. The baseline profiles were obtained from urothelial cells prepared from the urethers of nephrectomies. Then we searched for abnormally expressed proteins in voided urine sediments of 94 patients with bladder cancer and validated the findings in a blinded set of 160 voided urine samples from patients with bladder cancer and unaffected controls. Finally we searched for abnormally expressed proteins in voided urine samples of 168 patients with history of bladder cancer and related the findings to pathological, clinical, and follow-up data. The baseline profiles for urine samples were obtained from 65 age matched healthy individuals.

Results: Data were preprocessed using Matlab scripts to (a) remove noise, (b) subtract baseline, and (c) identify peak locations. Using the intensities of peaks, we classified urine samples in the training set by defining average "normal" and "tumor" profiles, and computing correlations between samples. Based on their correlation scores samples were classed as "normal", "tumor", or "ambiguous". Leave-one out cross-validation was used to define the boundary values for dividing regions in the training set and were subsequently used to classify the samples from the blinded set to assess sensitivity and specificity. Algorithms allowed us to identify cancer and normal samples with specificity 78% and sensitivity 100% with the positive predictive value 81% and negative predictive value 100% for a blinded set.

Conclusions: Protein Profiling of voided urine sediments is a promising non-invasive detection tool for bladder cancer.

737 Positive-Block Ratio in Radical Prostatectomy Specimens Is an Independent Predictor of Prostate-Specific Antigen Recurrence

RA Marks, HQ Lin, MO Koch, L Cheng. Indiana University, Indianapolis, IN; Yale University, New Haven, CT.

Background: Tumor volume has been considered an important variable in determining the probability of disease progression in prostatic adenocarcinoma. There have been many studies that have tried to determine an appropriate method of calculating tumor volume, but no single methodology has been agreed upon. We tested the hypothesis that the ratio of tumor positive tissue blocks to the total number of blocks submitted (positive-block ratio) can be used as an independent prognostic indicator for disease recurrence.

Design: We analyzed 504 patients who underwent total radical retropubic prostatectomy between 1990 and 1998. None of the patients had preoperative radiation or androgen-deprivation therapy. Clinical records were reviewed.

Results: The mean positive-block ratio was 0.44 (median, 0. 43; range, 0.05-1.0). The positive block-ratio was significantly associated with Gleason score, pathologic stage, surgical margin status, extraprostatic extension, seminal vesical invasion, lymph node metastasis, perineural invasion, and preoperative serum PSA level (all P<0.001). Using a multivariate Cox regression model, controlling for pathological stage, Gleason score, and surgical margin status, positive-block ratio was an independent predictor of PSA recurrence (hazard ratio, 2.4; 95% confidence interval, 1.1-5.1; P=0.02). Five-year PSA recurrence-free survival was 67% for those patients with positive-block ratio ≤0.43, as compared to 42% those with positive-block ratio >0.43 (P<0.001).

Conclusions: Positive-block ratio is an independent predictor of PSA recurrence and we recommend that this variable be recorded in radical prostatectomy specimens.

738 The Relationship of Prostate Specific Antigen Recurrence and the Extent of Surgical Margin Positivity in Radical Prostatectomy Specimens

RA Marks, MO Koch, BE Juliar, L Cheng. Indiana University, Indianapolis, IN.

Background: The presence of positive surgical margins is a negative prognostic indicator in patients undergoing prostatectomy for prostate cancer; whether the extent of the positive margins affects the clinical outcome with regards to prostate specific antigen (PSA) recurrence, remains uncertain. We evaluated the linear extent of margin positivity as a prognostic indicator in a series of retropubic prostatectomy specimens.

Design: One hundred seventy-four consecutive margin-positive prostatectomy specimens were evaluated. The linear extent of margin positivity was measured with an ocular micrometer.

Results: The linear extent of margin positivity ranged from 0.05 mm to 75.0 mm (mean= 8.94; median=5.0). The linear extent of margin positivity was associated with tumor volume (P=0.03); but was not associated with patients' age at surgery, preoperative PSA level, prostate weight, pathologic stage, Gleason score, extraprostatic extension, seminal vesicle invasion, perineural invasion, high-grade prostatic intraepithelial neoplasia or PSA recurrence. In the full model multiple Cox regression, significant predictors for PSA recurrence were tumor stage (P=0.015), Gleason score (P=0.009), and preoperative PSA (P=0.011); extent of margin positivity was not predictive of PSA recurrence (hazard ratio=1.00; 95% CI=0.98 to 1.02; P=0.96), nor was tumor volume a significant factor when adjusted for other covariates (P=0.27).

Conclusions: Preoperative PSA, tumor stage and Gleason score remained significant prognostic factors in evaluating the likelihood of PSA recurrence in patients with positive surgical margins; the extent of margin positivity, however, is not a prognostic factor for PSA recurrence and should, therefore, not be necessarily included in the final report for radical prostatectomy specimens.

739 Direct Assessment of Telomeres in Testicular Germ Cell Tumors Reveals Evidence of Telomere Length Heterogeneity and Non-Telomerase Mediated Telomere Maintenance in Tumor Subsets

AK Meeker, JI Epstein, Y Konishi, GJ Netto. Johns Hopkins University School of Medicine, Baltimore, MD.

Background: Chromosomal termini (telomeres) are involved in genetic stability. Germ line telomeres are maintained by telomerase. Testicular Germ Cell Tumors (TGCT), arise from the germ cell lineage. Telomere loss plays a role in epithelial carcinogenesis but an unclear role in TGCT. Prior studies utilizing bulk measurement could not assess precursor lesions or intra-tumoral heterogeneity. Here, we used high resolution telomere FISH to assess telomere lengths in TGCT cells and intra-tubular germ cell neoplasia of the unclassified type (IGCNU), the presumed precursor of TGCT.

Design: A spectrum of TGCT were analyzed including 18 seminomas (Sm), 11 teratomas (Ter), 4 yolk sac tumors (YST), 4 embryonal carcinomas (EC), and 1 spermatocytic seminoma (SS). Telomere FISH staining in which fluorescent signal intensity is proportional to telomere length was performed, with adjacent H&E sections for histology. Telomeric signals in tumor cells were compared to those of adjacent stromal cells or, when present, cells within normal-appearing and/or atrophic seminiferous tubules containing IGCNU.

Results: Normal germ cells exhibited long telomeres while IGCNU were heterogeneous. **Sm:** 7/18 had telomeres shorter than normal spermatogonia, 6/18 equivalent to normal germ cells and 5/18 showed cell-to-cell heterogeneity. **Ter:** 7/11 comparable to normal somatic stromal cells, 3/11 comparable to normal germ cells and 1 had long telomeres. **EC:** 3/4 displayed striking heterogeneity spanning the telomeres of normal germ cells and had evidence of the telomerase-independent telomere maintenance mechanism known as ALT (Alternative Lengthening of Telomeres). 1/4 had homogeneous telomeres comparable to normal germ cells and lacked ALT. **YST:** 2 tumors were comparable to normal germ cells and 2 had highly heterogeneous telomeres, one showing evidence of ALT. **SS:** the single case had extremely long telomeres and was ALT+.

Conclusions: IGCNU display significant cell-to-cell telomere heterogeneity, thus, as with carcinomas, telomere shortening may play a role in the initiation and/or progression of TGCT. Length heterogeneity was also observed in many TGCT, particularly EC and YST which also exhibited ALT, heretofore only observed in sarcomas. ALT was also found in the single SS but was uncommon in the other TGCT types and not observed in any of the teratomas.

740 Molecular Signature and Clinical Implications of *TMPRSS2* and *ETS* Transcription Family Genes Fusions in a Surgical Cohort of American Men Treated for Clinically Localized Prostate Cancer

R Mehra, S Tomlins, R Shen, L Wang, J Wei, K Pienta, D Ghosh, MA Rubin, A Chinniayan, RB Shah. The University of Michigan, Ann Arbor, MI; Brigham's and Women's Hospital, Boston, MA.

Background: Novel recurrent gene fusions between androgen regulated gene *TMPRSS2* (21q22.3) and the *ETS* family members *ERG* (21q22.2), *ETV1* (7q21.2) or *ETV4* (17q21) have been recently identified as a common molecular event in prostate cancer. In this study we comprehensively analyzed the frequency and risk of disease progression for the *TMPRSS2* and *ETS* family members molecular subtypes in a cohort of American men surgically treated for clinically localized prostate cancer.

Design: A tissue microarray was constructed from 111 men surgically treated for localized prostate cancer and stained for 3 break apart (*TMPRSS2, ERG, ETV4*) and one fusion (*TMPRSS2-ETV1*) FISH probes. FISH signals were scored manually (100x oil immersion) in morphologically intact and non-overlapping nuclei in a minimum of 50 cells/case. The clinical significance and risk of disease progression of these genomic rearrangements was analyzed.

Results: *TMPRSS2*, *ERG*, *ETV1* and *ETV4* genes were rearranged in 65%, 55%, 2% and 2% respectively. Overall 54% of cases demonstrated *TMPRSS2:ERG* and 2% *TMPRSS2: ETV1* fusions. A deletion of 3' end of *TMPRSS2* and 5' end of *ERG* was identified in 40.5% and 38.8% of cases rearranged for respective genes, confirming the intronic loss of genomic DNA between them is a common mechanism of fusion. In 10.5% of cases *TMPRSS2* was rearranged without any known three *ETS* genes partners. There was a trend for prostate cancers with *TMPRSS2* and *ERG* gene rearrangement to be associated with high pathologic stage (p=0.06) and Gleason score >= 7 (p=0.058).

Conclusions: Our results confirm that recurrent chromosomal aberrations in *TMPRSS2* and/or *ETS* family members are found in over 70% of prostate cancers. Presence of these distinct molecular subtypes may provide insight into the causation of prostate cancer and may further define the risk of disease progression.

741 Expression of High Mobility Group A Gene Products in Prostate Cancer

J Melamed, L Chiriboga, H Yee, P Lee, J-J Wei. New York University, New York, NY.

Background: High mobility group A genes transcribe two non-histone DNA binding proteins (HMGA1 and 2). They are normally expressed in embryo to regulate cell differentiation and aberrantly expressed in many malignant neoplasms to promote tumorigenesis. A few studies have indicated that overexpression of HMGA1 mRNA is associated with an aggressive prostate cancer. In this large cohort study, we examined HMGA1 and HMGA2 proteins and analyzed their association with demographic and pathologic characteristics of prostate cancer.

Design: 1) A tissue microarray (TMA) consisted of prostate cancer samples from 100 consecutive radical prostatectomy cases. The unselected cohort had comprehensive demographic, pathologic and clinical annotation (age: 39 to 78 years old, tumor stages: pT2a to pT3b, tumor volumes: <5% to 75% and Gleason scores: 6 to 9); 2) All cases were represented in quadruplicate plus one core of non-neoplastic tissue; 3) immunohistochemistry for HMGA1 and HMGA2 was performed and results were scored using a semiquantitative scoring system; 4) Statistical analysis showed the net gain or loss of HMGAs in prostate cancer correlated with patients age, tumor volume, stage and grade.

Results: Increased immunoreactivity for HMGA1 and HMGA2 was identified in 84% (72/86) and 66% (56/86) of cases with net gains of 1.47±0.23 and 0.83±0.31, respectively. Overexpression of HMGA1 in prostate cancer positively correlated with that of HMGA2 (r=0.56). The values of net gain for HMGA1/2 in association with tumor stage, volume and Gleason score are summarized in Table 1.

Conclusions: This is the first study to examine HMGA protein expression in a large cohort prostate cancer population by immunohistochemistry. Our results demonstrate that increased HMGA proteins are evident in most prostate cancer. By semiquantitative analysis, HMGA1 and HMGA2 are the potential prognostic markers: the high levels of protein production are associated with advanced tumor stage, large tumor volume and high grade tumor.

Table 1 HMGA1/2 expression in relation to pathologic stage, tumor volume and grade in prostate cancer

	HMGA1			HMGA2		
Stage	pT2	pT3a	pT3b	pT2	pT3a	pT3b
mean±sem	1.05±0.35	2.24±0.59	2.93±0.64	0.20±0.37	1.57±0.65	3.16±0.96
Volume	<5%	5-25%	>25%	<5%	5-25%	>25%
mean±sem	0.76±0.53	1.55±0.39	2.44±0.34	0.35±0.55	0.89±0.44	1.49±0.71
Gleason score	G6	G7	G8-9	G6	G7	G8-9
mean±sem	1.21±0.36	1.67±0.46	2.45±0.92	0.41±0.44	1.01±0.40	3.70±1.28

742 Automated Immunofluorescence Analysis Defines Microvessel Area as a Prognostic Parameter in Clear Cell Renal Cell Cancer

KD Mertz, F Demichelis, R Kim, P Schraml, M Storz, PA Diener, H Moch, MA Rubin. Brigham and Women's Hospital, Boston, MA; University Hospital Zurich, Zurich, Switzerland; Cantonal Hospital of St. Gallen, St. Gallen, Switzerland.

Background: Microvessel density has been reported to have prognostic relevance for clear cell renal cell carcinoma (ccRCC). However, this finding is controversial due to the difficulty of microvessel density evaluation in this complex vascularized tumor type. A more objective and reproducible quantification of biomarker expression can be achieved by an automated quantitative analysis (AQUA) system. The present study evaluates the utility of the AQUA system for determination of tumor vascularization in ccRCC.

Design: The AQUA system was applied to tissue microarrays with 284 primary ccRCC tumors. To determine angiogenesis in ccRCC, we created an epithelial/stromal-mask consisting of CD10, Epithelial Membrane Antigen and Vimentin to distinguish epithelial tumor cells from CD34 positive endothelial cells. Using immunofluorescence and computer aided quantification of CD34 expression, we measured the relative microvessel area and compared the microvessel area to the manually counted microvessel density.

Results: The microvessel area determined by AQUA in a test set with 209 ccRCCs ranged from 0% to 30.3% (mean±SD, 10.1% ± 6.3%). The manually determined microvessel density ranged from 6 to 987 vessels per mm^2 (mean±SD, 416.8 ± 252.8 vessels per mm^2). Microvessel area and microvessel density were significantly correlated ($p<0.001$). A larger microvessel area was associated with histological grade ($p<0.001$), tumor stage ($p=0.008$), presence of metastasis ($p=0.005$), presence of sarcomatoid areas ($p<0.001$) and tumor specific survival ($p<0.001$). Using small and large microvessel areas as defined in the test set, all associations with clinical and pathological parameters were confirmed in a second independent validation set consisting of 75 ccRCCs.

Conclusions: Microvessel area determination by AQUA is an objective and reliable method to quantify tumor vascularization in ccRCC. A large microvessel area correlates with a high microvessel density and is associated with better patient prognosis.

743 Expression of Cytokeratins and E-Cadherin Provides a Novel Molecular Subclassification of Clear Cell Renal Cell Cancer

KD Mertz, F Demichelis, MS Hirsch, H Moch, MA Rubin. Brigham and Women's Hospital, Boston, MA; University Hospital Zurich, Zurich, Switzerland.

Background: Since clear cell renal cell carcinoma (ccRCC) is a clinicopathologically heterogenous group of tumors, the identification of novel diagnostic markers is mandatory to help predicting the clinical behaviour and the prognosis for this RCC subtype. We hypothesized that cytogenetic aberrations of ccRCC may be associated with the expression of immunohistochemical markers such as cytokeratins that have been reported to have variable protein expression in this RCC subtype.

Design: We performed a detailed immunohistochemical analysis for cytokeratins and other molecular biomarkers on a series of 185 renal tumors (containing 129 conventional ccRCC cancers) using tissue microarrays and a semi-automated quantitative system for *in situ* protein measurements. For 126 of the ccRCC cases, cytogenetics was available. In particular, we evaluated the keratin expression profiles of these tumors using different antibodies that recognize basic and acidic cytokeratins.

Results: We identified the most common cytogenetic alterations in 126 ccRCC tumors, most of them involving chromosome 3 through loss, deletion or translocation. Cases were annotated according to the common cytogenetic alterations and to their total number of alterations. 30 ccRCCs (24%) did not show any cytogenetic aberration. We compared the immunohistochemical and the cytogenetic profiles of these 126 ccRCCs by applying hierarchical clustering of the tumors based on the protein values. A subgroup of cases without cytogenetic alterations showed high expression of cytokeratins. Another subgroup lacking cytogenetic alterations consisted of E-cadherin positive tumors. Both cytokeratin and E-cadherin positive ccRCCs were highly enriched for low grade tumors (Fuhrman nuclear grade 2, FNG 2). In contrast, a third subgroup of cytokeratin and E-cadherin negative tumors expressed vimentin and showed few to multiple cytogenetic alterations. This was consistent with higher FNG and more aggressive clinical behaviour.

Conclusions: Low nuclear grade and lack of cytogenetic alterations are associated with high expression of cytokeratins and E-cadherin in ccRCC. Characterization of ccRCCs based on their immunohistochemical marker profile and their cytogenetic status has the potential to supply significant clinical insights in the biology of ccRCC with prognostic relevance.

744 Prostate Specific Membrane Antigen (PSMA) Protein Expression in Normal and Neoplastic Tissues: *Immunohistochemistry Study Using Multiple Tumor Tissue Microarray Technique*

P Mhawech-Fauceglia, S Zhang, L Terracciano, S Guido, FR Herrmann, R Penetrante. Roswell Park Cancer Institute, Buffalo, NY; Basel University Hospital, Basel, Switzerland; Geneva University Hospital, Geneva, Switzerland.

Background: The new commercially available marker, prostate-specific membrane antigen (PSMA) seemed to be very helpful in making the diagnosis of prostate adenocarcinoma (PaC). However, the expression of this marker in various tumor types is still widely unknown. The aims of this study is to determine PSMA expression in normal tissues as well as in 3367 benign and malignant tumors, and subsequently to define the sensitivity and specificity of this marker in PaC.

Design: Multiple tissue microarray of 3367 benign and malignant tumors was constructed. Sections were stained with PSMA monoclonal antibody.

Results: PaC was positive in 78/141 (55.3%) with various staining patterns including cytoplasmic, apical, apical/cytoplasmic, and cytoplasmic with membranous accentuation. From all tumor types, PSMA expression was seen in 1/97 (1.0%) squamous cell carcinoma of the head and neck, 1/9 (11.1%) adenocarcinoma of the esophagus, 6/71 (8.45 %) adenocarcinoma of the stomach, 1/48 (2.0%) adenocarcinoma of the pancreas, 1/48 (2.0%) astrocytoma, and 21/346 (6.0%) urothelial carcinoma of the bladder (UBC). In all those tumors, staining pattern was always cytoplasmic. The sensitivity and specificity of PSMA in PaC was 55.3% and 98.7% respectively.

Table 1. Summary of Prostatic adenocarcinomas cases stained with PSMA

Number of cases (n)		apical	apical + cytoplasmic	cytoplasmic + membranous	cytoplasmic
Untreated (total n 97)					
	negative (n 35)				
	weak (n 9)	8	1	0	0
	moderate (n 15)	11	3	1	0
	strong (n 38)	20	11	4	3
Treated (total n 44)					
	negative (13)				
	weak (n 6)	0	0	0	6
	moderate (n 7)	1	2	0	4
	strong (n 18)	8	3	3	4
Treated and untreated (total n 141)					
	negative (n 48)				
	weak (n 15)	8	1	0	6
	moderate (n 22)	12	5	1	4
	strong (n 56)	28	14	7	7

Conclusions: PSMA is not sensitive but highly specific for PaC. However, staining patterns such as apical, apical/cytoplasmic and cytoplasmic with membranous accentuation are highly specific for PaC, and can be of great help in metastatic disease, especially from or to urinary bladder.

745 Overexpression of Toll-Like Receptor 3 in Clear Cell Renal Cell Carcinoma: A Potential Therapeutic and Diagnostic Target

T Morikawa, A Sugiyama, H Kume, K Tomita, T Kitamura, S Ota, M Fukayama, T Kodama, H Aburatani. Research Center for Advanced Science and Technology, University of Tokyo, Tokyo, Japan; Perseus Proteomics Inc, Tokyo, Japan; University of Tokyo Hospital, Tokyo, Japan; Graduate School of Medicine, University of Tokyo, Tokyo, Japan.

Background: Renal cell carcinoma (RCC) is one of the most refractory cancers in terms of pharmaceutical treatment. The aim of this study is to discover a novel therapeutic target gene for clear cell RCC, which accounts for the majority of RCC.

Design: Gene expression profiles of 27 clear cell RCC and 9 normal kidney tissues as well as 14 various normal tissues were examined by GeneChip HG-U133plus2.0 array (Affymetrix). Among the genes specifically up-regulated in clear cell RCC, overexpression of toll-like receptor 3 (TLR3) was validated by quantitative RT-PCR and immunohistochemistry. The growth inhibitory effect of TLR3 ligand poly I:C against 8 RCC cell lines was examined by MTT assay.

Results: TLR3 gene was highly expressed in clear cell RCC, whereas only low expression was observed in normal tissues. On immunohistochemical analysis using a monoclonal antibody against TLR3, positive signals were observed in 184 of 189 cases of clear cell RCC (97.4%) whereas TLR3 expression was entirely absent in chromophobe RCC (0/8). TLR3 ligand poly I:C exerted a growth inhibitory effect by inducing apoptosis in RCC cell lines in a TLR3 dependent manner. Moreover, a combination of TLR3 ligand poly I:C and interferon-alfa exerted a synergistic growth inhibitory effect.

Conclusions: Our results suggest that TLR3 may be a diagnostic marker for clear cell RCC and open new clinical prospects for using TLR3 agonists as therapeutic agents in clear cell RCC.

746 Molecular Genetic Evidence Supporting the Neoplastic Nature of Stromal Cells in "Fibrosis" after Chemotherapy for Testicular Germ Cell Tumors

MJ Morton, S Zhang, M Wang, DD Davidson, J Huang, TD Jones, JJ Anagnostou, Jr, SD Beck, RS Foster, L Cheng. Indiana University, Indianapolis, IN; University of Rochester, Rochester, NY.

Background: A residual retroperitoneal mass containing only fibrosis and necrosis is present in 40-52% of patients with advanced testicular germ cell tumors after chemotherapy. The biological nature and genetic characteristics of stromal cells in these residual masses have not been adequately investigated.

Design: Twenty-seven patients underwent retroperitoneal lymph node dissection after chemotherapy for metastatic testicular germ cell tumor. Fibrosis and necrosis were observed in all 27 cases. None had metatastic teratoma or other germ cell tumors. The patterns of allelic loss in the stromal cells of the fibrous tissue and in the lymphocytes using 10 microsatellite DNA markers (D1S508, D2S156, D9S171, IFNA, D9S177, D9S778, D13S317, TP53, D18S46, and D18S543) were compared. Isochromosome 12p and 12p over-representation were studied by fluorescent *in situ* hybridization.

Results: Allelic loss in the stromal cells of the fibrosis was present in at one microsatellite DNA locus in 24 (88%) of the cases. The frequency of allelic loss in the stromal cells was 17% for D1S508, 15% for D2S156, 23% or D9S171, 28% for IFNA, 15% for D9S177, 35% for D9S778, 24% for D13S317; 28% for TP53, 24% for D18S46; and 31% for D18S543. A chromosome 12p anomaly (either isochromosome 12p or 12p over-representation) was present in 9 (33%) cases.

Conclusions: The high frequency of allelic losses and chromosome 12p anomalies in the stromal cells from residual retroperitoneal fibrous masses after chemotherapy for testicular germ cell tumors suggest that the stromal cells are derived from the same tumor progenitor cells as the preexisting metastatic germ cell tumor.

747 Telomere Shortening in Intestinal Metaplasia of the Urinary Bladder Demonstrated by Quantitative FISH

MJ Morton, S Zhang, A Lopez-Beltran, GT MacLennan, JN Eble, M Sung, PH Tan, R Montironi, L Cheng. Indiana University School of Medicine, Indianapolis, IN; Cordoba University, Cordoba, Spain; Case Western Reserve University, Cleveland, OH; Chang-Gung Memorial Hospital, Kaohsiung, Taiwan; Singapore General Hospital, Singapore; School of Medicine, Polytechnic University of the Marche Region (Ancona), United Hospitals, Ancona, Italy.

Background: Although intestinal metaplasia is often found in association with adenocarcinoma of the urinary bladder, it is unclear whether intestinal metaplasia of the bladder is a pre-malignant lesion. We used quantitative FISH to measure telomere length in urinary bladder specimens with intestinal metaplasia, as telomere shortening has recently been demonstrated in many human epithelial cancer precursors.

Design: Paraffin-embedded tissue blocks from 34 patients with intestinal metaplasia of the urinary bladder were evaluated. Tissue sections were prepared and hybridized with a telomere-specific peptide nucleic acid (PNA) probe. Quantitative FISH on interphase nuclei was used to assess telomere signal intensity. The intensity from 50 nuclei within populations of intestinal metaplastic cells was averaged and compared to the average intensity from 50 nuclei from adjacent normal urothelial control cells. The overall average intensities in these two cell populations were calculated and compared.

Results: In all 34 cases, reduced average telomere signal intensity was observed in the nuclei of intestinal metaplastic cells, compared to the same parameter in adjacent control nuclei. The total averages for all the nuclei examined revealed an intestinal metaplasia to control signal ratio of 0.55 ($p<0.001$).

Conclusions: Our findings indicate that intestinal metaplasia in the urinary bladder is associated with significant telomere shortening relative to telomere length in adjacent normal urothelial cells. Since telomere shortening has been documented in certain pre-malignant epithelial lesions, our findings support the hypothesis that intestinal metaplasia of the urinary bladder is a precursor lesion to and could be a marker in the development of adenocarcinoma of the urinary bladder.

748 Morphological Features of *TMPRSS2: ERG* Fusion Prostate Cancer

JM Mosquera, S Perner, F Demichelis, MD Hoffer, KD Mertz, P Paris, J Simko, C Collins, T Bismar, MA Rubin. Brigham and Women's Hospital, Boston, MA; Harvard Medical School, Boston, MA; University of Ulm, Ulm, Germany; SRA Division & Bioinformatics Group, Povo, Trento, Italy; University of California, San Francisco, CA; McGill University, Montreal, QC, Canada; MIT and Harvard Medical School, Cambridge, MA; Dana Farber Harvard Comprehensive Cancer Center, Boston, MA.

Background: *TMPRSS2:ETS* fusion prostate cancers (PCA) comprise 40-50% of the PSA screened hospital based PCA examined to date making it the most common genetic rearrangement in human cancer. The most common variant involves *TMPRSS2* and *ERG*. Emerging data from our group and others suggests that *TMPRSS2:ERG* PCA is associated with higher tumor stage and PCA specific death. The goal of this study was to determine if this common somatic alteration is associated with a morphologic phenotype.

Design: We assessed 253 PCA cases for *TMPRSS2:ERG* fusion status using FISH. Tumors were assessed for presence or absence of 8 morphologic features. The reviewers were blinded to the fusion status. Statistical analysis was performed to look for significant associations between morphologic features and *TMPRSS2:ERG* fusion status.

Results: Five morphologic features were associated with *TMPRSS2:ERG* PCA: **blue-tinged mucin** (85% of cases, n=23/27), **cribriform growth pattern** (68%, n=50/74), **macronucleoli** (78%, n=39/50), **intraductal tumor spread** (88%, n=38/43), and **signet-ring cell-like features** (82%, n=9/11) all with p-values<0.05. Only 24% (n=30/125) of tumors without any of these features displayed the *TMPRSS2:ERG* fusion. In contrast, 55% (n=38/69) of cases with one feature (RR=3.88), 86% (n=38/44) of cases with two features (RR=20.06), and 93% (n=14/15) of cases with three or more features (RR=44.33) were fusion positive ($p<0.001$).

Conclusions: This is the first study to our knowledge that demonstrates a significant link between a molecular alteration in PCA and distinct phenotypic features. The strength of these findings is similar to BRCA-1/2 breast cancers and HNPCC colon cancer. The biologic effect of *TMPRSS2:ERG* overexpression may drive pathways that favor these common morphologic features that pathologists observe on a daily basis. These features should also be helpful in diagnosing *TMPRSS2:ERG* fusion PCA which may have both prognostic and therapeutic implications. Validation studies are underway.

749 An Interphase FISH Panel Can Distinguish among Various Granular Renal Neoplasms

M Myrsiades, K Reichard, B Hall, J McKenney, M Che, D Grignon, J Hozier, L Cerilli. Univ of New Mexico, Albuquerque, NM; Univ of Arkansas, Little Rock, AR; Wayne St Univ, Detroit, MI.

Background: Diagnostic challenges exist in the differentiation of renal neoplasms with granular cytoplasm, namely among oncocytoma, chromophobe renal cell carcinoma (RCC) and classic or clear cell (CC) RCC. Importantly, these neoplasms each portend significantly different prognoses. Cytogenetic abnormalities have been reported for each tumor type but not in a comprehensive and comparative manner. We aim to identify a clinically feasible fluorescent *in situ* hybridization (FISH) probe set that discriminates between these neoplasms using FISH on paraffin-embedded sections.

Design: 91 tumors were identified, including 40 oncocytomas, 29 chromophobe RCC, and 22 CC RCC, the largest series studied by FISH to date. 24 normal kidney cores served as controls. Tissue microarrays (TMA) were constructed. FISH probes targeting the centromere region (CEP) of chromosomes 1, 3, 4, 8, 10, 12, 17, 18, X, and Y, and CCND1 (11q13) using a break apart probe were analyzed. Semi-automated FISH analysis on interphase nuclei was performed (MetaSystems™). Genetic profiles from each tumor type were compared as a group to other tumor types using clustering analysis.

Results: FISH was successful on all cases. Computational analysis revealed a set of 4 probes able to differentiate among tumor subtypes. Visual assessment of clustering analysis data showed distinct clustering of oncocytomas (CEP 8/10/17 diploid and CCND1 rearranged in 13/40), while chromophobe RCC was distinctly separate (CEP 8/10/17 loss and CCND1 rearranged in 0/29). Similarly, CC RCC (CEP 8/10/17 diploid and CCND1 rearranged in 3/22) clustered distinctly from chromophobe RCC, but overlapped with oncocytoma. Specifically, CCND1 rearrangements were detected in 13/40 (33%) of oncocytomas, 0/29 (0%) chromophobe RCC, and 3/22 (14%) CC RCC.

Conclusions: 1) A 4 probe FISH panel can help differentiate oncocytomas from chromophobe RCC, and CC RCC from chromophobe RCC: CEP 8, CEP 10, CEP 17 and CCND1. This data indicates that this probe panel helps classify a tumor, when conventional histology is ambiguous, and can be performed on routinely processed tissue. 2) Analysis of chromosomes 1,3,4,12,18,X,Y could not statistically discriminate among these three granular tumor types either singly or within a small panel. 3) CCND1 gene rearrangements are specific (100%) for differentiating oncocytomas from chromophobe RCC but insensitive (33%) as a single marker of oncocytoma.

750 Use of pHH3, Ki-67 and Survivin Immunoreactivity in Evaluating Urothelial Carcinomas of the Bladder

H Nakhla, O El-Zammar. State University of New York & Upstate Medical University, Syracuse, NY.

Background: Accurate grading of urothelial carcinoma of the bladder is important for predicting outcome and for choosing therapy. Low-grade urothelial carcinomas invade in less than 20 percent of cases, in contrast to high-grade urothelial carcinomas that are invasive in most cases. Almost all disease-related deaths from bladder neoplasms are due to high-grade tumors. This study investigated the immunoreactivity of the mitosis marker phospho-histone H3 (pHH3), and of the proliferation markers Ki-67 and survivin in evaluating urothelial carcinoma of the bladder.

Design: Twenty-three cases of urothelial carcinoma were reviewed without knowledge of the immunohistochemical results, and graded according to the WHO/ISUP classification. Immunostaining on formalin-fixed, paraffin-embedded tissue was performed on all cases for PHH3, Ki-67 and Survivin. Ki-67 and Survivin labeling index values were recorded as the percentage of positive nuclei in 1000 cells. For pHH3, the total number of mitoses per 10 high power fields (HPF) was determined. All markers were assessed in fields with the highest immunoreactivity.

Results: There were 11 low grade and 12 high grade cases. In high-grade lesions, the average pHH3 mitotic count was 84.1 per 10 HPF (range: 41-180) compared to 9.2 (range: 1-38) in low grade lesions. Survivin staining was predominantly nuclear except for three cases, which showed additional diffuse cytoplasmic staining. The mean labeling index for Ki-67 and Survivin was 10.1% and 3.6% in low grade lesions and 30.3% and 24.3% in high grade lesions, respectively.

Conclusions: Staining for pHH3, Ki-67 and Survivin is higher in high grade than in low grade urothelial carcinomas. These immunohistochemical markers, especially pHH3, may be useful adjuncts to histopathology in grading of bladder neoplasms.

751 Expression of Survivin, PHH3 and Serine/Threonine Kinase Mirk/Dyrk1B Distinguish Renal Oncocytoma from Chromophobe Renal Cell Carcinoma

MR Nasr, SS Shah, VS Chandan, JC Cheville, E Friedman, SK Landas. SUNY Upstate Medical University, Syracuse, NY; Mayo Clinic College of Medicine, Rochester, MN.

Background: Renal epithelial neoplasms include several tumors with distinctive morphology and natural history. Occasionally there is overlap of morphological features of chromophobe renal cell carcinoma (RCC) and renal oncocytoma (RO). Distinguishing these is important as it has critical prognostic and therapeutic implications. This study evaluated the use of the immunohistochemical mitosis marker phospho-Histone H3 (pHH3), the anti-apoptotic marker survivin, and a critical regulator of cell growth and differentiation marker, Mirk/Dyrk1B, in separating RO from chromophobe RCC.

Design: Immunohistochemical analysis for survivin and pHH3 was performed on formalin-fixed paraffin embedded sections of RO (n=5), chromophobe RCC (n=5) and conventional/clear cell RCC (n=5). Expression of Mirk/Dyrk1B was assessed in the same manner. Immunostained sections showing pHH3 expression were reviewed and the total number of mitoses for each renal lesion was counted and expressed per 15 high power fields (HPF). Survivin staining was scored separately as cytoplasmic or nuclear. Nuclear survivin staining was counted in each renal lesion, and expressed per 15 HPF. Only cytoplasmic expression of Mirk/Dyrk1B was regarded positive.

Results: Mirk/Dyrk1B showed strong and diffuse cytoplasmic immunoreactivity in all cases of RO (5 cases) and clear cell RCC (5 cases) while it was negative (4 cases) or showed only weak and focal reactivity (1 case) in cases of chromophobe RCC. Nuclear survivin expression was seen in chromophobe RCC (mean: 3.2/15HPF; range: 1-6/15HPF) and clear cell RCC (mean: 6.2/15HPF; range: 2-14/15HPF) cases, but was negative in all 5 cases of RO. Strong cytoplasmic survivin expression was seen in all 5 RO cases in contrast to chromophobe and clear cell RCC cases. No pHH3 expression was detected in any RO cases. All 5 cases of chromophobe RCC showed staining for PHH3 (mean: 4.4/15HPF; range: 1-8/15HPF), but 3 of 5 cases of clear cell RCC expressed PHH3 (mean: 2.6/15HPF; range: 0-9/15HPF).

Conclusions: These findings demonstrate potential diagnostic utility of an immunohistochemical panel comprised of these three markers in the differentiation of RO from chromophobe RCC.

752 Inflammatory Cells and Membrane Disruption in Prostate Carcinoma: Do They Have a Role in Tumor Invasion?

AM Nelson, A Tuteja, Y-G Man. Armed Forces Institute of Pathology, Washington, DC.

Background: Our previous studies in human breast tumors revealed that ducts or acini with a focal disruption in their surrounding basement membrane and myoepithelial cell layer had a significantly higher infiltration of leukocytes and mast cells, and a vast majority of infiltrates were located at these disruptions (Man and Sang. Exp Cell Res 301:103-118, 2004). Our subsequent studies further showed that tumor cells overlying these focal disruptions had a significantly higher rate of proliferation and expression of invasion-related genes (Man et al. Breast Cancer Res Treat 89:199-208, 2005). This study intended to assess if similar alterations could be seen in human prostate tumors.

Design: Consecutive sections at 4-5 µm thickness were prepared from human prostate tumors. Sets of immediate adjacent sections were double immunostained for cytokeratin 34βE12 or collagen IV, to elucidate the basal cell layers, and the basement membrane, respectively, and then for leukocytes, mast cells, and proliferation markers. Immunohistochemistry was done using Vector (Burlingame, CA) products and methods. The expression levels and frequencies of these molecules in ducts or acini with and without focally disrupted physical barriers were statistically compared.

Results: (see tables below)

Conclusions: Focal disruption of the physical barriers and leukocytes and mast cell infiltration appear to be correlated events that directly trigger or facilitate prostate tumor invasion. Therefore, the development of therapeutic agents to manipulate leukocytes and mast cells may have significant value in treatment and prevention of tumor invasion. Supported in part by grants PC051308, DAMD17-01-1-0129, and DAMD17-01-1-0130 from Congressionally Directed Medical Research Programs to Yan-gao Man, MD., PhD.

CELLS COUNTED	LEUKOCYTES	MAST CELLS
With Focal Disruptions	357	172
Without Focal Disruptions	100	54
DUCTS COUNTED		
With Focal Disruptions	48	54
Without Focal Disruptions	58	39

Averages

	LEUKOCYTES	MAST CELLS
With Focal Disruptions	7.4	3.2
Without Focal Disruptions	1.7	1.4
p value	0.028	0.641

753 Loss of p16 Expression and Chromosome 9p21 LOH as Predictors of Outcome in Patients with Superficial Urothelial Bladder Carcinoma

G Nesi, T Cai, LR Girardi, G Baroni, R Bartoletti. University of Florence, Florence, Italy.

Background: Molecular alterations of genes implicated in cell cycles are important molecular events in bladder carcinogenesis. Alterations of 9p21 locus, especially $p16^{INK4a}$ gene, are very promising predictors of clinical outcome because they affect both the p53 and pRb cell-cycle regulatory pathways. The aim of the present study was to assess the prognostic value of p16 expression and loss of heterozygosis (LOH) on chromosome 9p21 in patients affected by superficial urothelial carcinoma of the urinary bladder.

Design: Fifty-six consecutive patients diagnosed with urothelial bladder cancer were enrolled in this study. LOH analysis was performed on a blood/tumour pair sample from each patient by using multiplex polymerase chain reaction (PCR). Three loci on chromosome 9 were investigated. All tumours were stained immunohistochemically for p16. Results from p16 and LOH analyses were compared with follow-up data in order to evaluate the prognostic role of these markers. Correlations between p16 expression and LOH at chromosome 9p21 were also investigated.

Results: Loss of p16 expression was found in 33 patients (58.9%) and was significantly associated with a reduced recurrence-free probability ($p<0.0001$). No correlations with stage ($p=0.162$) or grade ($p=0.051$) were evident. Forty-three patients (76.7%) showed at least one alteration on chromosome 9. The most frequently altered locus was D9S171 (9p21), with a frequency of 51.1% ($p=0.001$). A significant association was observed between p16 and LOH ($p=0.005$). According to Kaplan-Meier survival curves, recurrence-free status significantly correlated with p16 expression ($p<0.0001$), but not with alterations on chromosome 9 ($p=0.063$). On multivariate analysis, p16 expression ($p=0.002$), tumour grade ($p=0.001$) and the number of lesions ($p=0.002$) were identified as independent factors of tumour recurrence.

Conclusions: Our study indicates p16 expression as an independent prognostic factor for bladder tumour recurrence and highlights the role of cell cycle regulators in predicting the clinical outcome of patients with superficial urothelial bladder cancer.

754 Prognostic Role of E-Cadherin mRNA Levels in Urothelial Carcinoma of the Bladder: Relationship with Clinical Course at 12 Years Follow-Up

G Nesi, T Cai, LR Girardi, R Bartoletti. University of Florence, Florence, Italy.

Background: E-Cadherin (E-CAD) is a transmembrane glycoprotein which mediates a calcium dependent homophilic interaction among epithelial cells. The altered expression of E-CAD has been associated with clinicopathological findings in bladder tumours and might constitute a prognostic factor in bladder carcinogenesis. The aim of this study was to define the role of E-CAD mRNA expression in recurrence, progression and survival in urothelial carcinoma (UC) of the urinary bladder over a long follow-up period.

Design: Twenty-seven patients, subjected to transurethral resection of the bladder or open surgery for UC, were selected for the study. Neoplastic tissue samples, normal-appearing bladder mucosa and blood samples were taken from each patient. All the tissues underwent mRNA extraction and Northern blot analysis, marked with specific probes for E-CAD, and were evaluated by gel-electrophoresis. Clinicopathological and molecular data collected for each case were linked to vital status information at 12 years follow-up.

Results: In comparing molecular results with pathological stage and grade, we found a significant correlation (stage, $p=0.002$; grade, $p=0.008$) demonstrating that superficial bladder tumours are more likely to be E-CAD positive than invasive ones. No correlation was noted between number ($p=0.643$), time relapse ($p=0.097$), or other parameters of recurrence and progression ($p=0.078$) and expressed E-CAD mRNA levels. On multivariate analysis, E-CAD mRNA levels significantly correlated with cancer-specific survival ($p=0.002$).

Conclusions: Our results demonstrate that E-CAD mRNA is an independent predictor of cancer-specific survival in bladder cancer patients. We add that a long follow-up period is needed in order to assess the prognostic significance of molecular factors in urothelial bladder carcinoma.

755 Concurrent Renal Oncocytoma and Malignant Renal Tumors: Analysis of 28 Cases

MM Nicolas, CG Wood, P Tamboli. M. D. Anderson Cancer Center, Houston, TX.

Background: A small percentage of renal oncocytomas (RO) are associated with concurrent malignant renal tumors (MRT). There is scant information in the literature regarding concurrent RO and MRT, except in cases of renal oncocytosis and Birt-Hogg Dube syndrome. Aim of this study is to analyze the pathologic features of concurrent RO and MRT.

Design: All available material from 28 cases of concurrent RO and MRT was analyzed. These were diagnosed between 1990 and 2005 at one center (15 consult cases, 13 in-house cases). These included: 21 radical nephrectomies (2 bilateral) and 7 partials.

Results: The 28 cases were from 27 patients (22 men, 5 women). 22 cases were from one kidney (12 right, 10 left); 6 cases were bilateral (RO in 1 kidney and MRT in the opposite kidney in 5 cases; 1 case with RO and MRT in both kidneys). The 13 in-house cases constituted 0.48 % of 2691 nephrectomies performed in the same time period, and 8% of all RO resected. The concurrent MRT included: 12 clear renal cell carcinoma (CRCC), 9 papillary RCC, 2 papillary RCC and CRCC, 1 papillary RCC and chromophobe RCC, 1 chromophobe RCC (ChRCC), 1 hybrid RO/ChRCC, 1 multilocular cystic RCC and 1 sarcomatoid urothelial carcinoma. The TNM stage of the MRT (in cases where it could be accurately assigned) was as follows: 14 pT1a, 7 pT1b, and 3 pT3b. Follow-up for 12 in-house patients ranged from 5 to 55 months (average 30 months, median 29 months): 11 were without evidence of disease and 1 had multiple metastases at last follow-up. In addition to the MRT, papillary adenomas were present in 8 case and angiomyolipoma in one. In 7/28 cases, RO was the dominant mass (size range: 1.5-13 cm), with MRT size range of 0.3 cm to 3.7 cm. In 21/28 cases MRT formed the dominant mass (size range: 1.1-8.5 cm), while the RO ranged from 0.1 to 4.8 cm. Two or more MRT nodules were identified in 6 cases. Three or more RO or oncocytosis were present in 7 cases.

Conclusions: Although concurrent RO and RC are rare (0.48% of all renal tumors in our series), their awareness is important for the practicing pathologist. RO may be associated with MRT other than ChRCC (CRCC was the most common concurrent MRT in this study). In patients with multiple renal tumors, adequate sampling of all tumor nodules may be necessary to avoid missing a potentially malignant tumor in the presence of a RO. Also, patients with multiple tumors undergoing a biopsy for diagnosis, should undergo biopsy of the other nodules if the dominant nodule is a RO, to avoid missing a possible RC.

756 Nucleophosmin, a Critical Regulator of Cell Proliferation, Is Overexpressed in Prostate Cancer

P Nigwekar, C Wu, JL Yao, PA Bourne, J Li, Z Zhuang, PA di Sant'Agnese, DC Walters, J Huang. University of Rochester Medical Center, Rochester, NY; National Institute of Health, Bethesda, MD.

Background: Hormonal therapy (androgen ablation and/or anti-androgen) is effective in treating advanced PC. Similarly, androgen withdrawal inhibits growth of androgen-dependent PC cell lines such as LNCaP. We hypothesize that by comparing the protein expression profiles of LNCaP cells cultured with or without androgen, we may identify proteins involved in PC proliferation.

Design: Proteins from LNCaP cells cultured in FBS or androgen-deprived FBS were separated by 2-D gel electrophoresis. Differentially expressed proteins were identified with Liquid Chromatography Mass Spectrometry and validated by immunohistochemical staining using tissue microarrays containing benign prostate, PIN and PC.

Results: Ten differentially expressed proteins were sequenced. One of the proteins downregulated after androgen withdrawal was nucleophosmin (NPM), a key regulator of cell proliferation. Immunohistochemical staining was subsequently performed using an anti-NPM antibody (ABCAM, Cat. #AB24412, 1:400 dilution). NPM was rarely expressed in benign prostate and PIN but was expressed in the majority of PC (Table 1). The staining difference between benign prostate and PC was statistically significant ($P<0.001$), as was that between PIN and PC ($P<0.001$). Its expression was more frequent in high grade PC (Gleason 4 and 5) that in low grade PC (Gleason 2 and 3) ($P<0.001$).

Conclusions: NPM is a nucleolar phosphoprotein whose expression rapidly increases after mitogenic stimuli. Increased NPM level is detected in highly proliferating and malignant cells. NPM locus is involved in chromosomal translocations or deleted in various hematological and solid tumors. NPM is also mutated and aberrantly localized

in the cytoplasm of leukemic blasts in about 35% of AML cases. Thus, it may play an important role in the regulation of cell growth, proliferation and transformation. Our proteomic and immunohistochemical study suggests that over-expression of NPM may be involved in the carcinogenesis of PC.

Expression of nucleophosmin in benign and malignant prostate tissue

	Positive	Negative
Benign Prostate	10%(11/106)	90% (95/106)
PIN	4% (1/26)	96% (25/26)
Low Grade PC	68% (38/56)	32% (18/56)
High Grade PC	100% (36/36)	0% (0/36)
All PC	80% (74/92)	20% (18/92)

757 Prepubertal Biopsies Predict Significance of Cryptorchidism-Associated Mixed Testicular Atrophy, Allowing Fertility Assessment

M Nistal, MM Cajaiba, ML Riestra, M Reyes-Mugica, R Paniagua. Hospital La Paz/ Universidad Autonoma de Madrid, Madrid, Spain; Yale University, New Haven, CT; University of Alcala, Alcala de Henares, Spain.

Background: Mixed atrophy of testis (MAT), a frequent finding in formerly cryptorchidic and/or infertile patients, is defined as the synchronous occurrence, in variable proportions, of seminiferous tubules containing germ cells (TCGC) and Sertoli cell-only tubules (SCOT). In TCGC, different types of spermatogenesis anomalies may occur and can help to predict fertility prospects in these patients. Identifying even small numbers of adult spermatids (AS) in testicular biopsies correlates with successful spermatozoa retrieval for in vitro fertilization (IVF). Currently, it is unknown if precursor lesions of MAT can be identified in cryptorchidic testes during childhood. We compared prepubertal and postpubertal biopsies from the same patient group establishing a correlation between childhood findings and occurrence of MAT, as well as the development of spermatogenic foci and their extension in adulthood.

Design: 18 formerly cryptorchidic adults underwent testicular biopsies during orchidopexy in childhood and a repeat testicular biopsy in adulthood to evaluate infertility. All biopsies were bilateral, allowing analysis of cryptorchidic and scrotal testes. Slides were assessed for diagnosis and morphometric studies. In prepubertal biopsies, lesions were classified into types I (slight alterations), II (marked germinal hypoplasia) and III (severe germinal hypoplasia). In postpubertal biopsies, TCGC and SCOT percentages were estimated. Anomalies in spermatogenesis were classified into lesions of adluminal or basal compartments of tubules, and the proportion of tubules displaying AS as more or less than 50% of tubules with complete spermatogenesis (TCS).

Results: Comparison between pre and postpubertal biopsies revealed that most specimens developing from type III lesions presented with basal compartment injury (88%, p = 0.049), and most MAT specimens related to type III lesions had less than 50% of TCS (94%, p = 0.015), including all cases lacking AS.

Conclusions: Severe prepubertal germinal hypoplasia (type III lesions) correlated with MAT features that confer a worse prognosis for IVF (less than 50% of TCS and basal compartmen lesions). MAT characteristics may be predicted in cryptorchidic children, allowing prognosis concerning fertility in adulthood.

758 Utility of Prostate Saturation Needle Biopsy in Prediction of Tumor Volume in Whole Prostates

A Nowrouzi, F Gonzalez, GL Andriole, Y Yan, G Ferguson, K Maxwell, V Fernandez-Salvador, PA Humphrey. Washington University Medical Center, St. Louis, MO.

Background: Cancer size (volume) in the whole prostate gland has been linked to patient outcome and is a component of the definition of pathologically insignificant vs. significant prostate cancer. Previous attempts to predict prostate tumor volume (TV) using tumor extent in 6 to 12 needle biopsy (NB) cores have shown a modest correlation. It is not known if increasing the degree of prostate gland sampling by obtaining more cores would result in a stronger correlation. In this study, we assessed, using a mean of 31 cores procured by a saturation NB technique, the strength of association of multiple measures of tumor extent in NB core tissue with TV in the whole gland.

Design: Saturation needle biopsy sampling of 100 excised prostate glands from radical prostatectomy (RP) specimens was performed, with procurement of a mean of 31 cores per case. Tumor extent in saturation NB core tissue was quantitated as total number of positive cores, % of positive cores, linear extent of tumor in millimeters (mm), length % of tumor (linear mm of tumor/linear mm of all needle core tissue), total % of carcinoma (TPC) in all cores by visual inspection, and greatest % of carcinoma (GPC) in a single core. TV in RP was determined by image analysis. Statistical analyses included Spearman correlation coefficient determinations for correlation analysis, and least square regression modeling.

Results: Multiple measures of tumor extent in saturation NB core tissue were strongly correlated with TV : % of core biopsies involved by tumor (r = 0.81), linear extent of tumor in mm in all positive cores (r= 0.80), length % of tumor (r = 0.77), TPC (r=0.76), and GPC (r=0.44) (all p<0.0001). Regression modeling demonstrated that linear extent of tumor in mm, TPC, and GPC together were all significant in association with TV. Gleason grade in saturation NB tissue and pre-operative PSA values were not significant in the final model.

Conclusions: Carcinoma extent in saturation NB tissue is strongly correlated with TV in the whole prostate gland and use of multiple measures of tumor extent provides significant information on TV in the prostate. Increasing number of NB cores to sample the prostate gland and reporting of multiple measures of carcinoma extent in NB core tissue may improve the ability to predict prostate cancer size, and potentially, insignificant vs. significant prostate cancer.

759 The Impact of Lymphovascular Space Invasion in Pure pT1 Tumors of the Bladder: A Clinical Pathologic Study of 73 Cases

S Olgac, T Koppie, SK Tickoo, H Al-Ahmadie, S Fine, A Gopalan, G Dalbagni, VE Reuter. Memorial Sloan Kettering Cancer Center, New York, NY.

Background: While urothelial carcinoma(UC) with lamina propria invasion(pT1) is considered “superficial disease” , up to 30% of them progress to become muscle invasive disease and approximately 10%metastasize.Depth and pattern of invasion of the lamina propria(LP) and lymphovascular space involvement(LVI) are thought to be important morphologic features that may have prognostic significance.Large studies that correlate these parameters with outcome are few,particularly in patients that have undergone cystectomy.

Design: 73 cases of pT1UC,that never had muscularis propria invasion,on TURBT and cystectomy were identified and reviewed.Depth of invasion (taking the muscularis mucosae as a landmark whenever possible),pattern of invasion, LVI on H&E stained sections were evaluated.CD31 stain is performed on a selected slide for each case. Clinical information including regional and distant metastasis and outcome were obtained.

Results: At cystecomy, all cases showed high grade UC; 40 papillary UC only, 14 CIS only and 19 showing both CIS and papillary disease.70 cases showed focal,superficial(FS) invasion above muscularis mucosae(MM).71cases had lymph node(LN) dissection at the time of cystectomy.3 patients had regional LN metastasis, 2 of which were suspicious for LVI on H&E but were negative for CD31. 9 patients developed distant metastasis(DM) following cystectomy. On H&E stained sections only 2 cases with LVI were identified and one of them developed metastasis. Follow-up was available for 72 patients(range 9-352 mo, mean 75mo). At last follow up 58 patients had no evidence of disease(NED),12 patients died of other causes(DOC),3 patients were dead of disease(DOD).None of the patients who were DOD had LN metastasis or LVI on H&E and CD31 stained sections.All 3 patients with regional LN metastasis had NED at 38, 66 and 89 months.Of the 10 patients who had DM, 3 were DOD, 3 were DOC and 4 had NED. The 2 patients that showed LVI by CD31had NED at 44 and 93 months respectively.

Conclusions: Despite early cystectomy, patients with pure pT1 may develop systemic disease(12.5%) and die(4%).Depth of LP invasion did not have a significant adverse effect on prognosis in our series but a larger cohort with more cases with deep LP invasion is needed to evaluate this issue appropriately.LVI is rare and hard to detect on H&E and CD31 stained sections in this setting.Presence of LVI did not correlate with regional and distant metastasis and death in this subset of patients.

760 Immunohistochemistry as an Adjunct in the Differential Diagnosis of Radiation-Induced Atypia vs Carcinoma In Situ (CIS) of the Bladder. A Study of 48 Cases

E Oliva, DS Kaufman, WU Shipley, B Spicer, GP Paner, AM Gown, MB Amin. Massachusetts General Hospital, Boston, MA; Cedars Sinai Medical Center, Los Angeles, CA; PhenoPath Laboratories, Seattle, WA.

Background: Muscle invasive urothelial carcinoma (Inv-UCa) has been treated traditionally with cystectomy with or without adjuvant therapy. In recent years, bladder sparing protocols consisting of local tumor resection, radiation and chemotherapy have been offered to selected patients who are closely followed with surveillance biopsies to exclude recurrence or frequently associated CIS. In this setting radiation-induced changes (RAD-Ch) may be very difficult to distinguish from CIS, and failing to recognize its reactive nature may lead to overtreatment. The goal of our study was to ascertain the role of immunohistochemistry in differentiating CIS and RAD-Ch.

Design: 29 patients with a history of bladder radiation (RT) [RT treated Inv-UCa (22), other sources (7)] and 19 with CIS were identified. p53 and CK20 immunostains were performed in selected blocks after confirmation of the diagnosis evaluating nuclear p53 and cytoplasmic/membranous CK20 intensity (weak, moderate, strong) immunoreactivity by percentage of positive cells (focal = <10%, multifocal = 10-50%, diffuse = >50%).

Results: Weak focal to multifocal p53 staining was seen in 23/29 RT cases, 4 showed moderate staining (2 focal; 2 multifocal) and 2 were negative. Strong and diffuse p53 staining was found in 8/19 CIS, moderate and multifocal in 1, weak in 8 and 2 were negative. CK20 showed strong cytoplasmic staining of umbrella cells in all RT cases when present (22/29). Additionally, 6/29 showed CK20 focal membranous staining in transitional cells. In contrast, 11/19 CIS showed diffuse and strong CK 20 membranous staining, 5 moderate and multifocal-diffuse, 1 moderate and focal and 2 were negative. 7 CIS with weak or negative p53 showed significant CK 20 staining.

Conclusions: Significant CK20 expression (>90%) was only seen in CIS. Even though strong and diffuse nuclear p53 expression was only seen in about 50% of CIS, strong p53 expresssion was absent in RT cases. No p53 positive CIS case was CK20 negative. Thus, a combination of CK20/p53 proves to be very helpful, with CK20 being more reliable than p53 in assisting in the differential diagnosis between CIS and RT atypia.

761 The “Symphony” Protocol for H&E Staining of Prostatic Adenocarcinoma on Needle Biopsy: A Critical Multicenter Analysis of 120 Cases

AO Osunkoya, C Magi-Galluzzi, AV Parwani, TZ Ali, EF Tamas, VG Untawale, H Kahane, JI Epstein. The Johns Hopkins Hospital, Baltimore, MD; The Cleveland Clinic Foundation, OH; University of Pittsburgh Medical Center, PA; University of Maryland Medical Center, MD; Quest Diagnostics, NJ; Dianon Systems, CT.

Background: The diagnosis of prostate carcinoma on biopsy is based on a constellation of architectural, nuclear, cytoplasmic, and other features. One of the most important is the presence of prominent nucleoli in the nuclei of suspect glands. Most specimens are processed by routine Hematoxylin and Eosin (H&E) stains. The absence of prominent nucleoli often precludes the diagnosis of cancer especially in limited foci.

Design: 120 cases of Gleason grade 3+3 =6 cancers involving 10%-30% of one core were retrieved from 4 academic institutions and 2 large laboratories in the United States (20 cases per institution). In all cases, tissue was formalin fixed, sectioned (2 levels) at each institution, with 1 routine H&E done at each institution and the other unstained slide sent to Ventana for their "Symphony" H&E protocol. The routine H&E and Ventana "Symphony" H&E protocol stained slides from the same case were reviewed centrally in a blinded fashion at one of the institutions. The mean percentage of prominent nucleoli per cancer was assigned to each case. After unblinding, the routine H&E from each institution was compared in a pair-wise T-Test with the corresponding "Symphony" slide.

Results: The mean number of nucleoli per case on all 120 cases on routine H&E was 19.3% (range 5%-50%) and with the "Symphony" stain was 37.2 % (range 5%-80%). The results of the pair-wise T-Test for the 6 institutions were as follows: Site A: p=0.0003; Site B: p=0.0005; Site C: p=0.0001; Site D: p=0.0005; Site E: p=0.0002; and site F: p=0.003, with in all sites, the "Symphony" slides showing more prominent nucleoli than the routine slides.

Conclusions: The underdiagnosis of limited adenocarcinoma of the prostate on needle biopsy is one of the most frequent problems in urologic pathology. Although various immunohistochemical studies can aid in the diagnosis of prostate cancer, each has its false positives and negatives, and the cornerstone of establishing a diagnosis of prostate cancer rests on its H&E appearance. The Ventana "Symphony" H&E staining protocol consistently highlights nucleoli in cancer to a greater extent than routine H&E stains and may increase the likelihood of making a diagnosis of limited adenocarcinoma of the prostate in challenging cases.

762 Colorectal Adenocarcinoma with Involvement of the Prostate: Report of 9 Cases with Immunohistochemical Analysis and Long Term Follow Up

AO Osunkoya, GJ Netto, JI Epstein. The Johns Hopkins Hospital, Baltimore, MD.

Background: Spread of colorectal carcinoma to the prostate is rare with few case reports in the medical literature. The distinction between prostatic duct adenocarcinoma and spread of colonic adenocarcinoma to the prostate is critical but challenging, especially if the possibility of the latter is not considered on needle biopsy. We present the largest series to date on this phenomenon.

Design: 9 cases of colorectal adenocarcinoma with metastasis or direct extension to the prostate were retrieved from the consult files of one of the authors.

Results: Clinical: Mean age of patients at diagnosis was 61 years (range 42 to78 years). 6 cases (66.7%) were initially diagnosed on needle biopsy and the others by TURP. 3 cases (33.3%) were diagnosed prior to biopsy of the colon and lead to the discovery of the colonic primary. The mean interval between the detection of the primary tumor and prostatic involvement in the other 6 cases was 30 months (range 1 to 52 months). Stage of colorectal carcinomas ranged from T1-T4 (T1=2, T2=2, T3=2 and T4=3) at primary diagnosis. 2 cases (22.2%) were associated with prostatic spread of rectal adenocarcinoma following recurrence at the anastomotic site of previous colonic cancer. 3 patients (33.3%) had simultaneous microscopic foci of usual type prostatic adenocarcinoma. Follow up was available on all patients with a mean of 29.2 months (range 3 to 88 months). 5 patients (55.5%) died of disease. Histology: Variable features were present including, necrosis n=7 (77.8%), chronic inflammatory response n=7 (77.8%), cribriform pattern n=6 (66.7%), villous architecture n=2 (22.2%), mucin production n=2 (22.2%), signet ring cells n=1 (11.1%) and perineural invasion n=1 (11.1%). Immunohistochemistry: Stains were positive for Beta-catenin in 6/6 cases (100%), CDX2 6/6 cases (100%), CEA 7/7 cases (100%), CK20 5/6 cases (83.3%), HMWCK 5/6 cases (83.3%), and Racemase 3/6 cases (50%). Stains were negative for PSA in 9/9 cases (100%), P501S (prostein) 6/6 cases (100%), and CK7 6/6 cases (100%).

Conclusions: The distinction between prostatic adenocarcinoma and spread of colorectal carcinoma to the prostate is critical in view of both therapeutic and prognostic implications. It should be considered in the differential diagnosis when there is a prostatic carcinoma with necrosis, mucin production, mucin-positive signet ring cells, villous architecture, or associated inflammation. IHC for Beta-catenin, CDX2, CEA, HMWCK, PSA, P501S, CK20 and CK7 can be helpful in making the distinction.

763 Mucin Producing Urothelial-Type Adenocarcinoma of Prostate: Report of 15 Cases with Immunohistochemical Analysis and Long Term Follow Up

AO Osunkoya, JI Epstein. The Johns Hopkins Hospital, Baltimore, MD.

Background: Prostatic urothelial-type adenocarcinoma is a very rare tumor arising from intestinal metaplasia of the prostatic urethra and, although arising in the prostate, is identical to primary adenocarcinoma of the bladder. Only 4 cases have been reported in the medical literature, 2 of which are included in this series. The distinction between secondary adenocarcinoma involving the prostate, conventional adenocarcinoma of the prostate, and prostatic urothelial-type adenocarcinoma can present a significant diagnostic challenge and has significant therapeutic implications.

Design: 15 cases of prostatic urothelial-type adenocarcinoma were retrieved from the consult files of one of the authors.

Results: Clinical: Mean patient age at diagnosis was 72 years (range 58-93 years). All men had negative colonoscopies, clinically excluding a colonic primary. Bladder primaries were ruled out clinically or pathologically in radical resection specimens. Follow up was available on all men with a mean of 50.3 months (range 2 to 161 months). All men presented with urinary obstruction symptoms with 3 (20%) also having mucusuria and 2 (13.3%) also having hematuria. 4 men (26.7%) developed metastatic disease and 8 (53.3%) died of disease. Histology: In 8/15 (53%) cases, glandular metaplasia of the prostatic urethra and contiguous transition to adenocarcinoma were identified. Multiple histologic patterns were observed including dissection of the stroma by mucin pools 15/15 (100%), villous features 7/15 (47%), necrosis 2/15 (13.3%), signet ring cells 3/15 (20%), perineural invasion 1/15 (6.7%), focal squamous differentiation 1/15 (6.7%), and a granulomatous inflammatory response 1/15(6.7%). Immunohistochemistry: Stains were negative for PSA in 15/15 cases (100%), PSAP 13/13 cases (100%), CDX2 10/10 cases (100%), and Beta-catenin 10/10 cases (100%). Stains were positive for HMWCK in 12/12 cases (100%), CK7 10/12 cases (83.3%) and CK20 10/12 cases (83.3%).

Conclusions: Prostatic urothelial-type adenocarcinoma is a rare aggressive cancer. The differential diagnosis includes conventional prostatic mucinous adenocarcinoma and secondary infiltration from a colonic or bladder adenocarcinoma. IHC for PSA, PSAP, and HMWCK along with morphology can help rule out conventional prostate carcinoma. Beta-catenin, CDX2, and clinical studies are needed to rule out colonic adenocarcinoma. Only clinical studies can exclude infiltration from a primary bladder adenocarcinoma.

764 PAX-2 in the Diagnosis of Primary Renal Tumors: Immunohistochemical Comparision with the Renal Cell Carcinoma Marker Antigen (RCCM) and Kidney-Specific Cadherin (KSC)

A Ozcan, J Zhai, A Kunda, C Hamilton, SS Shen, LD Truong. The Methodist Hospital, Houston, TX; Baylor College of Medicine, Houston, TX; Weill Medical of College of Cornell University, New York, NY; Gülhane Military Medical Academy & School of Medicine, Etlik, Ankara, Turkey.

Background: The diagnosis of renal cell carcinoma (RCC) remains problematic, especially in the context of metastasis or fine needle aspiration biopsy. RCCM and KSC are considered specific markers for RCC, but are expressed preferentially in specific subtypes of RCC of lower grades. PAX-2 is a transcription factor that promotes renal tubular differentiation during embryogenesis. This study aims at evaluating the utility of PAX-2 in the diagnosis of renal tumors and comparing it with those of RCCM and KSC.

Design: Immunostain was performed on 137, 111, and 94 renal tumors for PAX-2, RCCM, and KSP, respectively. Among them, staining of consecutive tissue sections for all three markers was done in 94 cases. Features selected for evaluation included the percentage of tumor positive for individual or combined markers stratified against histologic subtypes.

Results: The staining was nuclear for PAX-2; but limited to cell membrane and cytoplasm for RCCM and KSC. The percentages of positive cases were shown in Table-1. The results of the 94 cases with staining for all three markers on consecutive tissue sections were: All markers positive: 12 cases, all markers negative: 5, at least one marker positive: 89, only PAX-2 positive: 11, only RCCM positive: 4, only KSC positive: 2.

Conclusions: 1) PAX-2 is successfully detected in routine tissue specimens, with a distinctive nuclear staining pattern; 2) It is expressed in a majority of RCCs, regardless of histologic subtypes, and thus represents a novel and sensitive marker for RCC. 3) Although PAX-2 seems to be more sensitive than both RCCM and KSC, there are significant exceptions in relation to histologic subtypes, justifying a selective use of all three markers as panel.

Table 1: Renal Tumors Stained for PAX-2, RCCM and KSC

Markers	All Cases	Clear Cell	Papillary	Chromophobe	Collecting Duct	Oncocytoma
PAX-2	85 % (116/137)	85 % (77/91)	88 % (28/32)	86 % (6/7)	100 % (2/2)	75 % (3/4)
RCCM	74 % (82/111)	77 % (65/84)	89 % (16/18)	20 % (1/5)	0 % (0/1)	0 % (0/3)
KSC	21 % (20/94)	21 % (15/70)	6 % (1/17)	75 % (3/4)	0 % (0/1)	50 % (1/2)

765 Analysis of Observed Survival Outcomes in Histologically-Specified Renal Cell Carcinoma (RCC); 1993-1998 Cases from the National Cancer Data Base (NCDB)

GP Paner, J Ritchey, A Stewart, MB Amin. Cedars-Sinai Medical Center, Los Angeles, CA; Chicago, IL.

Background: Cancers of the kidney and renal pelvis are the 7th leading cancer type and the 10th most common cause of cancer death in males in the US (ACS, 2006). The NCDB, a joint project of the Commission on Cancer (COC) of the American College of Surgeons and the American Cancer Society (ACS), is used to assess health care delivered to cancer patients. The surveillance information from NCDB can assist in setting guidelines for management of cancer care in the US.

Design: From 1993-1998, the NCDB collected 149,424 cases of kidney tumors reported based on the ICD-O-2/3 disease topography code C64.9 (WHO, 2000). To restrict the study to the histologically-specified RCC cases only, we excluded the following: those with no documented surgical resection, undetermined pathological staging, unknown or unspecified histology, nephroblastomas and urothelial carcinomas. All cases have a minimum follow-up of five years (up to 2003).

Results: A total of 47,686 histologically-defined RCC fit our case criteria, including 5,674 further specified as clear cell RCC subtype. The patient age ranged from 1 to 103 years old (62.1 mean years old), the majority occurred in patients more than 40 years old (93.2%) with higher male incidence (M:F=1.6:1). The tumor size ranged from 1 to 25 cm (mean, 5.53 cm).

Observed survival		1 year	3 years	5 years
Sex	**M**	88.0	73.6	62.9
	F	89.3	76.9	68.1
Age, years	**≤ 40**	93.2	84.7	80.0
	> 40	88.3	74.4	64.2
Grade*	**1**	94.7	86.3	77.7
	2	92.1	79.5	69.6
	3	79.3	60.3	48.8
	4	51.4	44.7	35.3
TNM stage**	**I**	95.1	86.7	77.9
	II	94.6	83.2	72.7
	III	86.5	67.5	55.2
	IV	54.6	26.2	16.8
Tumor size, cm***	**≤ 4**	95.4	87.4	78.9
	4.1-7	94.8	85.5	76.4
	7.1-10	95.0	84.5	74.6
	> 10	93.9	81.1	69.3

* Cases with diagnosis of clear cell carcinoma; **AJCC 5th edition; *** organ confined tumors

Conclusions: This large NCDB experience in renal cancer confirms the importance of pathologic evaluation of traditional parameters of grade and stage in renal cancer. Data on histologic subtype of RCC is inconsistently reported or not easily accesible to the registry during the study period; standardized reporting of pathology elements as mandated by the ACS, COC in 2004 may help data acquisition to confirm the clinical utility of histologic subtyping. This NCDB data has important implications in setting stage definitions to increase the prognostic accuracy of the future editions of the TNM staging.

766 Trends in Gleason Grading of Prostate Cancer (PCa): Analysis of Reporting by Institutional and Central Review Pathologists in Four Radiation Therapy Oncology Group (RTOG) Protocols Spanning 17 Years and 2094 Needle Biopsies (bxs)

GP Paner, K Bae, DJ Grignon, M Pilepich, G Hanks, W Shipley, M Roach, D McGowan, TM Pisansky, H Sandler, E Hammond, MB Amin. Cedars-Sinai Medical Center, Los Angeles, CA; Radiation Therapy Oncology Group, Philadelphia, PA; Wayne State University, Detroit, MI.

Background: The Gleason grade is a seminal clinico-pathologic parameter used contemporarily in clinical decision making in patients with PCa. Interobserver reproducibility is an important limiting factor such that all RTOG PCa protocols presently undergo central pathology review.

Design: The aim of this study was to detect trends in reporting of Gleason grading in institutional and central review pathologists in 4 studies [RTOG protocols 8610 (1987-1991; 334 bxs); 9202 (1992-1995; 972 bxs); 9413 (1995-1999; 589 bxs); 9910 (2000-2004; 199 bxs). Protocols 8610 and 9202 enrolled patients with locally advanced PCa and 9413 and 9910 enrolled intermediate-risk patients.

Results: Concordance data between institutional and central review are as follows:

	Complete agreement			Agreement within +/- 1 Gleason pattern/score		
Time Period	Primary Gleason	Secondary Gleason	Gleason Score	Primary Gleason	Secondary Gleason	Gleason Score
1987-1991	51%	42%	43%	93%	84%	81%
1992-1995	54%	42%	48%	91%	84%	82%
1995-1999	67%	47%	57%	97%	92%	90%
2000-2004	80%	53%	56%	98%	91%	90%
Overall	60%	44%	50%	94%	87%	85%

Gleason pattern 1 was reported in institutional Gleason scores in 7.2%, 2.1%, 0%, 0% bxs compared 0.9%, 0%, 0%, 0% bxs by central review in protocols 8610, 9202, 9413 and 9910 studies. Gleason pattern 2 was reported in 28.7%, 22.9%, 7.3%, 6.5% institutional Gleason scores versus 19.8%, 4.4%, 1.2% and 0% in central review scores, respectively in the 4 studies.

Conclusions: There is a trend for greater concordance between the Gleason score of institutional pathologists and central review over 17 years of reporting Gleason grade in PCa. Endorsement of the Gleason system by all major medical organizations worldwide, and increased education efforts have potentially contributed to widespread acceptance and decreased interobserver variability. Further attempts to refine morphologic criteria for Gleason pattern 3 vs. 4 vs. 5 are required as the prognostic significance of primary and secondary Gleason patterns influence clinical decision making.

767 Prospective Peer Review of Diagnostic Prostate Biopsies as a Tool for Error Reduction in a Sub-Specialty Based Practice

AV Parwani, C Vrbin, S Raab, R Dhir. University of Pittsburgh Medical Center, Pittsburgh, PA.

Background: Studies have shown the value of review of pathology cases by a second pathologist. While there is agreement that a prospective review of cases by a second pathologist may reduce error rates (2.1% in one study), the types of cases to be reviewed is not clear.Studies have indicated that in a second review of prostate carcinomas, most commonly results in an upgrade of Gleason grade. Our goals in the current study were to perform a prospective blinded review of diagnostic prostate biopsies by a second sub-specialty trained pathologist in our clinical practice, which is primarily a subspecialty-based academic setting.

Design: During a two-month period, a total of 86 consecutive cases of diagnostic biopsies (total number of parts = 258) were prospectively reviewed by a second pathologist before release of the final diagnosis. As a control, data from the 100 retrospective patients (total number of parts = 355) was also reviewed. Blinded slides with no attached diagnosis and review sheets were distributed to a second pathologist for review. In cases, when there was a discreopancy between the initial review and the second prospective review, a consensus was reached between the two pathologists.

Results: A total of 258 diagnosis by part were reviewed and consisted of a final diagnosis of benign (n=168, 65.1%), high grade PIN (n=23, 8.9%), atypical/suspicious (n=8, 3.1%) and malignant (n=58, 22.4%). In the current study, 13 of the 182 diagnosis (7.1%) initially classified as benign by the initial reviewer, were upgraded to either high grade PIN (n=11) or atypical (n=2). Similarly, 2 of the 8 (25%) cases initially, classified as either suspicious or atypical were downgraded to high grade PIN in the final diagnosis. Interestingly, amongst the categories of high grade PIN (n=10) and malignant (n= 58), there were no changes between the initial review and the final diagnosis.

Conclusions: Traditionally, quality assurance in anatomical pathology has primarily focused on retrospective review of randomly selected cases. The utility of a prospective audit of diagnostic biopsies has not been previously conducted in our clinical practice. Our data indicates that disagreements, both undercalls and overcalls, do occur and it may be beneficial to have focused prospective audit of diagnostic biopsies. Such a review may increase pathologist time and increase turn around time, but may provide sufficient additional benefits such as error reduction in the final diagnosis even within a sub-speciality based practice.

768 Overexpression of MicroRNA let-7c in Prostate Cancer

L Peng, J Melamed, XT Kong, Y Zhao, M Ksionsk, Y Peng, P Lee, JJ Wei. New York University, New York, NY.

Background: MicroRNAs (miRNAs) are a newly discovered group of small noncoding RNAs. They are dysregulated in solid malignant tumors. The function has not been fully understood, but is likely through regulation of target gene activity in cell proliferation and apoptosis.Let-7c is highly overexpressed in prostate cancer cell line LNCaP. In this study, we examined the expression of miRNA let-7c in benign prostate and in low and high-grade prostate cancer.

Design: 1) Locked nucleic acid (LNA)-modified miRCURY let-7c probe was used for tissue microassay based in situ hybridization.The hybridization and detection conditions for paraffin embedded tissue were followed the instruction provided by Exiqon, Inc. Several high-density tissue microarray (TMA) populations were used, including benign prostate tissue (BP) (37 cases), benign prostate hyperplasia (BPH) (41 cases), low and high grade prostate cancer (PCa) (82 cases). 3) Expression level was scored based on the intensity of color detection. 4) The expression of let-7c between benign prostate and prostate cancer was analyzed and assessed for any association with pathological, demographic and clinic annotation.

Results: While let-7c expression is observed in normal prostate tissue, BPH and PCa, its level is highest in PCa (see table). The level of let-7c also positively correlates with the Gleason score (from G6 of 1.78 to G9 of 2.19). High let-7c level is found in high grade PCa (pT2a of 1.76 to pT3b of 2.24) and is associated with shorter survival. The mean net gain values of let-7c in patients who died was higher (mean = 2.19) than that who still alive (mean =1.86).

Conclusions: Overexpression of let-7c is a frequent finding in PCa. The level of let-7c seems to be linearly correlated with the grade of tumor. Let-7 have many target genes, some of which are dysregulated in PCa. The strong association with cancer and increase let-7c level with grade suggest that let-7c may be one of miRNAs involved in the pathogenesis and progression of PCa.

Table Differential expression of miRNA let-7c in benign and malignant prostate

	Benign	BPH	PCa
case number	37	41	82
let-7c expression level < +	15/37 (41%)	29/41(70%)	1/82 (1.2%)
let-7c expression level +	22/37 (59%)	11/41(27%)	3/82 (3.6%)
let-7c expression level ++	0/37	1/41(2%)	30/82 (37%)
let-7c expression level +++	0/37	0/41	33/82 (40%)
let-7c expression level ++++	0/37	0/41	15/82 (18%)
Overall mean	0.82+/-0.08	0.71+/-0.09	1.94 +/-0.09 (T-N)

T-N: tumor-normal

769 *TMPRSS2-ERG* Fusion Prostate Cancer: An Early Molecular Event Associated with Invasion

S Perner, J-M Mosquera, F Demichelis, MD Hofer, PL Paris, J Simko, C Collins, TA Bismar, AM Chinnaiyan, AM De Marzo, MA Rubin. Brigham & Women's Hospital, Harvard Medical School, Boston, MA; University of Ulm, Ulm, Germany; Dana Farber Cancer Institute, Boston, MA; University of California, San Francisco, CA; McGill University Faculty of Medicine, Montreal, QC, Canada; Johns Hopkins University School of Medicine & Bloomberg School of Public Health, Baltimore, MD; ITC-Irst, Povo (Trento), Italy; University of Michigan Medical School, Ann Arbor, MI.

Background: Prostate cancer (PCA) is one of the most prevalent cancers and a major leading cause of morbidity and mortality. *TMPRSS2-ERG* fusion was recently identified as a common chromosomal aberration in PCA.

Design: We interrogated a broad spectrum of benign, precursor and malignant prostatic lesions to assess indireclty the *TMPRSS2-ERG* fusion status by using a dual-color FISH break-apart assay. Samples from autopsies and surgical specimens from hospital based cohorts contained 237 localized PCA, 34 hormone naive metastases, 9 hormone refractory metastases, 26 high grade PIN , 15 BPH, 38 proliferative inflammatory atrophy (PIA), and 47 normal prostatic tissue.

Results: The *TMPRSS2-ERG* fusion was seen in 48.5% of localized PCA (Fig.1C,D), 30% of hormone naive metastases, 33% of hormone refractory metastases, and in 19% of high grade PIN lesions, whereas the majority of PIN lesions were fusion negative (Fig.1A,B). Almost all fusion positive cases showed homogenous distribution of the fusion pattern. None of the 100 samples from normal prostatic tissue, BPH, atrophy, and PIA demonstrated the *TMPRSS2-ERG* fusion.

Conclusions: Considering the high incidence of PCA and the high frequency of this fusion, *TMPRSS2-ERG* is the most common genetic aberration ever described in any malignancy. The detection of *TMPRSS2-ERG* by FISH is a very specific and sensitive assay for fusion positive PCA and thus, its clinical application as a biomarker and ancillary diagnostic test is promising.

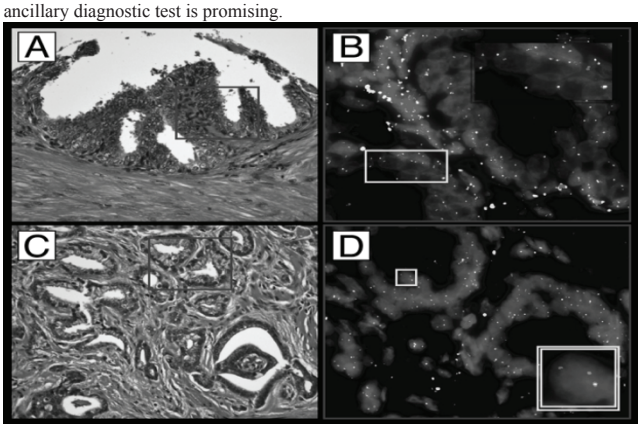

770 Expression of Phospho-mTOR in Different Renal Cell Carcinoma (RCC) Subtypes Using Tissue Microarrays (TMA)

A Petit, A Gaspa, X Garcia-Albéniz, B Mellado, I Nayach, L Gelabert, L Pla, C Mallofré. Hospital Clínic, Barcelona, Spain.

Background: The PI3K/Akt/mTOR pathway is considered to be a central regulator of cell proliferation, differentiation and survival. For its role in oncogenesis the proteins of this pathway have been proposed as interesting targets for therapeutic intervention in various malignancies including RCC. In this respect, trials using CCI-779 (inhibitor of mTOR) in patients with metastatic RCC are under evaluation. The active status of this pathway has been documented in RCC human cell lines. However there are few studies assessing the expression of the proteins of this pathway in RCC tissue samples. So that, the aim of this study is to characterize the expression of the activated form of mTOR in different RCC subtypes using TMA to evaluate its role in pathogenesis and as a therapeutic target.

Design: Eight Tissue microarrays (TMA) composed of triplicate 1.0 mm cores from 96 Clear Cell RCC (CRCC), 31 Chromophobe RCC (ChRCC), 14 Papillary RCC (PRCC) and 4 Mucinous tubular and spindle cell carcinoma (MTSCC) were constructed. In those arrays 122 cores of non-tumoral renal parenchyma were also included corresponding to the non-tumoral part of 61 RCC contained in the TMA. Immunohistochemical study was performed using polyclonal antibody phopho-mTOR (Cell Signaling). The percentage of positive stained cells was categorized as focal (1-25%), moderate (25-50%) and diffuse (>50%).

Results: Phospho-mTOR was expressed in most PRCC (93%) and all MTSCC (100%) being the diffuse extent of expression the most commonly found in these cases. Conversely, phospho-mTOR was detected mostly focally in 32% ChRCC and with an heterogeneous extent of expression in 65% CRCC (48% of CRCC positive cases were categorized as focal, 15% as moderate and 37% as diffuse). The pattern of expression was cytoplasmic with membranous reinforcement in all positive cases. In non-tumoral renal tissue phospho-mTOR immunostaining was only found in some tubules.

Conclusions: Our study highlights the activation of mTOR in the majority of PRCC and MTSCC and in some cases of CRCC in contrast to ChRCC. Further studies are needed to evaluate the meaning of these differences and the pathogenetic role of PI3K/Akt/mTOR pathway in RCC subtypes. Whether the extent of phospho-mTOR expression could be related to clinical or pathological parameters and whether it could be used as a marker to select patients to receive mTOR inhibitors demands more accurate investigation.

771 Association of Increased Levels of *TMPRSS2-ERG* Fusion Transcripts in pT2 and Well Differentiated Prostate Cancer

G Petrovics, S Shaheduzzaman, B Furusato, A Dobi, L Ravindranath, C Cook, Y Chen, V Srikantan, J Cullen, I Sesterhenn, DG McLeod, S Srivastava. CPDR, Rockville, MD; AFIP, Washington, DC; WRAMC, Washington, DC.

Background: Recent studies have highlighted genomic and expression alterations of the ETS related gene (*ERG*) as a common feature of the early stage prostate cancer (CaP). CaP patients with higher tumor vs normal indices of *ERG* expression exhibit better outcome after surgical treatment, in contrast to the low *ERG*-expressers. This study defines quantitative expression features of the *TMPRSS2-ERG* fusion transcripts in relation to clinic-pathologic characteristics in a cohort of 112 CaP patients.

Design: The expression of *TMPRSS2-ERG* fusions, and of *ERG*, was determined by QRT-PCR (normalized to *GAPDH*) in matched microdissected (LCM) tumor and benign epithelial cells from frozen prostatectomies (RP) of 112 CaP patients (224 specimens). Quantitative features of *TMPRSS2-ERG* fusion expression were analyzed for correlation with clinico-pathologic features of CaP patients (SAS version 9.1).

Results: Sixty nine (61.6%) out of 112 patients had detectable expression of *TMPRSS2-ERG* fusion transcripts in their CaP cells (fusion A:65 patients; both fusion A and B: 2 patients; fusion C: 1 patient). No expression of fusion transcripts was detected in benign prostate epithelium. A comparative sub-study of well differentiated (WD) and poorly differentiated (PD) CaP tumors revealed *TMPRSS2-ERG* fusion A transcripts in17 out of 20 (85%) WD tumors in contrast to the presence of the *TMPRSS2-ERG* fusion A transcripts in 8 of 20 (40%) PD tumors. Finally, patients with pT3-4 CaP had significantly lower expression of *TMPRSS2-ERG* fusion A transcript as compared to patients with pT2 stage disease.

Conclusions: This study establishes that most of the CaP associated *ERG* overexpression represent *TMPRSS2-ERG* fusion A transcripts (95%) and supports previous observations. Lack of detectable expression of the *TMPRSS2-ERG* fusion in benign cells of over 110 patients and its presence in only tumor cells supports diagnostic potential of the *TMPRSS2-ERG* fusion. Increased expression of *TMPRSS2-ERG* fusion transcript significantly associates with well differentiated tumors and with organ confined pT2 pathological stage of CaP. Taken together these data confirm our original observation suggesting for prognostic value of quantitative analyses of *TMPRSS2-ERG* fusion transcripts in CaP.

772 The Utility of PAX-2 in Distinguishing Metastatic Clear Cell Renal Cell Carcinoma from Its Morphologic Mimics

D Phan, JK McKenney, M Gokden, N Gokden. University of Arkansas for Medical Sciences, Little Rock, AR.

Background: PAX-2 is a homeogene strongly expressed during kidney development. Although immunohistochemical expression of PAX-2 has been described in a variety of primary renal cell carcinoma subtypes, its utility in a metastatic setting has not been previously evaluated. We studied PAX-2 expression in metastatic clear cell renal cell carcinoma (CC-RCC) and in a variety of neoplasms with clear cytoplasm that could potentially mimic CC- RCC.

Design: H&E stained slides and formalin-fixed paraffin embedded blocks representing 24 CC- RCCs metastatic to various organs were retrieved. The metastatic sites included brain (5 cases), paraspinal tissue (3 cases), bone (8 cases), lung (1 case), skin (1 case), soft tissue (2 cases), adrenal gland (2 cases), urinary bladder (1 case), and liver (1 case). Similarly, 28 neoplasms with clear cell change (CCC) mimicking CC-RCC were identified, including 5 hemangioblastomas, 6 chordomas, 1 extragonadal seminoma, 2 adrenal cortical carcinomas with CCC, 2 mucoepidermoid carcinomas with CCC, 2 hyalinizing clear cell carcinomas of salivary gland, 1 adenocarcinoma of parotid with CCC, 1 adenocarcinoma of lung with CCC, 1 huthle cell carcinoma of thyroid with CCC, 1 squamous cell carcinoma (SCC) of the vagina with CCC, 1 SCC of the skin with CCC, 2 hepatocellular carcinomas with CCC, 1 high grade prostatic adenocarcinomas with CCC, 1 SCC of tongue with CCC and 1 alveolar soft part sarcoma. All H&E stained sections were reviewed to confirm the diagnoses. Four micron sections were stained with anti-PAX-2 (Z-RX2; Zymed, San Francisco, CA) using a 1:100 dilution. Nuclear staining was scored semi quantitatively as follows: 1-25%:1+, 26-50%:2+, >50%:3+.

Results: 20 of 24 (83%) metastatic CC-RCCs showed nuclear immunoreactivity for PAX-2. Among these, the intensity of staining was 3+ in 12 (60%), 2+ in 2 (10%), and 1+ in 6 (30%) cases. The CC-RCCs without PAX-2 reactivity were from bone (2), brain (1) and skin (1). 6 of 8 (75%) CC-RCC in bone were reactive for PAX-2 despite prior decalcification. None of the 28 cases representing mimics of CC-RCC were reactive with PAX-2.

Conclusions: PAX-2 is a reliable marker of metastatic CC-RCC (sensitivity 83%) in various anatomic sites including bone following decalcification. In addition, none of the morphologic mimics of CC-RCC studied showed immunoreactivity for PAX-2 (specificity 100%). In this study, PAX-2 was a sensitive and specific marker for distinguishing metastatic CC-RCC from its potential mimics.

773 Hitherto-Unreported, Frequent Detection of the Same LOH on Chromosone 19q in Renal Oncocytoma and Chromophobe Renal Cell Carcinoma

MM Picken, B Chyna, RC Flanigan. Loyola University Medical Center, Maywood, IL.

Background: Benign Renal oncocytomas (RO) and Chromophobe renal cell carcinomas (ChRCC) are both derived from the distal nephron and, morphologically, show overlapping features. RO are cytogenetically heterogeneous with some tumors having a normal karyotype while others show loss of chromosome (chr) 1/1p. ChRCC show multiple chr losses: -1, -2, -6, -10, -17. The loss of chr 1/1p in both tumors has lead to the hypothesis that these two tumors may represent a spectrum of benign to malignant tumor progression. However, there is a paucity of data regarding any additional chromosomal/molecular abnormalities shared by both tumors.

Design: We sought to look for molecular abnormalities in RO and ChRCC in chr 19q which has been shown to be involved in oligodendroglioma and other tumors. LOH analysis was carried out using 2 microsatellite markers located on 19q (D19S412 and D19S112) and a PCR based assay. Paraffin sections from tumor and adjacent normal tissue were studied. DNA extraction, end-labelling and PCR amplification were performed as previously described *(BMC Clinical Pathology 2003;3:6).* DNA samples, heterozygous for any of the 3 loci, were considered informative, whereas homozygotes were deemed "non-informative" (NI). All tumors were defined morphologically using current diagnostic criteria *(J Urol. 2004; 2004;171:602).* Cytogenetic studies available for comparison in 16 RO, were performed as reported previously *(Arch Pathol Lab Med 2004; 128:1274).* Chromosomal data bases were searched for reports of abnormalities in chr 19 in ChRCC.

Results: Cytogenetic studies in 16 RO showed no detectable karyotypic abnormalities in chr 19. No abnormalities in chr 19 were previously reported in ChRCC. LOH studies were done in 22 RO and 12 ChRCC. LOH in one or both loci was seen in 13/22 RO (59%) and 8/12 ChRCC (67%); five RO and two ChRCC were negative for LOH in one locus, while the other locus was NI (x5) or could not be interpreted (x2). No LOH was detected in both loci in 4/22 (18%) of RO and 2/12 (17%) ChRCC.

Conclusions: In addition to the loss of chr 1/1p, RO and ChRCC share frequent LOH on chr 19. These results, which have not been previously reported, further support the presence of molecular similarities between the two tumors. Deletion of 1p and/or 19q in oligodendrogliomas predicts a survival advantage. Whether evaluation for LOH on 19q could be helpful in selecting prognostically favorable ChRCC/ other tumors derived from the distal nephron requires further studies.

774 Renal Oncocytoma and Chromophobe Renal Cell Carcinoma Share the Same LOH on the Short Arm of Chromosome 1; Comparison between FISH and LOH

MM Picken, B Chyna, RC Flanigan. Loyola University Medical Center, Maywood, IL.

Background: Renal oncocytomas (RO) and chromophobe renal cell carcinomas (ChRCC) share overlapping morphology. While some RO have a normal karyotype, others show loss of chromosome (chr) 1/1p. The latter is the most frequent karyotypic abnormality in RO, suggesting that genetic abnormalities related to the development of RO reside in this region. CHRCC is typically hypodiploid and also shows loss of chr 1. It has been postulated, but not universally accepted, that these tumors are genetically related and represent a spectrum of benign to malignant tumor progression.

Design: We sought to analyze chr 1 abnormalities in RO and ChRCC by FISH and LOH. For FISH, an LSI 1p36/LSI 1q25 dual color probe set from Vysis, Inc was used. LOH analysis was carried out using 3 microsatellite markers (D1S508, D1S199, D1S2734) and a PCR based assay. Paraffin sections from tumor and adjacent normal tissue were studied. DNA extraction, end-labeling and PCR amplification were performed as previously described *(BMC Clin Pathol 2003;3:6)*. DNA samples, heterozygous for any of the 3 loci, were considered informative, whereas homozygotes were deemed "non-informative" (NI). All tumors were defined morphologically using current diagnostic criteria.

Results: 17 RO and 12 ChRCC were studied by both techniques. By FISH, ten RO showed loss of chr 1, two of 1p; four were disomic and 1 RO was trisomic for chr 1; nine ChRCC showed loss of 1, one of 1p and two were disomic. The RO showed LOH as follows: in all 3 loci (x7), in 2 loci (x5) and in 1 locus (x3); 2 RO were NI. ChRCC showed LOH in all 3 loci (x5), 2 loci (x3) and 1 locus (x4). All ChRCCs and 15/17 (88%) RO showed LOH in at least one locus with LOH in the D1S2734 locus detected in 92% and 82% of tumors respectively. LOH in D1S199 was present in 50% and 53%, and in D1S508 in 67% and 59% of tumors, respectively. LOH was seen also in tumors disomic for chr 1 by FISH (2/4 RO and in 2/2 ChRCC), in one RO that was trisomic and in one ChRCC with -1p.

Conclusions: In this study, 100% of ChRCC and 88% of RO showed LOH in at least one locus, with LOH in locus D1S2734 detected in 92 and 82% of tumors respectively. An additional two loci were frequently affected in both groups. LOH was also seen in tumors that were disomic or trisomic for chr 1 by FISH. These results show similar patterns of genetic abnormalities within 1p in RO and ChRCC. These studies may lead to the delineation of a minimum deletion interval for the proposed tumor suppressor gene.

775 Chromosomal Analysis of Renal Cell Carcinomas with Mixed Histologic Patterns

O Pozdnyakova, LM Hutchinson, B Banner. UMASS Memorial Medical Center, Worcester, MA.

Background: Cytogenetic studies of renal cell carcinomas (RCC) have shown an association between a deletion of gene sequences on short arm of chromosome 3 (3p) in clear RCC and increase in number of chromosomes 7 and 17 in papillary RCC. Rarely RCC show mixed histologic patterns within one tumor, and the genetics of these tumors have not been studied. The aim of our study was to characterize chromosomal abnormalities in mixed RCC.

Design: We selected six resected tumors with mixed clear-cell and papillary patterns from the surgical pathology files. In addition, one pure clear-cell and one pure papillary RCC were selected for comparison. FISH was performed on the sections cut from paraffin blocks using centromeric probes for chromosomes 7 and 17 and a telomere probe for 3p. Signals were counted in 50 nuclei in identified areas with each pattern as well as in normal areas. FISH signals were expressed as the mean number of chromosomes per nucleus and the counts for each pattern were analyzed statistically.

Results: The mean numbers of chromosomes in each pattern were:

	Papillary pure	Papillary mixed	Clear pure	Clear mixed	Normal
Chromosome 7	3.2 ± 0.6	3.0 ± 0.9	1.8 ± 0.5	2.3 ± 0.8	1.9 ± 0.3
Chromosome 17	3.0 ± 0.7	2.5 ± 0.7	1.8 ± 0.5	2.1 ± 0.7	1.8 ± 0.4
Chromosome 3p	2.0 ± 0.4	1.9 ± 0.6	0.6 ± 0.5	1.2 ± 0.7	1.8 ± 0.4

There was a significant difference between the number of the signals for chromosomes 3p, 7, and 17 between papillary and clear-cell patterns in mixed tumors ($p<0.01$). The counts for pure and mixed papillary patterns were similar. However, the mixed clear-cell pattern showed abnormalities in all 3 chromosomes, unlike the pure clear-cell RCC.

Conclusions: In RCC with mixed histologic patterns, different chromosomal abnormalities may be associated with each pattern. The chromosomal abnormalities in papillary mixed RCC are the same as in the pure papillary RCC. In clear-cell pattern the chromosomal abnormalities are more variable. Our results suggest that RCC with mixed histologic patterns may be composite tumors with more than one tumor clone, and could have unpredictable biologic behavior.

776 Partial Atrophy in Prostate Needle Biopsies: A Detailed Characterization of Morphology, Immunophenotype and Proliferation Status

CG Przybycin, LP Kunju, A Wu, RB Shah. University of Michigan, Ann Arbor, MI.

Background: Partial atrophy (PA) is a distinct, relatively recently described and less studied variant of focal atrophy. It needs to be systematically characterized along three fronts: morphological, because it can be a mimic of prostate cancer (PCa), immunohistochemical, because it often shares the staining characteristics of PCa, and biological, because, it belongs to the larger group of focal atrophy, some of which have been shown to be proliferative and associated with chronic inflammation.

Design: PA lesions were prospectively identified from over 185 NBXs performed between 01/04 and 06/06. The morphological characteristics of each PA lesion along several architectural (circumscription, gland shape, stromal sclerosis, associated complete atrophy, presence of inflammation) and cytological (cytoplasm, nuclei size, nucleoli) criteria were assessed. An immunohistochemical profile for each PA lesion with basal cell (34betaE12 and p63) and P504S markers was generated. MIB-1 proliferation marker was evaluated quantitatively by Chromavision and compared with that of benign prostate glands.

Results: A total of 73 PA lesions were identified in 51/185 (27.5%) NBXs. PA lesions were characterized by circumscribed growth (70%), stellate/undulated glands (92%), associated complete atrophy (97%), lack of nuclear enlargement (100%) or macronucleoli (100%), clear cytoplasm (100%) and lack of inflammation (99%). Patchy basal cell staining was observed in 52/73 (71%) while 4/73 (5%) were completely negative with basal cell marker. P504S demonstrated variable expression in 7/73 (9.5%) PA lesions. A small subset of cases (6/51, 12%) created diagnostic difficulties due to poor circumscription, predominantly small poorly-formed round glands, presence of micronuleoli and/or overlapping staining characteristics of PCa. There was no difference between the mean proliferative index of the PA glands and that of the benign glands (5.3 and 4.7, respectively, p=0.68).

Conclusions: The vast majority of PA lesions are readily distinguishable morphologically from PCa. However, a small subset of PA may create diagnostic difficulties due to overlapping morphological and immunohistochemical features with PCa. Compared to other atrophic lesions, PA lesions are not associated with increased proliferative activity and/or inflammation.

777 Needle Biopsy (NBX) DNA Ploidy Versus Gleason Score for the Prediction of Disease Recurrence in Prostate Cancer

M Punar, CE Sheehan, B Varadarajalu, JS Ross. Albany Medical College, Albany, NY.

Background: Tumor Gleason grading is a standard of practice for the assessment of prostate cancer prognosis whereas the utility of DNA ploidy status remains controversial.

Design: 102 patients with clinical Stage A2-B2 prostatic adenocarcinoma (PAC) in 1989-1997 who were treated by radical retropubic prostatectomy (RPX) were included in this study. No patients received hormonal or radiotherapy prior to post-RPX disease recurrence. The study observation time ranged from 23 to 188 months, with a mean of 110 months. All patients without recurrence had at least 48 months observation time. The final tumor grade was the highest total combined Gleason score (GS) from the NBX specimens. Tumors were considered to be low grade when GS ≤ 6 and high grade when GS ≥ 7. Five micron sections from formalin fixed paraffin embedded NBXs containing the highest GS areas were Feulgen stained and analyzed for DNA content using the CAS-200 Image Analysis System. A non-diploid (aneuploid) histogram was defined as either a DNA index of greater than 1.23, a tetraploid peak greater 25% of total cells or the presence of multiple polyploid peaks. Disease recurrence was defined as an elevation of serum PSA by 0.4 nanograms per milliliter (ng/ml) at 2 occasions any time beginning one month after RPX.

Results: 31 (30%) of NBXs were high grade with 20 recurrences (PPV = 0.65) and 71 (70%) were low grade with 41 without recurrences (NPV = 0.58). 31 (30%) of NBX's were non-diploid with 24 recurrences (PPV = 0.77). 71 (70%) of NBXs were diploid 45 without recurrences (NPV = 0.63). The overall disease recurrence rate was 49%. 19 NBXs had both high Gleason score and non-diploid DNA content with 15 recurrences (PPV = 0.79). 59 NBXs had both low Gleason score and diploid DNA content with 39 without recurrences (NPV = 0.66). Both non-diploid DNA content and high Gleason score predicted disease recurrence with DNA ploidy status ($p<0.001$) out-performing tumor grading ($p=0.039$).

Conclusions: In this cohort of patients originally diagnosed with PAC from 9 to 17 years prior to the study, NBX DNA ploidy status continues to out-perform Gleason grading in the prediction of disease recurrence in prostate cancer. Given the increasing interest in new watchful waiting programs and alternatives to RPX, the potential addition of DNA ploidy measurements to tumor grading on NBX specimens to increase the accuracy of pre-treatment prognostic assessment warrants further study.

778 The 5-alpha-Reductase Inhibitor Dutasteride Decreases Cancer Volume and Induces Multiple Phenotypic Changes in the Human Prostate

J Qian, L Liu, J Ma, I Meiers, K Lang, SM Hewitt, TH Wilson, RS Rittmaster, DG Bostwick. Bostwick Laboratories, Glen Allen, VA; NCI, HIH, Bethesda, MD; GlaxoSmithKline, Research Triangle Park, NCS.

Background: To evaluate the treatment effects of the 5a-reductase inhibitor-dutasteride on cancer at radical prostatectomy in a multicenter trial.

Design: We analyzed the pathologic findings in 50 men who were treated with dutasteride, an inhibitor of Types 1 and 2 receptors of 5a-reductase, for 18 weeks prior to radical prostatectomy, and compared the findings from 25 men received no therapy for 8 weeks prior to radical prostatectomy. In treatment group, 26 and 24 men were treated with 0.5 mg and 3.5 mg dutasteride, respectively. The histopathologic features of benign epithelium and cancer were recorded and treatment effect was scored. Digital image analysis was used to measure stroma:epithelium ratio, epithelial height, and nuclear area in cancer. Tissue microarray technology was used to assess the expression of cathepsin B, Stefin A, CD34, p53, TUNEL, and lipoxygenase-5.

Results: In benign epithelium, treatment caused distinctive architectural and cytologic changes, including atrophy, a decrease in epithelium height, and an increase in stroma: epithelium ratio. In cancer, volume was significantly lower ($p<0.04$) in the dutasteride 0.5mg group (mean, 1.97cc) and in the 3.5mg group (mean, 1.70cc) compared to the untreated group (mean, 2.30cc).). Cancer treated with high dose (3.5 mg) dutasteride showed a lower stroma/epithelium ratio than untreated cancer (mean, 0.35 vs. 0.49, P=0.05). Using quantitative tissue microarray technology, we found that the mean staining intensity for CD34 (P=0.03) and p53 (P=0.03) was lower in cancer treated with high dose (3.5 mg) dutasteride than untreated cancer, while TUNEL intensity (P=0.03) was higher in high dose (3.5 mg) dutasteride-treated group.

Conclusions: Epithelial shrinkage of benign epithelium and decreased cancer volume were identified after 4 months of dutasteride treatment. Higher dose of dutasteride induced more changes in histology and phenotype than lower dose. These findings indicate that dutasteride induces significant and reproducible phenotypic alterations in the benign and neoplastic prostate, supportive of a chemopreventive or chemoactive role.

779 Double Immunohistochemistry for CK20/P53 in the Diagnosis of Neoplastic and Non-Neoplastic Bladder Biopsies

R Recavarren, S Mohanty, S Bastacky, F Monzon, R Dhir, AV Parwani. University of Pittsburgh Medical Center (UPMC), Pittsburgh, PA.

Background: The distinction between non-neoplastic and neoplastic bladder lesions is therapeutically and prognostically important. Previous studies have demonstrated the diagnostic utility of p53 and CK20 immunohistochemistry (IHC) in assessing neoplasia/dysplasia in bladder biopsies. We describe the use of double IHC (DIHC) for CK20/p53 as a tool for detecting synchronous expression of both markers in bladder biopsies.

Design: Sixty-four bladder biopsies were retrieved from our surgical pathology files, including 38 benign/reactive, 10 dysplasia and 16 urothelial carcinomas (UC) (9 carcinoma in situ (CIS) and 7 invasive carcinomas). H&E and CK20/p53-DIHC (DAKO, Carpinteria, CA) were examined for each case. CK20 stain was evaluated as 0 (negative), 1+ (weak), 2+ (moderate) and 3+ (strong). CK20+ cells were also assessed for location in upper third-umbrella cells, 2/3 urothelium sparing basal layer, or full-thickness stain including the basal layer. P53 was scored as 0 (negative), 1+ (<15%, weak), 2+ (15-50%, moderate) and 3+ (>50%, strong).

Results: (1) Benign/reactive cases were CK20 negative or only positive in the upper 1/3 urothelium in 35/38 cases (92%). (2) Among dysplastic cases, CK20 stained 2/3 urothelium in 6/10 cases (60%) (p53-). One case was CK20+ in 1/3 superficial urothelium (p53-). Three cases were CK20+ (full-thickness), with only one p53+ case. (3) Among CIS cases, 8 of 9 (89%) had CK20+ (full-thickness), and of those 5 of 8 (62%) were p53+. One case showed CK20+ (1/3 upper urothelium) but displayed strongly p53+. (4) Among invasive carcinomas, 5 of 7 (71%) were CK20+ and p53+, with strong dual staining involving the entire urothelium.

Conclusions: (1) CK20/p53-DIHC is useful in differentiating non-neoplastic vs. neoplastic lesions in bladder biopsies. (2) Dual staining not only allows for histologic correlation and diminishes the risk of losing the area of interest in limited biopsy specimens. (3) Benign/reactive lesions consistently show CK20+ umbrella cells and/or upper third urothelium, and most are p53 negative or express weak or no staining. (4) Dysplastic lesions have CK20 staining involving two-thirds to full-thickness urothelium, with variable or no p53 staining. (5) CIS and invasive UC have full thickness CK20+ and p53+ strong *dual* staining. (6) Our studies have demonstrated that CK20/p53 cocktail (if commercially available) may be a useful diagnostic marker in the assessment of bladder biopsies.

780 Testicular Germ Cell Tumors Express Kruppel-Like Factor 6 Splice Variants (KLF6-SVs)

J Regadera, F Sanz-Rodriguez, ML Botella, MM Cajaiba, A Serrano, M Nistal, P Gonzalez-Peramato, M Reyes-Mugica. Universidad Autonoma de Madrid, Madrid, Spain; CSIC, Madrid, Spain; Guadalajara General Hospital, Guadalajara, Spain; Yale University, New Haven, CT.

Background: Kruppel-like factor 6 (KLF6), a candidate tumor suppressor gene frequently mutated in prostate and colon carcinomas, encodes a zync finger protein, which acts as a transcription factor; its well-known target gene p21, inhibits cell proliferation interacting with cyclin D1. KLF6 polymorphisms in prostate tumors result in alternative splicing, and similar protein products may translate from truncating mutations. KLF6 splice variants (KLF6-SVs) lack the domain needed for transcription, and antagonize wild-type KLF6 resulting in decreased expression of p21. Interestingly, wild-type KLF6 was shown to be located in the nucleus, while KLF6-SVs are expressed in the cytoplasm.

Design: 77 testicular germ cell tumors (21 seminomas, 12 embryonal carcinomas, 7 immature teratomas, 6 yolk sac tumors, 4 mature teratomas, and 27 mixed tumors), and 4 normal adult testes were studied by immunohistochemistry (IHC) using a polyclonal anti-KLF6 antibody. Western blot and RT-PCR (using primers for both, total and wild-type KLF6) were applied in 13 tumors and 2 normal samples.

Results: Normal testis showed nuclear KLF6 expression in spermatogonia, Sertoli and Leydig cells. In contrast, tumor cells lacked nuclear immunoreactivity but featured strong and diffuse cytoplasmic expression in all tumor types (including areas of intra-tubular germ cell neopasia - ITGCN), except in cases of undifferentiated embryonal carcinoma, which revealed only weak and focal expression. Western blot revealed higher KLF6 expression in cancer samples than normal tissues, displaying a molecular weight compatible with a splice variant. RT-PCR showed, in addition to the wild-type KLF6 transcript, higher amounts of lower molecular weight amplicons in tumor but not in normal samples.

Conclusions: IHC detection of KLF6 in testicular germ cell tumors, including ITGCN, suggests that it may participate in the development and progression of testicular cancer. Western blot and RT-PCR analysis indicate that the aberrant cytoplasmic IHC expression is due to the presence of splice variants, supporting its role in tumorigenesis.

781 Anterior Prostatic Anatomy: A Modern Surgical Pathology Perspective

VE Reuter, H Al-Ahmadie, A Gopalan, S Tickoo, SW Fine. Memorial Sloan Kettering Cancer Center, NY.

Background: Over 25 years ago, McNeal described our current model of prostatic zonal anatomy based on autopsy dissections in various planes. As opposed to the cone-shaped organ seen in vivo, radical prostatectomy (RP) specimens are typically spherical, due to tissue contraction, and are sectioned from apex to base, yielding topography at the Surgical Pathology "sign-out" that may vary from traditional anatomy. There are no in depth studies of anterior anatomic variability, including the peri-urethral region (PUR), peripheral (PZ) and transition (TZ) zones, anterior fibromuscular stroma (AFMS), and anterior extraprostatic space (EPS) in modern RP specimens.

Design: Original slides of 197 entirely-submitted, whole-mounted RP containing anterior-predominant tumors were studied with attention to topographic relationships.

Results: Prostatic Apex: muscular contraction of the apex results in RP sections that begin closer to the urethral angle. Similar collapse of the lateral prostatic border causes posterior urethral bulging ("promontory"), which may be mistaken for the verumontanum. Surrounding the urethra is a thin layer of peri-urethral glands and stroma, followed by semicircular vertically-oriented striated muscle fibers. Anteriomedially (AM), the variably wide AFMS serves as a barrier for the PUR. In the absence of marked benign prostatic hypertrophy (BPH), the PZ extends far anteriorly and AM. **Prostatic Mid Gland:** the true verumontanum and bilateral lobes of the TZ are observed. PZ tissue encompasses the anterolateral (AL) prostate and may still extend AM. AFMS may be more limited on sections due to increased glandular density. **Prostatic Base:** from mid to base, the PUR is progressively invested by circumferential bands of short smooth muscle fibers which abut an enlarged AFMS. Proximally, TZ tissue recedes, PZ occupies the AL prostate, and the AFMS merges imperceptibly with large smooth muscle fibers of the bladder neck (BN). **Anterior EPS:** no clear 'capsule' is present at the anterior-most prostate, with significant variablity in the AL area. Fat and vessels seen AM are remnants of the ligated dorsal venous complex, which become admixed proximally with BN smooth muscle.

Conclusions: 1. Topography seen in RP specimens varies from traditional anatomy due to orientation and contraction of the prostate. 2. In the absence of BPH, virtually all glandular tissue at the apex is of PZ origin. 3. The AFMS is a prime region for expansile tumor growth which may be of TZ or PZ origin. 4. Anterior extraprostatic extension by tumor may involve fat and/or BN muscle.

782 Renal Lymphoma – A Clinicopathological Study of 27 Cases

B Richendollar, M Zhou, X Xie. Cleveland Clinic, Cleveland, OH.

Background: Lymphomas with primary presentations involving the kidney are difficult to diagnose. However, the distinction of renal lymphoma from much more common renal cell carcinoma is critical as the management of the two diseases is drastically different. This study reports the clinicopathological features of 27 renal lymphomas, the largest series reported so far.

Design: A review of medical records identified patients with a diagnosis of renal lymphoma from 1981-2006. Clinical, radiological and pathological data were reviewed. When available, the slides were also reviewed. The WHO classification system (2001) was used to classify these cases.

Results: Renal lymphomas account for 0.55% (27/4890) of all renal tumors at our institution, and include 17 men and 10 women. The mean age at presentation was 61 (28-80) years. Clinical histories were available for 19 of 27 cases. Of 19 patients, 15 (78.9%) had renal involvement as the primary presentation of lymphoma with 11 (73.3%) found to have concurrent lymphadenopathy. 4 patients had a known history of lymphoma at the time of renal diagnosis and the time interval between the initial diagnosis and the diagnosis of renal lymphoma ranged from 3-10 years. Of 16 patients with known presenting symptoms, 8 had abdominal / flank pain, 4 had acute renal failure, 1 had gross hematuria, while 3 were incidental findings. Of 17 patients with known radiological findings, 14 were found to have renal masses ranging between 1.7-27.0 cm in maximum diameter with 7 extending into the perirenal fat and 3 directly invading the adrenal gland. Based on clinical and radiological findings, 9 were classified as lymphoma, while 8 were initially classified as renal cell carcinoma. All 27 cases (100%) were B cell lymphomas, including 12 (44.4%) small B cell lymphomas, 11 (40.7%) large B cell lymphomas, 2 (7.4%) large B cell post-transplant lymphoproliferative disorders, 1 (3.7%) precursor B lymphoblastic lymphoma and 1 (3.7%) plasmacytoma. 2 patients presented with concomitant renal cell carcinoma, and 1 patient presented with concurrent transitional cell carcinoma.

Conclusions: Primary lymphomatous involvement of the kidney is rare and the overwhelming majority is B cell non-Hodgkin lymphoma. T cell lymphoma and Hodgkin lymphoma is not observed in our series. Awareness of possible renal involvement by lymphoma that presents as a mass, especially in patients with concurrent lymphadenopathy or known history of lymphoma, may prevent patients from having unnecessary nephrectomy procedures.

783 Molecular Fixative-Induced Epithelial-Stromal Separation in Prostatic Carcinomas: A Potentially Helpful Feature

P Robinson, M Nadji, N Block, A Morales. University of Miami, Jackson Memorial Hospital, Miami, FL.

Background: Epithelial-stromal separation (ESS), commonly known as retraction artifact may occasionally be seen in a number of carcinomas. This microanatomical alteration, however, is not readily discernible in formalin-fixed routinely process tissue. Alcohol-based fixatives on the other hand, amplify this separation to a considerable degree. We investigated the effect of a methanol-based fixative (Molecular Fixative, Sakura) on the microarchitecture of neoplastic and non-neoplastic prostatic tissue.

Design: Parallel blocks of tissue from prostatectomy specimens of 52 patients with biopsy proven prostatic carcinoma were fixed in both 10% buffered formalin and the Molecular Fixative (MF), from twelve to forty-eight hours at room temperature. They were then processed by a microwave-assisted rapid processing system (Xpress, Sakura) and stained with H and E. Adjacent sections from each block were stained for high molecular weight cytokeratin (34BE12, Dako). An additional 676 prostatic needle biopsies that were all fixed by MF were similarly reviewed.

Results: All prostatectomy samples contained both neoplastic and non-neoplastic glands. Of the 676 prostatic needle biopsies, 168 had areas of adenocarcinoma with Gleason's grades of 6 through 9. ESS was observed in the neoplastic glands of 48 (92%) of MF-

exposed prostatectomy samples and 164 (98%) of needle biopsies. Conversely ESS was seen in the neoplastic glands of only 4 (8%) of formalin-fixed prostatectomy specimens. Of interest was the presence of partial ESS of individual non-neoplastic glands adjacent to carcinomas in 9 (17%) of prostatectomy samples. This partial detachment corresponded to partial loss of basal cells as revealed by 34BE12 staining.

Conclusions: Epithelial-stromal separation is seen in the neoplastic glands of most prostatic adenocarcinomas that are fixed by the MF. This microanatomic feature could be of diagnostic value in selected cases. It is possible that the partial detachment of benign glands with loss of basal cells may signal an early neoplastic change.

784 Utility of Cytogenetics on Diagnosis of Renal Cell Tumors

PA Rodriguez Urrego, D Ang, R Kannan, H Aviv, B Fyfe. RWJMS-UMDNJ, New Brunswick, NJ.

Background: Histologic subtyping of renal cell tumors (RCT) has a prognostic value independent of staging. Cytogenetics was integrated into the 2004 WHO classification schema and has an established role in accurate diagnosis. This study aims to determine the utility of cytogenetic analysis in the accurate diagnosis of RCT in daily surgical pathology practice.

Design: From 3/ 05 to 6/ 06; 74 fresh RCT were sampled and cytogenetic studies were performed as part of the RCT protocol at RWJUH. Microscopic and karyotypic diagnosis were then reviewed retrospectively.

Results: The microscopic variants were conventional renal cell carcinoma (CRCC), papillary RCC (PRCC), chromophobe RCC (CHRCC), oncotyoma (OC), RCC associated with translocation Xp11.2 (tXp11.2), multilocular cystic (MLCRCC) and unclassified RCC (URCC). Microscopic and karyotypic diagnosis were correlated and sub classified: concordant (CC), discordant (DC) and uninformative (UC) cytogenetics (table 1). 61 % of the cases were CC. UC (31%) were due to lack of growth (n=9) and inadequate sampling (n=14). Inadequate sampling was defined either as normal karyotype (n=5), unspecific cytogenetic abnormalities (n=3), and low grade component/ stromal overgrowth (n=6). MLCRCC (2/2) and CHRCC (3/6) generally failed to grow in culture. DC (8%) included CRCC (n=4), PRCC (n=1) and CHRCC (n=1). Further review of these cases favored the primary histologic diagnosis (5/6). Additional investigations including FISH are being performed to better elucidate discrepancy. The time between collection of the specimens and processing, was ≥ 2 days in 6% of CC and 22 % of UC.

Conclusions: 1. Cytogenetic studies have a supportive role for the microscopic diagnosis of RCT to grant accuracy and to potentially elucidate newly defined entities (i.e. RCC tXp11.2). 2. In the case of discordant microscopic/karyotypic diagnosis, a review to ascertain the reason for the discrepancy and special studies (FISH) should be performed if necessary. 3. Timely handling of the specimen is necessary to maintain viability of the tissue. 4. The nature of the specimen should be evaluated at gross examination to establish what special studies (karyotype, FISH, EM) should be utilized to confirm diagnosis (i.e. MCRCC or CHRCC).

CORRELATION OF MICROSCOPIC AND CYTOGENETIC DIAGNOSIS

MICRO. / KTYPE	CRCC n=43	PRCC n= 12	CHRCC n= 6	OC n=4	RCC tXp 11.2 n=1	MLCRCC n=2	URCC n=6
CC n= 45	29	9	1	2	1	0	3
DC n= 6	4	1	1	0	0	0	0
UC n=23	10	2	4	2	0	2	3

785 Identification of a Unique Epigenetic Sub-Microenvironment in Prostate Cancer

J Rodriguez-Canales, JC Hanson, MA Tangrea, HS Erickson, PA Albert, BS Wallis, AM Richardson, PA Pinto, WM Linehan, JW Gillespie, MJ Merino, SK Libutti, KW Woodson, MR Emmert-Buck, RF Chuaqui. National Cancer Institute, NIH, Bethesda, MD.

Background: GSTP1 promoter methylation is the most frequent genomic alteration in prostate cancer. Previously, we found GSTP1 methylation in the tumor-associated stroma in addition to the tumor cells. An important next step is to better characterize the methylation and its anatomical distribution. The aim of this study is to quantify GSTP1 methylation in a 3-dimensional (3D) reconstuction of an entire cancer prostate.

Design: A cancerous prostate was obtained from a patient treated on an IRB-approved clinical trial at the NIH Clinical Center. The prostate was sectioned from apex to base, and contained 2 independent tumor foci Gleason 3+4=7. A second, control prostate with benign prostate hyperplasia (BPH) was processed as above. Using laser microdissection we performed an anatomical mapping from apex to base. The samples were normal epithelium and stroma, tumor epithelium, and tumor-associated stroma from both tumor foci. The BPH prostate was sampled for epithelium and stroma throughout. Methylation percentages of 15 CpG within the GSTP1 promoter were quantified with pyrosequencing.

Results: Normal epithelium and stroma both had a mean methylation of ≤15%. Tumor epithelium showed methylation ≥ 70% throughout. Tumor stroma was found to be methylated only in the apical pole of the tumor foci (40%). Morphologically, the apical pole of the tumors was comprised of predominantly non-reactive stroma and a Gleason pattern 3, while the stroma towards the base was reactive and a more aggressive tumor pattern. PIN was found at the apical region. The BPH prostate showed mean methylation ≤15% throughout.

Conclusions: The integration of pyrosequencing data and the 3D reconstruction of the prostate reveals a sub-region in the apical pole of the tumors. The presence of PIN and a lower tumor pattern in this region, combined with previous morphometric studies (i.e. apex is comprised of peripheral zone, and peripheral zone tumors show a tendency to spread vertically towards the base) suggest that this region could be the initial site of these tumors and the methylation of the tumor stroma could be important at the initial stages of tumorigenesis. Further studies on this tumor sub-region can improve the understanding of tumorigenesis.

786 Distinction of Bronchogenic Cyst from Metastatic Testicular Teratoma: A Histologic and Immunohistochemical Study of 56 Cases

AA Roma, M Varsegi, C Magi-Galluzzi, TM Ulbright, M Zhou. Cleveland Clinic Foundation, Cleveland, OH; Indiana University School of Medicine, Indianapolis, IN.

Background: Bronchogenic cysts (BC) are rare developmental abnormalities that result from abnormal budding of the primitive foregut. Although usually found above the diaphragm, they can occur in the retroperitoneum (RP) and posterior mediastinum where distinction from metastatic teratoma is essential. This study details the diagnostically important histologic and immunohistochemical features of BC and teratoma.

Design: 22 BCs (1 retroperitoneal, 17 mediastinal, 4 intrapulmonary) and 34 metastatic teratomas to RP in men with testicular germ cell tumors were studied for epithelial types, mesenchymal components, salivary-like glands, immature elements, nuclear atypia and necrosis. An architectural grade (0-2) was assigned based on the degree of differentiation towards normal tracheobronchial architecture. Each case was immunostained for CK7, CK20, CDX-2, TTF-1, chromogranin and Ki-67.

Results: 17/22 BCs (77%) showed either well (grade 2) or moderate (grade 1) architectural differentiation, whereas none of the teratomas did. Other helpful features included the absence of enteric-type epithelium, the predominance of respiratory epithelium, the presence of salivary-like glands, the absence of immaturity, atypia, necrosis, and CDX-2 staining and the infrequent expression of CK20 and Ki-67 in BCs compared to metastatic teratomas. Also, 32% of teratomas had glands that co-expressed CDX-2 and TTF-1, whereas such co-expression occurred in no BC.

Conclusions: BC can be reliably distinguished from teratoma. BC has more differentiated architecture, is composed predominantly of respiratory-type epithelium that is positive for CK7 and often for TTF-1. These features contrast with those of metastatic teratomas, which have mixed enteric and respiratory type epithelium as evidenced by positive stains for CK7, CK20, CDX-2 and TTF-1. Aberrant glandular differentiation, as demonstrated by CDX-2 and TTF-1 positive cells in the same glands, is only found in teratoma.

		BC (n=22)	Teratoma (n=34)
Architecture*	2	10 (45%)	0
	1	7 (32%)	0
	0	5 (23%)	34 (100%)
Epithelium*	Enteric	0	28 (82%)
	Respiratory	20 (91%)	0
	Other	2 (9%)	6 (18%)
IHC	CK7	22 (100%)	33 (97%)
	CK 20*	9 (rare cells) (41%)	34 (100%)
	TTF-1*	4 (18%)	17 (50%)
	CDX-2*	0	34 (100%)
	TTF-1 & CDX-2*	0	11 (32%)
	Chromogranin*	2 (9%)	29 (85%)
	Ki-67*	0	31 (91%)

*p<0.05

787 OCT-4 Expression in Malignant Epithelial Tumors of the Genitourinary Tract

AJ Saenz, GP Nielsen, S Campbell, E Oliva. Massachusetts General Hospital and Harvard Medical School, Boston, MA.

Background: Metastatic tumors to the testis account for a significant proportion of testicular tumors, the most common being prostate cancer, followed by lung, melanoma, kidney and lower-gastrointestinal tract. OCT-4, a transcription factor of the POU family expressed in embryonic stem and germ cells, is involved in the maintenance of pluripotent stem cells in an uncommitted state and is a relevant biomarker. OCT-4 is purported to be a highly sensitive and specific biomarker for germ cell neoplasia, i.e., intratubular germ cell neoplasia, seminoma/dysgerminoma/germinoma, and embryonal carcinoma, however, it can be expressed in non-germ cell tumors. We undertook a study to evaluate OCT-4 immunostaining in urinary, prostatic and renal neoplasms as they may cause problems in the differential diagnosis with germ cell tumors, in particular with seminoma.

Design: Twenty-seven tissue blocks including prostate carcinoma (P-Ca) Gleason score 8 or higher (8), grade 3 transitional cell carcinoma (TCC-3) (9), and clear cell renal cell carcinoma (RCC) (10) were stained for OCT-4. Percentage of positive tumor cells (<10%, 10-50%, or >50%) and staining intensity (weak, moderate, or strong) was evaluated.

Results: Moderate to strong nuclear OCT-4 positivity was seen in 5/9 TCC-3 ranging from <10% (2) to >50% (3) of the tumor cells. Normal urothelium was also positive. Weak to moderate nuclear OCT-4 positivity was present in 3/8 P-Ca ranging from <10% (1) to >50% of the tumor cells but normal prostate epithelium was negative. Weak nuclear OCT-4 positivity was observed in 4/10 RCC ranging from <10% (1) to >50% (3) of the tumor cells, expression was confined to solid areas while the glandular/cystic areas were negative. The proximal and distal renal tubular epithelium was negative for OCT-4.

Conclusions: Prominent OCT-4 positivity was found in a significant number of TCC-3. This finding should be considered especially when evaluating a poorly differentiated tumor at a metastatic site, even though the intensity of staining is not in most cases as strong as seen in seminoma. Furthermore, in our opinion, OCT-4 expression in these tumors it does not necessarily represent germ cell differentiation as staining was seen even in normal urothelium. OCT-4 expression was weaker in high-grade P-Ca and RCC. These results indicate that OCT-4 may be a helpful adjunct when considering prostate or renal carcinoma in the differential diagnosis of a testicular seminoma.

788 Prostatic Ductal Adenocarcinoma Presenting as a Small Urethral Polyp: A Clinicopathological Analysis of 8 Cases of a Lesion with the Potential To Be Misdiagnosed as a Benign Prostatic Urethral Polyp

H Samaratunga, B Letizia. Sullivan Nicolaides Pathology, Brisbane, Queensland, Australia.

Background: Ductal adenocarcinoma, a distinct variant of prostatic adenocarcinoma commonly involves the periurethral region as friable polypoid masses protruding from ducts near the verumontanum. Marked cytological atypia is seen in most cases while some display mild atypia causing diagnostic difficulty. Rarely, these can present as a single polyp mimicking a benign polyp. Such lesions have not been formally studied.

Design: We studied the clinicopathological and immunohistochemical findings of 8 cases of ductal adenocarcinoma presenting as a single urethral polyp. Immunostaining was recorded as the number of cells staining; absent (0); < 25% (1+); 25-50% (2+) ;> 50% (3+).

Results: The mean age was 76 years with patients presenting with urinary symptoms and haematuria. The mean serum PSA was 7.01 ng/ml (range: 1.04 to 21). All lesions were < 10 mm diameter single polyps in the prostatic urethra or bladder neck on cystoscopy, prompting a clinical diagnosis of benign polyp. Tumor cells had tall columnar pseudostratified nuclei with amphophilic cytoplasm in 5 cases and pale or clear cytoplasm in 3. Commonest patterns were cribriform (6 cases) and papillary (3 cases). Three cases had marked nuclear atypia. Five had mild atypia, 3 of which were initially diagnosed as a benign prostatic urethral polyp. All cases were positive for PSA and 34 β E12 (1+ or 2+). All 7 cases tested were positive for AMACR (a-methylacyl-CoA racemase), p 63 (1+ or 2+) and cytokeratin 7 and 70% for cytokeratin 20. Follow-up ranging from 3 months to 4 years revealed 4 patients with large volume prostatic cancer in other specimens, predominantly or entirely ductal adenocarcinoma.

Conclusions: Prostatic ductal adenocarcinoma can present as a small urethral polyp not uncommonly lacking marked atypia, causing confusion with prostatic urethral polyps. Basal cell markers are positive in these lesions causing further confusion. The propensity of ductal adenocarcinoma to grow into pre-existing ducts explains this finding. Positive AMACR is helpful in this distinction. Presence of nuclear pseudostratification and even mild atypia contrasts with prostatic urethral polyps lacking any atypia. Awareness of the morphological spectrum can prevent misdiagnosis of this aggressive, high-grade cancer. The immunoprofile can also distinguish this lesion from villous adenoma and other carcinomas.

789 Survival Following the Diagnosis of Non-Invasive Bladder Cancer: WHO/ISUP vs. WHO Classification Systems

AR Schned, AS Andrew, CJ Marsit, KT Kelsey, MS Zens, MR Karagas. Dartmouth Medical School, Lebanon, NH; Harvard School of Public Health, Boston, MA.

Background: The 1998 WHO/ISUP classification of bladder cancer divides urothelial tumors into a lesion with low probability of recurrence or progression, called papillary urothelial neoplasm of low malignant potential (PUNLMP), and two categories of papillary carcinoma: low- and high-grade (LGCa and HGCa). The traditional WHO 1973 classification divides urothelial tumors into three categories of carcinoma: grades 1, 2, and 3. Few studies have reported patient survival data based on the WHO/ISUP classification; none have demonstrated clear superiority over the 1973 WHO system. As part of a large epidemiological study, we compared survival using the two classification systems in a non-selected population of patients with non-invasive bladder cancer.

Design: All New Hampshire residents with bladder cancer newly diagnosed between July 1, 1994 and June 30, 2000, were identified through the State Cancer Registry. Slides were retrieved from over 90% of cases and reviewed by a single pathologist. Tumors were classified according to both WHO and WHO/ISUP criteria. Survival was determined from the Social Security Administration's September 2005 Death Master File. Hazard ratios were adjusted for age, gender, and smoking status.

Results: 504 patients comprised the study population. Using the WHO/ISUP system, survival times were lower for HGCa than PUNLMP or LGCa, but there was no survival difference between PUNLMP and LGCa. Hazard ratios were 0.9 (95% CI=0.3-2.7) for PUNLMP *vs.* LGCa, and 2.3 for PUNLMP *vs.* HGCa (95% CI=0.7-7.6). For tumors classified according to the 1973 WHO system, there was a gradient of survival times from grade 1 to grade 3 tumors, with progressively lower survival times for higher grade tumors. Hazard ratios were 1.7 (95% CI=1.1-2.8) for grade 1 *vs.* grade 2 tumors, and 2.4 (95% CI=1.3-4.4) for grade 1 *vs.* grade 3 tumors.

Conclusions: Our data show no difference in survival between PUNLMP and low grade papillary carcinomas classified according to WHO/ISUP criteria, in contrast to significant survival differences between grades 1, 2, and 3 in the WHO 1973 classification. Our results, along with others, call into question whether the WHO/ISUP system provides prognostic advantage in patients with non-invasive bladder tumors.

790 Renal Cell Tumor Typing According to WHO 2004 Scheme: Application to 935 Carcinomas Diagnosed from 1989 to 2003

MF Serrano, AS Kibel, T Bullock, PA Humphrey. Washington University School of Medicine, St. Louis, MO.

Background: In 2004 the World Health Organization (WHO) published a classification scheme which reflects significant advances made in the understanding of distinctive pathologic and genetic neoplastic entities in the kidney. In the past, this classification system was not widely and consistently applied. We sought to uniformly type a consecutive, large series of all renal cell tumors from a single institution to characterize the incidence of specific types over this time period and to identify the type(s) of renal tumors previously typed as specific entities no longer in the 2004 WHO scheme, including "granular" cell renal cell carcinoma (RCC).

Design: We reviewed and typed 935 RCCs from 918 patients according to the 2004 WHO classification; data on Fuhrman grade, tumor size, and pathologic stage were also recorded.

Results: 679 of 918 (74%) tumors were RCC of clear cell type, 138 (15%) were papillary, 32 (3.4%) were chromophobe, 13 (1.4%) were multilocular cystic, and 49 (5.3%) were unclassified. The remaining cases were as follows: 3 (0.3%) translocation carcinomas, 3 (0.3%) collecting duct carcinomas and 1 (0.1%) renal medullary carcinoma. Mean tumor size was 5.6 cm, with a median of 4.5 cm (range 0.2 to 22 cm). 523 tumors (60%) were stage pT1, 88 (9.4%) stage pT2, 184 (19.6%) stage pT3, and 62 (6.6%) stage pT4. 9 tumors had been classified as "granular RCC"; 2 of them were re-classified as clear cell carcinomas, 1 as papillary, 1 chromophobe and 5 unclassified. 13 tumors had been diagnosed as "granular and clear cell" type, these were reclassified as follows: 8 clear cell carcinomas, 2 papillary, 2 chromophobe, and 1 unclassified.

Conclusions: This large, consecutive, single-institution series highlights the incidence rates of newly-defined and rare carcinomas in the kidney. It is striking that in this era of 1989 to 2003, most surgically-resected renal cell tumors are organ-confined. Renal cell carcinomas previously classified as "granular cell" type are comprised of a number of different tumor types, using the WHO 2004 scheme.

791 Incidence of Renal Tumors: 1989-2003

MF Serrano, T Bullock, AS Kibel, PA Humphrey. Washington University School of Medicine, St. Louis, MO.

Background: We typed a consecutive series of all renal masses to identify changes in the histologic typing and incidence of benign renal masses and renal cell carcinomas (RCC) over time.

Design: Using a computer database search for partial and radical nephrectomies performed at Barnes-Jewish and St. Louis Children's Hospitals during the years 1989 to 2003, we identified a total of 1201 consecutive cases of renal masses. All tumors were typed according to the 2004 WHO classification.

Results: The study group included 935 RCC and 165 benign masses. 679 of 918 (74%) RCC were of clear cell type, 138 (15%) papillary, 32 (3.4%) chromophobe, 13 (1.4%) multilocular cystic, and 49 (5.3%) unclassified. 76 (46%) of the 165 benign masses were oncocytomas, 40 (24%) angiomyolipomas (AML), and 43 (26%)simple cysts.

Incidence of Mayor Types of RCC 1989-2003

Year	Clear cell (% RCC)	Papillary	Total RCC (% total masses)	Total Renal Masses
1989	24 (80)	5 (16)	30 (71)	42
1990	23 (88)	3 (11)	26 (72)	36
1991	28 (71)	9 (23)	39 (81)	48
1992	24 (66)	7 (19)	36 (80)	45
1993	17 (59)	7 (24)	29 (76)	38
1994	27 (75)	5 (13)	36 (75)	48
1995	39 (76)	7 (13)	51 (85)	60
1996	44 (68)	7 (10)	64 (80)	80
1997	49 (73)	13 (19)	67 (74)	91
1998	41 (76)	9 (16)	54 (62)	86
1999	51 (67)	16 (21)	76 (73)	104
2000	70 (70)	20 (20)	100 (77)	130
2001	75 (80)	11 (11)	93 (83)	112
2002	86 (81)	5 (4)	106 (82)	129
2003	97 (75)	15 (11)	128 (84)	152

Incidence of Mayor Types of Benign Renal Masses 1989-2003

Year	Oncocytoma (% benign)	AML	Simple Cyst	Total benign (% of total)
1989	0	3 (100)	0	3 (7)
1990	5 (83)	1 (17)	0	6 (16)
1991	3 (100)	0	0	3 (6)
1992	1 (33)	2 (66)	0	3 (6)
1993	2 (100)	0	0	2 (5)
1994	5 (100)	0	0	5 (10)
1995	4 (100)	0	0	4 (6)
1996	3 (60)	0	1 (20)	5 (6)
1997	10 (58)	1 (5)	5 (29)	17 (18)
1998	8 (36)	3 (13)	11 (50)	22 (25)
1999	8 (36)	8 (36)	6 (27)	22 (21)
2000	7 (36)	7 (36)	5 (2)	19 (14)
2001	6 (50)	2 (16)	2 (16)	12 (10)
2002	7 (33)	6 (28)	8 (38)	21 (16)
2003	7 (33)	7 (33)	5 (23)	21 (13)

Conclusions: The percentage of surgically-excised benign renal masses increased from 8% in 1989-1996 to 17% in 1997-2003. The incidence of different types of renal cell carcinoma remained constant over time.

792 Epithelial Cell Transcriptome of Poorly and Moderately Differentiated Prostate Cancers

S Shaheduzzaman, C Gao, Z Wang, B Furusato, G Petrovics, V Srikantan, L Ravindranath, M Nau, Y Chen, Y Chen, J Cullen, DG McLeod, I Sesterhenn, M Vahey, S Srivastava. CPDR, Rockville, MD; AFIP, Washington, DC; WRAMC, Washington, DC; NHGRI, NIH, Bethesda, MD; WRAIR, Rockville, MD.

Background: The focus of this study is to identify prostate cancer (CaP) associated gene expression of poorly differentiated (PD) and well differentiated (WD) prostate cancer cells.

Design: Laser capture micro-dissected (LCM) epithelial cells from benign and malignant prostate glands of 2 CaP patients groups ("high risk"(HR)poorly differentiated, Gleason score 8-9, PSA recurrence and "moderate risk" (MR) well with or without poorly differentiated, Gleason score 6-7, no PSA recurrence). Genes differentially expressed between benign and tumor epithelium of HR and MR groups (N=40), were analyzed by Affymetrix HG U133 Plus 2.0 GeneChips. for biochemical pathways/networks.

Results: CaP specific expression alterations of genes involved in cancer and inflammatory pathways were highlighted by various bio-informatics approaches. Several genes that were differentially altered in tumor cells of MR groups were part of cell morphology and cell death pathways. Huntington-interacting protein-1 (Hip-1) interactor (*HIPPI*)

associating with HR specimens was among genes noted in two independent GeneChip experiments. *HIPPI* has also been implicated in apoptosis pathway. Further analysis of the expression of *HIPPI* in tumor and benign epithelial cells of 96 CaP patients by QRT-PCR. significantly discriminated CaP in HR group (up-regulated) from MR group (down-regulated). In addition, statistical analysis revealed a significant correlation of *HIPPI* expression with Gleason sum (ANOVA, p=0.0006) and pathological T stage (T-test, p=0.0243).
Conclusions: Our study defines gene expression signatures that have potential to distinguish MR and HR CaP. Among the genes *HIPPI*, exhibited differential expression patterns in both MR and HR CaP by GeneChip and QRT-PCR assays. Further evaluations of HR and MR associated gene expression signatures have potential to define functional targets/pathways involved in CaP progression.

793 Mechanisms of Downregulation of *Lactotransferrin (LTF)* in Prostate Cancer

S Shaheduzzaman, A Vishwanath, B Furusato, J Cullen, Y Chen, L Banez, M Nau, L Ravindranath, KH Kim, A Mohammed, Y Chen, M Ehrich, V Srikantan, I Sesterhenn, DG McLeod, M Vahey, G Petrovics, A Dobi, S Srivastava. CPDR, Rockville, MD; AFIP, Washington, DC; WRAMC, Washington, DC; NHGRI, NIH, Bethesda, MD; WRAIR, Rockville, MD; Sequenom, Inc, San Diego, CA.
Background: Anti-tumorigenic effects of Lactotransferrin (*LTF*) in carcinogenesis models have provided *impetus* to evaluate features and mechanisms of *LTF* expression alterations in human prostate cancer (CaP). Frequent downregulation of *LTF* was observed in epithelial cell transcriptomes of benign and malignant prostate glands by laser capture microdissection (LCM) and GeneChip analysis. In this study we aim to validate our gene profiling findings by examining *LTF* mRNA and protein expression CaP samples and evaluate the mechanism of down regulation in CaP cells.
Design: Quantitative analysis of *LTF* mRNA expression in epithelial cells of CaP specimens was evaluated by QRT-PCR (N=100). LTF protein expression was determined by immunohistochemistry (IHC) (n=30) and by ELISA (Cancer, N=34 and Control, N=35). Methylation analysis of the first intronic CpG island of *LTF* gene was performed in LNCaP cells, treated with 5-azacytidine (Epitzper)a bisulfite-treatment based MALDI-TOF MS method. Cell proliferation was evaluated in LNCaP cells treated with LTF.
Results: Quantitative analysis of *LTF* mRNA expression in epithelial cells revealed prostate tumor cell associated *LTF* downregulation in 74% of CaP patients (n=100; 200 specimens). Surprisingly, downregulation of *LTF* mRNA expression showed significant association with decreased PSA recurrence-free survival in patients after radical prostatectomy. Moreover, low levels of LTF protein expression were observed in tumor tissues as well as in serum by IHC and ELISA Assessment of the mechanism of *LTF* downregulation revealed that a CpG island within the *LTF* promoter downstream region was heavily methylated in LNCaP cells. Furthermore, inhibition of cell proliferation was observed by LTF treatment in LNCaP cell culture model.
Conclusions: This study identifies and defines the potential of *LTF* expression alterations in CaP as a biologically relevant prognostic marker and unravels the mechanism and cell biologic effects of decreased expression of *LTF*.

794 Distant Metastasis of Bladder Cancers: Distribution and Association with Lymph Node Metastasis, Pathologic Stage, and Lymphovascular Invasion

SS Shen, GE Amiel, SF Shariat, A Vazina, GS Palapattu, Y Lotan, PI Karakiewicz, CG Rogers, PJ Bastian, A Gupta, MP Schoenberg, AI Sagalowsky, SP Lerner. The Methodist Hospital and Weill Medical College of Cornell University, Houston, TX; Baylor College of Medicine, Houston, TX; University of Texas Southwestern Medical Center, Dallas, TX; University of Montreal, Montreal, QC, Canada; The Johns Hopkins Hospital, Baltimore, MD.
Background: Distant metastasis is the strongest predictor of survival for bladder cancer patients. Pathways and establishment of distant organ metastasis include lymphatic or blood vascular invasion. Our hypothesis is that patterns of distant organ metastasis may be predicted by histolopathologic parameters and has prognostic significance.
Design: We reviewed a multicenter cystectomy database with 956 bladder cancer patients to identify distant organ metastases. Relevant clinico-pathologic parameters were summarized and correlated with organ metastasis and survival analysis was performed by using Kaplan-Meier method and log-rank test. Cox-regression was used for multivariate analyses for prediction of distant metastasis.
Results: A total of 174 (18.2%) patients with distant metastases were identified from 956 patients who underwent cystectomy for bladder cancer. The mean patients' age was 64 years with a male:female ratio of 4.1:1. The most common sites involved were: bone 52, lung 49, liver 36, lymph node 28, brain 8. 96 of 174 (55%) had one and 51 (29%) had two or more sites of metastasis. The average time from cystectomy to metastasis were 17.0 months. The 1-year, 2-year, and 5-year survival rates for patients with distant metastasis were 39%, 25%, 11%, respectively. The overall survival did not correlate with the numbers of metastasis (p=0.13). However, nodal or lung metastasis only had better overall survival than bone metastasis (p=0.015). Multivariate analysis showed that pathologic stage, nodal metastasis and lymphovascular invasion were independent variables to predict distant metastasis.
Conclusions: The most frequent organ metastases of bladder cancer are bone, lung, and liver. The average time to metastasis from cystectomy was 17 months. Distant metastases occur frequently in the absence of nodal metastasis. Survival has a stronger association with the site rather than number of metastases. In addition to the pathologic stage and nodal metastasis, lymphovascular invasion is an independent variable to predict distant organ metastasis.

795 Lymph Nodes Metastases in Patients with Renal Cell Carcinoma: Correlation with Histopathologic Features

SS Shen, JY Ro, B Zhao, SJ Jung, LD Truong, AG Ayala. The Methodist Hospital, Houston, TX.
Background: Approximately 30% of the patients with renal cell carcinoma (RCC) have distant metastasis at the time of diagnosis. However, regional lymph node metastasis is less common and the role of lymphadenectomy at the time of nephrectomy is not well defined and controversial. To determine whether pathologic features of tumor can predict nodal metastasis, a retrospective study was performed.
Design: To identify any histologic features that are associated with nodal metastasis, we reviewed 254 radical nephrectomies (1990-2005) that include lymph node dissection and correlated the histologic subtype, tumor size, Fuhrman nuclear grade, and presence of sarcomatoid changes with nodal metastasis. Fisher's exact or x^2 test was used to comparing categorical variables and t-test was used for continuous variable between the groups. Kaplan-Meier method was used for survival analysis.
Results: Of the 254 patients with nodal dissection, nodal metastases were found in 44 (17%) patients. Lymph node metastases were detected in 15% (28/187) of clear cell RCC, 40% (10/25) of papillary RCC, 0% (0/14) of chromophobe RCC, 100% (2/2) of collecting duct carcinoma (CDC), and 67% (4/6) of unclassified RCC. Papillary RCC, CDC and unclassified RCCs were more likely to have nodal metastasis than clear cell and chromophobe RCCs ($P< 0.05$). Sarcomatoid changes were seen in 13 of 44 (33%) nodal positive RCCs, but only in 9 of 210 (4.3%) nodal negative RCCs ($P < 0.001$). The average tumor sizes for node positive and node negative groups were 9.84±3.4 and 7.26±4.3, respectively ($P<0.001$). High grade (Furhman's nuclear grade 3 & 4) tumors were seen in 35 of 44 (80%) node positive RCCs, but only in 60 of 210 (29%) node negative RCCs ($P<0.001$). Similarly, local advanced tumors (T3 and T4) were seen much more often in nodal positive group than nodal negative group (77% vs. 38%, $P<0.001$). The median survival times for patients with and without nodal metastases were 75 and 112 months, respectively ($P < 0.001$).
Conclusions: Nodal metastasis is strongly associated with poor survival in patients with RCC. Certain histological subtypes (i.e. papillary RCC and CDC), greater tumor size, high nuclear grade and stage, and sarcomatoid change are significantly associated with nodal metastasis and this information may have an implication for surgical planning for lymph node dissection at the time of radical nephrectomy.

796 The Sensitivity of Transurethral Biopsy for Detecting Prostatic Involvement by Transitional Cell Carcinoma in Patients with Bladder Cancer

SS Shen, TM Wheeler, G Amiel, LD Truong, SP Lerner. The Methodist Hospital and Weill Medical College of Cornell University, Houston, TX; Baylor College of Medicine, Houston, TX.
Background: We have shown recently that patterns and extent of prostatic involvement is prognostically relevant (Human Path 2006) in patient with bladder transitional cell carcinoma (TCC). Knowledge of prostatic involvement preoperatively is important for surgical planning and choice of urinary diversion for cystectomy. To date, no studies have described the detailed patterns of prostatic TCC and correlation with transurethral biopsy.
Design: Total of 173 cystoprostatectomies for bladder TCC with matched preoperative transurethral biopsy of prostatic urethra were identified and included in this study. The prostate were examined by whole mount sections and urethral biopsy was obtained from 5 to 7 o'clock position of the verumontanum. The patterns of prostatic TCC involvement examined by whole mount sections were correlated with the findings of transurethral biopsy of the prostatic urethra.
Results: Prostatic involvement of TCC was detected in 65 patients (37.6%) by either prostatic urethral biopsy or whole mount sections. Of the 65 patients with prostatic TCC involvement, 33 had CIS, and 32 had invasive TCC, of which 8, 12, 12 of them were lamina propria invasion, prostatic stromal invasion and extracapsular/seminal vesical invasion, respectively. Ten of the invasive TCC were direct penetrating invasion from bladder cancer, and the rest were arising from the prostatic urethra or duct (lateral spreading). Forty-eight of 55 cases of lateral spreading prostatic TCC were detected by prostatic urethra biopsy for a detection rate of 87.3%. Seventeen cases of prostatic TCC were missed by prostatic urethral biopsy, of which over half (53%) of them were penetrating bladder cancers. Interestingly, 12 cases of prostatic TCC detected by prostatic urethral biopsy were not detected by whole mount sections. Eleven (92%) of these cases were CIS only.
Conclusions: Prostatic involvement by TCC is a common finding in patients with bladder cancer. Using the appropriate sampling strategy, the sensitivity of prostatic urethra biopsy for detection of lateral spreading prostatic TCC is 87.3%. Awareness of pattern of prostatic involvement by TCC in patient with bladder cancer should help guide the management of patients.

797 Change in Prostate Cancer Grade over Time in Men Followed Expectantly for Stage T1c Disease

TB Sheridan, JI Epstein. The Johns Hopkins Hospital, Baltimore, MD.
Background: To assess whether the Gleason grade changes in men followed expectantly with nonpalpable prostate cancer diagnosed on needle biopsy (stage T1c).
Design: We studied 241 men with stage T1c prostate cancer who underwent watchful waiting with repeat yearly needle biopsy sampling to assess for cancer progression. Following the initial cancer diagnosis, all men had at least 1 other biopsy demonstrating cancer.
Results: The median age was 66. The number of biopsies showing cancer over time was: two in 119 (49.4%); three in 74 (30.7%); four in 33 (13.7%); and ≥5 in 15 (6.2%). The average follow-up for those without progression was 32.3 months. 45/241 cases (18.7%) showed a significant change in grade from Gleason score ≤6 to Gleason score

≥7 (Gleason score 7 in 31 cases; Gleason score 8 in 4 cases). 24/45 (53.3%) cases that showed progression did so within 24 months of diagnosis. The actuarial risk of grade progression at various years from diagnosis is shown below.

Follow-up (years)	Risk of Grade Progression	No. of Men at Risk
1	3%	240
2	11%	145
3	20%	75
4	31%	38
5	35%	24

Conclusions: Within the first 3 years after diagnosis of Gleason score 6 prostate cancer, there is a relatively low risk of grade progression. Within the first 3 years, our data suggests that in most cases tumor grade did not evolve but rather that the higher grade component was not initially sampled since: 1) most grade changes occurred relatively soon after biopsy; and 2) within a few months after needle biopsy showing Gleason score 6 tumor, 20% of radical prostatectomies in general are found to have Gleason score ≥7 cancer (our 3 year risk of grade progression was 20%). Grade progression does appear to occur in some men with long-term follow-up who had multiple biopsies showing Gleason score 6 followed by higher grade cancer.

798 Evaluation of Expression of Human Kidney Injury Molecule-1 (hKIM-1), P504S, S100, Vimentin and EMA in Renal Cystic Lesions

J Shi, XJ Yang, PL Zhang, ST Chuang, H Hwang, C Luan, WK Han, JV Bonventre, F Lin. Geisinger Medical Center, Danville, PA; Northwestern Memorial Hospital, Chicago, IL; Brigham and Women's Hospital, Boston, MA.

Background: Cystic clear cell renal cell carcinoma (CCRCC) may potentially mimic other benign renal cyst lesions (RCL), such as adult polycystic kidney disease (APKD), multilocular renal cysts (MLRC), and simple cysts (SC). Recently, we reported a sensitive and specific marker, hKIM-1, for identifying clear cell RCC and papillary RCC (AJSP, in press). In addition, we also reported two markers, P504S (AMACR) and S100, frequently expressed in renal cell carcinoma. The utility of these 3 markers in the detection and differentiation of those renal cystic lesions has not been investigated.

Design: The diagnostic value of hKIM-1, S100, P504S, vimentin, and EMA in 60 cases of RCL was determined immunohistochemically. The 60 cases included 22 cases of CCRCC, 11 cases of MLRC, 9 cases of APKD, and 18 cases of SC. The staining intensity was graded as weak, intermediate, or strong. The distribution was recorded as negative, 1+, 2+, 3+, or 4+.

Results: The positive immunoreactivity for hKIM-1, P504S, S100, vimentin and EMA in the various cystic lesions is summarized in Table 1. Concurrent expression of hKIM-1, vimentin, and EMA and concurrent expression of these three markers plus S100 were present in 16 of 22 cases (73%) and 15 of 22 cases (68%) of CCRCC, respectively, whereas none of other cystic lesion showed these 2 profiles. hKIM-1 was also expressed in 6 of 11 cases (55%) of MLRC. Co-expression of vimentin and EMA was present in 100% of CCRCC and 3 of 9 (33%) APKD.

Table 1. Immunostaining Results in 60 Cases of Cystic Renal Lesions

Type of Cyst	hKIM-1	P504S	S100	Vimentin	EMA
CCRCC (n=22)	16 (73%)	10 (45%)	20 (91%)	22 (100%)	22 (100%)
APKD (n=9)	0 (0)	3 (33%)	6 (67%)	3 (33%)	9 (100%)
MLRC (n=11)	6 (55%)	4 (36%)	6 (55%)	1 (9%)	11 (100%)
SC (n=18)	1 (5.5%)	1 (5.5%)	6 (33%)	0 (0)	18 (100%)

Conclusions: These data indicate 1) hKIM-1 is a sensitive and relatively specific marker for identifying CCRCC; 2) a combination of positive immunostaining for hKIM-1/S100/vimentin/EMA is a specific staining profile for CCRCC; 3) hKIM-1 may play a role in the pathogenesis/transformation of a mophologically benign cyst into CCRCC and a subset of MLRC could be a precursor lesion of CRCC; and 4) S100 and P504S have a limited value in distinguishing cystic CRCC from benign cystic lesions.

799 Prostate Cancer Is Associated with Increased Expression of Nuclear Cyclin D1

R Simon, PA di Sant'Agnese, JL Yao, PA Bourne, KA Bohrer, J Huang. University of Rochester Medical Center, Rochester, NY.

Background: Cyclin D1 is a critical regulator of cell cycle progression. In prostate cancer (PC), it has been proposed that its role may be to regulate androgen-dependent transcription and cell cycle progression. Despite the potential significance of this molecule in the carcinogenesis of PC, few studies have compared its expression in benign and malignant prostate tissue in detail.

Design: Immunohistochemical staining was performed on tissue microarrays containing benign prostate, prostatic intraepithelial neoplasia (PIN) and PC using a monoclonal anti-cyclin D1 antibody (Novacastra, Cat# NCL-L-Cyclin D1-GM, 1:50 dilution), which gives nuclear staining in positive cells. The staining was analyzed using the ACIS II imaging system (Dako/Chromavision, Carpinteria, CA) that generated scores of 0 to 5 based on percentage of positive cells and intensity. Based on controls, negative staining was defined as a score of < 1.75 and positive staining as > or = 1.75. Statistical analysis was performed by Fisher Exact Test.

Results: The majority of benign prostate and PIN were negative for cyclin D1 while the majority of low grade PC (Gleason patterns 2 and 3) and all high grade PC (Gleason patterns 4 and 5) were positive (Table 1). The difference in nuclear cyclin D1 expression between benign prostate and PIN was not statistically significant. The difference in nuclear cyclin D1 expression between benign prostate and PC was statistically different (P<0.001), as was that between PIN and PC (P<0.001). The difference in nuclear expression of Cyclin D1 between low grade PC and high grade PC was not statistically different.

Conclusions: 1. Cyclin D1 is significantly over-expressed in PC in comparison to benign prostate and PIN, suggesting that aberrant cell cycle regulation plays an important role in the carcinogenesis of PC. 2. Expression of cyclin D1 is not significantly increased in PIN over benign prostate, suggesting that aberrant cell cycle regulation may be a later event in the carcinogenesis of PC.

Nuclear Expression of Cyclin D1 in Benign and Malignant Prostatic Tissue

	Positive	Negative
Benign Prostate	16% (17/109)	84% (92/109)
PIN	30% (8/27)	70% (19/27)
Low Grade PC	91% (61/67)	9% (6/67)
High Grade PC	100% (39/39)	0% (0/39)
All PC	94% (100/106)	6% (6/106)

800 Novel Anti-PSMA Monoclonal Antibodies Show Superior Tissue Specificity

K Sircar, N Bernard, AC Cuello, HU Saragovi, P Gold, AG Aprikian, S Moffett. McGill University, Montreal, QC, Canada; ProScan Rx Pharma, Montreal, QC, Canada.

Background: PSMA, a type II membrane protein expressed on prostatic acinar cells, is a potentially attractive target for prostate cancer diagnostics and therapeutics. We have generated novel murine monoclonal antibodies(mAb) against a specific extracellular peptide epitope of PSMA and tested their tissue reactivity by immunohistochemistry.

Design: We have used mAbs called 17G1 and 20F2 to screen tissue microarrays of 22 different normal tissues and 19 different tumor types in order to characterize their recognition specificity. The immunohistochemistry was performed on antigen retrieved, formalin fixed, paraffin embedded material. Anti-PSMA mAbs J591 and 7E11 were used as reference standards.

Results: 17G1 and 20F2 both showed the expected immunoreactivity to the apical surface of prostatic acinar cells in benign, premalignant and malignant prostatic tissues. Similar to J591, staining of cancer sections was more intense than benign.

Anti-PSMA tissue specificity

Tissue	J591	17G1	20F2
Skeletal muscle	+	+	-
Small bowel	weak	+	+
Kidney tubules	+	+	-

Nonreactive normal tissues included fat, bladder, brain, colon, esophagus, gallbladder, heart, liver, lung, pancreas, rectum, skin, spleen, stomach, testis, thymus, thyroid, tonsil.

Anti-PSMA tumor specificity

Tumor	J591	17G1	20F2	7E11
Rhabdomyosarcoma	-	+	-	+
Melanoma	-	+	-	+
Thyroid Carcinoma	-	-	-	+
Gastric Carcinoma	-	+	-	weak

Nonreactive tumors included astrocytoma, carcinoid, colon Ca, epithelioid sarcoma, Ewings sarcoma,, hepatocellular Ca, Hodgkin's and non-Hodgkin's lymphoma, lung Ca, leiomyoma, MFH, mesothelioma, pancreatic Ca, renal Ca.

Conclusions: Our study demonstrates that anti-PSMA mAb 20F2 shows superior tissue specificity compared to J591. While maintaining prostate tumor specificity, it did not recognize kidney or skeletal muscle which were stained by J591 and 17G1.

801 Multiple Anti-Cancer Target Expression in Hormone Refractory Prostate Cancer

K Sircar, M Blumenkrantz, I Zlobec, G Chen, M Fahmy, A Aprikian, MC Guiot. McGill University Health Center, Montreal, QC, Canada; Centre Hospitalier Universitaire de Montreal, Montreal, QC, Canada.

Background: Simultaneous inhibition of multiple anticancer targets is increasingly being exploited in numerous clinical trials. Treatment options for hormone refractory prostate cancer(HRPCa) are limited with preliminary data showing a synergistic effect when combining standard docetaxel based chemotherapy with targeted therapy . We evaluated the co-expression pattern, in HRPCa, of multiple targets for which synthetic inhibitors are available.

Design: Androgen independent prostate cancer tissues were obtained from transurethral resectates of 37 patients with hormone refractory prostate cancer(mean, 62.9 years; PSA 310). A tissue microarray(TMA) was constructed from these tissues using quadruplicate 1 mm cores. The TMA was immunostained with antibodies against EGFR, VEGF, c-Kit, COX-2 and Her2/neu. FISH was performed with a dual colored probe against the EGFR gene and CEP 7.

Results:

Frequency distribution of multi marker phenotypes

EGFR	VEGF	c-Kit	COX-2	Her-2/neu	N(%)
-	+	-	+	-	9(25%)
-	-	-	+	-	6(16.7%)
-	+	+	+	-	5(13.9%)
+	+	-	+	-	4(11.1%)
+	+	+	+	-	3(8.3%)
-	+	-	+	+	3(8.3%)
+	+	-	+	+	2(5.6%)
-	-	+	+	-	2(5.6%)
-	+	+	+	+	1(2.8%)
+	-	+	+	+	1(2.8%)

The EGFR gene was not amplified in any of the cases by FISH.

Frequency distribution of tumor markers

	Positive	Negative	p-value	Interpretation
EGFR	10(28%)	26(72%)	0.0077	Significantly more negative
VEGF	28(76%)	9(24%)	0.0018	Significantly more positive
c-Kit	13(35%)	24(65%)	0.071	No difference
COX-2	37(100%)	0(0%)	<0.0001	All positive
Her-2/neu	7(19%)	30(81%)	0.0002	Significantly more negative

Conclusions: Though Cox-2 inhibitors appear uniformly indicated in this setting, the broad distribution of multi-marker phenotypes seen in HRPCa supports an individualized, tailored approach to realize the full synergistic effect of anti-cancer targeted therapy.

802 Histologic Landmarks That Define Extraprostatic Extension (EPE) at the Prostatic Apex: Characteristics of Extraprostatic Tissue at the Apex as Dissected by Robotic Radical Prostatectomy (RP)

SJ Sirintrapun, GP Paner, J Tomaszewski, N Narula, D Lee, T Ahlering, A Tewari, MB Amin. Cedars-Sinai Medical Center, Los Angeles, CA; University of Pennsylvania, Philadelphia, PA; University of California-Irvine, Orange County, CA; Cornell University, New York, NY.

Background: In contemporary surgical pathology of the prostate, EPE is not generally diagnosed at the apex due to the lack of a well defined "capsule" in this region. We have frequently observed the presence of adipose tissue in prostates resected by robotic prostatectomy. The aim of this study was to define apical extraprostatic tissue (AEPT); the involvement of which by prostatic carcinoma (PCa) would imply pT3 disease at the apex.

Design: The apices of 75 consecutive specimens from a multi-institutional study of robotically-assisted RP performed by the da Vinci robotic system (Intuitive Surgical Inc., Sunnyvale, CA), sectioned according to a standard protocol; and examined by a single observer were evaluated for AEPT.

Results: The AEPT was relatively well demarcated from the prostatic fibromuscular parenchyma/skeletal muscle, and from the parenchyma to the ink margin revealed (a) loose connective tissue with variable neurovascular tissue; (b) striated muscle which was contiguous with muscle within the prostate; (c) adipose tissue and (d) smooth muscle, all in variable proportions and combinations. AEPT was seen in 92% of samples, it was composed of loose connective tissue (LCT) only in 1.3%, LCT with adipose tissue in 17.3%, and LCT, adipose tissue and smooth muscle in 73.2%. Fat was focal (single cluster of adipocytes) in 41.3% of cases, was moderate (more than a cluster but less than 75% of AEPT in at least one section) in 21.3% of cases, and abundant in (>75% of a section with AEPT containing fat) in 28.0% of cases. PCa involved the apex in 40.0% of cases and extended to the surgical margin in 6.6% at sites where AEPT was absent. AEPT was uninvolved by PCa in this series.

Conclusions: Our study expands the histology of the prostatic apex beyond that described in the current literature with very frequent observations of adipose tissue at this site. The tissue boundaries beyond those traditionally described in perineal and retropubic RP are most likely attributable to the enhanced visibility and facilitated dissection of the apex provided by the robotic technique. These observations have important implications for diagnosing pT3 disease in PCa at the apex of the gland.

803 The RNA Binding Protein IMP3: A Noval Molecular Marker To Predict Aggressive Superficial Urothelial Carcinoma of the Bladder

L Sitnikova, Q Liu, G Mendese, BA Woda, D Lu, KL Rock, Z Jiang. University of Massachusetts Medical Center, Worcester, MA.

Background: The Majority (75%) of urothelial carcinomas (UC) of the bladder is superficial tumors. It is clinically important to identify a subgroup of the aggressive superficial UCs with tumor progression (deeper invasion or metastasis). In this study, we investigated whether the RNA binding protein-3 (IMP3), an oncofetal protein, can serve as a new biomarker to predict progression and metastasis of superficial UC of the bladder.

Design: Survival analyses were performed on 214 patients with superficial UCs in their bladder biopsies (Ta, n=171; Tis, n=14; T1, n=29). The expression of IMP3 was evaluated by immunohistochemistry. 28 metastatic UCs were also evaluated for IMP3 expression.

Results: The expression of IMP3 protein was observed in the cytoplasm of tumor cells, but not in benign tissue adjacent to the cancer. 21% (45 of 214) of primary superficial UCs and 93% (26 of 28, P<0.001) of metastatic UCs expressed IMP3. Kaplan-Meier plots showed that patients without IMP3 expression in their superficial UCs had significant longer progression-free survival and disease-free survival than patients with IMP3 expression (P=0.0002). The 5-year progression-free survival rate was 90% in IMP3 negative patients versus 60% in IMP3 positive patients (P=0.0002). The 5-year disease-free survival rate was 96% in patients without expression of IMP3 versus 75% in patients with IMP3 expression (P=0.001). In Ta disease, 19% of IMP3 positive patients versus 6% of IMP3 negative patients showed progression (P=0.0098). In T1 disease, 60% of IMP3 positive patients versus 22% of IMP3 negative patients were found to have tumor progression (P=0.03) while 60% of IMP3 positive patients developed metastasis and no metastasis was found in IMP3 negative patients (P=0.0017). Multivariable analyses assessing the simultaneous contribution of other risk factors (tumor stage, grade, size and multiplicity, and patientstreatments et al) showed that the expression of IMP3 in the superficial UCs was an independent predictor of tumor progression. The hazard ratios of IMP3 status in superficial UCs were 3.87(progression-free survival, P=0.002) and 6.86 (metastasis-free survival, P=0.03).

Conclusions: IMP3 is an independent prognostic marker that can be used at the time of initial diagnosis of superficial UCs to identify a group of patients with a high potential to develop progression and metastasis, and who might benefit from early therapy.

804 LAMC2 mRNA and Protein Expression in Carcinoma of the Bladder

SC Smith, HF Frierson, D Theodorescu. University of Virginia Health System, Charlottesville, VA.

Background: LAMC2 (the laminin 5 gamma 2 subunit) is a component of the heterotrimeric laminin 5 basement membrane glycoprotein. We recently found LAMC2 to be overexpressed in a metastatic gene expression signature in a mouse model of human bladder carcinoma (BC).

Design: We examined the mRNA and protein expression of LAMC2 in BC-derived cell lines and primary tumor tissues by oligonucleotide DNA microarrays and a tissue microarray for immunohistochemistry (IHC).

Results: Using IHC, we found positivity for LAMC2 in 17 of 30 BC cell lines. In a cohort of BCs and normal urothelia (N=65 and N=20, respectively), we observed overexpression of LAMC2 mRNA in all BC (2.6-fold, P=.002) and especially in muscle invasive T2+ BCs (5.1 fold, P=.002) compared to normal urothelia. mRNA overexpression also occurred in muscle invasive T2+ BCs compared to superficial BCs (4.2-fold, P=.004). Using immunohistochemistry and a tissue microarray of BCs (N=167), we found significant associations of LAMC2 positivity with grade (P=.0003) and nodal status (P=.005). Moreover, LAMC2 positivity was associated with recurrence at 40 months, approaching significance in this cohort (P=.07).

Conclusions: These results suggest that LAMC2 has a role in promoting invasion and metastasis in human bladder carcinoma, and we propose investigation of the role of LAMC2 in these processes.

805 Grade Is More Influential on Prognosis Than Depth of Invasion in Penile Squamous Cell Carcinoma. An Outcome Study Comparing Paradoxical Superficial High Grade and Deeply Invasive Low Grade Tumors

FA Soares, I Werneck da Cunha, ML Oliveria L, GC Guimaraes, EF Velazquez, JJ Torres, A Chaux, AL Cubilla. Hospital do Cancer AC Camargo, Sao Paulo, Brazil; Harvard Medical School, Boston, MA; Instituto de Patologia e Investigacion; Facultad de Ciencias Medicas, Asuncion, Paraguay.

Background: There is a correlation of progressively deeper infiltration, higher tumor grade and adverse prognosis in penile cancer. However there are some superficial tumors depicting a high histological grade as well as deeply infiltrating neoplasms showing low grade histology. The outcome of these unusual presentations is not known.

Design: The aim of this study was to evaluate outcome in superficially invasive high grade (SHG) and in deeply invasive but low grade tumors (DLG). Penectomies, bilateral groin dissections and outcome were recorded in 30 SHG and 6 DLG neoplasms. These tumors were identified from a group of 375 penectomies for SCC treated at the Hospital do Cancer AC Camargo in Sao Paulo, Brazil. Superficial tumors were defined as neoplasms invading lamina propria and/or superficial corpus spongiosum up to 5 mm from tumor surface. Lesions invading deep corpus spongiosum and/or corpus cavernosum were considered as deep tumors. Carcinomas with any proportion of anaplastic cells were classified as high grade. The remainder were low grade.

Results:

Tumors	Cases	Neg nodes	Pos nodes# (%)	DOD# (%)
SHG	30	12	8 (27)	3 (10)
DLG	6	6	0 (0)	0 (0)

SHG: superficial high grade; DLG:deep low grade; Neg: negative; Pos: positive: DOD: dead of disease.

Conclusions: Twenty seven percent of patients with superficial high grade tumors showed lymph node metastases and 10% died of the disease. Interestingly, no matter how deep the tumor invaded, none of the patients with low grade SCCs had positive nodes or died of the disease. Histological grade appears to be more important than tumor depth in these unusual and paradoxical clinical presentations.

806 Quantitative Tissue PSA mRNA Expression as a Predictor of Outcome in Radical Prostatectomy and Alterations in the Androgen Signaling Pathway

J Sterbis, C Gao, B Furusato, J Cullen, Y Chen, L Ravindranath, DG McLeod, I Sesterhenn, G Petrovics, S Srivastava. CPDR, Rockville, MD; AFIP, Washington, DC; WRAMC, Washington, DC.

Background: While pre-operative serum PSA is a documented predictor of biochemical outcome following radical prostatectomy, tissue PSA expression has not been similarly investigated. As such, we compared tissue PSA mRNA expression in malignant cells to clinical outcome. We also hypothesized that as an androgen-dependent gene, tissue PSA expression could provide a functional assessment of androgen signaling in prostate cancer.

Design: Laser-capture microdissection (LCM) identified benign and malignant epithelial cells in 121 patients following radical prostatectomy. Expression of tissue PSA mRNA was determined by quantitative real-time RT-PCR. PSA expression within malignant cells was compared with matched benign cells, serum PSA, Gleason score, pathologic tumor stage and biochemical survival. Regression tree analysis delineated high and low tumor PSA expression groups, which were compared to androgen-dependent (PMEPA1, ERG, DD3) and androgen-independent (LTF, AMACR) gene expression within tumor cells.

Results: Paired T-test demonstrated that malignant cells expressed lower tissue PSA levels than matched benign cells (p=0.0133). Spearman correlation analysis found that PSA serum protein and tissue mRNA levels are not related (p=0.9635). Univariate analysis identified that tissue PSA expression was related to biochemical recurrence (p=0.0130) and pathologic T stage (p=0.0065). Kaplan-Meier analysis confirmed that tissue PSA expression in malignant epithelial cells predicted biochemical recurrence (p=0.0205). While androgen-independent genes demonstrated expression levels independent of tissue PSA, expression of androgen-dependent genes significantly correlated with each other at high tissue PSA.

Conclusions: Independent of serum PSA, increased neoplastic tissue PSA expression predicts biochemical recurrence and pathologic T stage and may represent changes in the androgen-signaling pathway.

807 Annexin II in the Atrophy To PIN Continuum

JM Stewart, N Fleshner, HL Cole, JM Sweet. University Health Network, Toronto, ON, Canada; Princess Margaret Hospital, Toronto, ON, Canada.

Background: Atrophy (ATR) associated with inflammation is a putative precursor to prostatic intraepithelial neoplasia (PIN). A precursor relationship requires direct morphologic continuity. Annexin II (ANXII) is a novel biomarker, proposed as a negative marker of PCa and PIN. In a tissue microarray (TMA) of ATR we evaluated ATR to PIN transitions, proliferation and ANXII expression to investigate the ATR to PIN continuum.

Design: A TMA was constructed from foci of ATR adjacent to PCa from 43 radical prostatectomies and each case was represented by three 1mm cores. Inflammation was noted for each core. Immunohistochemistry for ANXII and Ki-67 was performed. Ki-67 was used to score the proliferative index (number of positive nuclei versus the total number of epithelial cells)(PI). ANXII expression was scored based on the percentage of cells with cytoplasmic staining. Morphologic features were examined on a serial H&E section. ANXII and PI scores were assigned to PIN, ATR and PCa.
Results: 125 cores contained ATR, 52 PIN and 16 PCa. PIN comprised all cells with pinpoint nucleoli and nuclear atypia, consistent with high and low grade PIN. Inflammation and proliferation were observed in 76 and 52 cores containing ATR, respectively. In addition 4 and 13 cores containing PCa and PIN respectively demonstrated proliferation. All ATR epithelial cells demonstrated positive ANXII reactivity in the cytoplasm. Loss of ANXII was observed in all PIN and PCa cells. 35 cores showed both ANXII positive and ANXII negative reactivity, representing 53% of patients. Correlation with the serial H&E sections showed that cells with ANXII loss had morphological features of PIN whereas ANXII positive cells had features of ATR. These glands demonstrated a transition between ATR and PIN. No correlation was found between inflammation and ANXII loss or co-existence of ATR and PIN in the same gland. No difference in PI was observed between cores containing ATR into PIN transitions and those without. T-test analysis revealed a significantly higher PI in ATR with adjacent inflammation (p=0.04).
Conclusions: We confirm that ATR is proliferative and show that ATR with inflammation is more proliferative than that without. We demonstrate direct continuity of PIN and ATR in individual glands validating the existence of an ATR-PIN transition. ANXII proves to be a negative marker of PIN and a positive marker of ATR. ANXII may aid in the identification of transitioning glands in order to determine their role in prostatic neoplastic progression.

808 Inflammatory Myofibroblastic Tumor of Urinary Bladder: Immunohistochemical, Molecular, and Cytogenetic Characterization and Comparison

WR Sukov, AW Carlson, BM Shearer, KL Grogg, JC Cheville, RP Ketterling. Mayo Clinic, Rochester, MN.
Background: Inflammatory myofibroblastic tumor (IMT) of urinary bladder is a rare neoplastic spindle cell proliferation that can display cytologic atypia, cellularity, infiltrative growth and mitotic activity mimicking malignant tumors such as leiomyosarcoma, rhabdomyosarcoma, and sarcomatoid carcinoma (SC).
Design: Formalin-fixed, paraffin embedded tissue of primary urinary bladder spindle cell lesions obtained by transurethral resection, resection and cystectomy including 21 cases of IMT, 16 cases of leiomyosarcoma, 8 cases of SC, 3 cases of reactive myofibroblastic proliferations (including postoperative spindle cell nodule) and 3 cases of embryonal rhabdomyosarcoma were obtained from Mayo Clinic and consultation files. All cases were studied for expression of ALK-1, muscle, epithelial, neural, and follicular dendritic cell differentiation markers by immunohistochemistry and for EBV RNA by in situ hybridization. Also, all cases were studied in a blinded manner for *ALK* gene translocations by fluorescence in situ hybridization (FISH) using probes toward the regions flanking the *ALK* gene on chromosome 2p23.
Results: Clinical follow up for 11 of the 21 cases of bladder IMT ranging from 7 to 70 months with a mean follow up time of 36 months (median 34 months) identified no recurrences. Immunohistochemical analyses using markers for muscle, epithelial, neural, and follicular dendritic cell differentiation showed significant overlap between IMT with and without *ALK* gene translocations, and between IMT and malignant spindle cell tumors of the urinary bladder. In situ hybridization for EBV RNA was negative in all cases. In IMT of bladder, ALK-1 protein expression was identified in 13 of 21 cases (62%) and *ALK* gene rearrangements were present in 14 of 21 cases (67%). All cases of IMT that demonstrated ALK-1 expression carried *ALK* gene rearrangements and one case that was negative for ALK-1 protein expression by immunohistochemistry exhibited the *ALK* gene rearrangement. All cases of leiomyosarcoma, SC, embryonal rhabdomyosarcoma, and reactive myofibroblastic proliferations were negative for both ALK-1 protein expression by immunohistochemistry and *ALK* gene rearrangements by FISH.
Conclusions: We confirm the utility of immunohistochemical detection of ALK-1 protein, and FISH analysis for *ALK* gene translocations in separating IMT from malignant spindle cell tumors of the urinary bladder.

809 Clear Cell Adenocarcinoma of the Urinary Bladder and Urethra: Another Adenocarcinoma Positive for P504S

Y Sun, Y Huan, P Unger. Mount Sinai Medical Center, New York, NY.
Background: Clear cell carcinoma of the urinary bladder/urethra is a rare tumor histologically resembling the neoplasms in the female genital tract. Adequate characterization of this tumor has been hampered by its rarity. P504S was originally reported in prostatic adenocarcinoma, however, other adenocarcinomas have now been found to be reactive to this antibody (papillary renal cell carcinoma and gastrointestinal neoplasmas). In this study, we investigated the immunohistochemical staining profile in four primary clear cell carcinoma of urinary tract, including P504S, which has not been previously evaluated in these tumors.
Design: Four cases of clear cell adenocarcinoma were selected from our archives; 2 cases from urinary bladder (one male patient and one female patient) and two cases from urethra (both female patients; one in a diverticulum). Immunohistochemistry performed on the cases were P504S, K903, CK7, CK20, CA125, and p63. Staining was graded with a semiquantitative scale, with 0 indicating less than 5% of the tumor cells are positive; +, 5-25%; ++, 25-50%; and +++, more than 50% are positive; NA, not available.
Results:

Results of immunohistochemistry analysis

	P504S	CK7	CK20	CA125	K903	P63
1	+++	+++	++	++	+++	0
2	+++	+++	++	+	+++	0
3	+++	+++	0	0	+++	0
4	+	+++	0	NA	NA	NA

Conclusions: We found that clear cell carcinomas had a distinct immunoreactive profile: positive for P504S, K903, CK7, CA125 and usually positive for CK20; negative for p63. Although this immunohistochemical profile has some similarity to conventional urothelial carcinoma, it deviates from these tumors in being P504S positive and P63 negative. This staining profile may suggest a non-urothelial origin for these tumors which needs to be further investigated.

810 α-Methylacyl-CoA Racemase (P504S)/34βE12/p63 Triple Cocktail Stain in Prostatic Adenocarcinoma Following Hormonal Therapy

MT Sung, Z Jiang, R Montironi, GT MacLennan, R Mazzuccelli, L Cheng. Indiana University School of Medicine, Indianapolis, IN; Chang Gung Memorial Hospital-Kaohsiung Medical Center, and Chang Gung University College of Medicine, Kaohsiung, Taiwan; University of Massachusetts Medical School, Worcester, MA; School of Medicine, Polytechnic University of the Marche Region (Ancona), Ancona, Italy; Case Western Reserve University, Cleveland, OH.
Background: Our current investigation was conducted to evaluate the expression of AMACR in patients with prostate carcinoma following hormonal therapy and assess its diagnostic utility in combination with p63 and high molecular weight cytokeratin (34βE12) staining.
Design: Prostate tissues from 49 patients who had been treated with hormonal therapy were immunohistochemically analyzed for AMACR, 34βE12 and p63 expression by a triple antibody cocktail stain.
Results: All malignant acini were completely negative for both basal cell markers (34βE12 and p63). Tumor cells failed to demonstrate expression of AMACR in 14 of 49 cases (29%). In the remaining 35 cases (71%), positive immunostaining for AMACR was noted, but with variable intensities and percentages of cells stained. Positive staining for AMACR in benign glands was not seen in any case. In all cases, basal cells were strongly stained by p63 in benign acini with a mean positive percentage of 96%. Similarly, basal cells in benign acini displayed moderate staining intensities for 34βE12 in 3 of 41 cases (7%) and strong immunostaining for this marker in the remaining 38 cases (93%). AMACR expression may be substantially diminished or entirely lost in prostate carcinoma following hormonal therapy. This variation in AMACR expression does not correlate with the metastatic status, the modality of hormonal therapy or the extent of therapy-related effect.
Conclusions: It is important that pathologists be aware that some hormonally treated prostate carcinomas do not express AMACR, and that immunostaining in such cases must be interpreted with caution. A triple cocktail stain employing AMACR, 34βE12 and p63 can be helpful in evaluating prostate specimens for the presence of residual or recurrent carcinoma following hormonal therapy for cancer.

811 Urothelial Inverted Papilloma: A Clinicopathologic Analysis of 75 Cases

MT Sung, GT MacLennan, A Lopez-Beltran, R Montironi, L Cheng. Indiana University School of Medicine, Indianapolis, IN; Chang Gung Memorial Hospital-Kaohsiung Medical Center, and Chang Gung University College of Medicine, Kaohsiung, Taiwan; Case Western Reserve University, Cleveland, OH; Cordoba University, Cordoba, Spain; School of Medicine, Polytechnic University of the Marche Region (Ancona), United Hospitals, Ancona, Italy.
Background: Inverted urothelal papilloma is an uncommon urothelial neoplasm. Although it is traditionally regarded as a benign tumor, conflicting data on multiplicity, recurrence rate and association with urothelial carcinoma have left uncertainties concerning its biologic behavior.
Design: The authors analyzed the clinicopathological characteristics of 75 patients of inverted papillomas in the urinary tract without prior or concurrent urothelial carcinoma to determine its biologic behavior and prognosis, and to correlate these findings with surveillance strategies.
Results: These patients ranged in age from 26 to 85 years (mean, 60 years). Of the 46 patients for whom tobacco use history was available, 28 gave a history of smoking. Inverted papilloma were located in the urinary bladder (67 cases), prostatic urethra (4 cases) and ureter (4 cases). The majority of vesical tumors arose from the trigone or near the bladder neck. Common presenting complaints included included hematuria, dysuria and irritative voiding symptoms. In one case of vesical inverted papilloma, recurrence of inverted papilloma occurred. All other patients were free of tumor recurrence or progression during a mean follow-up of 68 months (range, 2-240 months).
Conclusions: Both the extremely low incidence of tumor recurrence (1%) and strikingly favorable prognosis suggest that inverted urothelial papilloma, when diagnosed according to strictly defined criteria, is a benign urothelial neoplasm not related to urothelial carcinoma. Therefore, complete transurethral resection of inverted papilloma is adequate surgical therapy, and surveillance protocols as rigorous as those employed in the management of urothelial carcinoma seem unnecessary.

812 Primary Mediastinal Seminoma: An Immunohistochemical Study

MT Sung, GT MacLennan, A Lopez-Beltran, R Montironi, L Cheng. Indiana University School of Medicine, Indianapolis, IN; Chang Gung Memorial Hospital-Kaohsiung Medical Center, and Chang Gung University College of Medicine, Kaohsiung, Taiwan; Case Western Reserve University, Cleveland, OH; Cordoba University, Cordoba, Spain; School of Medicine, Polytechnic University of the Marche Region (Ancona), United Hospitals, Ancona, Italy.

Background: Accurate diagnosis of mediastinal seminoma is critical because of its favorable response to radiation therapy and/or cisplatin-based chemotherapy. However, variability in genetic alterations and immunoprofiles between mediastinal and testicular seminomas has been reported, bringing into question the usefulness of diagnostic markers for gonadal seminoma when applied to its mediastinal counterpart.

Design: We evaluated the staining characteristics of a battery of immunohistochemical stains applied to 20 primary mediastinal seminomas, and assessed the utility of these stains in the diagnosis of this tumor.

Results: Moderate to strong nuclear OCT4 staining was identified in all 20 cases (100%) of mediastinal seminoma, and positive staining in more than 50% of tumor cells was noted in all but one case. 15 tumors (75%) showed membranous expression of c-kit, with moderate to strong staining intensities and variable staining percentages. Weak to moderate staining intensity for PLAP was noted in 10 cases (50%) with occasional background staining artifact. No more than 50% of tumor cells were positively stained by PLAP in any case. The incidences of positive staining was 50% for AE1/3, 45% fo high molecular weight cytokeratin (34ßE12), 60% for Cam 5.2, 45% for CK7 and 5% for EMA respectively. In most cases these epithelial markers highlighted only a small portion of tumors cells, usually less than 25%, with variable intensities. Immunostains for CD30 and CK20 were completely negative in all cases.

Conclusions: OCT4 immunostaining, with its superior sensitivity and easy interpretation compared to other markers, appears to be a strong and reliable marker for diagnosing primary mediastinal seminoma. In addition, the patterns of cytokeratin expression in mediastinal seminoma may imply a higher degree of differentiation than in testicular seminomas, and pathologists must exercise caution in the interpretation of keratin immunostains in mediastinal neoplasms.

813 Immunohistochemical Analysis of a Novel Diagnostic Marker TT902 for Prostate Cancer and Comparison with AMACR

H Takahashi, H Kuruma, M Nakano, S Egawa, M Furusato, H Hano. The Jikei University School of Medicine, Minato-ku, Tokyo, Japan.

Background: We have found a novel protein TT902, highly expressed in LNCaP cells, by high molecular weight proteomics techniques. To investigate this protein as a diagnostic marker for prostate cancer, we performed an immunohistochemical analysis in clinical prostate cancer specimens. We also compared expression patterns of the protein to those of AMACR.

Design: Forty-six cases of clinical prostate cancer were used in this study. A polyclonal antibody for TT902 was generated and immunohistochemically stained on these cases. Simultaneously, AMACR (P504S) immunostaining was performed in the same sets. Staining intensity and distribution in whole tumor areas by these 2 antibodies were evaluated as 0, 1+, 2+, and 3+. Subsequently, the staining intensity was evaluated in the same manner on Gleason score (G.S.): 4-6 and G.S.: 7-10 area, separately.

Results: Results were summarized on Table 1 and 2. As shown, the staining intensity was stronger and the distribution was more widely spread in AMACR than in TT902. The AMACR protein was expressed widely both in GS:4-6 and 7-10 area. Whereas, TT902 was more intensely expressed (2+, 3+) in G.S. 7-10 area than in G.S. 4-6 area (p=0.0001). The more intense expression of TT902 was observed in Gleason pattern 4 tumors than in pattern 2 or 3. Such tendencies were not obsereved in AMACR expression.

Conclusions: A novel protein TT902 should have a potential as an alternative diagnostic marker for prostate cancer. Especially, this protein is suggested to selectively correlate with high grade tumor unlike AMACR.

Table 1 Immunohistochemical results in whole tumor area

	0	1+	2+	3+
TT902	1	10	30	5
AMACR	0	4	13	29

Table 2 Intensity of 2 proteins in G.S.4-6 area vs. 7-10 area

	0	1+	2+	3+
TT902 G.S. 4-6*	5	19	9	0
TT902 G.S. 7-10*	0	7	26	7
AMACR G.S. 4-6**	0	2	12	19
AMACR G.S. 7-10**	0	2	12	26

*distritution: statistically significant (p=0.0001); **not significant

814 Detection of Residual Tumor Cells in Bladder Biopsy Specimens: Pitfalls in the Interpretation of Cytokeratin Stains

EF Tamas, JI Epstein. Johns Hopkins Hospital, Baltimore, MD.

Background: The detection of a few residual tumor cells in bladder specimens with prior biopsy site changes can be challenging based on histology alone. Immunohistochemistry for CKs may be used as an adjunct in this situation.

Design: Immunohistochemistry for a panel of antibodies (AE1/AE3, CAM 5.2, high molecular weight cytokeratin, SMA, desmin and ALK) was performed on 29 cases of bladder biopsies with prior biopsy site changes.

Results: Of 29 patients, 25 had a prior history of bladder tumor: 17 had invasive high grade urothelial carcinoma (T1: 5 cases; T2: 11 cases; T3:1 case); 7 had noninvasive high grade papillary urothelial carcinoma; 1 had noninvasive low grade papillary urothelial carcinoma). One of the patients with noninvasive high grade papillary urothelial carcinoma and one of the patents with invasive high grade urothelial carcinoma had associated CIS. Four patients had prior benign bladder diagnoses. Of the 29 cases, 6 (21%) had cells with staining for at least two of the CK markers. AE1/AE3 was positive for cells in 8/29 cases (28%). In 6 of these cases cells displayed a spindle cell and 2 cases a more epithelioid morphology. CAM5.2 was positive in 5/29 cases (17%); 3 of the cases had spindle cell and 2 cases epithelioid morphology. High molecular weight cytokeratin was expressed in cells in 2/29 cases (7%) with 1 case having spindle cell and 1 epithelioid morphology. SMA was positive in cells with a spindle cell morphology and negative in the more epithelioid CK positive cells. Desmin was positive in 3/6 CK positive spindle cells and negative in CK positive epithelioid cells. ALK was negative in all the cases. Three cases with spindle cell morphology and positivity for at least one of the CKs and SMA stains were interpreted as aberrant keratin expression in myofibroblastic cells based on the staining and the morphology of the spindle cells. Another 3 cases with concurrent staining for at least one of the CKs, SMA and desmin were consistent with smooth muscle cells based on their cellular morphology. Another 2 cases had cells which expressed at least two CK markers but did not express SMA, desmin, or ALK and a more epithelioid morphology. These cells were interpreted as residual tumors cells.

Conclusions: When interpreting CK stains for detection of residual tumor cells, one should pay attention to the nature of the cells and not assume all CK staining cells are residual tumor cells.

815 Lympoepithelioma-Like Carcinoma of the Urinary Tract: A Clinicopathologic Study of 30 Cases

EF Tamas, JI Epstein. Johns Hopkins Hospital, Baltimore, MD.

Background: Lymphoepithelioma-like (LELC) of the urinary tract is rare and its prognosis remains uncertain due to the limited number of small series described in the literature.

Design: We studied 30 cases of LELC of the urinary tract from the consults files of one of the authors and from The Johns Hopkins Hospital between 1990-2005.

Results: The mean clinical follow up was 32 months. The mean age of the patients was 67. 6 years. All cases but two were located in the urinary bladder with one case located in the renal pelvis and one case in the urethra. Twenty cases (66.7%) were pure, 7 cases (23.3%) predominant (>50%), and the remaining 3 cases (10%) focal LELC. Of the 10 cases without pure LELC, the associated conventional component was invasive urothelial carcinoma (n=9) and invasive adenocarcinoma (n=1). One case of pure LELC had invasive squamous cell carcinoma on a subsequent cystoprostatectomy specimen. The surface demonstrated carcinoma in-situ (CIS) in 6 cases, non-invasive high grade papillary urothelial carcinoma in 3 cases, and in-situ adenocarcinoma in 1 case. In 19/30 (65.5%) of cases, the inflammatory component consisted of a heavy lymphocytic infiltrate and in the remaining 11/30 (34.5%) cases a mixed inflammatory infiltrate. All 28 cases were strongly positive for AE1/AE3 and 18/24 (75%) cases overexpressed p53. All cases were negative for EBER by in situ hybridization. Tumor stages at presentation were as follows: 7 cases T1 (23.3%); 14 cases T2 (46.6%); 7 cases T3 (23.3%); and 2 cases T4 (6.6%). Treatment consisted of cystoprostatectomy in 10/30 cases (33.3%); radical cystectomy in 3/30 cases (10.0%); partial cystectomy in 4/30 cases (13.30%); nephrectomy in 1 case (3.3%), and transurethral resection followed by radiation or chemotherapy in 12/30 (40.0%) cases. 8 of 27 cases with follow-up (30%) cases had recurrence of tumor. Of the 27 patients, 7 (26%) patients had metastases. 7/24 cases (29%) of pure/predominant LELC cases with follow-up had recurrence of tumor with 6 (25%) patients having metastatic disease. The 5-year actuarial recurrence-free risks were 68.5% and 71% for all and pure/predominant LELC, respectively.

Conclusions: In contrast to what the literature suggests, the current study demonstrates that LELC, whether in pure or predominant form, appears to have a similar prognosis to ordinary urothelial carcinoma.

816 Atypical Spindle Cell Proliferations in Adipose Tissue Adjacent to Renal Cell Carcinomas, a Lesion Mimicking Well-Differentiated Liposarcoma

MR Tanas, C Sthapanachai, A Oliveira, BP Rubin. University of Washington, Seattle, WA; Mayo Clinic, Rochester, MN.

Background: Two cases of renal cell carcinoma (RCC) encountered in consultation demonstrated marked cytological atypia in the peri-nephric fibroadipose tissue, mimicking well-differentiated liposarcoma. Additional cases were examined to determine the frequency of these lesions. Fourteen such cases are presented.

Design: The clinical and pathological records of 59 consecutive nephrectomies containing RCC, spanning 14 months in the UWMC database, were reviewed. Immunohistochemistry (IHC) was performed by the avidin-biotin-peroxidase complex method using commercially available antibodies to the following antigens: AE1/AE3, Cam 5.2, cytokeratin 7, EMA, S-100 protein, smooth muscle actin (SMA), and desmin. Fluorescence in situ hybridization (FISH) for *MDM2*, an oncogene commonly amplified in well-differentiated liposarcoma, was performed in 5 selected cases.

Results: Twelve cases (20%) contained cytological atypia in the perinephric fat similar to the two index cases. The cytology of these cells ranged from enlarged, hyperchromatic spindle cells to floret-type multinucleate cells. Ten (17%) invaded through the renal capsule into the perinephric adipose tissue. Of those cases, 3 (30%) contained the aforementioned atypical cells. In contrast, 9 cases without extrarenal invasion (18%) contained the atypical spindle cells. Of the cases with atypical spindle cells, three (25%) were associated with extrarenal involvement. The atypical spindle cells exhibited focal to variable positivity for SMA and desmin in 3 of the 14 cases each. Pan-cytokeratin, Cam 5.2, CK7, EMA, and S-100 were negative in all cases. No *MDM2* amplification was found in the atypical spindle cells.

Conclusions: The atypical spindle cells were not uncommon, present in 20% of all cases, and more common (30%) in those with extrarenal involvement. The IHC and FISH results essentially exclude the possibility that these cells represent infiltrating

single RCC cells or the spindle cells of a well-differentiated liposarcoma. Instead, they suggest that the atypical cells are likely reactive (myo)fibroblasts. An association with extrarenal extension suggests they are reacting to infiltrating RCC cells. Despite the low likelihood of a concurrent RCC and liposarcoma, recognition of these atypical (myo)fibroblasts and their ability to mimic a liposarcoma may help in avoiding the potential pitfall of diagnosing a second malignancy.

817 Papillary Renal Carcinomas with Clear Cells: Clinicomorphological Features

DA Teixeira, A Billis, RF Stelini, AAA Vital-Brasil, F Denardi. School of Medicine, University of Campinas, Unicamp, Brazil.

Background: The significance of clear cell change in papillary renal carcinomas is not established.

Design: Between 1996 and 2006 we found 25 papillary tumors showing clear cells. Five tumors were pure papillary (4 type 2 and 1 mixed types 1 and 2). The remaining tumors presented additionally areas with non-papillary arrangement (solid, tubular, glomeruloid or other patterns). All tumors were classified as having <65% or 65-100% of the area with papillary arrangement and <35% or 35-100% of the area with clear cells. The TNM classification of malignant tumors (2002) was used for stage grouping and T category.

Results: The patient age ranged from 40 to 82 years (mean:46) with male predominance (19 males and 6 females). Six (24%) tumors showed clear cells only in papillary areas, 2 (8%) tumors only in non-papillary areas, and 17 (68%) tumors in both papillary and non-papillary areas. Three (30%) and 7 (70%) of tumors with <65% papillary pattern, and 10 (66.7%) and 5 (33.3%) of tumors with 65-100% papillary pattern corresponded to categories T1a/T1b and T2, respectively. Five (50%) and 5 (50%) of tumors with <65% papillary pattern and 11 (73.3%) and 4 (26.6%) of tumors with 65-100% papillary pattern corresponded to stage grouping I/II and III/IV, respectively. Eight (53.3%) and 7 (46.7%) of tumors with <35% clear cells, and 5 (50%) and 5 (50%) of tumors with 35-100% clear cells corresponded to categories T1a/T1b and T2, respectively. Eleven (73.3%) and 4 (26.7%) of tumors with <35% clear cells, and 5 (50%) and 5 (50%) of tumors with 35-100% clear cells corresponded to stage grouping I/II and III/IV, respectively.

Conclusions: Papillary tumors with non-papillary areas, and tumors with more extensive areas with clear cells tend to have higher diameter and higher stage grouping (TNM, 2002). It has to be established whether papillary tumors showing non-papillary patterns represent papillary differentiation in the progression of conventional clear cell renal carcinomas or combined tumors.

818 Müllerian-Type Stroma in Kidneys: Possible Metaplastic Response to Obstruction

SK Tickoo, LR Harik, JJ Tu, A Gopalan, HA Al-Ahmadie, SW Fine, S Olgac, VE Reuter. Memorial Sloan-Kettering Cancer Center, New York, NY; Weill Medical College of Cornell University, New York, NY.

Background: The presence of Müllerian-type (MT) stroma is a well known feature in renal mixed epithelial and stromal tumor (MEST) and cystic nephroma. It has been suggested that estrogen and progesterone-receptor (ER and PR) positivity in MEST may be etiologically related to hormonal therapies- a more frequent phenomenon in the recent years. We have observed MT stroma in many non-neoplastic, as well as in tumor-bearing kidneys away from the tumor, in the past few years, and herein we present our experience with 10 such cases.

Design: In a prospective manner, whenever we noted MT stroma, immunohistochemical stains for ER and PR were performed on kidneys removed for any cause. Detailed morphologic analysis of the lesion, as well as the rest of the kidney was performed, and clinical details were obtained from the clinical records.

Results: There were 8 males and 2 females in the group. The ages ranged from 11 months to 71 years. To the best of our knowledge, none of the males was on hormone therapy. In 6 cases, the nephrectomies were performed for a non-functional kidney, and in 3 cases for tumors [1 each of chromophobe, conventional, and acquired cystic disease (ACD)-associated renal cell carcinoma]. One case was a partial nephrectomy for vesico-ureteric reflux with upper pole hydronephrosis. The MT stroma was present in 9 cases as a non-mass forming proliferation around dilated, inflamed pelvicalyceal system. In one case MT stroma was present at the periphery of a markedly cystic ACD-associated RCC. The only common finding in all cases was a global or segmental hydronephrosis, or changes related to localized obstruction within the renal parenchyma most likely due to tumor compression. On immunohistochemical staining, the stroma was positive in variable proportions for ER in all 10 cases, and for PR in 8.

Conclusions: MT stroma can be present in the kidney, not only as a part of MEST or cystic nephroma, but also in association with other neoplastic and medical conditions. It is almost always associated with obstruction to the urinary outflow, and most likely represents a metaplastic change.

819 Primary Clear Cell Renal Cell Carcinoma (CRCC) and Its Paired Metastasis: A Comparative Histomorphologic and Immunohistochemical Study

SK Tickoo, A Gopalan, HA Al-Ahmadie, SW Fine, S Olgac, VE Reuter. Memorial Sloan-Kettering Cancer Center, New York.

Background: In evaluating a metastasis (M) from a renal primary (P), it is generally assumed that M will have morphologic and immunohistochemical (IHC) features similar to the tumors at the P site. However, few detailed studies supporting this assumption are available. Therefore, we performed a detailed morphologic and IHC investigation on P CRCC and their paired M.

Design: 40 consecutive cases of CRCC with M, which were part of another ongoing study, were studied. Detailed morphologic analysis was performed on both the P and their M. IHC staining was performed on one representative paraffin block from both the sites, using Cam5.2, CD10, Vimentin, and CK7 antibodies, as well as hypoxia-inducible pathway markers- HIF-1a and carbonic anhydrase IX (CA IX). The IHC results were graded as 0 (0-5% positive cell), 1+ (6-25), 2+ (26-50) and 3+ (>50% cells).

Results: The M sites included lungs (12), bones (6), lymph nodes (7), adrenal and brain (4 each), pancreas (3), thyroid, ovary, spleen and retroperitoneum (1 each). Size of the P ranged from 2-13.5 cm (mean, 8.4).The pT stages were 1 (4 cases), 2 (1), 3a (14), 3b (20) and 4(1). 35 of 40 P (87%) were nuclear grade 3 or 4 (HG), either exclusively (14; 35%) or associated with grade 1 or 2 (LG) areas (21; 52%). In 30/40 cases, M was exclusively HG, irrespective of whether the P was purely, predominantly, or focally HG. Some unusual morphologic features observed at both sites included focal to prominent papillary (6 cases), sarcomatoid (3), and rhabdoid (2) areas. Overall, 2 or 3+ positivity with CA IX, HIF-1a, CD10, Vimentin, Cam5.2 and CK7 was observed in 84, 66, 77, 64, 45, and 5% of P, and 89, 82, 70, 79, 45, and 8% of M, respectively. Although, the overall staining between P and M does not appear significantly different, comparison of individual pairs of tumors showed difference of positivity by more than 1 grade in 24, 29, 31, 26, 39, and 11% for CA IX, HIF-1a, CD10, Vimentin, Cam5.2 and CK7. For each antibody, there was an almost equal proportion of cases in which M showed either greater or lesser positivity than P.

Conclusions: 1) M from CRCC are often exclusively HG, even when the P shows only focal HG areas. This makes the examination of all material from the P essential to establish the source. 2) Among the antibodies used, diffuse CA IX positivity appears to be the most sensitive for CRCC, even in M. 3) The possibility of P CRCC cannot be excluded based solely of differences in IHC staining between the P and M.

820 Carbonic Anhydrase (CA9) Expression in Clear Cell (Conventional) Renal Cell Carcinoma (CRCC): Comparison of a Commercially Available Antibody with a Previously Frequently Utilized, Research-Based Antibody

SK Tickoo, HA Al-Ahmadie, D Alden, S Olgac, SW Fine, A Gopalan, P Russo, RJ Motzer, VE Reuter. Memorial Sloan-Kettering Cancer Center, New York, NY.

Background: CRCC is the most common subtype of renal cell carcinoma (RCC). It accounts for nearly 90% of all metastases from RCC and is resistant to most conventional treatment modalities such as chemotherapy and radiotherapy. CA9 is a membrane-bound protein with roles in regulating cell proliferation, oncogenesis and tumor progression. Its expression is regulated by VHL-hypoxia inducible factor pathway. Immunohistochemical (IHC) studies have shown CA9 is preferentially overexpressed in a majority of CRCC, making it an important diagnostic marker in such tumors. Prognostically, low CA9 expression levels have been shown to indicate poor survival and low response to interleukin therapy. In most IHC-based studies, clone M75 has been utilized. However, this antibody is not commercially available, limiting its utilization. We evaluated a recently developed, commercially available antibody to asses its expression in a large number of CRCC and compared that to results using clone M75.

Design: One hundred four cases of CRCC with different nuclear grades were assembled in a tissue microarray block and 2 sequential sections were stained by IHC with 2 different antibodies against CA9; clone M75 and clone NB100-417, the latter available from Novus Biologicals, Littleton, CO. Immunoreactivity was evaluated independently and the results were compared to the extent and pattern of staining.

Results: Available for evaluation by both antibodies were 97 cases. Overall, staining grade was the same with both antibodies in 87% of samples, and differences in CA9 expression between the 2 antibodies were not statistically significant (p=0.256). CA9 was expressed in >85% of tumor cells in 85 cases (88%) with NB100-417 and in 88 cases (91%) with M75 (p=1.0). Similar correlation was observed in cases with both moderate as well as low levels of expression. Most cases with high nuclear grade (HNG) were immunoreactive by both antibodies.

Conclusions: The majority of CRCC consistently express CA9 intensely in the majority of tumor cells. CA9 expression using both antibodies is comparable. CA9 expression is retained in tumors with HNG. Thus, the newly available antibody can be used as a diagnostic and possibly as a prognostic marker in CRCC, with the added advantage of its commercial availability.

821 Significance of Tertiary Gleason Grade 5 on Needle Biopsy

K Trpkov, M Chan, L Kmet, A Yilmaz. Calgary Laboratory Services and Centre for Advancement of Health, Calgary, AB, Canada.

Background: Significance of tertiary Gleason Grade 5 (T5) has been previously studied on radical prostatectomy, but the significance of T5 on biopsy is unknown. Recent consensus of the International Society of Urological Pathology recommended that T5 be added to the most prevalent grade to derive the composite biopsy Gleason score.

Design: We retrieved from our institutional database clinical and biopsy data on all patients with biopsy Gleason 5 between 07/2000 and 06/2006. T5 was found in 53 patients and primary/secondary Gleason 5 (P/S5) was found in 119 patients (total 172 patients). Only 20 patients had radical prostatectomy (RP) (8 with T5 and 12 with P/S5), while 152 patients were treated without RP. Biopsies and RP were reviewed and clinical follow-up was obtained.

Results: Clinical variables, age, and biopsy cancer extent were not significantly different between T5 and P/S5 patient groups, except for the lower prevalence of abnormal ultrasound in patients with T5 (39.6% vs. 56.3%; p=0.035). When stratified by treatment, patients who had RP were younger (T5: 62 years; P/S 5: 65 years) than patients who did not have RP (T5: 71 years; P/S 5: 70 years) (medians; p=0.001). Patient who underwent RP had fewer cancer positive cores on biopsy (T5: 5, P/S5: 4) than patient who did not have RP (T5: 7, P/S5: 8) (medians; p=0.005). Patients treated with RP had lower prostate-specific antigen (T5: 8.6; P/S5: 6.2) than patients treated without RP (T5: 16; P/S5: 16.2) (ng/ml; p=0.001). Biopsy T5 remained T5 on RP in 6/8 patients and in 2/8 was upgraded to secondary 5. On RP, 4/8 patients with biopsy T5 had pT3 disease vs. 8/12 with P/S5 (NS). On RP, positive margins were found in 5/8 T5 vs. 6/12 P/S5 and positive nodes were found in 0/8 T5 vs. 2/12 P/S5 (NS). Median tumor volume was

27.5% vs. 20% in T5 vs. P/S5 (NS). Patients with biopsy T5 had less lymphatic/vascular invasion than P/S5 (p=0.007). After a mean follow-up of 26.4 months, same disease progression rate was observed in patients who had RP: T5 (25%) vs. P/S 5 (25%), which was similar to patients with T5 who had no RP (16%).
Conclusions: Clinical and biopsy findings in patients with T5 and P/S5 who had RP were similar and reflected patient selection by the urologist. While RP findings did not differ significantly in T5 vs. P/S5, small patient numbers do not allow ruling out substantial differences in T5 vs. P/S5. Clinical and biopsy findings in patients not treated with RP, who had biopsy T5 and P/S5, were also similar, but were distinctly different from patients who had RP.

822 TMPRSS 2: A Prostate Cancer Marker of Metastasis and a Potential Molecular Target for Therapy

LD True, J Lucas, S Hawley, M Matsumoro, B Knudsen, R Etzioni, PS Nelson. University of Washington, Seattle, WA; Fred Hutchinson Cancer Research Center, Seattle, WA.
Background: The fusion of the TMPRSS2 promoter with members of the ets family of growth factors has been implicated as an important event in the development of prostate cancer. Given the importance of the TMPRSS2 in the development and progression of prostate cancer, we studied expression of this gene product in primary and metastatic prostate cancer.
Design: We made a monoclonal antibody to a peptide in the extracellular domain of the TMPRSS2 gene product. Specificity was assessed by Western blot and blocking immunohistochemical stains. Using tissue microarrays representing a spectrum of grades and stages of ⟩100 primary prostate cancers and of 20 metastatic prostate cancer samples, we characterized expression of TMPRSS2 using an indirect immunoperoxidase method. An additional TMA included tissue from 50 patients treated with 2 doses of 5-α reductase inhibitor dutasteride (0.5 mg and 3.5 mg). Stains were evaluated on a 4-point scale (absent, equivocal, present in a minority of cells, present in a majority of cells). Statistical evaluation used logistic expression analysis addressing the hypotheses that cancer cells stain more than normal cells, that staining differs by grade, and that metastases stain more than primary tumor cells.
Results: TMPRSS 2 is overexpressed more in prostate cancer compared with normal prostate cells and more in metastases than in primary cancers ($p \langle 0.01$). Trends for more intense staining by grade and decrease in staining in patients administered progressively greater doses of dutastasteride were not statistically significant ($p \langle .1$).
Conclusions: TMPRSS2 is overexpressed in prostate carcinoma in a stage-associated manner. As a membrane protein, it is a possible target for molecular therapy, as well as a prognostic marker. A question raised by our study is the relationship between overexpression of TMPRSS2 and recent findings that fusion of the TMPRSS2 promoter with a separate gene family - the ets family - is a frequent event in prostate carcinoma. Our finding raises the possibility that TMPRSS2 may be involved in two possibly unrelated molecular events in prostate carcinoma. One allele may by silenced as its promoter is translocated to the ets-located chromosome. The second may be promoted in prostate carcinoma by an independent mechanism.

823 Frequent TMPRSS2/ERG Gene Fusion in Prostate Cancer: Identification of Fusion Variants and Correlation to Histological Grades

JJ Tu, J Kao, S Rohan, YT Chen. Weill Medical College of Cornell University, NY, NY.
Background: TMPRSS2/ERG and TMPRSS2/ETV1 gene fusions were identified in 79% (23/29) of prostate cancer in the initial report (Science 310:644, 2005), leading to overexpression of ERG/ETV1. Two TMPRSS2/ERG fusion variants were described. We have analyzed a larger series by RT-PCR to identify novel fusion variants, and the frequency of gene fusion was correlated to ERG/ETV1 overexpression and to histological grades.
Design: RNA was extracted from 83 cases of prostate cancer, using paraffin sections from prostatectomy specimens. TMPRSS2/ERG and TMPRSS2/ETV1 translocations were analyzed by nested RT-PCR and direct sequencing. Quantitative RT-PCR was performed to evaluate overexpression of the downstream ERG and ETV1 transcripts, using 18S rRNA and 5ETV1 as endogenous controls.
Results: Successful RT-PCR was achieved in 75 of 83 cases. TMPRSS2/ERG fusion PCR product was detected in 34 cases (45%), indicating translocation. Concordant downstream ERG overexpression was seen in 30/34 cases, with 4 cases showing no significant change at ERG transcript levels. Conversely, only 3 cases with detectable ERG overexpression failed to PCR amplify TMPRSS2/ERG transcript, indicating either a fusion event outside of the PCR primer range, or an ERG activation mechanism unrelated to TMPRSS2 fusion. Thirty-eight cases (50%) showed neither fusion PCR products nor ERG overexpression, and the maximal frequency of TMPRSS2/ERG fusion in our series was thus estimated at 45-55%, lower than that previously reported. Among carcinoma of different grades, TMPRSS2/ERG fusion was seen in 7/11 (64%) Gleason's score 6, 22/48 (46%) Gleason's 7, and 5/16 (31%) Gleason's 8-10 tumors, suggesting that fusion-related hormone-driven prostate cancers tend to be of lower histological grades. DNA sequencing revealed four TMPRSS2/ERG fusion variants, including two novel variants. Surprisingly, ETV1 overexpression was detected in only two cases in our series, and no TMPRSS2/ETV1 translocation was identified by RT-PCR, indicating TMPRSS2/ETV1 fusion as a much less frequent event.
Conclusions: We confirmed TMPRSS2/ERG rearrangement and associated ERG overexpression as a frequent event in prostate cancer, but not TMPRSS2/ETV1 translocations. The overall translocation frequency was lower in our series than that previously reported, which may be partially due to the higher percentage of high grade tumors in our series, as a trend of lower translocation frequency was observed in these tumors. Finally, new fusion transcript variants were identified.

824 Diagnostic Utility of Molecular Markers in Separating Renal Oncocytomas from Chromophobe Renal Cell Carcinomas

AH Uihlein, SD Finkelstein, RS Saad, JL Lindner, JF Silverman, YL Liu. Allegheny General Hospital, Pittsburgh, PA; Pittsburgh, PA.
Background: Distinguishing oncocytoma (OC) from chromophobe renal cell carcinoma (ChRCC) can occasionally be challenging in the nephrectomy specimen and especially in core needle biopsies when based strictly on histologic features. To date, there are no reliable immunohistochemical markers to separate these two neoplasms, which differ significantly in prognosis and treatment. We investigated the diagnostic utility of molecular markers to discriminate OC from ChRCC.
Design: Forty cases were retrieved from the hospital pathology files. This study examined the mutational change (allelic imbalance [LOH]) for 22 polymorphic DNA markers (13 genomic sites) as well as DNA sequence mutation of mitochondrial DNA of 24 patients with OC and 16 patients with ChRCC. After review of each case, one representative slide of the tumor was selected in which 2 representative target areas were microdissected, and DNA was extracted. Mutations were quantitatively determined for a broad panel of LOH markers (1p, 3p, 5q, 9p, 10q, 11q, 12q, 13q, 14q, 17p, 17q, 21q, 22q, and mitochondrial DNA) using PCR/electrophoresis. Statistical analysis was performed using the SPSS statistical program.
Results: Mitochondrial DNA mutation was identified in 20/24 (83%) of OC, compared to 4/16 (25%) of ChRCC, which was statistically significant ($r = 0.58$, $P<0.001$). In addition, mutations at the 14q locus showed statistically significant correlation with OC ($r =0.35$, $P< 0.005$). High amplitude LOH mutations, defined as greater than 75% of the tumor cells demonstrating mutations, were significantly higher in ChRCC than OC ($r = 0.82$, $P< 0.001$). The combination of no mitochondrial mutation, no 14q mutation, and the presence of high amplitude LOH mutations had 100% specificity and 69% sensitivity for ChRCC.
Conclusions: The combination of mitochondrial DNA sequence mutation, 14q mutation, and the lack of high amplitude LOH mutations is characteristic of OC. The combination of no mitochondrial mutation, no 14q mutation, and the presence of high amplitude LOH mutations is unique to ChRCC. We believe that mutations of mitochondrial DNA and 14q, and the amplitude of LOH mutations can be helpful in differentiating OC from ChRCC in problematic granular renal cell neoplasms where histologic and immunohistochemical evaluation does not provide a definitive diagnosis.

825 Morphologic Changes in Prostate Cancer Samples Following Intraprostatic PSA-Based Vaccine Administration

D Val, JL Gulley, P Pinto, J Schlom, WM Linehan, MJ Merino. NCI, Bethesda, MD.
Background: Prostatic cancer is one of the most common causes of cancer in men classically treated with surgery, radiation, hormonal therapy and occasionally chemotherapy. Recently, the search for new molecular targets and vaccines has increased options for patients refractory to treatment and disease progression. We herein report the morphologic changes of prostatic biopsies of patients with recurrent prostate cancer, after receiving intraprostatic PSA-based vaccine.
Design: Nine patients ranging in age from 52-75 (m 59.7) had biopsies performed both before enrolment and 113 (±7) days after vaccination and three subsequent booster vaccinations. The second biopsy was taken 28 days after the final intraprostatic vaccine. All the samples were fixed in 10% neutral buffered formaline. H&E slides were obtained, as well as immunohistochemistry for PSA, cytokeratin AE1/AE, 34BE12, CD20, CD3, CD4 and CD8.
Results: The morphologic changes in the post- vaccine biopsy, were characterized by: striking eosinophilia, diffuse lymphoid infiltration, necrobiotic-type changes of the stromal component, and rare necrosis of the tumoral epithelial component. The residual tumor when present, was similar to the original lesion. Some glands showed focal markedly abnormal changes with macronuclei and prominent nucleoli. None of these features were recognized in the previous diagnostic biopsy. Further categorization of the lymphoid population by immunohistochemistry showed immunoexpression of CD3/CD4 + and CD3/CD8+, the latter with a predilection for intraepithelial location. PSA was identified in all the post vaccine biopsies.
Conclusions: Although immunotherapy is becoming a promising alternative for the treatment of patients with advanced cancer including prostate cancer, the associated morphologic changes are not well known. We herein described the morphologic changes characterized by intense inflammation, necrobiotic necrosis and marked atypia of residual epithelium, of patients with prostate cancer treated with PSA-vaccine.

826 The Predictive Value of Cytogenetic Abnormalities in Urine Samples

RJ Van Kirk, Jr, JF Tomashefski, Jr, M Chung-Park, A Khiyami. Case Western Reserve University/MetroHealth, Cleveland, OH.
Background: Fluorescent in-situ hybridization by Urovysion® (Vysis, Inc., Downers Grove, IL) is used to detect four of the most common chromosomal abnormalities associated with transitional cell carcinoma (TCC) cells present in urine samples. It can be used either as a screening test for TCC or to test for recurrence in patients with a known history of TCC. The criteria for a positive test result requires that multiple chromosomal gains be present in multiple cells, or that loss of 9p21 be demonstrated in multiple cells. The purpose of this study was to correlate the type of chromosomal abnormality present in the positive Urovysion® test with subsequent biopsy findings.
Design: The study included all cytogenetic results for urine samples accessioned from 1/1/2004 to 9/1/2006 by the Department of Pathology at MetroHealth Medical Center. The surgical pathology results from those subjects with positive findings were reviewed. A positive Urovysion® test is defined by the manufacturer as: *a*) either the presence of 4 or more cells with a gain of chromosomes 3 and 7, 3 and 17, or 7 and 17, or *b*) at least 12 cells with loss of 9p21. The cases with positive results were stratified into those with only the chromosome gains, those with only the 9p21 loss, or those with both the gains and the 9p21 loss.

Results: A total of 20 patients had a positive Urovysion® test during the study period. Of these, eleven were positive by chromosome gains, five were positive by loss of 9p21, and four cases could have qualified by either. All five cases with only the 9p21 loss were negative for TCC (four had only reactive atypia on biopsy and one had prostate cancer). Furthermore, there were six cases where the biopsies showed only reactive atypia, and all six had only the chromosome gains or only the 9p21 loss, but not both. There were eight cases where cells with both gains and losses were identified of which six had TCC of grade II or higher and two had metastatic TCC.
Conclusions: In this study population, the presence of only the loss of 9p21 in 12 or more cells did not accurately predict TCC. However, loss of 9p21 when present in conjunction with chromosome gains of 3, 7 and 17 may be associated with advanced disease. Our findings suggest that the predictive value of the Urovysion® screening test may be improved by eliminating loss of 9p21 as a sole criterion for a positive test.

827 Penile Verruciform Tumors: Extended Classification, Differential Diagnosis and Outcome in 104 Cases

EF Velazquez, FA Soares, I Werneck da Cunha, A Lopes, JE Barreto, AL Cubilla. Harvard Medical School, Boston, MA; Hospital do Cancer AC Camargo, Sao Paulo, Brazil; Instituto de Patologia e Investigacion, Asuncion, Paraguay.
Background: Verruciform tumors are exophytic, usually low grade penile neoplasms of variegated morphology and etiology that can be classified in different subtypes. New tumor subtypes have been recently reported. However, there is no much information regarding tumor behavior and prognosis of these subtypes. Clinicopathological studies are needed to validate the importance of subclassifying penile verruciform tumors.
Design: This study was designated to delineate the morphological features and determine the patient's outcome of the various verruciform tumor types in a well-characterized cohort of patients from one institution, many of which with extended follow-up. After pathologic review of 375 penile squamous cell tumors, which included 372 invasive squamous cell carcinomas (SCCs) and 3 giant condylomas, 104 verruciform tumors were selected. The selected material consisted of 104 penectomies and 56 groin dissections. Data documented were: age, tumor site, size, histological grade (1, 2 and 3), thickness, anatomical level of invasion, groin nodal status and final outcome. Follow up was obtained in 92 patients (88%).
Results: Tumors were classified in: verrucous carcinoma (25 cases), warty carcinoma (25 cases), papillary carcinoma (18 cases), carcinoma cuniculatum (3 cases), giant condyloma (3 cases) and mixed verruciform SCC (30 cases). Our study showed that giant condylomas affect patients at a significantly younger age than other variants. High histological grade areas were only present in warty and mixed verruciform SCCs. Nodal metastasis were present in warty (16%), papillary (13%) and mixed SCCs (7%) but not in giant condylomas, verrucous carcinoma or carcinoma cuniculatum. Mortality was documented in papillary (12%) warty (8%) and mixed tumors (7%) but not in the other types. No significant differences were found in regards to site, size, depth and level of invasion in this series.
Conclusions: Verruciform tumors show variegated albeit distinctive morphological features and in general have a better prognosis compared with other types of penile SCCs. A careful identification of the various subtypes is important because of the metastatic potential and mortality associated with especial variants such as papillary, warty and mixed verruciform SCCs. Verrucous carcinoma, carcinoma cuniculatum and giant condylomas have an excellent prognosis.

828 Small Cell Carcinoma of the Prostate: A Study of 118 Cases

WL Wang, JI Epstein. The Johns Hopkins Hospital, Baltimore, MD.
Background: Small cell carcinomas of the prostate (SCC) are rare and reported as case reports or small series.
Design: 118 cases of SCC were found from our institution and the consult service of one of the authors. In 96 cases, H&E slides were available. SCC specimens included 72 needle cores, 32 TURPs, 5 radical prostatectomies, and 12 biopsies from metastases (some with >1 procedure). 105/118 were prostatic specimens with the rest from metastases or pelvic disease. For cases with paraffin blocks or unstained slides, immunoreactivity in the small cell component was analyzed for PSA, p501S (prostein), PSMA (prostate specific membrane antigen), and neuroendocrine markers.
Results: Men ranged from 44-92 years old (mean: 69 yrs.). While serum PSA could be very high (up to 1896 ng/ml), the median value was only 4.0 ng/ml. 33/78 (42%) men with available information had a history of usual prostatic adenocarcinoma. The interval between the diagnosis of SCC and prior prostate cancer ranged from 1-300 months (median 25 months). 87% of men died with the time to death from diagnosis of SCC ranging from 1-98 mos. (median 10 mos.). Pure SCC was seen in 54/95 (57%) of cases with the remaining admixed with prostate adenocarcinoma. In cases with adenocarcinoma, 20.5% had sharp demarcation from SCC with in other cases merging of the 2 components. In mixed cases, SCC predominated (median: 80% of the tumor); the Gleason score of the adenocarcinoma was ≥8 in 85% of these cases. In 61cases (64%), SCC was classic morphology with remaining still diagnostic of SCC yet having somewhat more cytoplasm. Of the 96 cases: necrosis was seen in 40% (2%-95% of the tumor); giant bizarre cells in 19%; Indian filing in 21%; rosette formation in 29%; focal vacuolated cytoplasm in 18%; and desmoplasia in 20%. 88% of SCC were positive for at least 1 neuroendocrine marker.

	Rare	1%-10%	10%-50%	>50%	Total Positive
PSA	6/14 (43%)		4/14 (29%)	4/14 (29%)	14/80 (18%)
P501s	4/19 (21%)	2/19 (11%)	1/19 (5%)	12/19 (63%)	19/65 (29%)
PSMA	4/16 (25%)	5/16 (31%)	3/16 (19%)	4/16 (25%)	16/65 (25%)

Conclusions: In this the largest study of prostatic SCC we highlight the presence of morphological features that may result in its underdiagnosis, such as the presence of larger cells with more cytoplasm, Indian file formation, giant cells, vacuolated cells, and desmoplasia. Other more classic features of SCC along with rosettes are critical for its accurate diagnosis. P501s and PSMA were better in identifying the prostatic origin of SCC than PSA, although the majority (81%) of prostatic SCC were negative for all 3 markers.

829 Amplifications of *EGFR* Gene and Protein Expression of *EGFR, Her-2/Neu, C-Kit* and Androgen Receptor in Phyllodes Tumor of the Prostate

X Wang, TD Jones, S Zhang, JN Eble, DG Bostwick, J Qian, A Lopez-Beltran, R Montironi, L Cheng. Indiana Univ, Indianapolis, IN; Bostwick Laboratories, Richimond, VA; Cordoba Univ, Cordoba, Spain; Polytechnic Univ of Marche Region, Ancona, Italy.
Background: Phyllodes tumor of the prostate is a rare neoplasm. It may undergo sarcomatous transformation with early recurrence and may metastasize. This study investigated epidermal growth factor receptor (*EGFR*) gene amplification and protein overexpression of *EGFR, Her-2/neu, CD117* (c-kit), and androgen receptor (*AR*). Ultimately, this study will provide insight into the molecular pathogenesis and to define potential therapies for this neoplasm.
Design: This study included 11 patients. Amplification of *EGFR* gene was performed by fluorescence in situ hybridization and the overexpression of *EGFR*, *Her-2/neu*, *c-kit*, and *AR* was performed on the paraffin-embedded tissue sections using avidin-biotin-peroxidase method.
Results: In the stromal elements, *EGFR* gene amplification was present in 4 of 11 tumors and polysomy chromosome 7 was present in 2 of 11 tumors. No amplification was present in the epithelial components. Only 1 of 11 tumors had polysomy of chromosome 7 in the epithelial components. Immunohistochemically, in the stromal components, *EGFR* expression was demonstrable in 4 of 11 tumors and *AR* was demonstrated in 6 of 10 tumors. Neither *Her-2/neu* nor *c-kit* expression was seen in the stromal components of any of the 11 tumors. In the epithelial components, *EGFR* expression was present in all 11 tumors with strong staining in the basal cell layers and weak or no staining in luminal epithelium; *AR* expression was seen in 7 of 10 tumors; *Her-2/neu* was weakly positive in 4 of 11 tumors; and *c-kit* expression was present focally and weakly in 2 of 11 cases with only 2-5% of cells staining. The highest staining intensity and the highest percentage of positively-staining cells were seen with *EGFR* immunostaining in both the stromal and epithelial (mainly basal cells) components. *AR* staining showed the next highest staining intensity and percentage of positive cells in both components. *Her-2/neu* and *c-kit* were only weakly or infrequently expressed in the epithelial components of prostatic phyllodes tumors.
Conclusions: Our data indicate that *EGFR* and *AR* are frequently and strongly expressed in both epithelial and stromal components of prostatic phyllodes tumors. *EGFR* gene amplification is frequently present in the prostatic phyllodes tumors and may account for one of the mechanisms leading to protein overexpression.

830 Epidermal Growth Factor Receptor Protein Expression and Gene Amplification in Small Cell Carcinoma of the Urinary Bladder

X Wang, S Zhang, GT MacLennan, JN Eble, A Lopez-Beltran, X Yang, C Pan, R Montironi, L Cheng. Indiana Univ, Indianapolis, IN; Case Western Reserve Univ, Cleveland, OH; Cordoba Univ, Cordoba, Spain; Northwestern Univ, Chicago, IL; Univ of California at Davis, Sacramento, CA; Polytechnic Univ of Marche Region, Ancona, Italy.
Background: Small cell carcinoma of the urinary bladder is a highly aggressive malignancy. Epidermal growth factor receptor (EGFR) is overexpressed in many malignancies, and its overexpression has been associated with poor prognosis. Furthermore, anti-EGFR targeted therapies have been successful in the treatment of colon and lung cancers. This study was performed to investigate EGFR protein expression and gene amplification in a large series of urinary bladder small cell carcinomas and to correlate the findings with clinicopathologic parameters.
Design: Fifty-two cases of urinary bladder small cell carcinoma were included. Immunostaining for EGFR was performed using avidin-biotin-peroxidase method. Gene amplification for EGFR was performed by fluorescence in situ hybridization (FISH). EGFR expression was correlated with clinicopathologic parameters.
Results: Fifty-two cases (41 males and 11 females; age: 36 to 85 years) were analyzed. All patients except one had advanced disease (T2 or above) at presentation. Pathologic stage was T1 in1, T2 in 26, T3 in 22, and T4 in 3 cases, respectively. Immunohistochemically, positive EGFR expression was observed in 14 of 52 cases (27%) (7 with 10-25%; 4 with 25-50%; 1 with 50-75%; and 2 with 75-100% staining, respectively). No EGFR gene amplification was observed in any of 52 cases by FISH. Forty cases had polysomy and the remaining 12 cases displayed disomy. No correlation between EGFR protein expression and gene amplification was demonstrated (P=0.99). There was no correlation between EGFR expression and clinicopathologic characteristics including age (P=0.64), gender (P=0.26), history of smoking (P=0.67), clinical stage (P=0.13), pathologic T stage (P=0.53), lymph node metastasis (P=0.27), distant metastasis (P=0.34) or survival (P=0.91).
Conclusions: EGFR is expressed in a subset of urinary bladder small cell carcinomas (27%); however, expression of EGFR does not correlate with clinicopathologic parameters. At the molecular level, EGFR over-expression in small cell carcinoma of the bladder does not appear to be caused by gene amplification. The expression of EGFR raises the possibility that EGFR may be a potential therapeutic target in the treatment of this malignancy.

831 Lymphatic Vessel Density Does Not Associate with Tumor Grade in Prostate Cancer

Y Wang, E Genega, Y Fu. Beth Israel Deaconess Medical Center, Boston, MA.
Background: Prostate cancer (PCa) is one of the most common malignancy and third-leading cause of cancer death in men. High grade PCa has been associated with regional lymph node metastasis and poor prognosis. There are a number of controversal reports regarding the association of lymphangiogenesis with tumor grade and its role in predicting prostate cancer metastasis. In this study, we used CD31, an antibody that stain both lymphatics and blood vessels, and D2-40 which only stain lymphatics to stain a series of prostate carcinomas and compared their lymphatic and blood vessel patterns.

Design: Paraffin sections of archived radical prostatectomy specimens from 12 high-grade PCa (Gleason score >=7(4+3)) and 12 lower grade PCa (Gleason score 6(3+3)) were immunostained with CD31 and D2-40 antibodies. Fifteen representative images of intra-tumor, peri-tumor and non-tumor area were taken from each case. Microvessel density (MVD) and lymphatic vessel density (LVD) were evaluated using IPlab Scientific image software and analyzed using paired t-test and Kruskal-Wallis test.
Results: All tumor samples studied have CD31 positive microvessels in intra-tumor, peri-tumor and non-tumor areas. There was significant increase in average intra-tumor MVD than non-tumor areas for all cases studied (3.8 vs 0.6; $p< 0.05$). Unlike blood vessels, lymphatics were not present inside the tumor but rather seen at the tumor infiltrading edge and adjacent benign prostate. In some areas where tumor cells invading inbetween normal prostate glands, rare lymphatics can be seen within the tumor but all are present adjacent to benign glands that were "entrapped" by the tumor. No lymphatics were seen in tumor areas that are exclusive of benign prostate glands. There is no significant difference in intra-tumor lymphatic patterns among high and lower grade tumors.
Conclusions: All carcinomas showed markedly increased microvessel density compared to the adjacent non-neoplastic prostate. There are no intra-tumor lymphatics present in either high or lower grade PCa. The rare lymphatics seen inside the tumor mass are likely native lymphatics related to "entrapped" benign glands instead of true tumor lymphatics. Our data indicates that intra-tumor lymphangiogenesis likely plays no significant role in prostate cancer metastasis. The peri-tumor lymphatic vessel density, their structural abnormality and the tumor induced micro-environment at the tumor infiltrating edge may instead play key roles in prostate cancer progression and dissemination.

832 Utility of Anti-Phosphorylated H2AX Antibody (gamma]-H2AX) in Diagnosing Metastatic Renal Cell Carcinoma

MJ Wasco, RT Pu. University of Michigan, Ann Arbor, MI.
Background: Renal cell carcinoma (RCC), hepatocellular carcinoma (HCC), and adrenocortical carcinoma (ACC) have overlapping morphologic features. Frequently, all three need to be considered in a differential diagnosis. Immunohistochemical markers including RCC marker (RCC-Ma) have been employed with varying success in differential diagnosis of RCC. Gamma-H2AX is an antibody that specifically reacts with phosphorylated histone H2AX (at position Ser-139) and has been used to detect bladder, breast, lung, and colon cancers and precursor lesions. Our preliminary tissue microarray study demonstrated that γ-H2AX stained many primary RCC strongly and did not stain HCC or ACC, prompting us to evaluate γ-H2AX in these tumors and to compare it with RCC-Ma.
Design: 71 cases of metastatic RCC, 18 HCC, and 21 ACC were identified. Paraffin-embedded tissue sections were stained for γ-H2AX and RCC-Ma. Staining intensity and pattern were recorded for each case. Data were analyzed to determine and compare sensitivity and specificity of each marker.
Results: RCC-Ma demonstrated abundant cytoplasmic staining of some cases of HCC and ACC as well as normal tissues, but a membranous pattern of staining was found to be 74.6% sensitive (53/71 cases of metastatic RCC stained), and 100% specific for RCC (none of the ACC or HCC stained). γ-H2AX had a similar sensitivity of 70% (50/71 cases positive, with greater than 25% of nuclei staining) and a specificity of 76.9% for RCC. In contrast, γ-H2AX stained one of 18 HCC (5%) and 8 of 21 (38%) ACC. More importantly, of RCCs that were negative for RCC-Ma, 12 of 18 (67%) were positive for γ-H2AX. In metastatic RCC, 83% (39/47) of tumors with a higher nuclear grade (equivalent of Fuhrman 3 or higher) stained with γ-H2AX, compared to 46% (11/24) of low nuclear grade (equivalent of Fuhrman 2 and lower) tumors. RCC-Ma had similar rate of staining in low and high grade tumors, 75% (18/24) and 72% (33/47), respectively. 37.5% of low grade tumors stained only with RCC-Ma, as compared to 10.6% of high grade tumors. 8.3% of low grade tumors and 23.4% of high grade tumors stained for γ-H2AX only.
Conclusions: γ-H2AX is a useful adjunct in diagnosis of metastatic RCC. It often stains RCC which are negative for RCC-Ma. It also stains higher grade RCC, which are often a diagnostic challenge, more frequently than RCC-Ma. A nuclear pattern of staining of γ-H2AX has a comparable sensitivity to RCC-Ma, and the interpretation is easier and more reliable. RCC-Ma is 100% specific for RCC, but only when a membranous pattern of staining is interpreted as positive.

833 Pseudoglandular (Acantholytic) Squamous Cell Carcinomas of the Penis. A Report of 7 Cases

I Werneck da Cunha, FA Soares, AM Souza, EF Velazquez, JJ Torres, A Chaux, AL Cubilla. Hospital do Cancer AC Camargo, Sao Paulo, Brazil; Harvard Medical School, Boston, MA; Instituto de Patologia e Investigacion; Facultad de Ciencias Medicas, Asuncion, Paraguay.
Background: About 60% of penile carcinomas are squamous cell carcinomas (SCCs) of the usual type but there is a variegated spectrum of other subtypes. We found no reports of pseudoglandular SCCs.
Design: The aim of this study was to delineate clinicopathologic features and outcome of an unusual variant of penile SCC. Clinical charts and pathologic materials from 375 penectomies with SCC of the penis treated at the Hospital do Cancer AC Camargo in Sao Paulo, Brazil were reviewed and 7 SCCs with prominent pseudoglandular (acantholytic) features were identified (2%). The following information was obtained: patients' age, tumor site, size, histological grade (1, 2 and 3), thickness, anatomical level of invasion (CS, corpus spongiosum, CC, corpus cavernosum), vascular and perineural invasion, groin nodal status and follow up in months.
Results: Median age was of 54 years. Tumors were large (av 4.6 cm) and involved multiple sites. Microscopically, there were acantholytic areas ranging from solid nests with early necrosis to empty pseudoluminal spaces lined by one layer of squamous or cuboidal cells strikingly simulating glands. Most tumors were deeply infiltrating (4 invaded CC and 2 CS) and of high histologic grade (6 cases). Vascular invasion was present in 4 cases and perineural invasion in 2. There was regional nodal metastasis in 3 patients, 2 of which died from disease. The other 5 were either alive with no evidence of disease (12 and 21 years after diagnosis) or died from causes other than penile cancer (3, 4 and 7 years after diagnosis).
Conclusions: Pseudoglandular SCCs of the penis are large, locally aggressive neoplasms with metastatic potential. The mortality rate in our series was 28.5%. Pseudoglandular penile SCC should be differentiated from adenosquamous carcinomas, an unusual penile carcinoma variant with areas of true glandular differentiation.

834 Utility of a Comprehensive Immunohistochemical (IHC) Panel in the Differential Diagnosis of Spindle Cell Lesions of the Urinary Bladder

D Westfall, AL Folpe, GP Paner, E Oliva, LC Goldstein, AM Gown, MB Amin. Cedars-Sinai Medical Center, Los Angeles, CA; Mayo Clinic, Rochester, MN; Massachusetts General Hospital, Boston, MA; PhenoPath Laboratories, Seattle, WA.
Background: Spindle cell lesions of the urinary bladder are relatively uncommon, but pose a significant diagnostic challenge, as the morphology and immunoprofile of pseudosarcomatous processes in this location significantly overlap with spindled epithelial and mesenchymal tumors. The utility of a panel including antibodies to the recently described basal cell markers p63 and cytokeratin 5/6 (CK5/6) along with those to pan-cytokeratin (CK), smooth muscle actin (SMA) and ALK1 protein has not been analyzed in this diagnostic context.
Design: 46 spindle cell lesions including 10 pseudosarcomatous myofibroblastic proliferations (PMP) (related and unrelated to prior procedure), 23 sarcomatoid urothelial carcinomas (Sarc Ca), 12 leiomyosarcomas (LMS) and 1 leiomyoma were immunostained for p63, CK5/6, CK, SMA, and ALK1.
Results: IHC profile of spindle cell lesions of the urinary bladder:

	Score	Keratin	p63	Alk-1	SMA	CK5/6
PMP (n=10)	0	3/10	9/9	8/10	0/10	9/9
	1+	0/10	0/9	1/10	1/10	0/9
	2+	4/10	0/9	1/10	4/10	0/9
	3+	3/10	0/9	0/10	5/10	0/9
	Total +(%)	7/10(70)	0/9(0)	2/10(20)	10/10(100)	0/9(0)
Sarc Ca (n=23)	0	7/23	12/23	23/23	6/23	17/23
	1+	2/23	3/23	0/23	8/23	1/23
	2+	2/23	3/23	0/23	6/23	1/23
	3+	12/23	5/23	0/23	3/23	4/23
	Total +(%)	14/23(61)	11/23(49)	0/23(0)	17/23(74)	6/23(26)
Smooth muscle tumors (n=13)	0	6/13	10/13	13/13	2/13	12/12
	1+	3/13	2/13	0/13	2/13	0/12
	2+	3/13	1/13	0/13	2/13	0/12
	3+	1/13	0/13	0/13	7/13	0/12
	Total +(%)	7/13(54)	3/13(23)	0/13(0)	11/13(85)	0/12(0)

Score: 0, < 5% +; 1+, 5-10% +; 2+, 11-50% +; 3+, >50% +
Conclusions: Although clinically and biologically distinct, PMP, Sarc CA and LMS of the bladder show significant immunophenotypic overlap, even using an extended panel of antibodies. Although clinical and morphologic correlation remain the cornerstones of this differential diagnosis, an IHC panel composed of CK, SMA, ALK1, p63 and CK5/6 is a useful diagnostic adjunct: the combination of CK-SMA-ALK1 (+) / p63-CK5/6 (-) supports PMP; CK-p63-CK5/6 (+) / SMA-ALK1(-) favors Sarc Ca, and SMA (+) / CK-p63-CK5/6-ALK1 (-) is seen most often in LMS.

835 Renal Cell Carcinoma in Children and Young Adults: Clinicopathological Spectrum with an Emphasis on Translocation Associated Carcinomas

AJ Wu, LP Kunju, RB Shah. University of Michigan Medical Center, Ann Arbor, MI.
Background: Renal cell carcinomas (RCCs) in children and young adults are rare. Certain distinct variants of RCC with unique recurrent translocations, which primarily occur in children and young adults, are increasingly being recognized in the new classification of renal tumors.
Design: To further characterize RCC in children and young adults, clinical, morphologic, immunohistochemical and cytogenetic/molecular data were analyzed in RCCs diagnosed in patients younger than 30. RCCs were classified according to the 2004 WHO criteria for renal neoplasms. A broad immunohistochemical panel of cytokeratin (CK) cocktail; CAM5.2; EMA; CK 7; CD10; RCC; WT1; HMB45; P504S; and TFE3 protein (which correlates with the presence of the *TFE3* gene fusion product), was performed.
Results: Of all RCCs diagnosed at our institution between 1986 and 2006, 24 occurred in patients younger than 30. Morphologic and immunohistochemical characterization of these RCCs revealed five distinct groups: 1) clear cell RCC, sporadic (n=5) or associated with vHL syndrome (n=6); 2) Xp11.2 translocation associated RCC (n=4); 3) papillary RCC, type 1 (n=1) and type 2(n=2); 4) chromophobe RCC (n=1); and 5) RCC, unclassified (n=5). All (100%) clear cell RCCs, both sporadic and vHL associated, and the chromophobe RCC presented with low stage disease (pT1), while the majority (67%) of papillary, translocation associated, and unclassified RCCs presented with higher stage disease (≥pT2), sometimes with nodal involvement and/or distant metastases (33.3%). Xp11.2 translocation associated RCCs were negative/very weakly positive for cytokeratins/EMA, negative for WT1, HMB45, and positive for CD10, RCC, P504S and TFE3. Three of 5 unclassified RCCs had an "oncocytoma-like" morphology with focally prominent cystic change resembling cystic nephroma, low nuclear grade, cytoplasmic vacuoles and inclusions, EMA, CD10, RCC and P504S expression, and lack of expression for other cytokeratins, WT1, HMB45, and TFE3. One unclassified carcinoma had a mixed morphology and arose concurrently with angiomyolipoma in a patient with tuberous sclerosis.
Conclusions: Our results demonstrate that distinct genetic associations characterize a significant proportion of RCCs in children and young adults. Clear cell RCC, either sporadic or vHL associated, is a subtype with a favorable prognosis. Additional follow up, immunomarkers, and molecular studies are currently ongoing to further characterize this subset of RCCs, especially the unclassified RCCs.

836 Pathological Characterization of Residual Prostate Cancer (PCa) in a High Risk Neoadjuvant Chemotherapy Surgical Model

AJ Wu, J Friedman, M Hussain, RB Shah. University of Michigan Medical Center, Ann Arbor, MI.

Background: Because residual disease contributes to relapse in patients with high risk PCa, neoadjuvant chemotherapy has been attempted to improve outcomes. Although the morphologic features of PCa following neoadjuvant hormonal therapy have been well documented, there are only limited studies on the pathologic characteristics in pure neoadjuvant chemotherapy models.

Design: This study was designed to determine the effect of 3-6 cycles of docetaxel and capecitabine on the morphology of PCa and on select proteins which are known to be regulated by these chemotherapeutic agents. Fifteen patients with high risk localized PCa (either clinical stage >T2, PSA≥ 15 or Gleason ≥8) were enrolled. Prechemotherapy biopsies and postchemotherapy prostatectomies were scored (0-4, 4 =strongest) for the following morphologic features of treatment effect: 1)necrosis; 2)glandular breakdown; 3)apoptosis/pyknosis; 4)clear cell change; 5)cytoplasmic vacuolation; and 6)fibrosis. Immunostains for thymidine phosphorylase (TP; an enzyme responsible for activation of capecitabine to 5-FU) and Survivin (an anti-apoptotic protein) were performed on pre and postchemotherapy specimens; percentage of tumor staining was documented. The morphologic and immunostain profiles were correlated with postchemotherapy decreases in PSA.

Results: Prechemotherapy biopsies and postchemotherapy prostatectomies were available for seven patients. Only four prostatectomy specimens showed overall chemotherapy response; all of these were mild. The most common features were focal clear cell change (n=6 with score=1-2) and glandular breakdown (n=5 with score 1-3). Four specimens showed focal apoptosis/pyknosis (score=1-2) and a few (n=1-2) showed focal (score=1) necrosis and vacuolation of cells. Only one of the three PSA responders (>50% decrease in PSA) showed mild chemotherapy response. There was no discernable pattern of TP expression in prostatectomies compared to prechemotherapy biopsies (3 increased, 3 decreased, 1 with unchanged TP expression). Four prostatectomies showed decreased Survivin expression. TP and Survivin expression did not correlate with PSA response.

Conclusions: Neoadjuvant chemotherapy results in only a mild pathologic response in a subset of patients and may lead to a moderate decrease in Survivin expression. Additional studies with larger sample sizes will be required to further characterize these trends.

837 Can Additional Levels and Secondary Review of Negative Diagnoses Reduce Errors in Interpretation of Prostate Needle Specimens?

HH Wu, TM Elsheikh. Ball Memorial Hospital, Muncie, IN.

Background: Routine processing of prostate needle core biopsies in our laboratory includes an average of two serial sections placed on each of 3 slides. Slides 1 and 3 were stained with Hematoxylin and Eosin (H&E) while slide 2 was left unstained for possible immunohistochemistry. This study was carried out to determine whether additional sections or second review of negative biopsies would detect possible cancer missed on initial evaluation.

Design: Additional four unstained serial sections from each paraffin block were placed on slide 4 and slide 5 (two sections each) for 100 consecutive blocks of prostate needle biopsies. After the final reports were issued, all the unstained slides from slides 2, 4 and 5 were stained with H&E, and were reviewed by the authors. Significant pathologic findings such as adenocarcinoma, high grade prostate intraepithelial neoplasm (HGPIN), and atypical small acinar proliferation (ASAP) were documented and compared to the original slides.

Results: Each block contained one to four cores of tissue with a total of 217 cores in 100 blocks (mean 2.17 cores per block). There were 14 adenocarcinomas, 2 ASAP and 1 HGPIN identified in original reports and were also present on the additional 4 serial sections of tissue. However, there was one additional 2 mm focus of adenocarcinoma (Gleason grade 3+3) and one 1 mm focus of ASAP identified in the additional serial sections that were not documented in the original reports. On retrospective examination of the original slides, these foci of adenocarcinoma and ASAP were present in the original slides, which indicated that they were missed by the original pathologists. Eighty-one blocks of needle biopsies contained benign prostate tissue.

Conclusions: Our study reveals a 2% false negative rate and a 0% positive rate. All the cancer cases were reviewed and confirmed by a second pathologist according to our departmental policy. However, negative needle biopsies were not required for mandatory second review. Second review of all negative prostate needle biopsies may be useful in reducing the false negative rate. Two to three H&E stained slides with at least 6 serial sections of tissue appear to be adequate for histologic examination of the prostate needle biopsy, as extra sections did not reveal additional significant pathology.

838 Expression of Mineralocorticoid Receptor and 11β-Hydroxysteroid Dehydrogenase Type II in Renal Cell Neoplasms: A Tissue Microarray Study

E Yakirevich, DJ Morris, R Tavares, M Lechpammer, LJ Wang, E Sabo, RA DeLellis, MB Resnick. Rhode Island Hospital, Brown Medical School, Providence, RI.

Background: The kidney is an important target for mineralocorticoids. Aldosterone is the major endogenously secreted mineralocorticoid, acting by binding to mineralocorticoid receptors (MRs) present in distal renal tubular epithelium. The ability of non-selective MR to bind mineralocorticoids is mediated by the enzyme 11β-Hydroxysteroid Dehydrogenase Type II (11βHSD2), which inactivates cortisol to cortisone, preventing binding of glucocorticoids by MR. Our goal was to determine whether MR and 11βHSD2 expression could be used to characterize and distinguish major types of renal cell neoplasms (RCNs).

Design: In this study, we retrospectively analyzed paraffin embedded microarray specimens from 128 consecutive patients with RCNs for MR and 11βHSD2 expression by IHC. A recently described mouse MAb MR1-18 (Gomez-Sanchez, 2006) was used for MR; a rabbit polyclonal Ab H-145 from Santa Cruz was used for 11βHSD2. The cases were stratified into 83 clear cell renal cell carcinomas (CRCC), including 8 cases with predominant granular histology (GCRCC); 13 papillary RCC (PRCC), 18 chromophobe RCC (CHRCC), and 14 oncocytomas (OC). The level of protein expression was scored semiquantitatively on a scale of 0-3+.

Results: Both MR and 11βHSD2 expression were present in normal kidneys in distal convoluted tubules, collecting ducts and Henle's loops with a predominant nuclear localization for MR and cytoplasmic staining for 11βHSD2. OC demonstrated a significantly greater degree of strong MR staining than CHRCC (71% vs 33%; P=0.03). CHRCC demonstrated membranous and cytoplasmic 11βHSD2 staining while OC showed diffuse cytoplasmic reactivity. There was a strong correlation between MR and 11βHSD2 staining (R=0.7, P<0.0001).

Expression of MR and 11βHSD2 in RCNs

	CRCC	GCRCC	PRCC	CHRCC	OC
MR	0/75	0/8	0/13	13/18 (72%)	13/14 (93%)
11βHSD2	2/75 (2.6%)	0/8	0/13	17/18 (94%)	14/14 (100%)

Conclusions: The vast majority of CHRCC and OC express MR and 11βHSD2 thereby distinguishing them from eosinophilic variants of CRCC and PRCC. Additionally, the levels of MR expression appear to be useful in distinction of CHRCC from OC. This expression pattern reflects the histogenetic origin of CHRCC and OC from the distal nephron, whereas absence of immunoreactivity in CRCC and PRCC is consistent with their origin from proximal convoluted tubules. MR and 11βHSD2 should be included in the IHC panel to more accurately subtype RCNs.

839 Upregulation of Both Decoy Receptor 1 and c-FLIP May Counteract the Function of DR5 in Renal Cell Carcinoma

B Yang, N Chen, H Zeng, R Huang, YT Zhang, XQ Chen, YD Huang, Q Zhou. West China Hospital, West China Medical School, Sichuan University, Chengdu, Sichuan, China.

Background: The tumor necrosis factor receptor-associated apoptosis induced ligand (TRAIL) can bind to the death receptor 4 (DR4) or DR5, leading to binding and activation of caspase 8 (hence cell death), which can be competitively inhibited by cFLIP. On the other hand, binding of TRAIL with the decoy receptor (DcR1 and DcR2) does not result in caspase activation as these receptors lack functional intracellular domains necessary for interacting with the caspases. Although activation of DRs may be an effective approach to inducing cell death in various neoplasms, expression of DcRs and cFLIP may counteract this effect. We investigate in the present study the relative mRNA expression level of DR4, DR5, DcR1, and cFLIP in renal cell carcinoma (RCC), as a means of evaluating potential responsiveness of TRAIL-induced cell death in RCC.

Design: The relative mRNA levels of DR4, DR5, DcR1, and cFLIP were assessed by semi-quantitative RT-PCR in 29 fresh samples of conventional (clear cell) RCCs and 29 paired normal renal cortical tissue samples. Primers were designed and synthesized (Invitrogen) according to c-DNA sequences in the GenBank. The relative mRNA was calculated against actin which was used as internal control.

Results: DR5 mRNA was readily detected in 72% (21/29) of the RCCs, as was in the control cell line (human cervical cancer cell HeLa), but was absent or only present at low level in the 29 paired normal renal cortical tissue samples. DR4, however, was only detected in 10% (2/21) of the RCCs. On the other hand, DcR1 and c-FLIP1 were detected in both RCC and normal renal tissue, but were quantitatively more abundant in the former.

Conclusions: Although DR5 was more frequently expressed in RCC than in normal renal tissue, the co-upregulation of both DcR1 and c-FLIP may lead to inhibition of its function and insensitivity to TRAIL-induced cell death.

840 Expression of Androgen Receptor Target Gene c-FLIP in Prostate Cancer Stromal Environment and Its Role in Tumor Growth and Progression

H Ye, Y Li, L Chiriboga, P Pearce, J Melamed, Z Wang, JJ Wei, I Osman, P Lee. New York University School of Medicine, New York, NY; UT MD Anderson Cancer Center, Houston, TX; NYU School of Medicine, New York, NY; New York Harbor Healthcare System, New York, NY.

Background: In prostate cancer, the tumor stromal environment plays an active role in tumor initiation, progression and metastasis. Androgen receptor (AR), a transcription factor of the steroid receptor family, is expressed in both stromal and epithelial cells of prostate. Upon association with ligand, AR migrates into the cell nucleus, and then binds to cognate androgen response elements to activate the expression of AR target genes, which play important roles in the regulation of prostate cell growth. Studies on the stromal expression and function of AR and its target genes in prostate cancer are limited. c-FLIP, an inhibitor of Fas/Fas-L mediated apoptosis has recently been shown by us to also be an androgen receptor target gene, promoting survival of prostate cells. In this study, we examined the expression and function of stromal c-FLIP in prostate cancer.

Design: We examined the expression of c-FLIP in stromal cells in prostate cancer by immunohistochemical analysis of archival radical prostatectomy cases (n = 59) using a polyclonal antibody. We quantified the expression of c-FLIP in stromal cells comparing the relative expression in the areas of benign prostate with areas of cancerous prostate. We further stratified the increase and compared with other clinicopathological variables specifically patient age, race, PSA, tumor grade and stage.

Results: There is a statistically significant increase of stromal c-FLIP expression ($p < 0.001$) within the neoplastic gland stroma as compared with benign areas of prostate distant from the cancer foci. There is an association between increased tumor stromal c-FLIP expression and patient's PSA, tumor grade and stage, but not patient's age and race. These results corroborate our in vitro data that stromal c-FLIP expression promotes prostate cancer growth and invasion.

Conclusions: The results of this study underscore the importance of the stromal microenvironment in prostate neoplasia. The increased expression of an androgen receptor target gene in stromal cells within the immediate vicinity of neoplastic glands suggests that a pathway mediated by androgen receptor and its downstream genes may play an important role in the development and progression of prostate cancer.

841 Aberrations of Chromosome 9 Detected by Fluorescence In Situ Hybridization in Urothelial Carcinoma In Situ: Correlation with $p16^{INK4}$ Immunohistochemical Expression

M Yin, K Cieply, K Cumbie, S Bastacky, R Dhir. University of Pittsburgh Medical Center, Pittsburgh, PA.

Background: Mutations of INK4a, located at 9p21, are found to be involved in urothelial carcinogenesis. Using $p16^{INK4}$ immunohistochemical stains, we previously documented a marked increased expression in urothelial carcinoma in situ (CIS); a moderate expression in invasive urothelial carcinoma (UC); and minimal staining in urothelium adjacent to carcinoma (UAC). The aim of this study was to evaluate specifically the relationships between the previously documented levels of $p16^{INK4}$ expression and chromosome 9 alterations.

Design: Bladder specimens with CIS (n=15), high-grade UC (Ta/T1: n=7; T2-T4: n=9), and UAC (n=18) were obtained. Five-micron sections were analyzed with standard fluorescence in situ hybridization (FISH) methodology, using dual-color LSI 9p21 & CEP-9 probes. The targeted areas were identified on a corresponding section with $p16^{INK4}$ stain. An average of 60 interphase cells was evaluated. Normal control bladder specimens from organ donors (n=12) were incorporated into the assay, leading to the establishment of positive cut-off levels.

Results: Both loss of 9p21 and gain of chromosome 9 were observed in different forms of UC and in UAC (table 1), with CIS showing the higher frequecy of the chromosomal changes. The 9p21deletion became less frequent with disease progression. Polysomy 9 was observed in both in situ and invasive UCs. UAC shows less numerous genetic changes, consistent with its low $p16^{INK4}$ expression.

Conclusions: 1. Both deletion of 9p21and hyperploidy of chromosome 9 are abundant in UCs. 2. Increased immunohistochemically detected $p16^{INK4}$could be due to polysomy 9 (increased gene copies leading to increased protein expression) or 9p21 deletion (stable mutated protein). 3. Invasive UCs show much more frequent polysomy 9 and less frequent 9p21 deletion, implying role in aggressive disease. 4. The molecular changes confirm the value of $p16^{INK4}$ immunohistochemical stain in detecting CIS, especially in differentiating CIS from reactive atypia.

Alterations of chromosome 9 in UCs and UAC

	CIS	Ta/T1 UC	T2-T4 UC	UAC
% of cells with loss of 9p21	17.0	10.5	4.4	4.0
% of cases with loss of 9p21	66.7	85.7	33.3	61.0
% of cells with polysomy 9	24.7	13.7	42.8	3.0
% of cases with polysomy 9	73.3	57.1	66.7	50.0

Data are presented as mean.

842 Diagnostic Utility of P501s (Prostein) in Comparison to Prostatic Specific Antigen (PSA) for the Detection of Metastatic Prostatic Adenocarcinoma

M Yin, R Dhir, AV Parwani. University of Pittsburgh Medical Center, Pittsburgh, PA.

Background: Immunohistochemical detection of prostate specific antigen (PSA) is widely used to identify metastatic prostatic adenocarcinoma (MPA). However, PSA may not be expressed in some poorly differentiated prostatic carcinomas and its immunoreactivity has been found in some non-prostatic tissues. P501s (prostein) is a prostate-specific marker that is expressed in the cytoplasm of benign and malignant prostatic glandular cells. It has not been detected in any other normal or malignant tissues. The purpose of this study was to evaluate the expression of P501s in MPA and compare its expression with PSA.

Design: Immunohistochemical stains with monoclonal mouse anti-P501S antibodies were performed on five-micron sections of tissue microarray (TMA) specimens. The TMA is constructed with normal donor prostates (NDP, n=24); prostatic adenocarcinoma (PRCA, n=135); non-neoplastic prostatic tissues adjacent to malignant glands (NAT, n=36); benign prostatic hyperplasia (BPH, n=35); high-grade prostatic neoplasia (PIN, n=35); metastatic prostatic adenocarcinoma (MPA, n=54); and samples of benign testis, colon, adrenal and kidney (n=24). The metastatic lesions were also subjected to immunohistochemical stains with monoclonal antibodies to PSA. A composite score (ranging from 0 to 3) was assigned to score intensity of staining.

Results: Granular staining pattern is seen in benign and malignant epithelial cells at the apical aspect of cytoplasm, predominantly adjacent to the nuclei, corresponding to the location of Golgi complex. No staining was seen in samples of testis, colon, adrenal and kidney. The staining intensity and percentage of negative P501s and PSA stains are shown in table 1. Five MPA cases (9.3%) were negative for either P501S or PSA. Only two metastatic lesions (3.7%) showed negative stains for both markers.

Conclusions: P501S is an organ specific marker for benign and malignant prostatic epithelial cells. Its characteristic cytoplasmic stain pattern provides an additional valuable immunomarker for detection of metastatic prostatic malignancy, even though the intensity of its expression is reduced, as in the case with PSA. Simultaneous stains with P501S and PSA will greatly improve the detection rate and identify a significant majority of the metastases.

	NDP	PRCA	NAT	BPH	PIN	MPA
P501s scores	1.95	1.59	1.77	2.10	2.11	0.84
P501s negative cases	0%	5.9%	5.6%	0%	0%	13%
PSA scores						1.46
PSA negative cases						13%

Data are expressed as mean.

843 Molecular Profiling of the Novel Thyroid-Like Renal Cell Carcinoma (RCC) and Tubulocystic RCC by High-Density Oligonucleotide Microarrays

AN Young, GP Paner, GT MacLennan, JC Cheville, A Vieillefond, O Hes, JK McKenney, F Paraf, DJ Grignon, JI Epstein, JR Srigley, MB Amin. Emory University Hospital, Atlanta, GA; Cedars-Sinai Medical Center, Los Angeles, CA.

Background: The clinico-pathologic significance of common adult renal neoplasms has been strenghtened by discovery of unique gene expression profiles in each tumor subtype. Thyroid-like and tubulocystic RCCs are new emerging distinct subtypes of renal epithelial neoplasm. We compared the gene expression profiles of thyroid-like and tubulocystic RCCs with common RCC subtypes, using high-density oligonucleotide microarrays. Thyroid-like and tubulocystic RCCs are rare, and frozen specimens were unavailable for this analysis. Therefore, novel technologies were applied for microarray analysis of formalin-fixed paraffin-embedded tissues.

Design: Specimens included 5 clear RCC, 4 chromophobe RCC, 3 thyroid-like RCC and 4 tubulocystic RCC. Total RNA was isolated from fixed tissue blocks using the Arcturus Paradise reagent system, and expression profiles were characterized with Affymetrix X3P microarrays. These extraction reagents and microarrays are optimized for use with fixed tissue. Normalized microarray results were analyzed with unsupervised and supervised clustering algorithms to test for unique expression profiles and candidate biomarkers of thyroid-like and tubulocystic RCC. A Gene Ontology analysis program (GO/stat) was used to determine if specific biological processes were highly represented in tumor expression profiles.

Results: Compared to clear cell and chromophobe RCC, thyroid-like RCC overexpressed 135 and underexpressed 46 genes, while tubulocystic RCC overexpressed 53 and underexpressed 126 transcripts. Several differentially expressed transcripts have been annotated for function using the Gene Ontology controlled vocabulary. Using the /GO/stat program, thyroid-like RCC was found to overexpress cell cycle-related genes, while tubulocystic RCC expressed cell cycle and biomolecule metabolism genes differentially.

Conclusions: Unique gene expression signatures were identified in thyroid-like and tubulocystic RCC by microarray analysis of fixed tumor specimens. Differential gene expression may provide insights into the distinct biology of these rare renal tumors. In addition, selected biomarkers have potential to be translated into immunohistochemical panels for the microscopic differential diagnosis of renal tumors with unusual histology.

844 Diffuse Membranous Immunoreactivity for D2-40 (Podoplanin) Distinguishes Primary and Metastatic Seminomas from Other Germ Cell Tumors and Metastatic Neoplasms

H Yu, GS Pinkus, JL Hornick. Brigham and Women's Hospital, Boston, MA.

Background: Podoplanin is a glycoprotein expressed in a variety of human cell types, including glomerular epithelium, lymphatic endothelium, and mesothelium. Recently, podoplanin has been shown to be expressed in primary germ cell tumors (GCT), with conflicting results regarding specificity. However, podoplanin expression in metastatic GCT and other metastatic tumors has not been extensively examined. The goal of this study was to evaluate the distribution and specificity of podoplanin in primary testicular and metastatic GCT compared to other metastatic neoplasms.

Design: 122 tumors were studied: 43 primary GCT [14 seminomas (SEM), 4 teratomas, 2 embryonal carcinomas (EC), 23 mixed GCT]; 32 metastatic GCT; 11 metastatic melanomas; 25 metastatic carcinomas (5 each from breast, colon, lung, stomach, kidney); 10 lymphomas [5 diffuse large B-cell lymphoma, 5 anaplastic large cell lymphoma (ALCL)]. Immunohistochemical studies were performed following epitope retrieval (0.01M citrate buffer, pH 6.0; pressure cooker) using monoclonal antibody D2-40 (Signet Labs) and an EnVision+ peroxidase detection system (Dako). The intensity, pattern, and extent of immunoreactivity were evaluated.

Results: In primary GCT, all foci of SEM showed strong diffuse membranous staining for D2-40 in >90% of cells. In contrast, no other GCT components showed diffuse membranous staining. Of EC, 11% showed focal complete membranous staining in <5% of cells; 89% of EC and 50% of yolk sac tumors showed focal weak cytoplasmic and partial membranous staining. Of teratomas, 50% showed focal apical staining in epithelium. All foci of choriocarcinoma were negative. Intratubular germ cell neoplasia showed strong diffuse membranous staining in all cases. Similarly, in metastatic GCT, all foci of SEM showed strong complete membranous staining in nearly all tumor cells, whereas other GCT components showed only focal cytoplasmic and/or partial membranous staining. Among non-GCT, only 1 metastatic melanoma, 1 ALCL, and 1 metastatic carcinoma each from breast, lung, and kidney showed focal weak cytoplasmic staining.

Conclusions: Diffuse membranous immunoreactivity for podoplanin as detected by monoclonal antibody D2-40 is highly sensitive and specific for primary and metastatic SEM. Podoplanin expression in other GCT components is generally focal, weak, and cytoplasmic and/or partially membranous. Immunodetection of podoplanin may be useful to support SEM in the differential diagnosis of poorly differentiated epithelioid malignant neoplasms.

845 Diagnosing Metastatic Renal Cell Carcinoma (RCC). The Utility of PAX-2 Compared with the Renal Cell Carcinoma Marker Antigen

J Zhai, A Ozcan, A Kunda, C Hamilton, SS Shen, LD Truong. The Methodist Hospital, Houston, TX; Weill Medical of College of Cornell University, New York, NY; Baylor College of Medicine, Houston, TX; Gülhane Military Medical Academy & School of Medicine, Ankara, Turkey.

Background: The diagnosis of metastatic (Met) renal cell carcinoma (RCC) remains problematic, since the Met may 1) long precede or lag much behind the onset of RCC; 2) be less differentiated than the primary RCC and not conform to the known morphologic spectrum of RCC; and 3) develop in patients with history of both RCC and another

cancer. PAX-2 is a transcription factor that promotes renal tubular differentiation during embryogenesis. PAX-2 expression in Met RCC is studied and compared with that of the RCC Marker antigen (RCCM).

Design: From an archive of 94 unequivocal cases of Met RCC, 64 cases were immunostained for PAX- 2 and 58 cases for RCCM. Among them, both PAX-2 and RCCM stain were performed on consecutive tissue sections for 28 cases. Features selected for evaluation included histologic type of the Met in relation to that of the primary tumor, staining intensity (graded 0-3), staining extent (% of positive tumor cells), and the correlation of staining of PAX-2 and RCCM relative to tumor type.

Results: For **PAX-2**, 47/64 (73%) cases showed positive stain (mean score 2.06) in 5-100% tumor cells (mean 55) with a nuclear pattern, and a weak nonspecific cytoplasmic pattern in 39 cases. The positive stain was not correlated with the tumor type or grade. For **RCCM**, 33/58 (57%) cases showed positive stain (mean score 2.5) in 2-100% tumor cells (mean 62) with a cytoplasmic pattern only. The positive stain was seen predominantly in Met with low nuclear grade, and clear cell or papillary features. The results of the 28 cases submitted to staining for both **PAX-2 and RCCM** were shown in Table 1.

Conclusions: 1) Immunostain for PAX-2 is successful in routinely processed human tissue, with a nuclear pattern, expected for a transcription factor; 2) PAX-2 expression, noted in a majority of Met RCC, should substantially facilitate a correct diagnosis. 3) PAX-2 is a significantly more sensitive marker than the RCCM, but there are rare cases with the – PAX-2/+ RCCM phenotype, justifying the use of both as a panel.

Table 1: 28 Cases Submitted for Both RCCM and PAX-2 Staining

	PAX-2 Positive (n=20)	PAX-2 Negative (n=8)
RCCM Positive (n=12)	10	2
RCCM Negative (n=16)	10	6

846 Expression of SmgDGS in Prostatic Adenocarcinoma and Its Function in Cancer Cell Migration

HY Zhi, XJ Yang, J Kuhnmuench, R Thill, CL Williams, CG Becker, R Li. Medical College of Wisconsin, Milwaukee, WI; Northwestern Memorial Hospital, Chicago, IL.

Background: SmgDGS, a guanine nucleotide exchange factor, actives small GTPases which promote malignancy of different carcinoma cells. Surprisingly, the expression and function of SmgDGS in human cancers have not been reported. In this study, we evaluated the expression of SmgGDS in benign prostatic tissue, prostatic adenocarcinoma and prostatic intraepithelial neoplasia (PIN) using immunohistochemistry. In addition, we performed functional studies of SmgGDS using siRNA in different prostatic cancer cell lines.

Design: Large sections of 18 radical prostatectomy specimens contained invasive carcinoma (Gleason score G3-G5) and benign prostatic tissue, with or without PIN were selected. In addition, a section of tissue microarray containing 90 cases including 30 high grade PIN, 30 G3 and 30 G4/5 carcinoma, with or without benign prostatic tissues was also used. Totally, there were 108 cases including 44 PINs and 78 adenocarcinomas with 32 cases containing benign tissues. Immunohistochemistry was performed using a monoclonal anti-SmgGDS antibody (BD Transduction laboratories). In the functional studies, the LnCap and PC-3 cell lines were transfected with SmgGDS siRNA to silence SmgGDS expression. The MTT assay was used to measure cell proliferation and the Wound-Healing and Colloidal Gold Phagokinesis assays were used to measure cell migration.

Results: SmgGDS was either weakly expressed or undetectable in benign prostatic glands. Seventy of 78 (89.7%) invasive adenocarcinomas and 38/44 (86.4%) PINs showed a strong and increased staining when compared with adjacent benign glands. There was no difference of expression between different Gleason patterns with 30/33 (90.9%) in G3 versus 40/45 (88.9%) in G4/5 adenocarcinomas. Silencing SmgGDS expression slightly inhibited cell proliferation in both LnCap and PC-3 cells. However, silencing SmgGDS significantly diminished cell migration in PC-3 cell line.

Conclusions: 1) SmgGDS is overexpressed in prostatic adenocarcinoma and PIN, indicating a potential role as a marker in the diagnosis of prostatic cancer. 2) The increased SmgGDS expression in both adenocarcinoma and PIN suggest its role in early prostatic carcinogenesis. 3) SmgGDS enhances the migration of the androgen-independent PC-3 cells. This finding indicates that SmgGDS may be used as a potential target in the treatment of advanced prostatic cancers, because androgen-independence is correlated with advanced tumor stage after hormonal therapy.

847 Cancer Risk Associated with High Grade Prostatic Intraepithelial Neoplasia (HGPIN) in a Contemporary Single-Institution Cohort

M Zhou, E Klein, C Magi-Galluzzi. Cleveland Clinic, Cleveland, OH.

Background: HGPIN has been shown to denote a 25-30% risk of finding cancer in subsequent biopsies. Its significance, however, has been questioned recently as several studies have shown that the cancer risk associated with HGPIN is comparable to that associated with a benign initial diagnosis. This study examined the cancer risk associated with HGPIN in a contemporary cohort of patients evaluated at a single institution.

Design: Patients met the following criteria: (1) initial and subsequent prostate biopsies were performed after January 2003; (2) initial biopsy contained ≥ 6 cores; (3) time interval between the initial and 1st repeat biopsy ≤24 months; (4) initial biopsy had a diagnosis of benign prostatic tissue (BPT), HGPIN, atypical glands suspicious for cancer (ATYP). All the biopsies were diagnosed by the GU pathology service at the authors' institution.

Results: 262 patients were included in this study. The initial diagnosis was BPT in 28.2%, HGPIN in 47.3%, and ATYP in 24.4%. The mean number of re-biopsy was 1.2 (range 1-3), and the time interval between the initial and subsequent biopsy (ies) was 10.6 (range 0.5-39.5) months. Of the patients with an initial HGPIN diagnosis, 33.1% had PCa in subsequent biopsies, compared to 14.9% cancer risk associated with an initial BPT diagnosis ($p<0.01$, Table 1). If the initial biopsy had ≥ 10 cores, the cancer risk associated with HGPIN was 33.7%, significantly higher than that associated with the initial BPT biopsy (12.5%, $p<0.01$). However, the cancer risk associated with HGPIN was not significantly different from that associated with the initial BPT biopsy (30.4% vs 19.2%, $p>0.05$) when the initial biopsy had 6-9 cores.

Table 1: The Cancer Risk Assessment with BPT, HGPIN and ATYP in Initial Diagnosis

		PCa in Subsequent Biopsy		
		Biopsy core #6-9	Biopsy core # ≥10	All Cases
Initial Diagnosis	BPT	5/26 (19.2%)*	6/48 (12.5%)**	11/74 (14.9%)^
	HGPIN	7/23 (30.4%)*	34/101 (33.7%)**	41/124 (33.1%)^
	ATYP	5/9 (55.6%)	22/25 (40%)	27/64 (42.2%)

*p>0.05, **p<0.01, ^p<0.01

Conclusions: HGPIN is associated with a significantly increased cancer risk in our contemporary cohort. However such increased cancer risk is only significant when the initial biopsy has ≥ 10 cores. Our study suggests that HGPIN in needle biopsy should still be considered as a risk factor for PCa. In addition, a biopsy scheme with ≥ 10 core is recommended in order to detect such an increased cancer risk associated with HGPIN.

848 Expression of Carbonic Anhydrase IX (CA9) in Renal Neoplasms: Implications for Use as Diagnostic Marker

M Zhou, C Magi-Galluzzi. Cleveland Clinic, Cleveland, OH.

Background: CA9 is a tumor associated antigen found on the cell surface of a number of human cancers. Recently, CA9 has been shown to be a useful diagnostic and prognostic biomarker for clear cell renal cell carcinoma. Its expression in other renal neoplasms, and its utility as a differential diagnostic marker, however, is not well documented.

Design: A tissue microarrays (TMA) was constructed from 60 normal kidneys, 23 clear cell renal cell carcinoma (CCRCC), 20 papillary renal cell carcinomas (PRCC), 16 chromophobe renal cell carcinomas (ChRCC), and 19 oncocytomas (ONC), 14 pelvic urothelial carcinoma (TCC) and 20 angiomyolipoma (AML). The TMA was immunostained for CA9. Membranous CA9 expression was scored as negative, weak and strong. The percentage of positive cells was also recorded.

Results: CA9 expression was absent in normal renal tissues. Strong and weak positive staining was present in 83% and 4% of CCRCC, respectively, with an average of 47.6% of tumor cells positive for CA9 expression (Table 1). Thirteen % of CCRCC was negative. Ten % of PRCC was also positive for CA9. One such case had papillary structures lined with clear cells. All pelvic TCCs were positive for CA9, with strong expression in 86% and weak expression in 14% of cases. However, only an average of 11.3% of tumor cells were positive for CA9. All ChRCC, ONC and AML were negative for CA9.

Table 1: Expression of CA9 in Renal Neoplasms

CA9 Expression	CCRCC	PRCC	ChRCC	ONC	TCC	AML
Strong Positive	19/23 (83%)	2/10 (10%)	0	0	12/14 (86%)	0
Weak Positive	1/23 (4%)	0	0	0	2/14 (14%)	0
Negative	3/23 (13%)	18/20 (90%)	16/16 (100%)	19/19 (100%)	0	20/20 (100%)
% postivie cells [mean (range)]	47.6% (3-100)	21.5% (20-23)	N/A	N/A	11.3% (5-50%)	N/A

Conclusions: Although expressed by the majority of CCRCC, CA9 is also found in all the renal pelvic TCC and in a minority of PRCC, but is absent in ChRCC and oncocytoma. CA 9 may potentially be useful in the differential diagnosis of selected renal tumors, such as CCRCC vs ChRCC, and TCC vs ChRCC.

Gynecologic

849 p16 Is Expressed in Ovarian Clear Cell Carcinoma

AJ Adeniran, ED Euscher, MT Deavers, A Malpica. M.D. Anderson Cancer Center, Houston, TX.

Background: p16 is a cyclin-dependent kinase-4 inhibitor that is expressed in tumors of the female genital tract. Of the gynecologic tumors, p16 expression in cervical carcinoma (squamous, glandular, and small cell) is best studied and characteristically overexpressed. p16 expression in low grade and benign ovarian tumors is reported to be low while ovarian serous carcinomas are reported to have overexpression. The expression of p16 in ovarian clear cell carcinoma has not been studied. This study evaluates the expression of p16 in a series of fifteen cases of ovarian clear cell carcinoma.

Design: Fifteen cases of pure clear cell carcinoma of the ovary were retrieved from the pathology files of M.D. Anderson Cancer Center. H&E slides were reviewed in all cases. Immunohistochemical analysis for p16 (clone 16P07, dilution 1:25, Labvision/Neomarkers, Fremont, CA) was performed on formalin-fixed, paraffin embedded archival tissue utilizing standard avidin-biotin technique. Nuclear and cytoplasmic expression in tumor cells was considered positive with results scored semiquantitatively (0, no staining; 1+, 1-25%; 2+, 26-50%; 3+, 51-75%; 4+, 76-100%) by two independent observers.

Results: Fourteen of the 15 (93%) cases over-expressed p16 immunohistochemically. Eleven of 15 (73%) cases had a score of 3+ or 4+, and 3 of 15 (20%) cases had a score of 1+ or 2+. One of fifteen cases (7%) had no p16 expression.

Conclusions: The majority of ovarian clear cell carcinomas overexpress p16, although the mechanism for this is unknown. p16 may be less useful as a marker to distinguish metastatic cervical carcinoma to the ovary from a primary ovarian carcinoma. However, p16 may be a useful marker in an immunopanel to distinguish a primary ovarian clear cell carcinoma from a metastatic carcinoma with clear cell morphology to the ovary.